

**Tip Clearance
Measurement in
Aero and Industrial
Turbomachinery**

Edited by Geoff Sheard

Sigel
Press

Copyright © 2013 Sigel Press

Sigel Press
51A Victoria Road
Cambridge CB4 3BW
England

4403 Belmont Court
Medina, Ohio 44256
USA

Visit us on the World Wide Web at: www.sigelpress.com

The rights of Geoff Sheard, identified as editor of this work, have been asserted by him in accordance with the Copyright, Designs and Patents Act 1988.

All rights reserved. No part of this publication may be reproduced, stored in a retrieval system, or transmitted in any means, electronic, mechanical, photocopying, recording, or otherwise without prior written permission of the publisher.

Internal Design: Professional Book Compositors, Lorain, Ohio, USA
Cover Design: Harp Mando
Cover Image: Alessandro Corsini, Sapienza University of Rome

ISBN 10: 1-905941-20-X
ISBN 13: 978-1-905941-20-9

A catalogue record for this book is available from the British Library.
Typeset in Times Roman

The publisher's policy is to use paper manufactured from sustainable forests.

In Memory

There is no such thing as a self-made man. We all work in and are part of teams. The research in this volume is no different to any other of life's endeavours, and as such, the above applies as well to this collection as it does to any other facet of life.

In 1990, George Westerman was a young man who wished to study engineering at university. He was looking for a summer job in an engineering company after completing his first year in the sixth form. I put George to work as a laboratory assistant, where he quickly became part of the team. As part of the team it was natural that George should also co-author reports. At the time this did not seem in any way out of the ordinary as I took excellence for granted.

George died on July 7, 1993. He was 19 years old. There are no words to express my thanks to George for the contribution that he made to the research in this volume, nor my grief (and that of his family, friends and colleagues) at his untimely death. Those of us lucky enough to have known him still miss his sharp mind, his infectious wit and warmth of heart.

Geoff Sheard
Fläkt Woods Group

Permissions Acknowledgements

Chapter 1, *An Electromechanical Measurement of Turbomachinery Blade Tip-to-casing Running Clearance*, was originally published in the proceedings of the 37th American Society of Mechanical Engineers Gas Turbine and Aeroengine Congress, paper number 92-GT-50. Reprinted with the permission of The American Society of Mechanical Engineers. Permission to publish received April 18, 2012.

Chapter 2, *A Technique for the Measurement of Blade-tip Clearance in a Gas Turbine*, was originally published in the proceedings of the 25th AIAA / ASME / SAE / ASEE Joint Propulsion Conference, paper number AIAA 89-2916. Reprinted with the permission of the American Institute of Aeronautics and Astronautics, 1801 Alexander Bell Drive, Suite 500, Reston, VA 20191-4344, USA. Permission to publish received June 28, 2012

Chapter 3, *Blade-by-blade Tip Clearance Measurement*, was originally published in the International Journal of Rotating Machinery, Volume 2011, an Open Access publication. Reprinted under the terms of the Hindawi Publishing Corporation's Creative Commons Attribution license.

Chapter 4, *An On-line Calibration Technique for Improved Blade-by-blade Tip Clearance Measurement*, was originally published in the proceedings of the 38th ISA International Instrumentation Symposium. Copyright © 1992 ISA. All rights reserved. Used with permission of ISA. Permission to publish received April 17, 2012.

Chapter 5, *A High-speed Capacitance-based System for Gauging Turbomachinery Blading Radius during the Tip Grind Process*, was originally published in the Proceedings of the 37th American Society of Mechanical Engineers Gas Turbine and Aeroengine Congress, paper number 92-GT-365 and subsequently in the transactions of the American Society of Mechanical Engineers Journal of Engineering for Gas Turbines & Power, Volume 116. Reprinted with the permission of The American Society of Mechanical Engineers. Permission to publish received April 18, 2012.

Chapter 6, *A Blade-by-blade Tip Clearance Measurement System for Gas Turbine Applications*, was originally published in the proceedings of the 39th American Society of Mechanical Engineers Turbine and Aeroengine Congress, Paper Number 94-GT-40 and subsequently in the transactions of the American Society of Mechanical Engineers Journal of Engineering for Gas Turbines & Power, Volume 117. Reprinted with the permission of The American Society of Mechanical Engineers. Permission to publish received April 18, 2012.

Chapter 7, *Capacitive Measurement of Compressor and Turbine Blade Tip-to-casing Running Clearance*, was originally published in the proceedings of the 41st American Society of Mechanical Engineers Gas Turbine and Aeroengine Congress, paper number 96-GT-349, winning the Controls, Diagnostics and Instrumentation Technical Committee best paper award. The paper was subsequently published in the transactions of the American Society of Mechanical Engineers Journal of Engineering for Gas Turbines & Power, Volume 119. Reprinted with the permission of The American Society of Mechanical Engineers. Permission to publish received April 18, 2012.

Chapter 8, *Turbine Tip Clearance Measurement System Evaluation on an Industrial Gas Turbine*, was originally published in the proceedings of the 42nd American Society of Mechanical Engineers Gas Turbine and Aeroengine Congress, paper number 97-GT-466. Reprinted with the permission of The American Society of Mechanical Engineers. Permission to publish received April 18, 2012.

Chapter 9, *High-temperature Proximity Measurement in Aero and Industrial Turbomachinery*, was originally published in the proceedings of the 42nd American Society of Mechanical Engineers Turbine and Aeroengine Congress, paper number 97-GT-198 and subsequently in the transactions of the American Society of Mechanical Engineers Journal of Engineering for Gas Turbines & Power, Volume 121. Reprinted with the permission of The American Society of Mechanical Engineers. Permission to publish received April 18, 2012.

Appendix 1, *Capacitance Transducer Apparatus and Cables*, was originally published as Patent Number WO 97/28418. Reprinted in accordance with the requirements of the Copyright, Designs and Patents Act, Section 30 (1) and Section 47 (1).

Appendix 2, *Gap Measurement Device*, was originally published as Patent No. US 5,760, 593. Reprinted in accordance with the requirements of the Copyright, Designs and Patents Act, Section 30 (1) and Section 47 (1).

Appendix 3, *Capacitive Gap Measurement Device*, was originally published as Patent No. GB 2 325 305 B. Reprinted in accordance with the requirements of the Copyright, Designs and Patents Act, Section 30 (1) and Section 47 (1).

Contents

List of Figures	ix
List of Tables	xxi
Foreword	xxiii
Acknowledgements	xxv
About the Editor	xxvii
Introduction: Tip Clearance Measurement Geoff Sheard	xxix
Summary of Chapters Geoff Sheard	xxxv
Chapter 1 An Electromechanical Measurement of Turbomachinery Blade Tip-to-casing Running Clearance A.G. Sheard and S.R. Turner	1
Chapter 2 A Technique for the Measurement of Blade-tip Clearance in a Gas Turbine J.W.H. Chivers	25
Chapter 3 Blade-by-blade Tip Clearance Measurement A.G. Sheard	53
Chapter 4 An On-line Calibration Technique for Improved Blade-by-blade Tip Clearance Measurement A.G. Sheard, G.C. Westerman and B. Killeen	81
Chapter 5 A High-speed Capacitance-based System for Gauging Turbomachinery Blading Radius during the Tip Grind Process A.G. Sheard, G.C. Westerman, B. Killeen and M. Fitzpatrick	111
Chapter 6 A Blade-by-blade Tip Clearance Measurement System for Gas Turbine Applications A.G. Sheard and B. Killeen	139

Chapter 7	Capacitive Measurement of Compressor and Turbine Blade Tip-to-casing Running Clearance	161
	D. Müller, A.G. Sheard, S. Mozumdar and E. Johann	
Chapter 8	Turbine Tip Clearance Measurement System Evaluation on an Industrial Gas Turbine	189
	S.J. Gill, M.D. Ingallinera and A.G. Sheard	
Chapter 9	High-temperature Proximity Measurement in Aero and Industrial Turbomachinery	211
	A.G. Sheard, S.G. O'Donnell and J.F. Stringfellow	
Appendix 1	Capacitance Transducer Apparatus and Cables	233
	J.F. Stringfellow, L. Wayman and B. Knox	
Appendix 2	Gap Measurement Device	241
	A.G. Sheard and D.C. Lawrence	
Appendix 3	Capacitive Gap Measurement Device	251
	A.G. Sheard	
	Bibliography	259
	Author Index	265
	Subject Index	267

List of Figures

Figure 1.1	An example of Amsbury and Chivers' (1978) design of electromechanical clearance measurement system probe and actuator	2
Figure 1.2	A schematic layout of the electromechanical clearance measurement system installation and component parts	3
Figure 1.3	A 100 mm installed length, 6 mm stroke probe cartridge. Probes with installed lengths from 50 mm to 1.5 m may be used	6
Figure 1.4	The mini electromechanical clearance measurement system actuator design, with a probe cartridge shown for clarity	8
Figure 1.5	Removal of the probe cartridge from a mini electromechanical clearance measurement system actuator	10
Figure 1.6	The mini and micro electromechanical clearance measurement system actuators, which are 23% and 18% the volume of Davidson <i>et al.</i> 's (1983) first generation system	10
Figure 1.7	The 19" rack-mount electromechanical clearance measurement system controller	11
Figure 1.8	Controller operating modes which the operator may set up and change via the 19" rack-mounted controller's RS232 interface	12
Figure 1.9	Mini electromechanical clearance measurement system calibration as delivered and after 48 hours' continuous operation, illustrating system accuracy	14
Figure 1.10	An end view of the UCF6 facility with three traverse actuators, labelled A, B and C, and four of Davidson <i>et al.</i> 's (1983) first generation electromechanical clearance measurement systems, labelled 1, 2, 3 and 4	16
Figure 1.11	Blade tip-to-casing clearance results (percentage design clearance versus percentage design speed) from UCF6 when fitted with four of Davidson <i>et al.</i> 's (1983) first generation electromechanical clearance measurement systems	17
Figure 1.12	Blade tip-to-casing clearance results (percentage design clearance versus percentage design speed) from UCF6 when fitted with the mini electromechanical clearance measurement system, plus three of Davidson <i>et al.</i> 's (1983) first generation electromechanical clearance measurement systems	18
Figure 1.13	A side view of the CTR1 facility with the mini electromechanical clearance measurement system probe and actuator fitted	19

Figure 1.14	The installation design for the mini electromechanical clearance measurement system in the full scale spool with the heavyweight and lightweight brackets used to match probe thermal growth to that of the spool casing	21
Figure 1.15	A close-up view of the probe tip region of the probes used on UCF6 and CTR1 (right) and full scale spool (left) illustrating their different geometries. The probe used on UCF6 and CTR1 has run for over 100 hours and whilst well worn, was still fully functional	21
Figure 1.16	A side view of the full scale spool with mini electromechanical clearance measurement system probe and actuator fitted prior to test	22
Figure 2.1	Optical triangulation: principle of operation	28
Figure 2.2	Folded optical triangulation probe	29
Figure 2.3	Variation of relative permittivity of air versus location through a gas turbine	34
Figure 2.4	Frequency modulated driven guard capacitive clearance measurement system schematic block diagram	35
Figure 2.5	Capacitive clearance measurement system sensor schematic diagram	36
Figure 2.6	Prototype compressor stage 2 (left) and stage 5 (right) capacitive clearance measurement system probes	40
Figure 2.7	Comparison of compressor stage 5 predicted and measured blade tip-to-casing clearance	43
Figure 2.8	High-pressure compressor blade tip-to-casing clearance measurements obtained during a flight cycle	44
Figure 2.9	Prototype turbine capacitance probe, installed in both high-pressure and intermediate-pressure turbine stages	46
Figure 2.10	High-pressure turbine blade tip-to-casing clearance data obtained during a flight cycle	49
Figure 3.1	Trends in tip clearance. Measured by Müller <i>et al.</i> (1997) using an electromechanical clearance measurement system (Sheard and Turner, 1992) and capacitive clearance measurement system (Stringfellow <i>et al.</i> , 1997) in the high-pressure turbine of a BMW Rolls-Royce GmbH BR700 development gas turbine	55
Figure 3.2	Frequency modulated driven guard capacitive clearance measurement system schematic block diagram	57

Figure 3.3	The blade analyser unit developed by Killeen <i>et al.</i> (1991) and used to measure individual pulse heights, schematic block diagram	59
Figure 3.4	Layout diagram of the complete capacitive clearance measurement system used to measure blade tip-to-casing clearance over every blade	60
Figure 3.5	Spinning rig design used to evaluate the performance of Chivers' (1989a) capacitive clearance measurement system. The capacitance probe is fitted on a traverse actuator with touch probe to enable on-line calibration	61
Figure 3.6	Capacitance probe and touch wire mounting arrangement on the traverse actuator carrier	63
Figure 3.7	The spinning rig used to evaluate performance of Chivers' (1989a) capacitive clearance measurement system	64
Figure 3.8	Close-up view of the traverse actuator mounting on the spinning rig housing showing the clamping arrangement of the capacitance probe and touch wire	64
Figure 3.9	Capacitive clearance measurement system output plotted against known clearance illustrating the one over distance nature of the system output. Each dot on the graph is a single measurement made over a single blade	65
Figure 3.10	Error in capacitive clearance measurement system output, calculated by subtracting the known clearance between probe and blade tip from that obtained using the measurement system calibration for each blade	66
Figure 3.11	Error in capacitive clearance measurement system output plotted against blade number around the spinning rig wheel, illustrating a ± 0.025 mm variation in blade height due to shaft eccentricity	67
Figure 3.12	Error in capacitive clearance measurement system output plotted against blade number around the spinning rig wheel after compensating the error due to spinning rig shaft eccentricity	68
Figure 3.13	Capacitive clearance measurement system output plotted against known clearance after compensating for spinning rig shaft eccentricity	69
Figure 3.14	Error in capacitive clearance measurement system output, calculated after compensating for spinning rig shaft eccentricity	70
Figure 3.15	Capacitive clearance measurement system output for the longest blade of the spinning rig wheel plotted against position, which was changed using the traverse actuator	71

Figure 3.16	Capacitive clearance measurement system calibration obtained without datuming the probe or knowing the length of each blade relative to the longest blade. The figure also shows the actual position of the data points used in the calibration	72
Figure 3.17	Capacitive clearance measurement system output for each blade of the spinning rig wheel plotted against known clearance, over-plotted with the recently acquired calibration	73
Figure 3.18	Error in capacitive clearance measurement system output over the 24 blades around the spinning rig wheel, calculated by subtracting the known clearance between probe and blade tip from that calculated from the measurement system calibration. The calibration was obtained without datuming the capacitance probe	74
Figure 3.19	The hybrid probe developed by Sheard and Killeen (1993) and used by Sheard and Killeen (1995) to measure the blade-by-blade tip-to-casing clearance in the C147 compressor at DRA Pystock	76
Figure 4.1	Capacitive clearance measurement system schematic block diagram	84
Figure 4.2	Blade analyser unit used to measure individual pulse heights, schematic block diagram	85
Figure 4.3	The prototype measurement head (without its cover), which integrates the capacitance probe, spark-discharge electrode and traverse actuator into a single unit	87
Figure 4.4	The 8 mm integrated probe with the adjustable electrode used in the prototype measurement head	88
Figure 4.5	The original traverse actuator design, used for radial and angular positioning of aerodynamic probes in a gas turbine annulus. The radial transport mechanism was utilised in the prototype measurement head for positioning the capacitance probe and spark-discharge electrode	89
Figure 4.6	The inter-relationship between the ground station modules, measurement head and host computer illustrating the system processor's key role as an interface accepting input commands and then transparently orchestrating the action of other modules to act on them	90
Figure 4.7	The prototype measurement head fitted to a computer numerically controlled (CNC) lathe with a Pratt & Whitney JT8 stage 11 compressor disc and blade set	91

Figure 4.8	Seventy-point data sets acquired from the capacitance probe at nine different traverse actuator positions. Each dot on the graph is a single measurement over a single blade	93
Figure 4.9	Capacitive clearance measurement system output for the longest blade of each data set plotted against known position, which was changed using the traverse actuator	95
Figure 4.10	Capacitive clearance measurement system calibration obtained with no knowledge of relative blade heights or the distance from spark-discharge electrode to capacitance probe tip. The known positions of the data points used in the calibration are also shown	96
Figure 4.11	Capacitive clearance measurement system output plotted against clearance illustrating the one over distance nature of the system output	98
Figure 4.12	Error in capacitive clearance measurement system output, calculated by subtracting clearance obtained using system calibration from that obtained assuming no knowledge of traverse actuator position	100
Figure 4.13	Capacitive clearance measurement system output plotted against corrected clearance illustrating that the data falls onto a curve with noticeably less scatter than before correction	102
Figure 4.14	The deviation of capacitive clearance measurement system output from the refined calibration, illustrating an error of ± 0.005 mm. The error degrades at increasing range due to the capacitance probe's decreasing sensitivity	103
Figure 4.15	Clearance measured over each blade around the JT8 stage 11 compressor disc, measured six times, calibrating then parking the probe before and after each measurement	105
Figure 4.16	Error in measured clearance of each blade around the JT8 stage 11 compressor disc, measured with a 1.2 mm diameter capacitance probe at a probe range of 0.25 mm	106
Figure 4.17	Clearance measured over each blade around the compressor disc, measured using an optical triangulation system and capacitive clearance measurement system following an on-line calibration	107
Figure 5.1	A schematic view of the electromechanical clearance measurement system probe and actuator mounted on a gas turbine, with the controller displaying distance from the probe's datum to the rotating blading	114

Figure 5.2	The electromechanical clearance measurement system actuator and probe cartridge. For tip-grind applications a bayonet-type probe cartridge with a soft copper tip facilitates rapid probe changes and prevents the probe electrode damaging the blading in the event that the electrode physically contacts the blade	115
Figure 5.3	A typical tip-grind machine, based on a manual grinding machine fitted with three axis read out and the electromechanical measurement system developed by Davidson <i>et al.</i> (1983)	116
Figure 5.4	The blading of a typical compressor drum and the datum discs illustrating how the radial and axial datum faces enable machining of blades with a hade angle	117
Figure 5.5	A schematic view of a bladed disc assembly fitted on a grinding machine with datum discs and an electromechanical measurement system	118
Figure 5.6	Layout of the measurement head designed for measuring radius of individual rotor and stator blades during their machining, developed by Sheard <i>et al.</i> (1992)	119
Figure 5.7	The computer numerically controlled lathe fitted with a grinding spindle, prototype measurement head, datum disc and Pratt & Whitney JT8 stage 11 bladed compressor disc	121
Figure 5.8	Offset of the JT8 stage 11 compressor blades from the longest blade, measured statically using a dial gauge and at 1800 rpm using the measurement head. Dial gauge measurements are offset to the left and measurement head measurements to the right for clarity	122
Figure 5.9	Radius of the JT8 stage 11 compressor blades prior to grinding, measured at 1800 rpm using the measurement head	123
Figure 5.10	Radius of the JT8 stage 11 compressor blades after a 0.05 mm cut, measured at 1800 rpm using the measurement head	125
Figure 5.11	Radius of the JT8 stage 11 compressor blades after a 0.10 mm cut, measured at 1800 rpm using the measurement head	126
Figure 5.12	Radius of the JT8 stage 11 compressor blades after a 0.15 mm cut, measured at 1800 rpm using the measurement head	127
Figure 5.13	Radius of the JT8 stage 11 compressor blades after a 0.20 mm cut, measured at 1800 rpm using the measurement head	128

Figure 5.14	Radius of the JT8 stage 11 compressor blades after a 0.25 mm cut, measured at 1800 rpm using the measurement head	129
Figure 5.15	Repeatability test conducted on the Pratt & Whitney JT8 stage 11 bladed disc at 1800 rpm. The capacitance probe used in the measurement head was recalibrated prior to each of the six measurements of radius	130
Figure 5.16	A close-up view of the pin-fixed blade root fixing arrangement of the Pratt & Whitney JT8 stage 7 blades	131
Figure 5.17	Radius of the JT8 stage 7 compressor blades prior the grinding, measured at 1800 rpm using the measurement head	132
Figure 5.18	Radius of the JT8 stage 7 compressor blades after the final 0.25 mm cut, measured at 1800 rpm using the measurement head	133
Figure 5.19	Radius of the JT8 stage 7 compressor blades after completing the 0.25 mm cut following Winfield's (1991) recommendation, measured at 1800 rpm using the measurement head	135
Figure 5.20	Radius of the JT8 stage 7 compressor blades after blade de-burring, measured at 1800 rpm using the measurement head	136
Figure 6.1	Clearance measured over the longest blade of a high-pressure turbine illustrating the 20% reduction in clearance achieved by applying shroud cooling air to the turbine casing	141
Figure 6.2	Turbine exit gas angle measured before applying shroud cooling air, with cooling air and after cooling air was removed, illustrating over ten degrees' change in gas angle in the blade tip region	142
Figure 6.3	A schematic view of the probe installation illustrating the factors used to calculate blade tip-to-casing clearance over the longest blade	144
Figure 6.4	A 100 mm installed length, 6 mm stroke blade-by-blade electromechanical clearance measurement system probe	145
Figure 6.5	A close-up view of a probe tip, with electrode (bottom), capacitance probe (top) and cooling holes (left and right)	146
Figure 6.6	The blade-by-blade electromechanical clearance measurement system actuator and probe	147
Figure 6.7	The blade-by-blade electromechanical clearance measurement system actuator and probe illustrating the actuator and probe cooling air inlet locations. The actuator cooling air inlet is on the top of the actuator and the probe cooling inlet is located at the bottom, immediately above the mounting flange	148

Figure 6.8	The interrelationship between ground station modules, electromechanical actuator and host computer	150
Figure 6.9	The C147 compressor at DRA Pyestock fitted with two of Davidson <i>et al.</i> 's (1983) electromechanical clearance measurement systems (A), a blade-by-blade electromechanical clearance measurement system (B), a radial traverse actuator (C) and two area traverse systems (D). Courtesy British Crown (1993)	152
Figure 6.10	The C147 fitted with two of Davidson <i>et al.</i> 's (1983) electromechanical clearance measurement systems (A) and a blade-by-blade electromechanical clearance measurement system (B). Courtesy British Crown (1993)	152
Figure 6.11	Measured distance from the blade-by-blade electromechanical clearance measurement system datum to the C147 compressor stage 5 longest blade during commissioning	154
Figure 6.12	Measured C147 compressor stage 5 clearance from Davidson <i>et al.</i> 's (1983) electromechanical clearance measurement system and results from the blade-by-blade electromechanical clearance measurement system	155
Figure 6.13	A typical capacitance probe output voltage signal after a spark-discharge to the longest blade (bottom) and tachometer signal (top)	156
Figure 6.14	Two data sets of blade tip-to-casing clearance versus blade number data acquired after 1 and 3 hours at the compressor design point	157
Figure 6.15	A clearance versus blade number data set, after subtracting the mean clearance	158
Figure 7.1	Capacitive clearance measurement system schematic block diagram	163
Figure 7.2	Capacitance probe, cable assembly and oscillator	164
Figure 7.3	Blade passing and staircase signal, blade thickness > 1 mm, clearance > 1 mm (hardcopy from a digital oscilloscope used to monitor measurement system dynamic outputs)	166
Figure 7.4	Capacitance probe calibration rig, originally developed by Chivers (1989a)	169
Figure 7.5	Capacitance probe mounted in the calibration rig. The capacitance probe is mounted on a traverse mechanism (right) with a reproduction of the gas turbine casing around the probe tip at the equivalent of 3 o'clock over the calibration disc blades	170

Figure 7.6	Typical calibration curve for a capacitive clearance measurement system probe and oscillator pair	171
Figure 7.7	A 20-channel capacitive clearance measurement system ground station	175
Figure 7.8	Blade tip-to-casing clearance data from Sheard and Turner's (1992) electromechanical clearance measurement system and a capacitive clearance measurement system	177
Figure 7.9	Typical circumferential probe positions around compressor stage 6, 8 and 10 plus high-pressure turbine stage 2	178
Figure 7.10	Capacitive clearance measurement system compressor tip-rub data acquired during the gas turbine running-in procedure	180
Figure 7.11	Capacitive clearance measurement system mean compressor blade tip-to-casing clearance data for a performance curve	181
Figure 7.12	Individual blade tip-to-casing clearance data from four circumferential positions around compressor stage 6	182
Figure 7.13	Deviation from mean blade tip-to-casing clearance for four circumferential probe positions around compressor stage 6	184
Figure 7.14	High-pressure turbine, stage 2 mean blade tip-to-casing clearance measured during a gas turbine cold stabilisation test	185
Figure 7.15	The capacitive clearance measurement system dynamic output of two circumferentially opposed capacitance probes	187
Figure 8.1	General Electric MS6001FA stage 1 turbine capacitance probe	193
Figure 8.2	General Electric MS6001FA gas turbine cross section. Photo courtesy of General Electric Company	195
Figure 8.3	Schematic of the 16 evaluation probe location around the Stage 1 turbine: view looking downstream	195
Figure 8.4	Isometric view of tip clearance probes in the turbine Stage 1 shroud	196
Figure 8.5	General Electric MS6001FA Stage 1 turbine blade tip geometry, and position of the capacitance probe used to measure blade tip-to-casing clearance relative to it	197
Figure 8.6	Calibration curves for average blade tip-to-casing clearance from Systems 1, 2 and 3	198
Figure 8.7	Histogram of measured blade fence thickness versus the nominal blade fence thickness used to specify the geometry of the capacitive clearance measurement system calibration disc	200
Figure 8.8	Configuration of the capacitance probes, electronics, signal conditioning electronics and data acquisition system	202
Figure 8.9	Blade passing outputs from Systems 1 and 2 at the full-speed no-load conditions	204

Figure 8.10	Plot of blade tip-to-casing clearance and speed versus time for Systems 1 and 2 positioned at location 1 on MS6001FA Stage 1 turbine	205
Figure 8.11	Average blade tip-to-casing clearance at location 7 on MS6001FA Stage 1 turbine during planned over-speed trip	206
Figure 8.12	Typical equivalent ‘thermal mass’ to flanges at horizontal joint (Ramachandran and Conway, 1996). Photo courtesy of General Electric Company	207
Figure 9.1	Traditional tri-axial capacitive sensor (top) originally developed by Chivers (1989a) and the new technology (NT) capacitive sensor (bottom) originally developed by Sheard and Lawrence (1998). This example of the new technology capacitive sensor was designed with side entry cable	213
Figure 9.2	Proximity measurement system component parts and cable configuration	214
Figure 9.3	Schematic diagram of the gas turbine-mounted capacitive displacement transducer (CDT) amplifier	216
Figure 9.4	Schematic diagram of the proximity measurement system 19" rack mount receiver	217
Figure 9.5	Traditional tri-axial capacitive sensor (left) originally developed by Chivers (1989a) and the new technology (NT) capacitive sensor (right) originally developed by Sheard and Lawrence (1998)	220
Figure 9.6	Finite element analysis of optimised new technology sensor tip. Predicted lines of constant voltage to target at one sensor diameter from the sensor tip	221
Figure 9.7	The new technology sensor range when coupled with authors’ developed proximity electronics and the sensor range of Grice <i>et al.</i> ’s (1990) original electronics and sensor design	222
Figure 9.8	The new technology sensor range when coupled with tip clearance electronics of Stringfellow <i>et al.</i> (1997) and the sensor range achieved by Gill <i>et al.</i> (1997) when using tip clearance electronics of Stringfellow <i>et al.</i> ’s (1997) and the original sensor design of Chivers (1989a)	223
Figure 9.9	Measured and theoretical isolation resistance for alumina-coated sensor components	227
Figure 9.10	Proximity measured system sensitivity	229

Figure A1.1	Schematic illustration of a prior art arrangement of a capacitive clearance measurement system oscillator circuit, tri-axial cable and probe arrangement	234
Figure A1.2	An enlarged cross-section through a tri-axial cable perpendicular to the longitudinal axis through a cable	238
Figure A2.1	A section through a practical embodiment of the sensor's first form according to the invention	243
Figure A2.2	Schematic representation of the sensor's second form according to the invention	247
Figure A2.3	Schematic representation of the sensor's third form according to the invention	248
Figure A2.4	Schematic representation of the modified form of the sensor in Figure A2.3	249
Figure A3.1	Schematic section through the composite sensor and tri-axial cable	256

List of Tables

Table 1.1	Gas turbine users of blade tip-to-casing clearance measurement systems	4
Table 1.2	Second generation electromechanical clearance measurement system specification	9
Table 1.3	Commissioning test vehicle conditions	13
Table 2.1	Environmental conditions within a gas turbine at the critical locations engineers fit tip clearance measurement sensors	33
Table 2.2	Combustion gas composition through a gas turbine's turbine	34
Table 3.1	Spinning rig wheel geometry	62
Table 3.2	Blade offset from the longest blade	62
Table 6.1	Blade-by-blade electromechanical clearance measurement system specification	146
Table 6.2	The C147 compressor overall design parameters	151
Table 6.3	Commissioning test vehicle conditions	151
Table 7.1	Capacitive clearance measurement system specification	168
Table 7.2	Capacitive clearance measurement system uncertainty analysis	172
Table 7.3	Comparison between gas turbine crank clearance and cold build clearance	179
Table 8.1	Vendor provided generic system requirements and system specifications	192
Table 8.2	Generic system uncertainty analysis results at 2.5 mm (0.100") clearance	199
Table 9.1	Clearance sensor comparison of capability in gas turbine applications, compiled from data contained in Burr (1994)	212
Table 9.2	Drive electronic specification	218
Table 9.3	Sensor specification	218
Table 9.4	Relative permittivity of silica and magnesia	225
Table 9.5	Cable specification	225

Foreword

Mankind continuously creates knowledge. Academics and industrialists alike undertake research which creates new knowledge that they then, classically, document in peer-reviewed academic papers. Each paper becomes part of an on-going conversation amongst an intellectual community, as that community works to expand its understanding of the world within which we live.

We are also continuously losing knowledge. Over a period of years, researchers may publish many academic papers during the course of a single research programme. If we do not make explicit the linkage between those papers, the work remains fragmented and may get buried in the ever increasing mass of new publications. Over time we may forget the original reason for the research and lose its wider contribution to knowledge.

Researchers must avoid losing what mankind has already discovered. If we are not to lose new knowledge, we must capture it in an accessible form. We must explain the rationale for undertaking the reported work and clarify the collective contribution to knowledge. We must give thought to how we will harness and apply that knowledge. Collected papers, such as the present volume, are a means of enabling this process.

This collection of papers is highly recommended reading, particularly for engineers who are concerned with controlling and measuring the turbomachinery blading tip-to-casing clearance. The need for more efficient turbomachinery drives the designer towards ever tighter tip clearances. This requires the development of highly accurate techniques to measure tip clearance.

The measurement of clearance between turbomachinery blades and the casing within which they run is an example of instrumentation that the turbomachinery community takes largely for granted today. The development of an accurate and reliable method by which we can measure this clearance represents well over a decade of effort. It is the results of that effort that serve as the basis for the academic papers in this volume. In collecting and editing these papers, Geoff Sheard has provided an important record which is an essential source of information to those who wish to develop these techniques further. The papers explain sensor and cable technology, analogue and digital electronics, as well as the more practical problems of in-service application. They show how the researchers met and overcame the challenges involved.

This story will also appeal to the wider readership of those who wish to understand the processes involved in the design and development of sophisticated instrumentation for use in hot, high-pressure, hostile environments, such as that found in modern rotating turbomachinery. All readers will be interested by following the painstaking development path described in this volume and will learn much in the process.

Martin Oldfield
Emeritus Professor of Engineering Science
University of Oxford
April 12, 2012

Acknowledgements

Many individuals have helped in writing the academic papers upon which this volume is based and it is my pleasure to acknowledge this. Foremost among these are my co-authors Michael Fitzpatrick, Scott Gill, Mike Ingallinera, Eric Johann, Bernard Killeen, Subir Mozumdar, Detlef Müller, Steve O'Donnell, John Stringfellow, Simon Turner and George Westerman.

I would also like to acknowledge the contributions of John Chivers, Vice President – Technology with Kulite Semiconductor Products, Inc. John was formally head of the Rolls-Royce (Derby) Electronics & Measurement Techniques Department. In that capacity John lead the original research effort that resulted in a first generation frequency modulated driven guard capacitive clearance measurement system. It was this first generation system that my co-authors and I progressively developed and documented that forms the basis of this volume. I am indebted to John for finding time in an already overcrowded schedule to assist with the organisation of this volume's content, and for his help during the development of the original academic papers into book chapters.

I would also like to acknowledge the contribution of Martin Oldfield, Emeritus Professor of Engineering Science, University of Oxford. Martin spent his working life developing and using experimental facilities to study the flow-field physics at play within turbomachinery blading. As a consequence of his professional focus, Martin spent much of his time developing advanced instrumentation techniques, their associated analogue and digital signal conditioning electronics. The constructive criticism that Martin offered during the development of this volume constituted a form of peer review for which I am most grateful.

I also wish to thank Thomas Sigel, first for his tremendous contribution in turning around extensive scripts into succinct and easily readable text, and second for his assistance with the process of converting the final text into this published volume.

Last, I would like to acknowledge the contribution of Kirsten Greenzweig, who converted the original academic papers upon which this volume is based into electronic files that could then be edited and typeset. Kirsten also recreated the original figures in electronic form, an undertaking that proved to be far more time consuming than either of us imagined.

Geoff Sheard
Fläkt Woods Group

About the Editor

Wearing many hats, Geoff Sheard is the Fläkt Woods Group Vice President of Fan Technology, a leading global supplier of energy-efficient solutions operating in both the air climate for buildings and air movement for the infrastructure and industry markets. He is a director of Fläkt Woods Limited, an Honorary Professor at the Aston University Department of Engineering and Applied Science, a Visiting Professor at *Sapienza* University of Rome *Dipartimento di Ingegneria Meccanica e Aerospaziale* and a Visiting Professor at the University of Northampton Business School.

Geoff is also a director of the Air Movement & Control Association (AMCA) and a member of the AMCA Executive Board. He is a member of the International Gas Turbine Institute (IGTI) Board of Directors and leads the IGTI Fans & Blowers initiative. He is also a member of the Institution of Mechanical Engineers (IMechE) Fluid Machinery Group and Chairman of the organising committee for Fan 2012, an international conference on fan noise, technology and numerical methods.

Geoff has doctorate degrees from the University of Oxford in turbomachinery aerodynamics and from the University of Northampton in leadership and team development. He also holds a masters degree in business administration from Cranfield University and a bachelor's degree in mechanical engineering from Liverpool University.

A chartered engineer, a Liveryman of the Worshipful Company of Engineers, a fellow of the Institution of Mechanical Engineers, a fellow of the Royal Aeronautical Society, a fellow of the American Society of Mechanical Engineers, and a fellow of the Chartered Institute of Building Service Engineers, Geoff has published widely in both technical and management areas. He has published three books, two monographs, over 100 articles, and is a member of the *Journal of Management Development* editorial advisory board and the *Leadership and Organisational Development Journal* editorial review board.

Introduction: Tip Clearance Measurement

Geoff Sheard

‘Those ignorant of history are destined to repeat it’, says the philosopher, warning us to learn from the past in order to avoid making the same mistakes again. But perhaps we should also read history for the inspiration it offers, through understanding the plans and triumphs of people who passed this way before¹.

This volume of collected papers documents research undertaken in response to a need: to make a reliable measurement of blade tip-to-casing clearance in aero and industrial turbomachinery. The volume arises from discussions around nine papers and three patents that collectively comprise the chapters and appendices. Each marks a milestone in the development of technology that underpins the capacitive measurement of blade tip-to-casing clearance.

The chapters relate to one of three separate, but complementary developmental phases, each of which is associated with an aspect of a development effort that commenced in the mid 1980s and ended in the late 1990s:

1. development and demonstration of components;
2. validation of those components; and
3. in-service verification of the components when combined into a clearance measurement system.

During the 1970s, the majority of researchers favoured an optical blade tip-to-casing clearance measurement system concept. However, optical clearance measurement systems did not transition well from the research to development environment. Consequently, interest grew in the development of electromechanical and capacitive clearance measurement systems. Although those involved at the time did not realise it, the developed electromechanical clearance measurement systems would go on to facilitate demonstration of the developed capacitive clearance measurement system accuracy.

In a laboratory environment, the developed capacitive clearance measurement system showed an accuracy of ± 0.01 mm, significantly better than anticipated, and equivalent to that which researchers achieved with larger and more complex optical

¹ An observation made by Professor Richard Darton FREng, Head of Department, Department of Engineering Science, University of Oxford in his forward to Alister Howatson’s ‘Machanicks in the Universitie’ published by the University of Oxford in 2008.

clearance measurement systems. As a consequence, those involved moved on from development and demonstration to validation. The objective was to continue the development effort in less demanding environments, before tackling the challenge of achieving the laboratory accuracy in a gas turbine compressor or turbine installation.

The developed capacitive clearance measurement system was then the subject of verification, with researchers applying it first on an aero and then an industrial gas turbine. The experience gained through in-service application facilitated a final optimisation of sensor geometry and signal conditioning electronics that effectively completed measurement system development.

Chapters 1, 2 & 3: Demonstration

During the 1970s, optical clearance measurement systems were the subject of intense research efforts. Despite their elegance and early promise, by the mid 1980s, gas turbine development engineers established direct-current capacitive clearance measurement systems as a low cost and reliable means of measuring blade tip-to-casing clearance in the relatively low temperature compressor environment.

Although early direct-current capacitive clearance measurement systems worked well enough in compressor environments, they did not perform in turbine environments. Development engineers favoured electromechanical clearance measurement systems in the more demanding turbine environment. Electromechanical clearance measurement systems were relatively bulky, making their application on multiple compressor stages challenging. Having to use different measurement systems on the compressor and turbine was far from ideal. The gas turbine community needed a clearance measurement system that they could apply in both compressor and turbine environments.

The reported research in Chapters 1, 2 and 3 clarifies the process that those involved at the time worked through to demonstrate the accuracy of a capacitive clearance measurement system based on a frequency modulated driven guard system concept. It was this system concept that enabled the clearance measurement system to make reliable measurements of blade tip-to-casing clearance in both compressor and turbine environments.

Chapter 1 presents a programme of work that developed a compact electromechanical clearance measurement system. At the time, the perceived need driving the development effort was to enable the reduction of the clearance measurement system size such that engineers could fit it to successive stages of a development gas turbine compressor. In order to reduce the system size, the authors had to miniaturise all components. It was this miniaturisation that went on to facilitate the use of the electromechanical clearance measurement system in the development of a capacitive clearance measurement system.

Chapter 2 reports the original research programme that established the optimal method for measuring blade tip-to-casing clearance in both gas turbine compressor and turbine environments. The chapter presents the evaluation of alternative measurement system concepts and explains the rationale for choosing a capacitive clear-

ance measurement system in combination with a driven guard electrode system. The research included an installation in both a gas turbine compressor and turbine environment, and in so doing, demonstrated the measurement system's potential.

Chapter 3 builds on Chapters 1 and 2, reporting a complementary laboratory research programme which established the accuracy with which the capacitive clearance measurement system presented in Chapter 2 could measure blade tip-to-casing clearance. The authors established accuracy using the electromechanical clearance measurement system presented in Chapter 1. In the laboratory environment the capacitive clearance measurement system was able to measure blade tip-to-casing clearance to an accuracy of ± 0.01 mm. The accuracy with which the authors could measure clearance was equivalent to that which other researchers could achieve with larger and more complex optical systems.

Chapters 4, 5 & 6: Validation

Accuracy of the developed capacitive clearance measurement system was high enough to encourage those involved to conduct further research. At the time there was much discussion as to exactly what form that further research should take. Finally, a consensus emerged: blade-by-blade tip-to-casing clearance measurement. Optical clearance measurement systems classically measured the clearance over individual blades. Although those measurements were typically combined into an average clearance over all blades, the individual measurements of clearances over every blade were, at least, in theory available. If the developed capacitive clearance measurement system was to be a viable alternative to optical measurement systems, then researchers reasoned that it must be capable of making the same blade-by-blade measurement of clearance.

Making a blade-by-blade tip-to-casing clearance measurement is an order of magnitude more difficult than measuring an average clearance over all blades. As such, those involved decided to avoid rushing into a development gas turbine environment. The more prudent course of action was to remain in the laboratory, moving towards gas turbine applications in small steps.

Chapter 4 builds on the work presented in Chapter 2 with the development of an on-line calibration technique for the developed capacitive clearance measurement system. The ability to calibrate the system immediately prior to a measurement of clearance would eliminate a significant proportion of the error sources that would otherwise degrade system accuracy in gas turbine applications.

Chapter 5 applies the developed capacitive clearance measurement system in the only application within which an optical measurement of blade-by-blade clearance had become routine — compressor manufacture. Gas turbine compressors classically comprise a drum into which successive stages of blades fit. The compressor design incorporated loose blades that only lock into their working position under the influence of centrifugal force when the compressor is rotating. It is impossible to achieve the target tolerance for compressor diameter over each stage by cutting individual blades to the required length and then fitting them into the compressor drum.

It is necessary to grind them to length *in situ* whilst the compressor is rotating. By fitting the developed capacitive clearance measurement system to a ‘tip grinding’ machine, the authors were able to develop the measurement system and its associated blade-by-blade data acquisition system. Making parallel blade-by-blade measurements using the tip-grinding machines optical clearance measurement system facilitated this development.

Chapter 6 takes the developed system for tip-grinding application, and repackages it into a form suitable for gas turbine application. Despite their success in a manufacturing environment, the authors remained cautious, not wanting to rush into a high-profile gas turbine development programme. Instead, they revalidated the repackaged system in a compressor test rig that they also fitted with an electro-mechanical clearance measurement system. In this way, they could validate the accuracy of the developed capacitive clearance measurement system when making a blade-by-blade measurement of tip-to-casing clearance against the measurement of minimum clearance using an electromechanical clearance measurement system.

Chapters 7, 8 & 9: Verification

Researchers concluded that the validation of the developed capacitive clearance measurement system was a success, with the next step to demonstrate that they could reproduce the performance that they achieved in laboratory, manufacturing and compressor rig environments in both aero and industrial gas turbine applications. The verification of system accuracy in gas turbine applications is made more challenging not only by the constraints on available space, vibration and temperature that occur with the application, but also the sensitivity of the recorded data. In effect, commercial considerations restrict what one can publish.

Despite the sensitivity associated with publication of the measured data, BMW Rolls-Royce GmbH granted permission to publish measurements on the first BR710 development gas turbine. Additionally, General Electric granted permission to publish measurements on a GE MS6001FA industrial gas turbine. Although there were significant constraints imposed upon what they could report, these two programmes of work effectively verified the ability of the developed capacitive clearance measurement system to operate successfully in the most demanding gas turbine compressor and turbine applications.

Chapter 7, in effect, repeated the researchers’ compressor and turbine measurements during initial demonstration of the developed capacitive clearance measurement system reported in Chapter 2. The difference between the two experimental campaigns is two-fold. First, the developed capacitive clearance measurement system that the authors tested was significantly improved when compared to that which they originally demonstrated. Second, they fitted many more clearance sensors which provided more extensive data with significantly greater accuracy. Much of the data remains necessarily confidential; however, enough was published to illustrate that the developed capacitive clearance measurement system was robust, reliable and able to provide data with accuracy comparable to that which researchers achieved in the laboratory environment. As observed by Peter Loftus² in January 2012, since its

original development the capacitive clearance measurement system has become a standard part of rig and development engine testing across the Rolls-Royce portfolio of products.

Chapter 8 differs from the work reported in Chapter 7 as the reported research focuses on an evaluation of alternative embodiments of the capacitive clearance measurement system. The evaluation aimed to establish which of the available alternatives would form the basis of a clearance control system under development for General Electric Power Generation's next generation 'H System' industrial gas turbine. The purpose of the clearance control system is to control the clearance between casing and the turbine blades to minimise tip clearance. In so doing, it maximises efficiency during loaded operation, whilst preventing rubs during start-up and shut-down. The evaluation was a success, identifying the developed version of the capacitive clearance measurement system that the authors used in Chapter 7 as the preferred embodiment of the clearance measurement system.

Chapter 9 closes out the technology development with a presentation of work that the authors undertook to optimise sensor geometry to maximise probe range. The work on sensor geometry was complemented with a final industrialisation of the electronic systems which the authors used to drive the sensors. Specifically, the authors finalised a complementary direct-current capacitive system that enabled them to double check the cold-build clearance between sensor and blades after compressor or turbine build, but before first-fire. This eliminated one of the most persistent error sources that occurred with the application of the developed frequency modulated capacitive clearance measurement system.

Low carbon energy

As observed by Philip Andrew³ in January 2012, since its initial evaluation, the capacitive clearance system has evaluated positively on multiple engine platforms, and is under consideration for application in future General Electric product derivatives. During General Electric's initial evaluation, Chapter 8, the authors observed that the purpose of the evaluation was to identify a tip clearance measurement system that could provide a measurement of clearance for a future closed-loop clearance control system.

General Electric implemented a closed-loop clearance control system on the gas turbine of the 50 Hertz 'H System' 480 MW combined-cycle power plant located at Baglan Bay on the south coast of Wales⁴. The developed clearance control system circulates air as a heat transfer medium at a controlled temperature through passages

² Loftus, P. (2012), Private communication with Mr. P. Loftus, Rolls-Royce plc, Head of Measurement Engineering, 3 January, 2012.

³ Andrew, P.L. (2012), Private communication with Dr. P.L. Andrews, GE Energy, Manager Thermal Systems Conceptual Design, 3 January, 2012.

⁴ Pritchard, J.E. (2003), 'H System Technology Update'. *Proceedings of the 48th American Society of Mechanical Engineers Gas Turbine and Aeroengine Congress*. Atlanta, USA, 16–19 June, Paper No. GT2003-38711.

in the turbine inner shell. By varying the circulating air temperature, operators can minimise the clearance over turbine blades during full load operation which maximises turbine efficiency.

Following the Tōhoku earthquake and tsunami on 11 March 2011, the Fukushima Daiichi nuclear disaster unfolded, comprising a series of equipment failures, nuclear meltdowns and releases of radioactive materials at the Fukushima I Nuclear Power Plant. It is the largest nuclear disaster since the 1986 Chernobyl disaster. Following the disaster, there is little enthusiasm globally for nuclear energy, although interest in low carbon energy remains.

The current move towards low carbon renewable energy is also a move towards a more unpredictable electricity supply. As renewable energy continues to make up an increasing proportion of electricity input to the grid, there will be an increasing need for a flexible and efficient method of managing variations in grid demand. Following the Fukushima Daiichi nuclear disaster, industrial gas turbines have emerged as a favoured technology that is capable of responding quickly and flexibly to variations in grid demand.

At the 2011 Turbo Expo, held from 6–10 June 2011, in Vancouver, Canada, General Electric announced that a clearance control system would form part of its next-generation FlexEfficiency 50 combined-cycle power plant. On 8 December 2011, Electricite de France (EDF), one of the world's largest utilities, and General Electric (GE) announced plans to jointly develop and showcase the first FlexEfficiency 50 plant which will connect to a national grid.

The FlexEfficiency 50 plant, which EDF and GE are co-developing, will showcase a combination of flexibility and efficiency with low emissions. The new combined-cycle plant will be located at Bouchain, an existing EDF power plant site in northern France, and will produce 510 megawatts. The FlexEfficiency 50 plant is the result of General Electric's \$500 million investment in research and development to deliver cleaner and more efficient energy.

Experts expect the plant to achieve greater than 61% efficiency at base load. Its operating flexibility will enable the plant to respond quickly to fluctuations in grid demand, paving the way for greater use of renewable resources such as wind and solar. EDF's decision to install the FlexEfficiency 50 plant will be an important example of how flexibility and efficiency can combine to enable greater use of renewable power globally.

The inclusion of a closed-loop clearance control system is not the only necessary technology for a flexible and efficient combined cycle power generation system. Development of a capacitive clearance measurement system that can provide the closed-loop input to a clearance control system does not alone constitute the development of a clearance control system. However, it does constitute a necessary prerequisite and perhaps also the most critical single component.

Summary of Chapters

Geoff Sheard

This chapter-by-chapter summary of technical contribution provides the reader with a detailed description of the work in each chapter. In so doing, it clarifies each chapter's content and summarises its contribution to knowledge. This summary augments the description of the work itself with discussion as to why the authors undertook the work. It also lays out the rationale for undertaking the research, and the logic underpinning the move from one reported research programme to the next. Therefore, this summary links each chapter and makes explicit its collective contribution to knowledge.

The paper comprising each chapter constitutes a complete collection of the published scholarly work relating to the developed capacitance clearance measurement system. The Editor selected them for inclusion based on the degree to which the content contributed towards the creation of a coherent body of knowledge.

Chapter 1 An Electromechanical Measurement of Turbomachinery Blade Tip-to-casing Running Clearance

The paper that forms the basis of this chapter reports the development of an electromechanical clearance measurement system. Although the authors did not know it at the time that they were developing the measurement system, it would become both the most successful electromechanical clearance measurement system, and also the last. The measurement system was successful as a consequence of its robust and reliable design, giving clearance data in even the most demanding high-pressure turbine applications. Second, the design was compact enough that one could fit the system to every stage of a gas turbine compressor.

The electromechanical clearance measurement system reported effectively moved blade-tip clearance measurements out of the research laboratory. Previous embodiments of the electromechanical clearance measurement concept had proven unreliable in practical installation. Through a combination of system design and increasing experience guiding practical application, the measurement of both compressor and turbine blade tip-to-casing clearance became a routine measurement on which gas turbine development engineers could rely.

The reported electromechanical clearance measurement system became a standard component within the suite of measurement systems that engineers used during gas turbine development programmes from the late 1980s and remained so for the next 10 years. The availability of accurate blade tip-to-casing clearance measurements

over blades within every stage of a gas turbine compressor and turbine contributed to the success of those development programmes, providing insight into the movement of gas turbine blades relative to the casings within which they ran.

Despite the success of the electromechanical clearance measurement system, it did have a limitation. The measurement system was only able to measure the clearance to the longest blade. As all blades are essentially the same length, initially this limitation was not a major handicap. More important was that blade tip-to-casing rubs occur as a consequence of the longest blade making contact with the casing at some points during the gas turbine cycle. Nevertheless, the electromechanical clearance measurement system's slow frequency response made the system not only incapable of identifying the extent of clearance change due to rotor and casing natural frequencies, but susceptible to damage as a consequence of them.

Although gas turbine development engineers became skilled at using the electromechanical measurement system during gas turbine transients, system response was not fast enough to allow the authors to derive an accurate estimate of casing thermal time constants from the measured clearance data. Difficulty in making an accurate measurement of casing thermal time constant was exacerbated when the authors attempted to resolve the contribution to change in clearance that occurred with disc thermal growth, and the effects of centrifugal force on clearance that occurred with changing gas turbine speed.

Although reliable and effective, the electromechanical measurement system's limitations, combined with the need for a 'line of sight' from actuator to target, ultimately limited its capability. The capacitive measurement of clearance overcame the electromechanical measurement system's inherent limitations. Although subject to other limitations, capacitive clearance measurement systems became the focus for further development.

Chapter 2 A Technique for the Measurement of Blade-tip Clearance in a Gas Turbine

During the 1970s, many researchers experimented with capacitive clearance measurement. Some developed direct-current systems that found wide-spread application in the relatively low-temperature environment associated with gas turbine compressors. Despite the promise that these direct-current systems showed, none effectively addressed the challenge of making a reliable measurement of blade tip-to-casing clearance in a high-pressure turbine environment. For a capacitive clearance measurement system to offer a real alternative to an electromechanical clearance measurement system, it had to offer, at least, the potential of routine and reliable clearance measurement in the high-temperature turbine environment.

The paper that forms the basis of this chapter presents the initial design, development and validation of a frequency modulated driven guard capacitive clearance measurement system. A critical aspect of the research was the identification of the frequency modulated system concept in combination with a driven guard electrode screen. This concept utilised changing blade tip-to-sensor capacitance to modulate

the frequency of an oscillator. The addition of the driven guard electrode screen ensured that the effects of temperature changes on the measurement of clearance were effectively removed and enabled the author to apply the technique in both gas turbine compressor and turbine environments.

Previous direct-current clearance measurement systems polarised the sensor electrode, and assumed that the target blades were at earth potential. They were then able to deduce the blade tip-to-sensor capacitive couple that was related to blade tip-to-casing clearance via a calibration. This system concept did not work in a turbine environment because combustion products were electrically charged. This electrical charge manifested itself in the direct-current clearance measurement system output as electrical noise. This noise reduced the system signal-to-noise ratio so far that it was for all practical purposes impossible to measure blade tip-to-casing clearance.

This chapter presents the identification and evaluation of different measurement system concepts and discusses the rationale for adopting a frequency modulated driven guard concept. In summary, a frequency modulated driven guard capacitive clearance measurement system offered the potential to be both compact enough to fit onto multiple compressor stages, insensitive to the effect of electrically charged combustion products in a turbine environment and insensitive to changes in sensor temperature.

The data that the author collected during measurement system testing on both a gas turbine low- and high-pressure compressor and a high-pressure turbine was of particular importance to Rolls-Royce plc. The data reported in this chapter was the first occasion on which experimental transient blade tip-to-casing clearance information had been made available. The quantity and quality of blade tip-to-casing clearance data that the author obtained during both compressor and turbine testing demonstrated a significant advance both in experimental measurement techniques and the understanding of the gas turbine mechanical structures' transient behaviour.

Chapter 3 Blade-by-blade Tip Clearance Measurement

It was the capacitive clearance measurement system's success in its first Rolls-Royce plc gas turbine compressor and turbine tests that provided the impetus for further measurement system development. By providing blade tip-to-casing clearance measurements in a compressor and turbine, the capacitive clearance measurement system had demonstrated beyond all reasonable doubt that the frequency modulated driven guard system concept was suitable for low-pressure compressor, high-pressure compressor and turbine application.

Despite the undoubted success of the capacitive clearance measurement system evaluation, as with any development effort, unforeseen problems did arise. In addition to the capacitive clearance measurement system under evaluation, the authors also fitted an electromechanical clearance measurement system. The intent was to compare average blade tip-to-casing clearance over all measured blades using the capacitive clearance measurement system with the measurement of minimum blade tip-to-casing clearance over the longest blade using the electromechanical clearance measurement system.

At the time of the evaluation, the electromechanical clearance measurement system was relatively rudimentary, and proved unreliable. The authors suspected that the gas turbine rotor was not well grounded electrically, and therefore the electro-mechanical clearance measurement system was unable to make any useful clearance measurement in either the compressor or turbine environments. Consequently, the capacitive clearance measurement system evaluation left some doubt as to the ultimate accuracy of the clearance measurements that the author obtained.

The evaluation of measurement system accuracy does not require a gas turbine. In many ways a laboratory environment is preferable, as this eliminates many of the error sources that occur with a gas turbine installation. As such, the authors initiated the programme of work that this chapter reports to identify the capacitive clearance measurement system's ultimate accuracy.

The approach that the authors adopted was to combine the developed electro-mechanical clearance measurement system with the capacitive clearance measurement system. In this way, they could move the capacitive sensor relative to the blades over which they mounted it, and positioned it a known distance from the longest blade as the electromechanical clearance measurement system registered that blade's presence. Further, the authors were able to crop each blade by known amounts relative to the longest blade. As such, once they knew the capacitive sensor's location relative to the longest blade, they could calculate its location relative to every other blade. Although in theory it would have been possible to attempt the above in a gas turbine installation, practical consideration would have made it impossible in practice.

The combination of an electromechanical clearance measurement system and cropped blades enabled the authors to know the clearance between capacitive sensor and every blade independently of any measurement that they made using the capacitive clearance measurement system. By then calibrating the capacitive clearance measurement system and measuring the blade tip-to-casing clearance over each blade, the authors established clearance. Subtracting the former measurement from the latter enabled the accuracy with which the authors established blade tip-to-casing clearance.

To the authors' astonishment, the capacitive clearance measurement system measured blade tip-to-casing clearance to an accuracy of ± 0.01 mm over a 1.00 mm range. This was comparable to the accuracy that other researchers achieved at the time with significantly larger and more complex optical clearance measurement systems. The established accuracy inspired the authors to redouble their efforts to further develop the capacitive clearance measurement system.

Chapter 4 An On-line Calibration Technique for Improved Blade-by-blade Tip Clearance Measurement

An aspect of the evaluation of accuracy that Chapter 3 reported was the successful measurement of blade tip-to-casing clearance over every blade. At the time the authors were not focused on the possibility of making a measurement of

blade-by-blade clearance in a gas turbine environment. The focus was purely academic: how accurately does this capacitive measurement system measure blade tip-to-casing clearance? For this, the authors considered a measurement of clearance over every blade helpful.

The capacitive clearance measurement system is an analogue electrical system. As the capacitive link between sensor and blade changes, so does the system natural frequency and in turn, system output voltage. Consequently, as a blade passes the sensor, the output voltage first rises as it approaches, and then falls as it departs. Each pulse's peak height is proportional to the gap size between sensor and blade when the blade is immediately opposite the sensor. Measurement system output is thus a pulse train, with each pulse's heights proportional to the gap size between sensor and blade tip.

We can derive a measurement of average blade tip-to-casing clearance over all blades simply by feeding the capacitive clearance measurement system output pulse train into a root-mean-square volt metre. The volt metre integrates the pulse train into an average voltage that one can then log using a data acquisition system. The above approach to average clearance measurement is attractive as it is simple, and results in an output that a traditional gas turbine test bed data questions system can easily log.

Measuring clearance over every blade requires a height measurement of each pulse in the output pulse train. To do this, the authors developed a peak detect, hold and reset circuit. This registered the voltage peaks' height and fed them to an analogue to digital converter. A dedicated microprocessor receives both the analogue to digital converter output, and a tachometer signal. Using the tachometer signal, the microprocessor splits the output from the analogue to digital converter into revolution-by-revolution data sets of pulse height over each blade.

The above digital electronic signal processing presented a significant challenge using late 1980's computer technology, and the authors did not attempt it during the initial measurement system development or gas turbine evaluation. They addressed and solved the challenge in the laboratory. After much debate and deliberation, the authors recognised that although their previous laboratory evaluation had been effective in establishing measurement system accuracy, it had also relied on using the electromechanical clearance measurement system in combination with the capacitive clearance measurement system. To move towards a gas turbine compressor or turbine measurement of blade-by-blade tip-to-casing clearance using the capacitive clearance measurement system, the authors reasoned that they needed to eliminate the electromechanical clearance measurement system.

The authors continued the evaluation presented in Chapter 3, this time focusing on the development of a calibration technique that did not require the involvement of the electromechanical clearance measurement system. They moved the capacitive sensor relative to blades of known length, and they established its distance from the longest blade using the electromechanical clearance measurement system. In this way the authors created a reference data set of clearance over each blade. They then focused on the capacitive clearance measurement system output at different locations as the capacitive sensor retracted by known amounts. In so doing, the authors

were able to develop an on-line calibration technique that enabled them to calibrate the capacitive clearance measurement system without knowing the location of the capacitive sensor relative to the longest blade. This eliminated the need for the electromechanical measurement of clearance to the longest blade.

Chapter 5 A High-speed Capacitance-based System for Gauging Turbomachinery Blading Radius during the Tip Grind Process

A desire to develop overall measurement system capability, as opposed to just the analogue electronics and sensor technology associated with the capacitive clearance measurement system, inspired the research in Chapter 5. The focus was on digital electronics, signal processing and computer-based post-processing of data.

The process of developing an on-line calibration technique for improved blade-by-blade tip clearance measurement was also a process of developing the overall measurement system from a set of prototype components into something more robust, that at least in theory, the authors could apply into the more demanding gas turbine compressor or turbine environment.

Despite a more robust measurement system, the authors remained cautious. Rushing into a gas turbine compressor or turbine environment was not attractive. It takes time for any developmental system to mature, and in order for that time to be available, the authors had to apply the system into a failure tolerant environment. Highly capable Chief Engineers classically lead gas turbine development projects. These Chief Engineers are many things, but failure tolerant is not one of them. The prudent course of action was to seek out a less demanding environment than that which a development gas turbine provided.

Compressors classically comprise a drum into which successive blade stages fit. These blades are necessarily a loose fit in the drum, only achieving their operating position under centrifugal load when the compressor is rotating. The tolerance imposed on bladed compressor diameter is typically a few hundredths of a millimetre. It is impossible to achieve such tight build tolerance by cutting individual blades to length and fitting them into the compressor drum. It is necessary to grind the compressor blades to length whilst the compressor is spinning using a 'tip grinding' machine.

During the 1970s, researchers had applied electromechanical clearance measurement systems into the compressor manufacturing environment. An electromechanical clearance measurement system would make a measurement of distance to a reference disc of known diameter, and then to the blades of unknown diameter. The difference between the two was the difference between the compressor stage and reference disc diameter. By the late 1980s, optical clearance measurement systems that could make compressor diameter measurement over every blade largely replaced these early electromechanical clearance measurement systems. A measurement of diameter over every blade was necessary for quality assurance purposes, to verify that every blade in a stage achieved overall stage diameter tolerance.

The authors' involvement with tip grinding machine manufacturers supplying electromechanical clearance measurement systems provided an opportunity for the Editor to re-establish contact. Although a more capable blade-by-blade optical clearance measurement system replaced the electromechanical clearance measurement system, the tip grinding machine manufacturers were receptive to the Editor's approach. The optical clearance measurement system was an order of magnitude more expensive than the electromechanical system that it replaced, and as it used a laser, it necessitated a variety of expensive modifications to the tip grinding machine itself to ensure the safety of operators. As such, there was enthusiasm for a collaborative research project to develop a capacitive clearance measurement system that could make a blade-by-blade measurement of compressor diameter in a manufacturing environment.

The research reported in this chapter presents a summary of the developed tip grinding machine measurement system results. It demonstrates the process by which the operator successively grinds a compressor stage to the correct diameter. The chapter shows that the system's repeatability, when using the previously developed on-line calibration technique, is self-consistent with the measurement system accuracy that the authors achieved in the laboratory.

What the chapter does not convey is that the reported results were the result of a 2-year collaborative development programme. During that time, the authors developed the prototype blade-by-blade measurement system from a laboratory prototype that only the authors could operate into a reliable measurement system that tip grinding machine operators could use unsupervised. This they did on many occasions to maintain production when the temperamental and unreliable optical clearance measurement system suffered a technical failure.

Chapter 6 A Blade-by-blade Tip Clearance Measurement System for Gas Turbine Applications

Although compressor manufacturing is not as 'glamorous' as gas turbine development testing, it is a failure tolerant environment. At least, initially the measurement of blade-by-blade diameter over each compressor's stage was highly unreliable, and failure was more common than success. Failure occurred as a consequence of the digital signal processing and computer-based post-processing of measured data. The dedicated micro-processor that converted analogue to digital converter output into data sets that could pass to a computer for post-processing proved a particular challenge.

An additional unforeseen challenge in the compressor manufacturing environment was the variety of compressors that could be subject to tip grinding in a single day. Each had a different number of stages, different number of blades per stage, different diameter per stage and diameter tolerance per stage. The authors needed to expand the computer-based software to include a library of possible compressors that might face the measurement system.

Despite the manifest limitations of the original laboratory prototype, it proved popular with the tip grinding machine operators. The development testing mostly

took place at the Rolls-Royce plc East Kilbride gas turbine overhaul facility in Scotland. This popularity was despite the authors' inability to understand the operator's Scottish accent, and indeed the operator's inability to understand a word that the authors said. In spite of the communication difficulties, all involved maintained a positive attitude, and retained a sense of humour as the capacitive clearance measurement system accidentally crashed into yet another compressor stage.

It is helpful to put the above into context, as at the time that the authors were developing this, a set of prototype blades for a development gas turbine cost Rolls-Royce plc an estimated £500,000 per set. In contrast, recycled compressor blades subject to tip grinding were for all practical purposes free of charge. This goes some way to explaining the operator's good natured tolerance of the authors' apparently never-ending efforts to perfect the measurement system's performance.

After a 2-year development period in a compressor manufacturing environment, the compressor diameter's blade-by-blade measurement had become a relatively routine measurement. At least, the authors had eliminated catastrophic errors that scrapped an entire stage of compressor blades. Consequently, they turned their attention back to gas turbine testing.

The trials and tribulations of their experience in the compressor manufacturing environment resulted in the authors remaining cautious. It was still too early to rush into a gas turbine development test. They needed a lower risk option. In this regard the authors were fortunate. The gas turbine research group at DRA Pystock was sympathetic, and offered the Editor the opportunity to fit a prototype blade-by-blade tip-to-casing measurement system on a C147 compressor. Researchers at DRA Pystock were to extensively instrument a C147 compressor in a drive to provide a complete data set to facilitate computational code validation.

The researchers at DRA Pystock already planned to instrument the C147 compressor test rig with the authors' electromechanical clearance measurement system. Consequently, the authors set about developing an embodiment of the capacitive clearance measurement system that they used in the compressor manufacturing environment that they could directly interchange with an electromechanical clearance measurement system actuator.

Although a compressor test rig represents perhaps the least difficult of gas turbine environments, it is significantly more challenging than a compressor manufacturing environment. The measurement system requires cooling, is subjected to significant vibration in operation and must fit into space crowded with other instrumentation and rig services. Despite the practical problems that occur with installation and operation, the C147 compressor test proved a success.

Blade-by-blade measurements of tip-to-casing clearance were in excellent agreement with the electromechanical clearance measurement system measurement of clearance to the longest blade. The blade-by-blade measurements revealed a ± 0.5 mm sinusoidal variation in tip clearance around the rotor that was self-consistent with clearance in the compressor rig bearings. The compressor blades also resealed in the compressor drum differently each time the researchers at DRA Pystock ran the compressor resulting in a ± 0.01 mm random variation in blade length from one compressor test to the next.

Chapter 7 Capacitive Measurement of Compressor and Turbine Blade Tip-to-casing Running Clearance

An on-going programme of laboratory development complemented the time that the authors spent in the compressor manufacturing and compressor rig test environment. The development effort focused on mineral-insulated cable that the authors used in the capacitive sensor and the sensor itself. At the time of investigation, much of the information was commercially sensitive and therefore the authors could not report it in an academic paper. However, they did patent the intellectual property.

Mineral-insulated cable is a technology in its own right. A rod, insulator and tube are classically mechanically drawn down from a starting diameter to the required diameter. The result is a metal and mineral cable that can withstand high-temperature application. As the authors applied capacitive clearance measurement system sensors into high-temperature environments, a mineral-insulated cable is a mandatory part of the sensor. Appendix 1 presents the development of a new mineral-insulated cable with very low guard conductivity. The developed mineral-insulated cable facilitated the use of longer sensor cable lengths. The authors needed longer sensor cables as development aero gas turbines require longer sensor cable lengths than sensors for application in a laboratory, compressor manufacturing or compressor test rig environments.

In addition, Appendix 1 also presents a developed form of the capacitive clearance measurement system oscillator. The original oscillator required a dedicated multi-core cable to connect it to its respective demodulator. This was acceptable in a laboratory, compressor manufacturing or compressor test rig environment, but presented a practical impediment in a gas turbine development test rig. The developed form of the oscillator routed power to, and signals from the oscillator using a standard 50 ohm co-axial cable, and in so doing, facilitated application of the capacitive clearance measurement system in a development gas turbine test bed using standard test bed wiring.

The research that the authors undertook to generate the intellectual property covered by the patent that forms the basis of Appendix 1 was never published in an academic paper, but was fundamental to the authors' ability to apply the capacitive clearance measurement system into a development gas turbine environment.

A parallel laboratory development effort focusing on the sensor itself was the subject of a second patent that forms the basis of Appendix 2. The original sensor contained ceramic components that mechanically separated the metal components and, in so doing, provided electrical isolation between them. These ceramic components were fragile, leading to handling problems and consequently a significant proportion of sensors breaking during installation. The 'new technology' sensors were inherently rugged and robust enough to withstand handling and installation.

The developments described above and presented in detail in Appendices 1 and 2 constituted enabling technology that combined with the measurement system that the authors progressively developed in the laboratory, compressor manufacturing

and compressor rig environments. The combination resulted in a capacitive clearance measurement system in which BMW Rolls-Royce GmbH had sufficient confidence to apply on the first BR710 development gas turbine. It is this developed measurement system that forms the basis of this chapter.

In hindsight it is remarkable that BMW Rolls-Royce GmbH allowed publication of any data from their first development gas turbine test. Despite the limitations imposed on what the authors could publish, data from compressor tip rubs, circumferential deviations of clearance and the thermal time constant of the stage 2 high-pressure turbine were published. In so doing, this clearly demonstrated the capacitive clearance measurement system capability.

Although not presented in detail, the paper that forms the basis of this chapter did showcase data from first application of a significant development in the measurement system's digital signal processing capability. The authors had previously used a personal computer to take blade-by-blade data sets of the measurement system output voltage to apply the appropriate calibration. In so doing, they converted blade-by-blade output voltage into a blade-by-blade clearance off line. The authors developed a 'staircase module' and 'lineariser module'. The staircase module held the peak voltage from the measurement system pulse train, and then updated that voltage as the next peak voltage became available. The lineariser module applied the measurement system calibration to the 'staircase signal' such that the system output was now a measurement of blade-by-blade tip-to-casing clearance in engineering units, which updated each time a blade passed a sensor.

The above signal conditioning was significant as in combination with a tachometer signal and a high-speed data acquisition system, development engineers could log a blade-by-blade measurement of tip-to-casing clearance and view that data in real time during a gas turbine test. Not reported in the paper that formed the basis of this chapter is a 'max/min' output capability included in the staircase module. By feeding a tachometer signal to the staircase module, the maximum blade tip-to-casing and the minimum blade tip-to-casing clearance could be output as a linearised clearance measurement, and updated revolution by revolution. The authors could display the resultant output in real time during a gas turbine test, clearly showing the bearing clearance during stable operation and then the extent of clearance transients that occurred as a consequence of casing and rotor vibration modes.

By making measurements at multiple circumferential locations around each stage, and on multiple compressor and turbine stages, the authors were able to deduce casing and rotor vibration modes in real time during the development gas turbine test. Although of the highest interest to both the authors and development engineers, the above data was too sensitive to publish. The disappointment that the authors felt at not being able to showcase the full capability of the capacitive clearance measurement system was partially mitigated when the paper that forms the basis of this chapter went on to win its respective conference best paper prize.

Chapter 8 Turbine Tip Clearance Measurement System Evaluation on an Industrial Gas Turbine

The success of the developed capacitive clearance measurement system when fitted to the first BR710 development gas turbine represented a ‘coming of age’ for the capacitive clearance measurement system. It was now possible to make the blade tip-to-casing measurements that development engineers had always wanted.

Success on the BR710 did not go unnoticed in the wider gas turbine community. Engineers at General Electric were evaluating a wide range of options for a technology upgrade for a forthcoming ‘H System’ industrial gas turbine. Industrial gas turbines have historically been the most challenging type of turbomachinery to instrument as a consequence of the very high turbine entry temperatures and the gas turbine’s size. As such, development engineers at General Electric were cautious. They did not accept the capacitive clearance measurement system’s claimed performance at face value. It would have to prove that it could repeat its success when fitted to an aero gas turbine on an industrial gas turbine.

The Editor agreed to an evaluation programme with General Electric. They would evaluate three blade tip-to-casing measurement systems on a MS6001FA industrial gas turbine’s high-pressure turbine. The first was the original embodiment of the capacitive clearance measurement system. The second was the developed capacitive clearance measurement system that the authors successfully used on the BR710 aero gas turbine. The third was a capacitive clearance measurement system which utilised a direct-current operating principle.

The authors fitted all three measurement systems to the MS6001FA industrial gas turbine’s stage 1 high-pressure turbine. The two frequency modulated clearance measurement systems operated successfully; however, the direct-current measurement system failed. The MS6001FA industrial gas turbine’s firing temperature was 1288°C making the sensor environment particularly challenging.

The evaluation provided a direct comparison between the capacitive clearance measurement system’s original embodiments and the developed measurement system. The developed measurement system demonstrated a signal-to-noise ratio approximately twice that of the original embodiment. The authors directly attributed this improvement to the application of the enhanced measurement system electronics, Appendix 1.

Following the successful evaluation of the capacitive clearance measurement system’s developed form, commercial consideration once again restricted what the authors could publish. It is therefore only possible to comment in general terms; however, it is helpful to remember the clearance measurement system evaluation’s explicitly stated purpose: to select a clearance measurement system to form the basis of a clearance control system for application as part of a future H System technology upgrade package.

The reasons why a gas turbine manufacturer would want a clearance control system are as follows. A reduction in stage 1 high-pressure turbine blade tip-to-casing

clearance has the potential to increase overall gas turbine efficiency by 1%. In a stage 1 high-pressure turbine that may already be 90% efficient, we can better conceptualise a 1% improvement as a 10% reduction in remaining aerodynamic losses. Achieving the same reduction via any other approach would be difficult, and thus the attractiveness of a clearance control system is apparent.

Clearance control systems have two roles to play in improving gas turbine efficiency. First, they provide a means by which one can minimise blade tip-to-casing clearance at full load. Second, they provide a means by which one can safely increase blade tip-to-casing clearance during those transients that would otherwise result in a rub between blade tips and casing within which they run that would, in turn, lead to increased blade tip-to-casing clearance under all subsequent operating conditions.

All closed-loop clearance control systems require blade tip-to-casing clearance real-time measurement as the primary input to the clearance control system. The blade tip-to-casing measurement system is only one clearance control system element, and if that system is to operate effectively, all elements must be robust and reliable. The difficulty that occurs with making all clearance control system elements robust and reliable means that effective clearance control systems still constitute a form of competitive advantage for those gas turbine manufacturers that have developed them. As such, virtually nothing is available in the public domain relating to the General Electric, or any other manufacturer's clearance control system.

Chapter 9 High-temperature Proximity Measurement in Aero and Industrial Turbomachinery

As the General Electric evaluation was under way, authors focused on the final documentation of those aspects of the capacitive clearance measurement system that had been a focus during the latter stages of the overall measurement system development effort.

The paper that forms the basis of this chapter briefly describes the new oscillator presented in the patent that forms the basis for Appendix 1. The chapter describes in detail the 'new technology' sensor technology that is presented in the patent that forms the basis of Appendix 2, and clarifies the specific advantages it offers over the original sensor design. The paper upon which this chapter is based does not report in detail the authors' 'next generation' sensor development work. The next generation sensor concept was the subject of a patent that forms the basis of Appendix 3.

The paper that forms the basis of this chapter also presented a developed form of a direct-current clearance measurement system that could use the same new technology sensors as the capacitive clearance measurement system. It is important to recognise that a frequency modulated operating principle limitation is that it only functions at blade passing frequencies above approximately 1 kHz. The direct-current system was able to make a blade tip-to-casing clearance measurement statically, and at blade passing frequencies up to approximately 1 kHz. The direct-current clearance measurement system's frequency response was just fast enough to allow it

to operate at the cold windmill speed for an aero development gas turbine. At cold windmill, compressor blades lock into their running position, and in so doing, the direct-current clearance measurement system was able to provide a cold-build clearance measurement before the development engineers first fired a gas turbine.

Although the above may appear as a technicality, the most common error source during a development gas turbine test that calls clearance measurement accuracy into question is errors in cold build clearance measurement. Cold build clearance is the distance that the capacitive sensor is recessed in the casing within which blades rotate. One measures the cold build clearance with a depth gauge during the development gas turbine build. By measuring the clearance between blades and casing with a feeler gauge, whilst holding the blade in its working position, one can calculate the total distance from sensor face to blade tip. The authors could then use the direct-current clearance measurement system to measure the distance from sensor face to blade tip at cold windmill. If the two measurements agreed, the development engineers could have confidence that they correctly calibrated both the measurement system and correctly measured the cold build clearance. If the two measurements did not agree, then an error existed that required resolving before the development gas turbine's first fire.

The paper that forms the basis of this chapter also reported one final research finding. The authors had observed that some high-temperature sensor installations had recorded a change in measured clearance as they adjusted cooling air flow to the sensor. From this, the authors concluded that the capacitive sensor was also a temperature sensor at high temperatures, something that they have very much hoped to avoid. The authors conducted an evaluation of magnesia's relative permittivity (the insulator that they used in the capacitive clearance measurement system's original embodiment) and silica (the insulator that they used in the clearance measurement system's developed embodiment). The authors had switched from magnesia to silica as silica has a relative permittivity approximately half that of magnesia. Consequently, a silica-insulated mineral-insulated cable could be twice the length of the equivalent magnesia-insulated cable. However, as the authors discovered, magnesia's relative permittivity is approximately constant with temperature, but after 600°C, silica's relative permittivity raises dramatically. From the time of this realisation onward, all sensors intended for installation in application with an installed temperature of 600°C or above utilised magnesia-insulated mineral-insulated cable.

Appendix 1 Capacitance Transducer Apparatus and Cables

The three appendices in this volume are each a developed form of a patent. Patents are written in a formal style that is difficult for those unfamiliar to penetrate. As such, we tend not to read or reference patents. To overlook patents, however, is to overlook a significant source of intellectual property. The three patents included in this volume each document one aspect of the intellectual property that the authors originated as part of the capacitive clearance measurement system development. We

have edited each into a more readable form, in an effort to make its content more accessible to the reader.

The patent that we have converted into this appendix's text supports the main body of the volume by providing insight into the electronics and cable technology that the authors developed as part of the capacitive clearance measurement system development.

The cable that the authors used in the capacitive clearance measurement system is a tri-axial mineral-insulate cable. Mineral-insulated cable represents a technology in its own right, and tri-axial mineral-insulated cables represent one of the most challenging embodiments of that technology. The challenge was all the more difficult as a consequence of a need to increase the mineral-insulated cable's length to 5 metres in order to enable the measurement system oscillator's placement in a low-temperature environment away from the hot compressor or turbine components.

As the authors increased the tri-axial cable length, the oscillator was progressively less able to drive the guard to the same instantaneous voltage as the centre wire. An investigation identified that as cable length increased, the high electrical resistance of the guard resulted in the voltage drop along the cable becoming significant enough to compromise measurement system performance. In effect, the voltage drop was limiting the length of mineral-insulated cable the system oscillator could drive.

The electrode, guard and the tri-axial cable's outer screen were traditionally manufactured from stainless steel for strength. The electrode and outer screen required mechanical strength in order to facilitate sensor manufacture. However, the guard was an entirely internal feature of both the sensor and the tri-axial cable. One could therefore manufacture the guard from a material with lower electrical resistance than that which stainless steel offered.

After some experimentation, the authors chose a nickel alloy as the preferred guard material due to its low electrical resistance. However, the nickel alloy had very low strength compared to stainless steel. Drawing down a stainless steel, nickel alloy, stainless steel combination during the tri-axial cable manufacturing process proved extremely difficult. The nickel alloy guard would either break up completely during manufacturing, or was so badly punctured that it was no longer electrically effective. The problems that occurred with manufacturing were exacerbated by some applications that required cable down to 2.0 mm diameter in lengths of up to 10 metres. The original cable was 3.5 mm in diameter and 160 mm long.

The authors spent over a year optimising the tri-axial cable manufacturing process. When perfected, the resulting cable was a smaller diameter (and hence more flexible) and with a lower electrical resistance guard (and hence longer) that together facilitated installation on larger civil gas turbines and the very much larger industrial gas turbines.

The patent that forms the basis of this appendix also presents a developed version of the capacitive measurement system oscillator. The original oscillator design incorporated a multi-core cable that linked the oscillator to the demodulator. This proved a practical impediment in both gas turbine compressor and turbine application. Gas turbine test cells are typically pre-wired with 50 ohm co-axial cable as

standard. Other cable requires separate installation. As such, the capacitive measurement system's original embodiment could not use standard test bed wiring.

The oscillator's developed form ran power from the demodulator to the oscillator by applying a voltage to a 50 ohm co-axial cable's centre wire that connected to the oscillator. The oscillator was able to draw current down the centre wire, whilst still returning and outputting voltage down the same cable to the demodulator. This development allowed the authors to install capacitive measurement systems in gas turbine test beds using standard test bed cable. In so doing, development engineers were able to treat the system as part of a test bed's standard suite of instrumentation.

Appendix 2 Gap Measurement Device

The patent that we have converted into the text of this appendix supports the main body of the volume by providing insight into the sensor technology that the authors developed as part of the capacitive clearance measurement system development. Two separate needs drove the sensor development effort. First, the original sensor design which the authors initially used when first developing the capacitive clearance measurement system was fragile. Second, the original sensor design did not electrically isolate the active sensor electrode well, resulting in unwanted thermally induced errors in the measurement system output.

The original sensor concept relied on a set of machined metal and machinable glass ceramic components that the authors assembled into the capacitive sensor. The machinable glass ceramic components were prone to shatter if the sensor was subjected to a shock load. Consequently, the authors took care when handling the sensors, but inevitably, the sensors' fragility resulted in failure during gas turbine compressor and turbine build.

The capacitive clearance measurement system concept incorporates a 'guard' screen into the sensor. The sensor's centre wire and electrode is isolated from the outer screen via an inner screen that 'guards' the centre wire and electrode. By driving the guard to the same instantaneous voltage as the centre wire and electrode, the measurement system becomes insensitive to changes in the relative permittivity of the insulator separating the guard from the centre wire. The insulator's relative permittivity is a function of temperature, and although this change is modest up to compressor delivery temperatures, it becomes significant at turbine entry temperatures. The original sensor concept relied on a single machinable glass ceramic component to separate the sensor's outer body from the electrode at the sensor tip. Mechanical constraints made it impossible to continue the guard to the sensor tip. Consequently, the capacitance between sensor electrode and outer body would increase at elevated temperature in turbine application, introducing an unwanted error source.

The 'new technology' sensor concept eliminated machinable glass ceramic components. Alumina coating the electrode and guard maintained electrical isolation. Machinable glass ceramic component elimination resulted in an inherently rugged capacitive sensor. Maintaining electrical isolation using thin layers of

alumina oxide, it became mechanically possible to continue the guard to the sensor tip. In this way, the new technology sensor concept addressed two fundamental issues with the original design, and in so doing, facilitated routine and accurate blade tip-to-casing clearance measurement in high-temperature turbine environments. As an added bonus, the elimination of the sensor tip capacitive link between sensor electrode and the sensor's main body significantly improved sensor sensitivity that, in turn, improved measurement system signal to noise ratio and hence range.

Appendix 3 Capacitive Gap Measurement Device

The patent that we have converted into the text of this appendix supports the main body of the volume by presenting a sensor concept that attempts to eliminate the sensor completely. The new technology sensor which the previous appendix describes constituted a conventional combination of assembled sensor components to the end of a cable.

The sensor concept in the patent that forms the basis of this appendix extended the mineral-insulated cable manufacturing process. Manufacturers produce mineral-insulated cable by taking a rod, insulator and tubes and combining them into a short, but large diameter version of the required cable. The cable then passes through successive dies until it draws down to the required length.

It is common practice when manufacturing mineral-insulated thermocouples to leave the cable a relatively large diameter, but to 'draw down' the cable's end to a smaller diameter. The thermocouple cables are then joined at the end of the 'draw down' and the cable's end are welded to form the thermocouple bead, and the outer screen sealed to seal the thermocouple inside the casing. This effectively minimises the thermocouple's size.

The authors applied the same mineral-insulated cable manufacturing technology to the manufacturing of a capacitive sensor. The authors drew down a tri-axial mineral-insulated cable to the required diameter, typically 3.0 mm; however, they did not fully draw down the cable's end, instead leaving it typically 8.0 mm. They then successively flamed sprayed the cable's end with insulator layers and metal to form and protect the sensor electrode. In this way, the capacitive sensor forms an adapted end to the flame-sprayed mineral-insulated cable, but it is not augmented with any manufactured ceramic or metal components. This eliminates all machined components, although a practical embodiment would require welding a mounting ring to the cable sensor's outer body to enable development engineers to first calibrate and then install it.

Electromechanical Measurement of Turbomachinery Blade Tip-to-casing Running Clearance

A.G. Sheard and S.R. Turner

ABSTRACT

It is difficult to reliably measure a running clearance in the hostile environment over gas turbine blading. When manufacturers require measurements during tests lasting many hours, or even days, system ruggedness and reliability are of primary importance.

This chapter describes how the authors developed a reduced size and weight second generation electromechanical tip clearance measurement system. Size and weight reduction facilitates the use of the measurement system for blade tip-to-casing measurements on all development tests from rig to flight-worthy gas turbines. During the course of commissioning, the authors tested the measurement system first in the laboratory, then on progressively more demanding test vehicles. The final test was on a military full-scale gas turbine's single spool core high-pressure turbine. During the course of this test, the authors measured mean turbine entry temperature which exceeded 1527°C through the blading over which they measured clearance. This turbine entry temperature is typical of the applications for this second generation system.

INTRODUCTION

This chapter describes a programme which the authors undertook to develop and test a second generation electromechanical clearance measurement system. Their objective was to reduce the clearance measurement system size and weight to enable its use in applications where available space is at a premium. This increased the installation envelope from the rig and test environments to flight-worthy gas turbines. In principle, this enables the use of a single blade tip-to-casing measurement system throughout an entire gas turbine development programme. The work falls

This chapter is a revised and extended version of Sheard, A.G. & Turner, S.R. (1992), 'An Electro-mechanical Measurement System for the Study of Blade Tip-to-casing Running Clearances'. *Proceedings of the 37th American Society of Mechanical Engineers Gas Turbine and Aeroengine Congress*. Cologne, Germany, 1–4 June, Paper No. 92-GT-50.

broadly into two sections. The first is the mechanical design of a new clearance measurement system. The second is its commissioning in four stages. The chapter concludes by reviewing the second generation system's performance during the commissioning exercise.

The measurement system described in this chapter is a development of a first generation measurement system which Davidson *et al.* reported (1983). Both first and second generation systems utilise an electromechanical stepper motor driven probe and a spark-discharge technique. These ascertain the proximity of an electrically grounded target, typically a rotating compressor or turbine blade. In the 1950s, the Fenlow Company introduced the first electromechanical clearance measurement system, but it suffered from thermal effects which limited its accuracy. Amsbury and Chivers (1978) overcame the thermal effect that limited accuracy of the 'Fenlow' probe. They developed an electromechanical clearance measurement system with a mounting face feature, allowing its placement in a working location close to the probe tip, Figure 1.1. Amsbury and Chilvers (1978) also cooled the electromechanical clearance measurement system design, enabling it to both survive and make useful measurements of high-pressure turbine blade tip-to-casing clearance with gas temperatures of 1527°C.

Despite the initial success of Amsbury and Chivers (1978), the system proved unreliable in practical application. Chivers (1989a) attempted to use Amsbury and Chivers' (1978) system to measure high-pressure compressor and high-pressure turbine tip clearance in a development gas turbine. Compressor rotors become electrically charged by the compressed air's scrubbing action. This charge on the rotor then



FIGURE 1.1. An example of Amsbury and Chivers' (1978) design of electromechanical clearance measurement system probe and actuator.

leaks to earth through the compressor bearings, and, in the case of a high-pressure compressor, through the bearings and gears in the external gearbox. Chivers (1989a) found that the compressor and turbine's blades were not effectively earthed. A spark failed to pass between the wire and the rotor blades, resulting in the wire driving into the rotor blades and damaging them.

Davidson *et al.* (1983) addressed and solved the thermal effect problems by developing a novel spring-loaded probe. The probe spring loaded against a 'datum' face (Figure 1.2) on the casing within which the compressor or turbine blades rotated. This maintained the probe's datum close to the measurement point, thus eliminating thermal errors. Davidson *et al.* (1983) also solved the problem of ineffective earthing with compressor and turbine rotors. They advocated fitting a carbon brush to the rotor and connecting it to earth. In practice, fitting a carbon brush proved challenging in development gas turbine applications; however, researchers successfully developed such techniques which enabled Davidson *et al.*'s (1983) electromechanical clearance measurement system to become the first measurement system that engineers could routinely apply in gas turbine development, as opposed to instrumentation research programmes.

In the current programme of work, the authors focused on minimising the size of Davidson *et al.*'s (1983) first generation electromechanical clearance measurement system without changing the system concept. The first generation system's spring-loaded probe resulted in a self-calibrating measurement system. Engineers could use Davidson *et al.*'s (1983) embodiment of the concept successfully over a wide range of temperatures. It is capable of ± 0.025 mm accuracy over a 6 mm range.

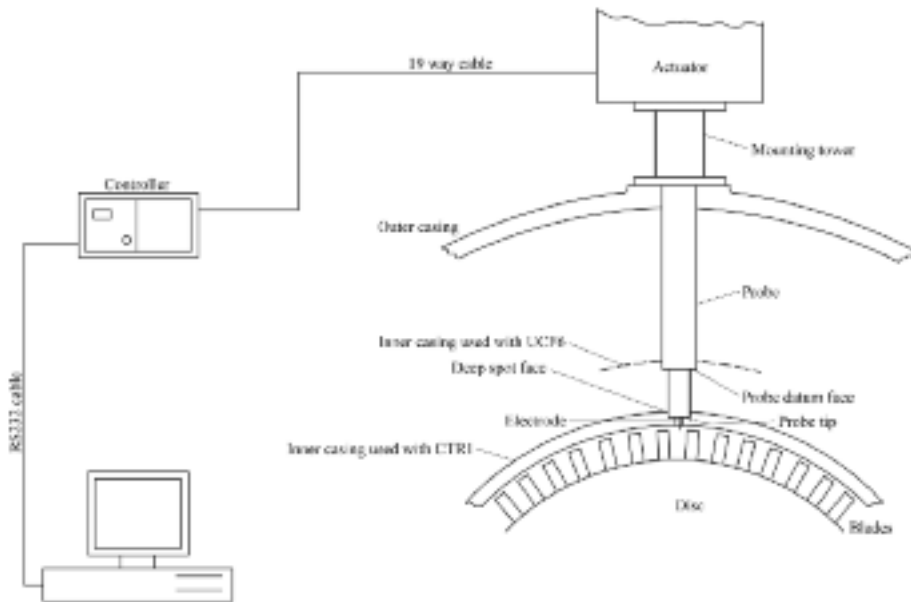


FIGURE 1.2. A schematic layout of the electromechanical clearance measurement system installation and component parts.

The authors decided to undertake this development exercise after a thorough review of the gas turbine community's current and future clearance measurement requirements. The clearance measurement systems currently available for use in high-temperature and high-vibration environments utilise one of five basic principles of operation. In addition to the electromechanical principle, clearance measurement systems may utilise optical, direct-current capacitive, frequency modulated capacitive or microwave operating principles, Table 1.1.

In the majority of applications, the measurement of blade tip-to-casing clearance to the longest blade is the most important parameter as the blade tip radii are normally ground to the same length. Chivers (1989b) and Parish (1990) have described other complementary capacitance-based systems which may provide tip-to-casing clearance on a blade-by-blade basis, but in practice, engineers typically use them to measure average clearance over all blades. These systems require calibrating prior to use, with the attendant risk that the calibration may drift.

With the continuing viability of a clearance measurement system utilising the electromechanical operating principle established, the authors undertook the development of a second generation electromechanical clearance measurement system. The first phase of the development programme was the design of a miniaturised electromechanical actuator. This chapter will summarise the system requirements

Table 1.1. *Gas turbine users of blade tip-to-casing clearance measurement systems.*

User	Electromechanical	DC cap	FM cap	Optical	Microwave
Pratt & Whitney	Hartford		O	E	
	Florida	D	O	O	
	Canada	D	O		
General Electric	Evendale	O	O		
	Lynn	D			
Rolls-Royce	Derby	O/D	O	O	O
	Bristol	D	C	K	
	Leavesden		C	K	
GTEC		O	O		
AGT	D		O		
Snecma	D		O		
MTU	O	O			
Textron			O		
WPAFB		O			
Turbomeca		O			
Alfa Avio		O			
Williams	D				
Teledyne CAE	D				
Fiat	D				

C = Chivers (1989a); D = Davidson *et al.* (1983) ; K = Killeen *et al.* (1991); O = own; E = experimental.

and the second generation system's conceptual design. It describes in detail the probe's mechanical design and mode of operation, the electromechanical actuator and its electronic controller, at which point we may consider the development programme's first phase complete.

CLEARANCE MEASUREMENT SYSTEM CONCEPT

The electromechanical clearance measurement system comprises three basic components (Figure 1.2); a probe, an electromechanical actuator and a rack-mounted controller. The probe spring loaded against a datum face which is physically close to the measurement point, typically on a casing around the blading. An insulated electrode runs through the probe which moved towards the blading using a lead screw and stepper motor drive assembly. The electromechanical actuator contains an electronics module and the stepper motor drive assembly. The electronics module generates 400 volts which apply to the electrode and detect, by low-energy electrical discharge, the passing blade's proximity. The controller generates the stepper motor drive pulses and interrogates the electronics module to ascertain detection of a target. When the controller senses that a discharge has occurred, the electrode retracts to an internal datum. The controller front panel displays the distance from the position at which the discharge occurred to the internal datum and the electrode then moves back in and the process repeats.

The controller can function as a stand-alone unit or one can interface it to a computer via an RS232 link. For multichannel installations, one can use a control program to set up multiple controllers and record clearance measurements from each.

The probe cartridge

The probe cartridge design is critical to system accuracy and to its ability to withstand the environment around gas turbine blading. The probe cartridge, Figure 1.3, has an installed length of 100 mm, the distance from its mounting flange to tip. One can vary the installed length from 50 mm to over a metre and, in particularly difficult installations, one may even angle it to enable an otherwise impossible tip-clearance measurement as Valentni *et al.* (1988) describe.

To understand the probe cartridge's operation, consider datum disc 1 (Figure 1.3). The datum consists of a metal disc mounted on the electrode with an insulated sleeve preventing it from shorting to ground. The figure shows the datum disc against the outer datum face with the electrode in its fully retracted position. During normal operation, the electromechanical actuator drives the electrode in until it senses that the 400 volts on the electrode has shorted to ground. This electrical discharge can occur for one of two reasons: either the electrode tip has discharged to a passing target (a blade) or the datum disc has contacted the inner datum and the electrode shorted to the ground through the probe centre housing. Once the controller senses that the electrode has shorted to ground, it retracts and recharges to 400 volts. The

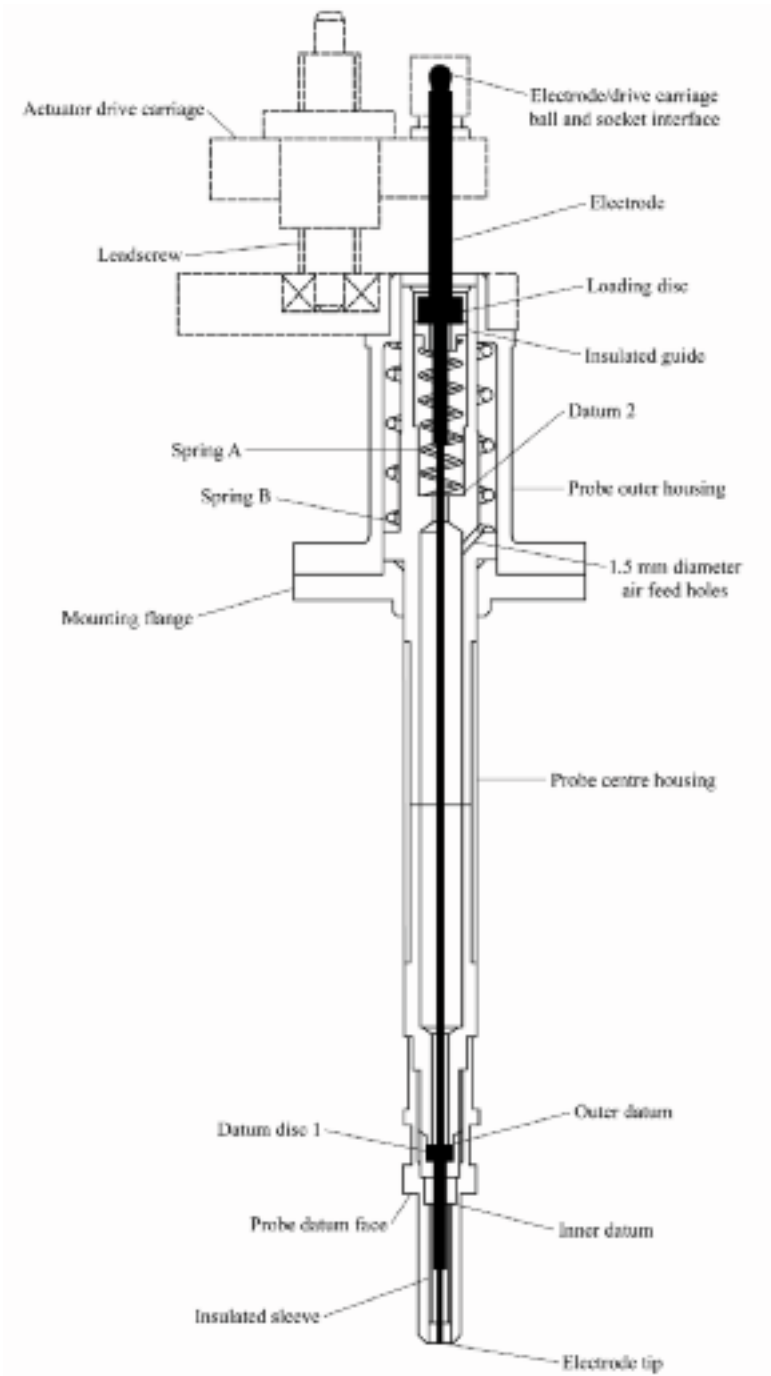


FIGURE 1.3. A 100 mm installed length, 6 mm stroke probe cartridge. Probes with installed lengths from 50 mm to 1.5 m may be used.

controller counts the stepper motor pulses as the electrode retracts until it senses a second discharge as the datum disc contacts the outer datum. The number of stepper motor pulses between first and second discharge are a measure of the distance from the first discharge point to the outer datum.

The probe cartridge's mechanical construction is such that the inner and outer datum faces are rigidly fixed relative to the probe datum face. The probe spring loads against the datum face. We will explain the mechanism which accomplishes this later. As the inner and outer datum faces are mechanically connected to the probe datum face, all three maintain themselves in a fixed position relative to each other. This point is significant as thermal effects result in the distance between the probe datum face and probe cartridge mounting flange changing. Second, due to the probe materials' coefficient of expansion, it grows when heated. By maintaining the probe datum physically very close to the electrode tip, changes in casing relative position and thermal effects do not influence the measurement of distance from the target to the outer datum.

When one installs a probe cartridge in a gas turbine application spring B keeps the probe cartridge against the probe datum face. Engineers usually keep the spring force below 50 N to minimise the load on the often light casings. Further compression of spring B takes up the probe centre housing's thermal expansion without altering the probe cartridge's relative position on the probe datum face.

The casings on which the mounting flange and probe datum face sit will also change their relative position due to thermal effects. We define the net effect of the combined change in casing relative motion and probe centre housing expansion as 'float'. Spring B accommodates the probe's float. If the thermal effects cause a reduction of spring compression (negative float) the force spring B exerts to keep the probe on its datum faces reduces. If they cause an increase (positive float), then it increases spring B's force. In practice, thermal effects almost always result in positive float as at a gas turbine design point the void between casings is usually at an elevated temperature, resulting in the probe cartridge centre housing expanding, with the inner casing at a higher temperature than the outer casing which results in its radius increasing more. The float range that the probe cartridge can accommodate is +5.0 to -1.0 mm, at which spring B loads are 10 Kg and 1 Kg, respectively.

The electromechanical actuator

The major design criterion when designing the electromechanical actuator was minimum overall size. The final design, Figure 1.4, incorporates two principal components: the stepper motor drive assembly and an electronics module. Table 1.2 summarises the design specification.

The stepper motor drive assembly consists of a miniature stepper motor and a lead screw on which the probe electrode drive carriage mounts. When one fits the probe to the actuator mounting tower the probe electrode sits in the ball and socket joint on the cartridge, Figure 1.3. By incorporating a ball onto the end of the electrode and socket in the carriage, the probe cartridge may readily change to facilitate the use of a single actuator with many probes for different installation geometries,

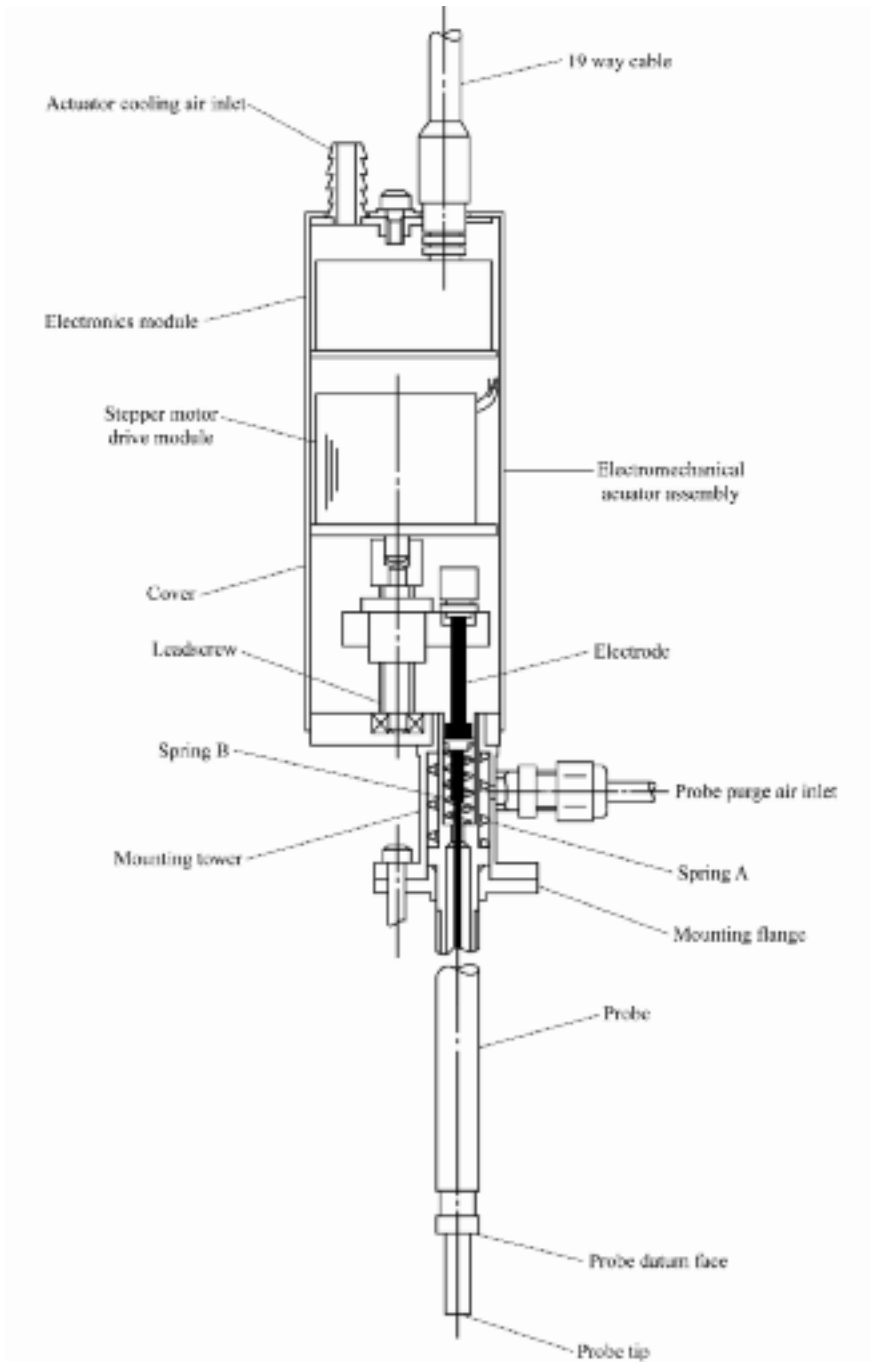


FIGURE 1.4. The mini electromechanical clearance measurement system actuator design, with a probe cartridge shown for clarity.

Table 1.2. Second generation electromechanical clearance measurement system specification.

Range	6.0 mm
Resolution	0.01 mm
Repeatability	+/-0.01mm
Accuracy	+/-0.025 mm
Sample rate	6 per second maximum
Minimum target presentation time	2 micro seconds
Probe diameter at the tip	3 mm minimum, 6 mm nom
Maximum uncooled probe temperature	627°C
Maximum gas temperature	1527°C
Actuator dimensions	44.5 × 48.2 × 165 mm
Actuator weight	0.75 Kg
Actuator environmental limit	50°C
Outputs from the control system	9.99 V = 9.99 mm probe position 9.99 V = 9.99 clearance RS232 output

Figure 1.5. The 200 step motor is half stepped to give 400 steps per revolution driving a 1.0 mm pitch lead screw, giving a step size of 2.5 microns. The electrode's spark gap to a passing blade is from 3 to 5 microns depending on gas temperature, pressure and target geometry. As the drive's step size is less than the spark gap, there is no possibility of the electrode physically contacting a passing blade under normal operating conditions.

The electronics module contains the high-voltage generator for the electrode and the spark-discharge detect circuit. The high-voltage generator is a direct current (DC) to DC converter which generates 400 volts from a 24 volt input. The authors chose 400 volts as the minimum which could successfully break down the dirt and oxide coatings on both electrode tip and target.

The spark-discharge detect circuit senses the electrode's sparking to a target and cuts the current off with less than 2 pico-Joules of transferred charge. By minimising the charge it transfers, one avoids the possibility of damage, due to, for example, sparking in a gas turbine's bearing. It also ensures that if the system operator accidentally touches the electrode, it may shock him or her, but it is not dangerous. In order for a spark to establish itself in the first place, the electrode must have a target for at least 2 microseconds. Compressors have typical blade tip velocities of 400 metres per second and thicknesses of 1.6 mm, presenting the blade tip to the 0.9 mm diameter electrode for approximately 6 microseconds.

Removing the electronics module completely and housing it in a separate box connected to the actuator via an armoured cable has achieved further miniaturisation. This concept resulted in a 'micro' electromechanical actuator, Figure 1.6, to complement the mini design. The mini design occupies 23%, and the micro design 18%, of the volume of Davidson *et al.*'s (1983) first generation electromechanical actuator, and 30% and 24%, respectively, of the weight.

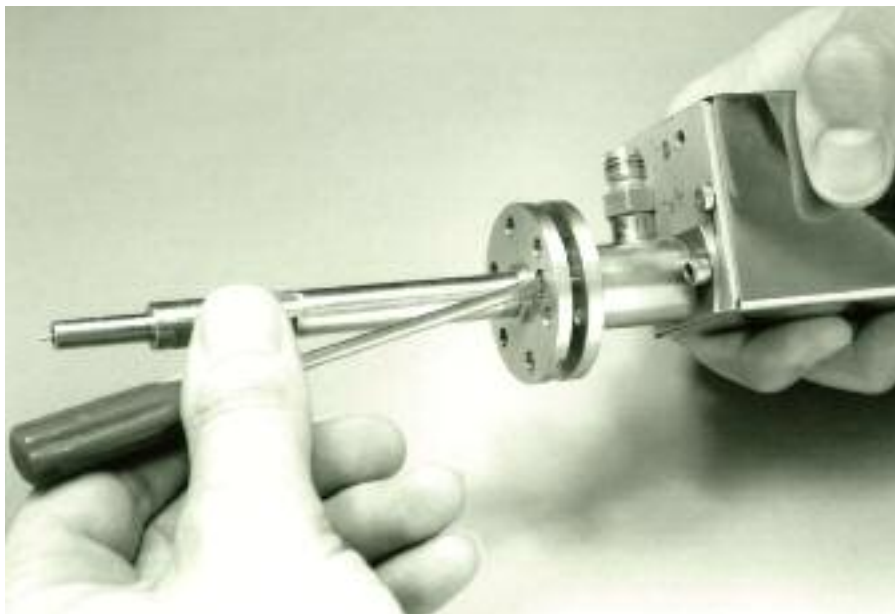


FIGURE 1.5. Removal of the probe cartridge from a mini electromechanical clearance measurement system actuator.

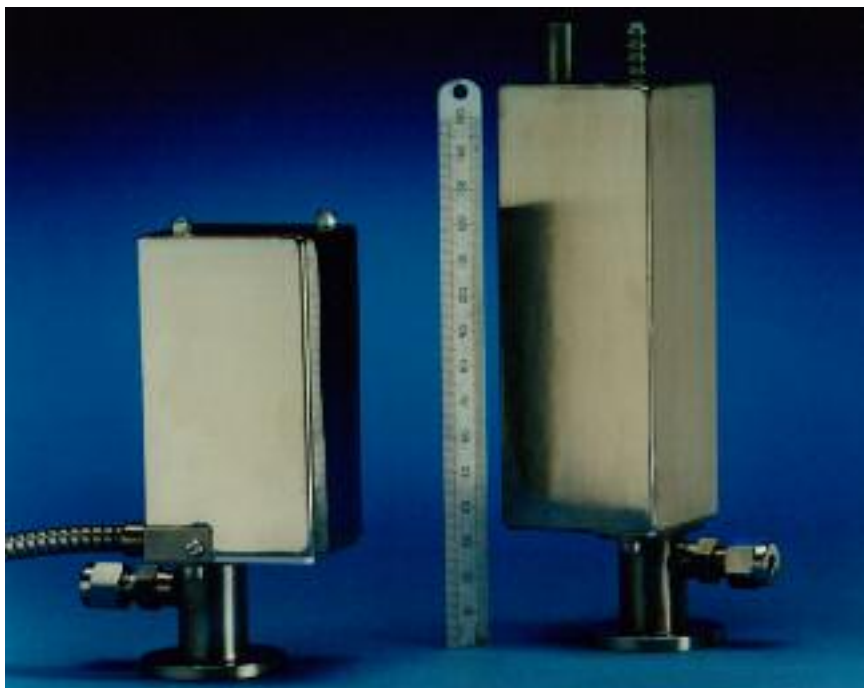


FIGURE 1.6. The mini and micro electromechanical clearance measurement system actuators, which are 23% and 18% the volume of Davidson *et al.*'s (1983) first generation system.

Cooling requirements

The electromechanical actuator and probe cartridge are designed for use in modern gas turbines where turbine entry temperature can exceed 1527°C and therefore require cooling. A dry purge air supply cools the probe cartridge. The purge air can be either compressor discharge air or externally supplied. It feeds into the mounting tower, Figure 1.4, and exits from the probe tip. The purge air also prevents contaminants from entering and causing false short circuits from the electrode to the ground. For this reason the purge air must be clean and supplied even at ambient conditions when no cooling is required.

The electromechanical actuator is also cooled. For high heat environments one can use a double-skinned air-cooled actuator case. Similarly, if the casing on which the mounting flange is fixed is hot, one can use a double-skinned water-cooled mounting tower interface washer to minimise thermal conduction up the tower.

The electronic controller

The microprocessor controller which the authors utilised to drive the electromechanical actuator comprises a half-width 19" rack. The half-width 19" rack incorporates a power supply module and controller module, Figure 1.7. The controller's

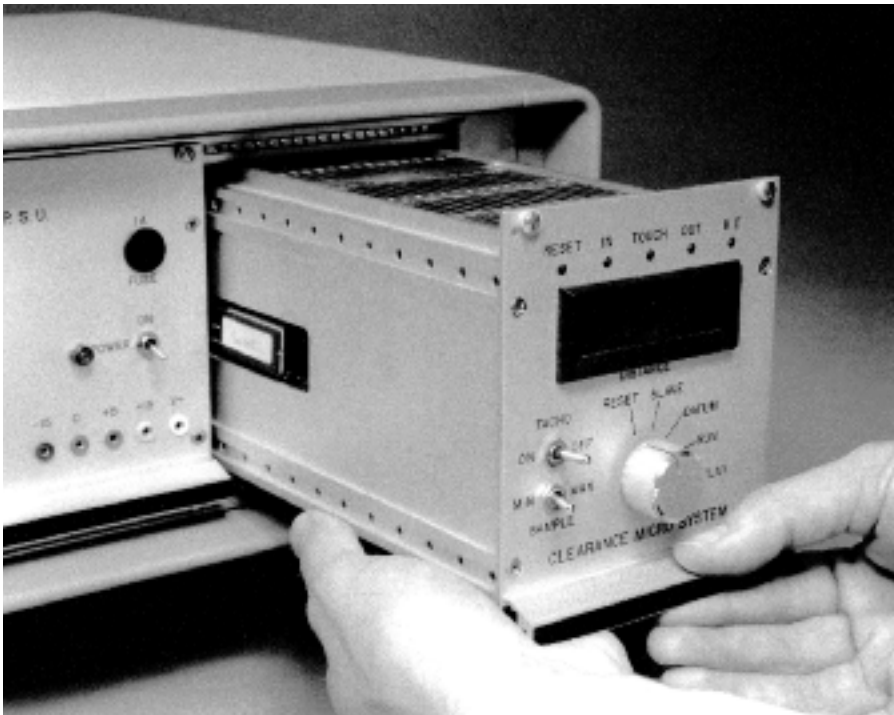


FIGURE 1.7. The 19" rack-mount electromechanical clearance measurement system controller.

primary function is to move the electrode inwards towards a target until it detects a spark-discharge. Once a spark-discharge occurs the controller retracts the electrode to its datum and the process repeats. The controller front panel displays the distance from target to datum and routes that distance to the rear panel as an analogue voltage.

The spark-discharge occurs on the longest blade which is closest to the electrode. To prevent mechanical contact there must be at least one complete rotor revolution between each of the actuator's inward steps. The inward step rate must be slow enough to ensure this. One can use a tachometer signal to synchronise the step rate to the rotor speed. This tachometer lock enables one to safely stop the rotor with no possibility of mechanical contact between electrode tip and the blading.

To ensure that failure of the electronics module will not cause the electrode to traverse into the blading, the microprocessor controller tests the electronics module prior to each and every motor step. A transistor gate between the electrode and the ground can close. The module senses a spark-discharge. Assuming that the microprocessor registers this spark-discharge, the gate opens, the module is hopefully functional and the motor then steps.

Figure 1.8 illustrates the controller's full range of operating parameters. When in the datum state the controller is not passive, but instructs the electromechanical actuator to continually hunt its outer datum, monitoring thermal growth which might otherwise damage the electrode. Once switched to run, the controller moves the electrode in until it detects a spark-discharge. The controller then retracts the electrode at

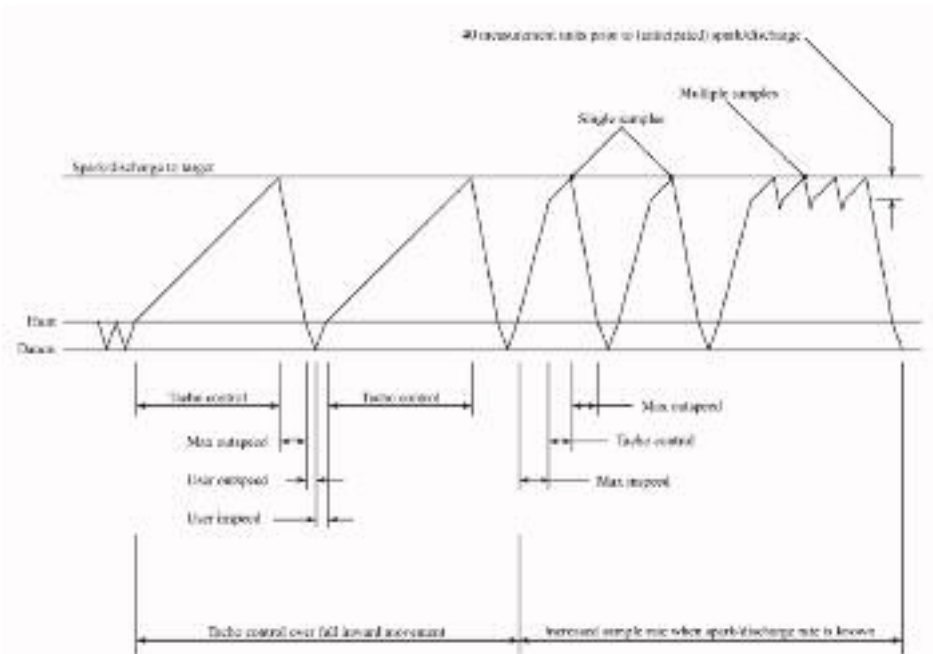


FIGURE 1.8. Controller operating modes which the operator may set up and change via the 19" rack-mounted controller's RS232 interface.

a user-defined speed until it reaches the hunt point when it reverts to a low withdrawal speed to contact the outer datum.

The authors set the user-defined parameters using an RS232 interface on the controller’s rear panel. One may download a pre-set configuration prior to a test and then interrogate the controller via the interface during the test. Additionally, probe position and clearance are available on the controller rear panel as 0–10 volts analogue outputs.

The controller performs all functions relating to the electromechanical actuator’s drive. The user may either link controller analogue outputs into a data logger, or acquire data via the RS232 interface. The controller front panel always displays the last valid measured clearance which one can record manually.

COMMISSIONING

Following the electromechanical actuator’s design, the authors undertook a four-stage commissioning programme comprising a laboratory test and a three-stage rig test. The authors chose the rig tests, which Table 1.3 summarises, as a gradual progression from the laboratory to a high-pressure military spool test. The spool test is representative of the most severe environment that one is likely to encounter.

Laboratory tests

The laboratory test comprised three separate investigations of different aspects of system performance. The authors calibrated the electromechanical actuator, left it running against a target for 48 hours, and then recalibrated it. Second, they ran it in an oven for 2 hours. Third, they performed a vibration test to ascertain its natural frequency. This test series gave the authors confidence that the electromechanical actuator was safe for use on a rig test.

The authors used a micrometre measuring tool with a traceable calibration to ascertain system accuracy. They used the micrometre as a target for the electrode. They retracted the micrometre in 0.5 mm steps and recorded the reading on the controller. They defined the difference between micrometre and controller reading as system error. The calibration of the electromechanical actuator (Figure 1.9), as they received it, and after 48 hours of continuous running, indicated an accuracy of +/-0.02 mm before and after the continuous test. Second, the results repeat closely

Table 1.3. *Commissioning test vehicle conditions.*

Rig	Gas temperature	Air temperature	Vibration
UCF6	127°C	25°C	10 mm/s
CTR1	377°C	35°C	20 mm/s
FSS	1527°C	50°C	50 mm/s

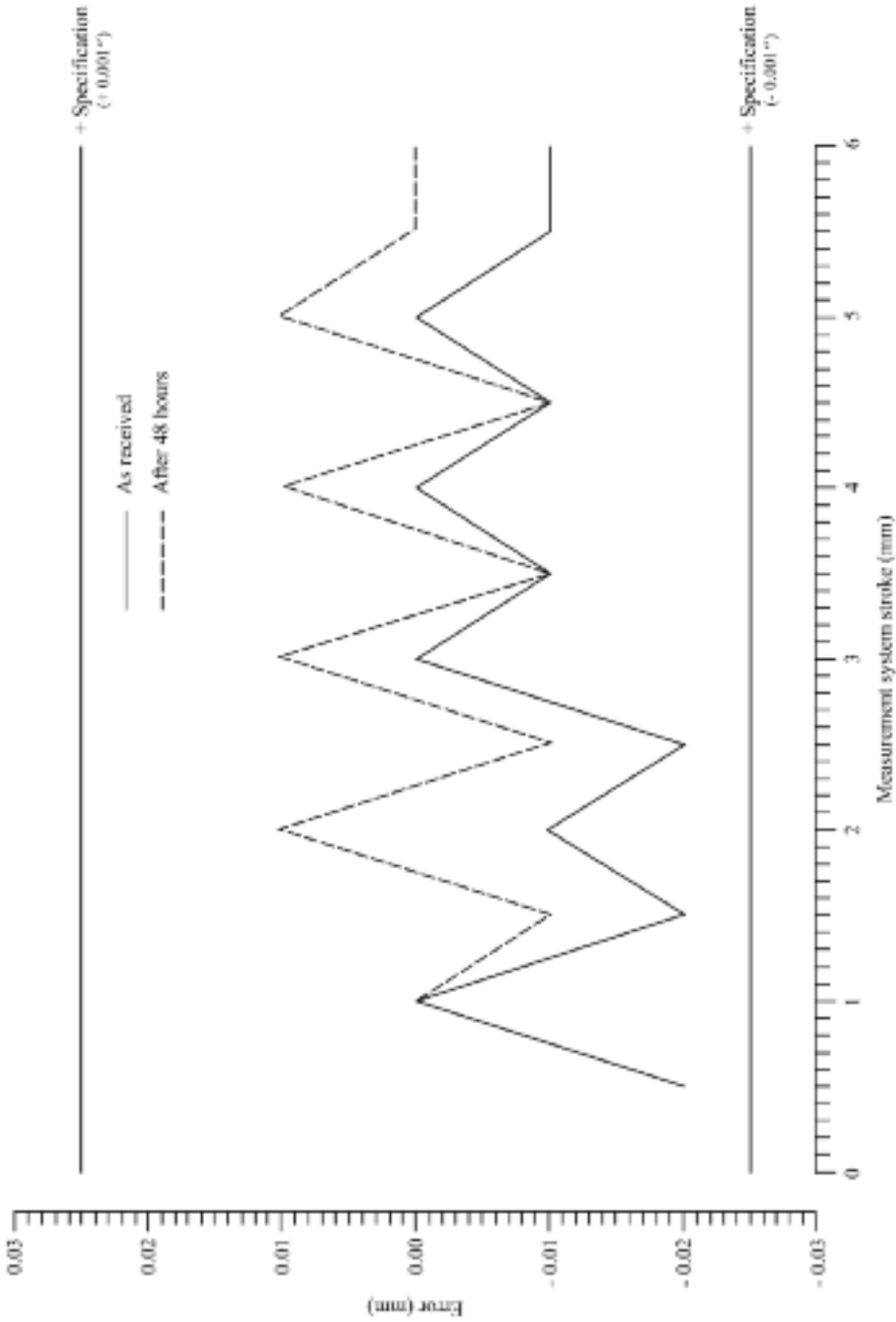


FIGURE 1.9. Mini electromechanical clearance measurement system calibration as delivered and after 48 hours' continuous operation, illustrating system accuracy.

enough to give confidence that there had been no degradation of performance during the 48 hours of operation.

The authors designed the probe-actuator assembly to run on hot turbine casings. In the vicinity of a turbine casing the ambient air temperature could reach up to 50°C. In order to verify the probe-actuator's ability to withstand this elevated environmental temperature, the authors ran it against a fixed target for 2 hours in an oven at 50°C. If ambient temperature exceeded 50°C, they could cool the actuator assembly to 50°C or below in operation if necessary.

The final laboratory test was a vibration test to ascertain the electromechanical actuator's vibration characteristics. The authors encountered a natural frequency at 720 Hz, corresponding to a first-order gas turbine excitation at a speed of 43,200 rpm. They allowed the electromechanical actuator to run against a stationary target whilst they subjected it to a 15 mm/s excitation at 720 Hz. They continued the vibration test for 12 hours, at the conclusion of which the electromechanical actuator was fully functional. At this point, the authors cleared the electromechanical actuator for rig testing.

Universal Cold Flow Rig Number 6 (UCF6)

The UCF6 facility is a general-purpose facility designed to accommodate 100% size aerodynamic models of high-pressure turbines. The facility achieves correct pressure ratio and non-dimensional speed, therefore achieving correct gas angles and Mach numbers through the stage. It does not achieve total temperature and pressure conditions and therefore the UCF6 facility does not achieve gas turbine Reynolds numbers or gas-to-wall temperature ratios.

The facility is extensively instrumented (Figure 1.10), with three traverse actuators and four electromechanical clearance measurement systems. The traverse actuators are able to position aerodynamic probes in the gas path, which Sheard *et al.* (1993) described. All three mount on a rotating casing to facilitate the flow field's area traversing.

In order to ascertain the electromechanical clearance measurement system performance, the authors ran a repeat test using four of Davidson *et al.*'s (1983) first generation systems as a basis for comparison. The test consisted of a slow 0 to 100% speed acceleration from a cold start, Figure 1.11. They then replaced the first generation number 4 measurement system with the mini electromechanical clearance measurement system and then repeated the test. The results, Figure 1.12, show the mini electromechanical clearance measurement system performance was comparable to that of the first generation system. In all, UCF6 ran for 30 hours with a mini electromechanical clearance measurement system fitted for 10 hours. The authors did not encounter operational problems.

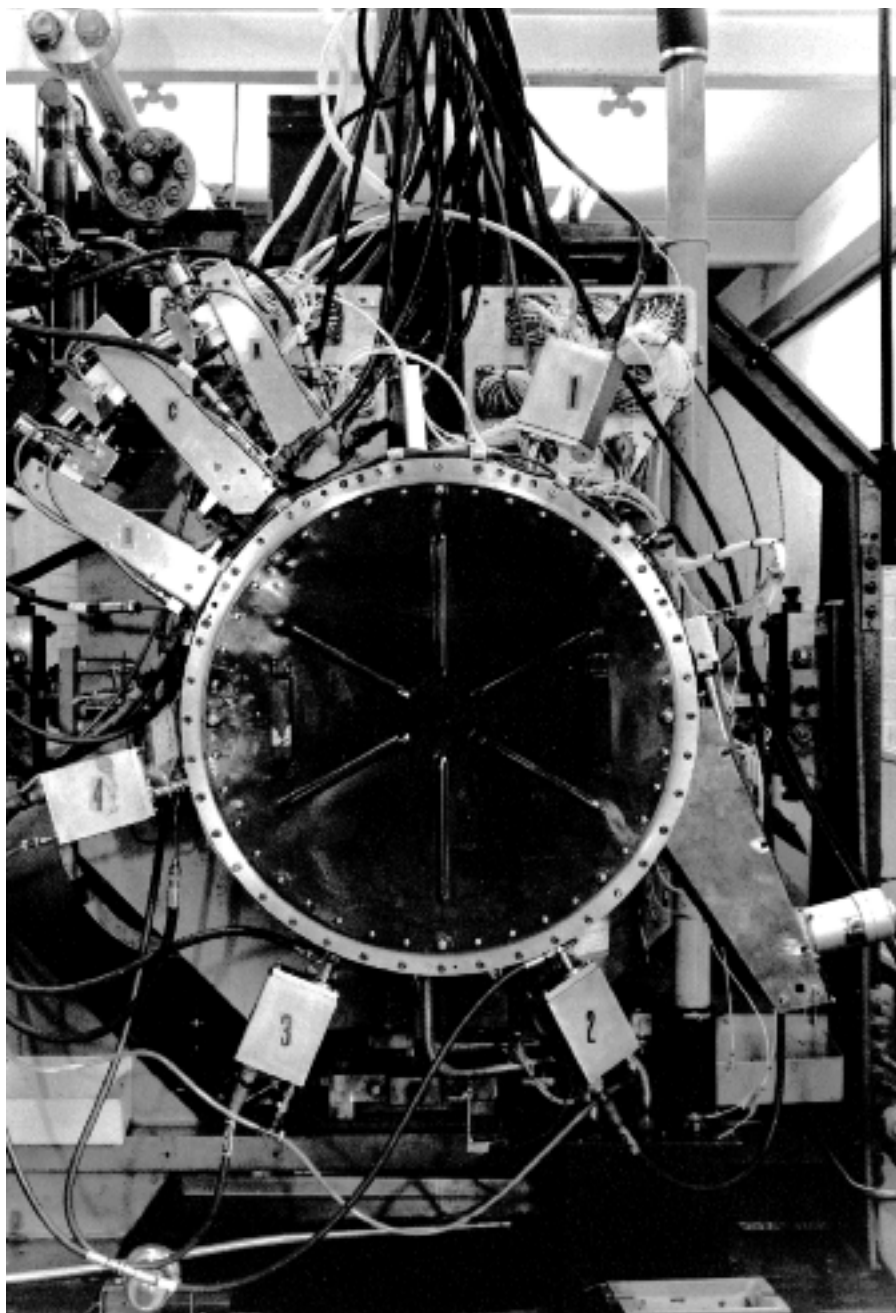


FIGURE 1.10. An end view of the UCF6 facility with three traverse actuators, labelled A, B and C, and four of Davidson *et al.*'s (1983) first generation electromechanical clearance measurement systems, labelled 1, 2, 3 and 4.

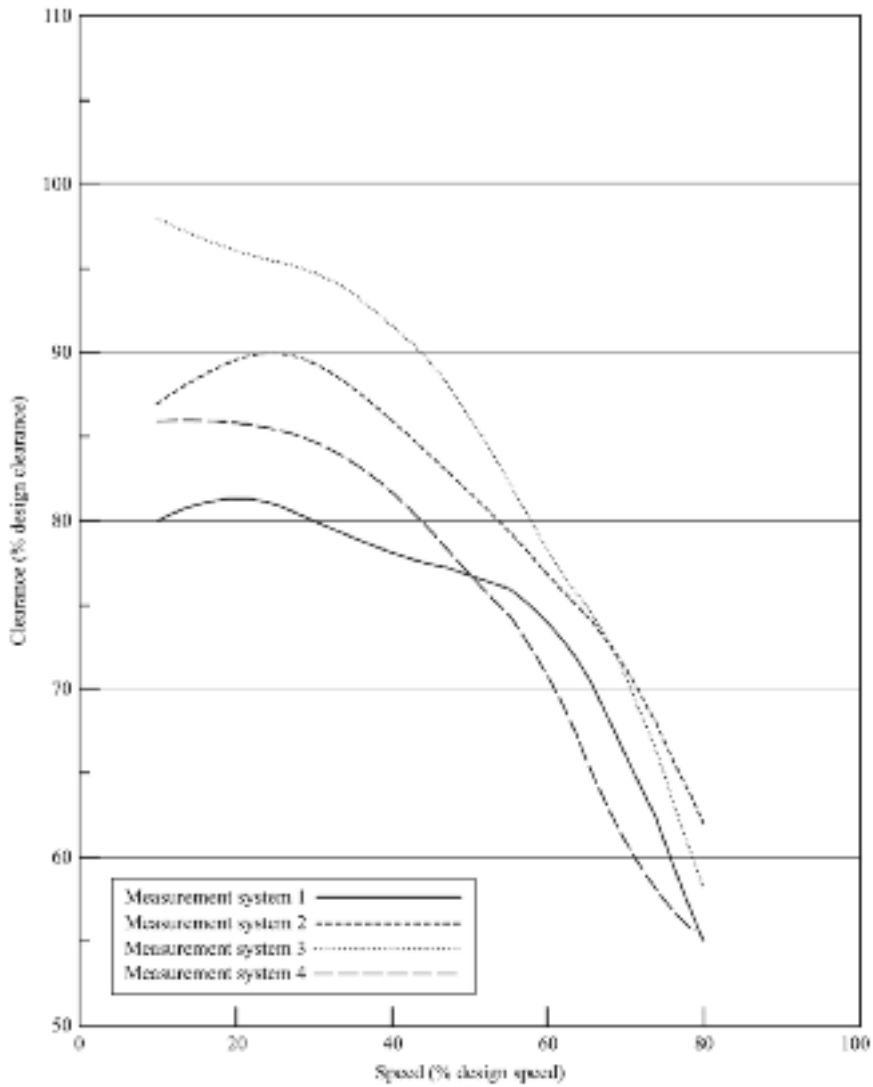


FIGURE 1.11. Blade tip-to-casing clearance results (percentage design clearance versus percentage design speed) from UCF6 when fitted with four of Davidson *et al.*'s (1983) first generation electromechanical clearance measurement systems.

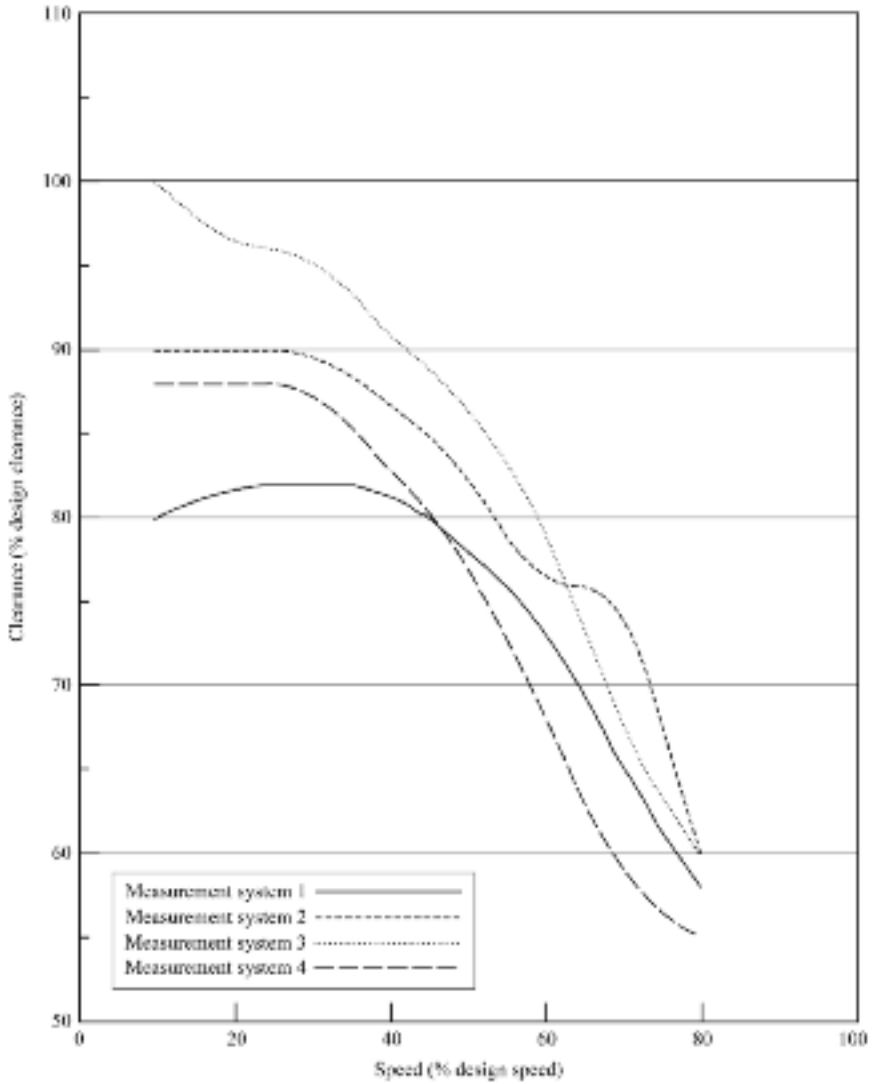


FIGURE 1.12. Blade tip-to-casing clearance results (percentage design clearance versus percentage design speed) from UCF6 when fitted with the mini electromechanical clearance measurement system, plus three of Davidson *et al.*'s (1983) first generation electromechanical clearance measurement systems.

Compressor Test Rig Number 1 (CTR1)

The CTR1 facility is a general-purpose compressor test facility. Its specification is similar to that of UCF6; however, as a compressor test facility, the mean gas path exit temperatures can reach 250°C, leading to an elevated ambient temperature in the test cell. Second, the vibration levels experienced on this facility are significant and therefore the equipment mounted on it requires some vibration tolerance.

The installation on CTR1, Figure 1.13, is externally similar to UCF6 with one significant difference. The installation technique which the authors utilised on CTR1,

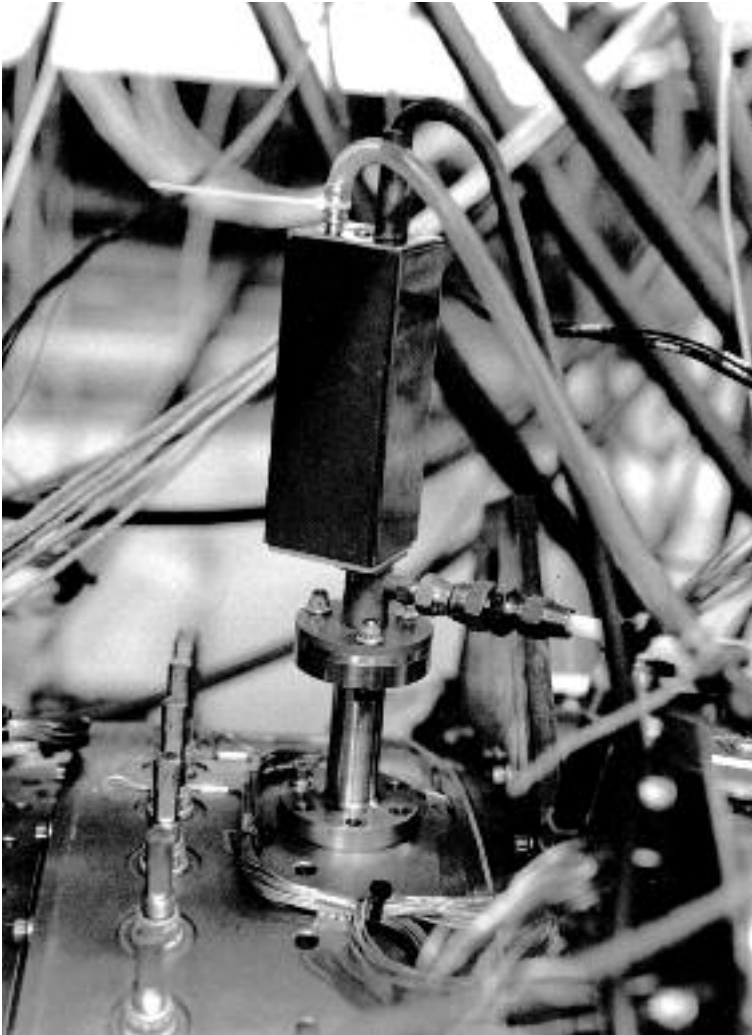


FIGURE 1.13. A side view of the CTR1 facility with the mini electromechanical clearance measurement system probe and actuator fitted.

which has thin lightweight inner casings, was to use the probe tip as a datum face with the rig casing machined with a deep spot face to give the tip a flat surface against which to rest, Figure 1.2. The UCF6 facility utilised the probe's intended datum face, not the probe tip. The CTR1 installation was more typical of those which engineers use in high-temperature applications where the thin inner casing prevents the machining of a shoulder deep enough to enable the use of the probe datum face. This, coupled with the gas turbine casings' real thermal shift, vibration during operation and the elevated environmental temperature around the actuator provided a good pre-run for the high-temperature installation.

The authors established CTRI test envelope limits using Davidson *et al.*'s (1983) first generation system. They then fitted a mini electromechanical clearance measurement system and completed the performance map. In all, the authors logged over 100 operating hours with the mini electromechanical clearance measurement system, during which they encountered no operational problems. They obtained results that were in accordance with those of Davidson *et al.*'s (1983) first generation system.

Full scale spool (FSS)

The full scale spool test that the authors utilised to evaluate the electromechanical clearance measurement system was a full scale test on a high-pressure military gas turbine core utilising flight standard discs, blades and casings. The turbine entry temperature was in excess of 1527°C at some points during the gas turbine cycle. As there was no low-pressure stage around the core, the outer casings were close to the gas stream and ran hot. There were very high peak and transient vibration loads during the test. The prime objective was simply a successful installation that was still functional at the conclusion of the test.

In hot applications probe installation considerations are paramount to the success of the test. The installation geometry, Figure 1.14, is deceptively simple; however, it was the product of hard won experience. First, the authors spring loaded the probe onto its tip against a spot face on the spool liner. The inner casing comprises individual liner segments which, whilst mechanically restrained, were free to move under thermal and differential gas loads. The cooling arrangement for the liners was also such that it severely restricted access to the spot face. The restricted access required the machining of two flats on the probe tip, Figure 1.15.

The authors fitted a seal washer around the probe as it passed through the outer casing. They fitted the actuator to a heavyweight bracket to transfer the electromechanical actuator's weight from the outer casing to a mounting flange, the far end of which they restrained with a lightweight bracket. The cold installation loaded the probe against the outer casing's far side. When the facility thermally soaks through at design point, the gas turbine outer casing expands more than the bracket and unloads the probe. The authors arranged the initial probe loading so that it was fully unloaded at design conditions. The lightweight bracket prevents the installation natural frequency falling low enough for the gas turbine to directly excite it, but it was flexible enough

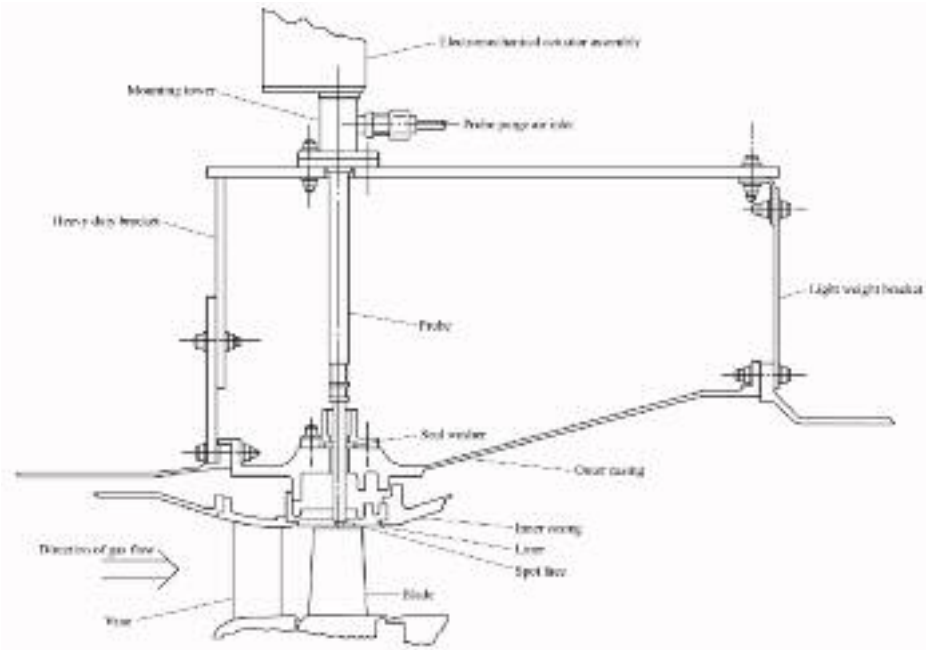


FIGURE 1.14. The installation design for the mini electromechanical clearance measurement system in the full scale spool with the heavyweight and lightweight brackets used to match probe thermal growth to that of the spool casing.

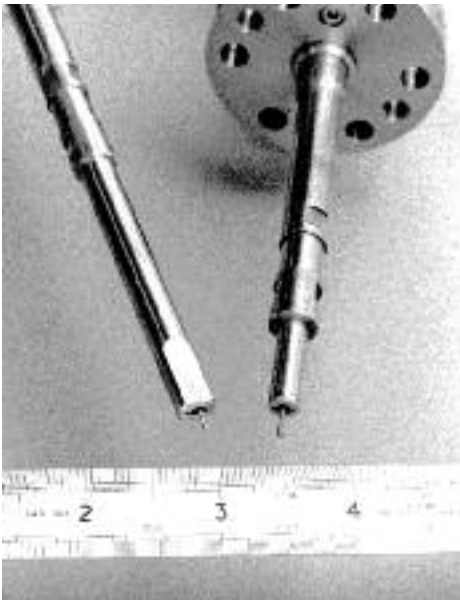


FIGURE 1.15. A close-up view of the probe tip region of the probes used on UCF6 and CTR1 (right) and full scale spool (left) illustrating their different geometries. The probe used on UCF6 and CTR1 has run for over 100 hours and whilst well worn, was still fully functional.

not to influence the heavyweight bracket's thermal behaviour. The actual installation, Figure 1.16, clearly shows the bracket arrangement with the electromechanical actuator standing off the outer casing. The electromechanical actuator's low weight would enable it to mount directly on the casing in future installation designs.

The authors repeated the method that they utilised during the CTR1 test on the full scale spool test, with Davidson *et al.*'s (1983) first generation system to ascertain the envelope's extremities. They also used a mini electromechanical clearance measurement system to fill in the performance map.

Whilst the test data are necessarily confidential, the mini electromechanical clearance measurement system survived the 10 hour full scale spool test. The obtained results were in accordance with those that the authors obtained using Davidson *et al.*'s (1983) first generation system. Following the full scale spool test, the authors stripped and inspected the mini electromechanical clearance measurement system probe and actuator. The high temperature in the probe tip region had resulted in it oxidising to dark blue, from which we may infer a probe tip temperature of over 300°C. The probe was, however, fully functional at the conclusion of the test as was the actuator, which gave the authors confidence that the electromechanical clearance measurement system was performing as they had originally envisaged.

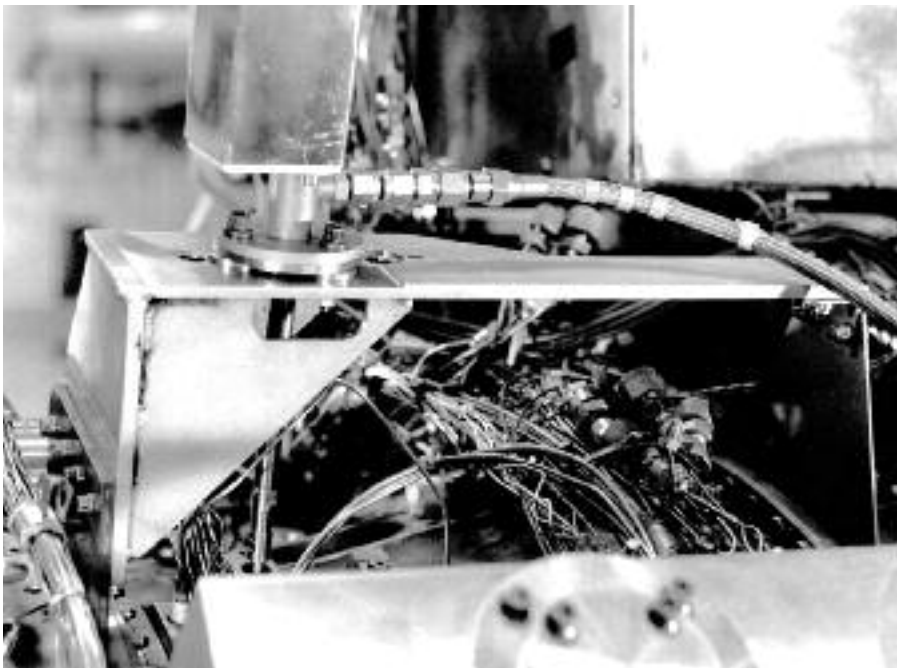


FIGURE 1.16. A side view of the full scale spool with mini electromechanical clearance measurement system probe and actuator fitted prior to test.

CONCLUSIONS

The authors designed a second generation electromechanical clearance measurement system with an actuator 23% of the size and 30% of the first generation system weight. The authors utilised the concepts in the first generation actuator design; however, a more compact stepper motor drive unit and electronics module have facilitated the reduction in size.

Housing the electronics module separately to produce a micro electromechanical actuator extended the mini electromechanical clearance measurement system concept. This reduced the actuator's size to 18% of the first generation design, facilitating a further increase in the range of possible installations.

The authors adapted the probe design to fit the reduced size actuator, but retained the same mechanism for spring loading it onto a datum face physically close to the measurement point.

The authors undertook a four-stage commissioning exercise following the design of the second generation system. The first stage involved a series of laboratory tests to verify the system's performance. Three rig tests followed these laboratory tests, starting with a cold flow rig, working up to the most demanding spool test. In all, the second generation system installations performed reliably and gave results which were in accordance with those which the authors obtained using Davidson *et al.*'s (1983) first generation system.

At the completion of the commissioning tests, the authors concluded that second generation system performance was comparable to that of the first generation system. The authors agreed that obtaining this level of performance on highly demanding test vehicles with an actuator 23% of the first generation size was excellent and therefore they concluded that the second generation system was fully commissioned.

REFERENCES

- Amsbury, C.R. & Chivers, J.W.H. (1978), 'System for the Measurement of Rotor Tip Clearance and Displacement in a Gas Turbine'. *AGARD Conference Proceedings, Seal Technology in Gas Turbine Engines*, vol. 234.
- Chivers, J.W.H. (1989a), *A Technique for the Measurement of Blade Tip Clearance in a Gas Turbine*. PhD thesis, University of London.
- Chivers, J.W.H. (1989b), 'A Technique for the Measurement of Blade Tip Clearance in a Gas Turbine.' AIAA Paper No. 89-2916.
- Davidson, D.P., DeRose, R.D. & Wennerstrom, A.J. (1983), 'The Measurement of Turbomachinery Stator to Drum Running Clearances'. *Proceedings of the 28th American Society of Mechanical Engineers Gas Turbine and Aeroengine Congress*. Phoenix, USA, 27-31 March, Paper No. 83-GT-204.
- Killeen, B., Sheard, A.G. & Westerman, G.C. (1991), 'Blade-by-blade Tip-Clearance Measurement in Aero and Industrial Turbomachinery'. *Proceedings of the 37th ISA International Instrumentation Symposium*. San Diego, California, USA, 5-9 May, pp. 429-47.

- Parish, C.J. (1990), 'Fast Response Tip Clearance Measurement in Axial Flow Compressors — Techniques and Results'. *Proceedings of the IMechE Part G: Journal of Aerospace Engineering*, vol. 204, pp. 51–6.
- Sheard, A.G., Killeen, B. & Palmer, A. (1993), 'A Miniature Traverse Actuator for Mapping the Flow Field between Gas Turbine Blade Rows'. *Proceedings of the IMechE: Machine Actuators & Controls Seminar*. London, UK, 31 March, pp. 1–11.
- Valentini, E., Lacitignola, P. & Casini, M. (1988), 'Progress on Measurement Techniques for Industrial Gas Turbine Technology'. *Proceedings of the 33rd American Society of Mechanical Engineers Gas Turbine and Aeroengine Congress*. Amsterdam, Netherlands, 6–9 June, Paper No. 88-GT-113.

A Technique for the Measurement of Blade-tip Clearance in a Gas Turbine

J.W.H. Chivers

ABSTRACT

This chapter is concerned with the development of a technique to measure steady and transient blade tip-to-casing clearances for use in the development and optimisation of gas turbines. The chapter discusses problems that occur with obtaining such a measurement in a gas turbine environment and derives a measurement specification which is applicable primarily to sea-level bench testing. The chapter also reviews previously published and unpublished work in the field of gas turbine tip clearance measurements. The chapter proposes a novel capacitance transduction technique which uses a frequency modulated oscillator in combination with an active guarded electrode assembly. The chapter evaluates the performance of a prototype clearance measurement system in the laboratory which the author then used on both a gas turbine compressor and turbine.

INTRODUCTION

In both gas turbine compressors and turbines, the aerofoil section blades rotate in close proximity to the stationary casings. The clearance which exists between the rotor blade tips and the casings is typically some 2% of blade height. For example, at the inlet and outlet of the high-pressure compressor of a gas turbine, the rotor blades would have heights of 125 and 50 mm giving nominal running clearances of 2.5 and 1.0 mm, respectively. During normal gas turbine operation in a flight environment, these clearances can vary from 0 to 4% of blade height. These small clearances have a profound effect on the design of compressors, turbines and the entire gas turbine. The main effects of large blade-tip clearances on a gas turbine are:

This chapter is a revised and extended version of Chivers, J.W.H. (1989), 'A Technique for the Measurement of Blade Tip Clearance in a Gas Turbine'. AIAA Paper No. 89-2916.

1. Reduced efficiency. Air can leak back over the rotor blade tips.
2. Reduced compressor surge margin. For a given rotational speed and airflow, increased tip clearance has the effect of reducing the pressure ratio and the surge line approaches the working line.
3. Reduced gas flow through the gas turbine.

Typically, for a large gas turbine, an increase in tip clearance of 0.125 mm in the high-pressure compressor can reduce compressor efficiency by 0.5% and increase the gas turbine's specific fuel consumption by 0.2%. In the case of the high-pressure turbine, a similar increase in tip clearance decreases the turbine efficiency by 0.5% and increases specific fuel consumption by 0.25%.

In his paper (Freeman, 1985), Chris Freeman studied the effects of tip clearances in axial turbomachinery and attempted to both identify the results of changes in tip clearances and list the causes. To summarise, thermal effects cause the changes in casing diameters, and centrifugal growth and thermal growth primarily cause the changes in rotor diameters. A time delay occurs with each of these changes for any change in gas turbine operating condition.

The rotor's growth, due to centrifugal force, tracks rotational speed and is thus virtually instantaneous. The casings' thermal growth is rapid as the structural mass is low, thus having a small thermal inertia. The rotor thermal growth is slower because the mass, and hence the thermal inertia, is relatively large and also the rotor discs, which retain the blades, are insulated from the hot gas path.

When considering tip clearance, we may summarise the measurement system requirement as follows: it provides a blade-tip-to-casing clearance measuring system which can integrate with the routine suite of instrumentation techniques that engineers use during research compressor and turbine rig testing and during the development phase of complete gas turbines on sea-level test beds.

MEASUREMENT SPECIFICATION

Range

For a large gas turbine in the thrust range 250 to 400 kN, it is necessary to measure turbine and compressor blade tip-to-casing clearances between 0.0 and 2.5 mm. In order to ensure that a tip clearance measuring system does not become damaged whenever a blade tip-to-casing rub occurs, it is essential to install a tip clearance sensor in the casing lining under-flush, typically by 0.5 mm. Accounting for the sensor recess, the required measuring range is 0.5 to 3.0 mm. An average clearance measure of all the blades in a rotor stage from a fixed circumferential position on a casing is of most use to both the research and development engineer. Individual blade clearance measurement is not an essential system requirement.

Accuracy

A system total error band of +5% and -5% of reading down to a minimum reading of 0.5 mm under all environmental conditions is a requirement during rig and development gas turbine testing. We can express this accuracy in terms of either component efficiency or gas turbine specific fuel consumption. For example, at the design clearance values for the last stages of a high-pressure compressor or a high-pressure turbine, the 5% of reading tip clearance error band is equivalent to a component efficiency error band of 0.3% or a specific fuel consumption uncertainty of 0.1%.

Environment

As the air passes through a gas turbine, the maximum gas temperature between the blade tips and the casings (the measuring gap of interest) typically varies from ambient at gas turbine inlet to a compressor delivery temperature of 527°C and a high-pressure turbine inlet temperature of 1227°C. The temperature adjacent to the gas turbine core casings under the fairings are typically 177°C above the compressors rising to 227°C above the turbines.

Dynamic response

Blade passing frequencies of up to 20 kHz are typical in large gas turbine compressors and turbines with rotational speeds of up to 10,000 revolutions per minute and 100 plus blades per stage. A blade-to-space ratio in the order of 1 to 10 is usual for a compressor, which implies that a tip clearance measuring system requires a bandwidth in the region of 2 MHz. Blades in a turbine generally have a thicker chord in order to contain the air cooling passages. The effective blade-to-space ratio is less than the compressor blade-to-space ratio by a factor of two, thus reducing the required system bandwidth by the same factor. The actual spatial resolution of any sensor that detects the blade tips will have a significant effect on the clearance system bandwidth requirements.

SURVEY OF PREVIOUS WORK

Between 1965 and 1980, the USA was the country most active in new research techniques for gas turbine blade tip-to-casing clearance measurement. One technique, optical triangulation, is conspicuous by the numerous researcher teams who have investigated and developed its application to gas turbines.

Researchers have referred to the optical triangulation measurement technique under various headings including a 'laser proximity probe', 'laser triangulation

probe' or 'laser optical clearance system.' Drinkuth *et al.* (1974), Ford (1980), Barranger and Ford (1981) and Hardy (1972) have investigated the technique at Pratt & Whitney Aircraft, White (1977) has researched at Avco Lycoming and Baker *et al.* (1978) have studied the subject at General Electric.

Figure 2.1 shows the triangulation system's principle of operation. Almost exclusively, researchers use a helium–neon laser as the light source, not for the light's coherent properties, but simply because the illumination is intense, has a small spot size and is well collimated. Rotor blade tip radial movement results in a spot of light's linear movement on either a position sensor or a vidicon tube which the researchers can then quantify.

Figure 2.2 shows a schematic diagram of a more practical triangulation principle embodiment. This arrangement requires only one access hole through the gas turbine casings and provides a more stable measurement than that derived from a separate transmitter/receiver optical system.

In the early 1950s, researchers developed the first commercially available clearance measuring system which they could use to continuously monitor turbomachinery blade tip-to-casing clearance. A British company, Fenlow Ltd, manufactured it. The 'Fenlow' probe is based on an electromechanical arrangement to measure the displacement of an electrically grounded target. The probe consists of an alternating current repeater motor which slowly moves an insulated wire towards an earthed target, typically a gas turbine blade tip. A remote transmitter electrically drives the repeater motor which, in turn, is mechanically driven by a direct current motor.

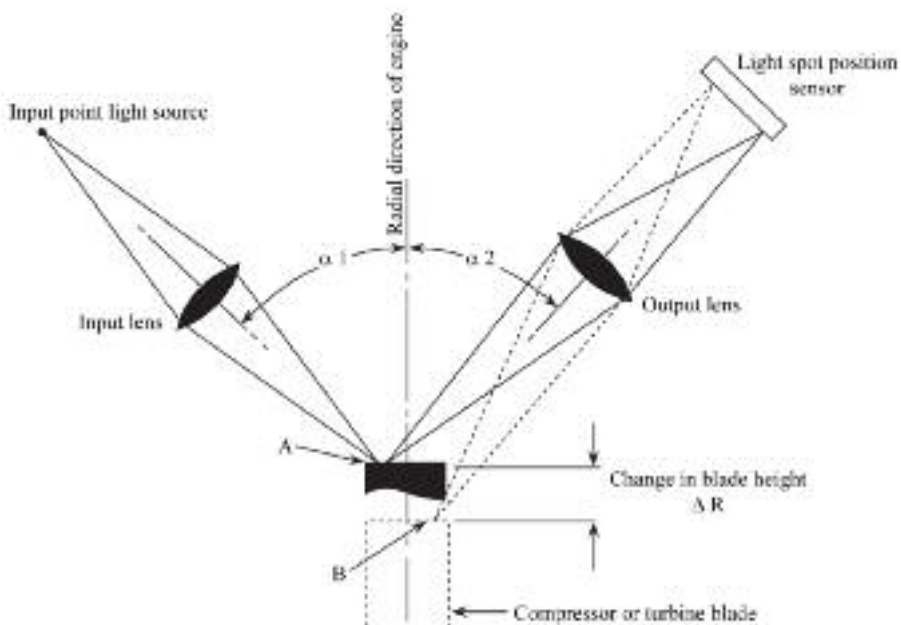


FIGURE 2.1. Optical triangulation: principle of operation.

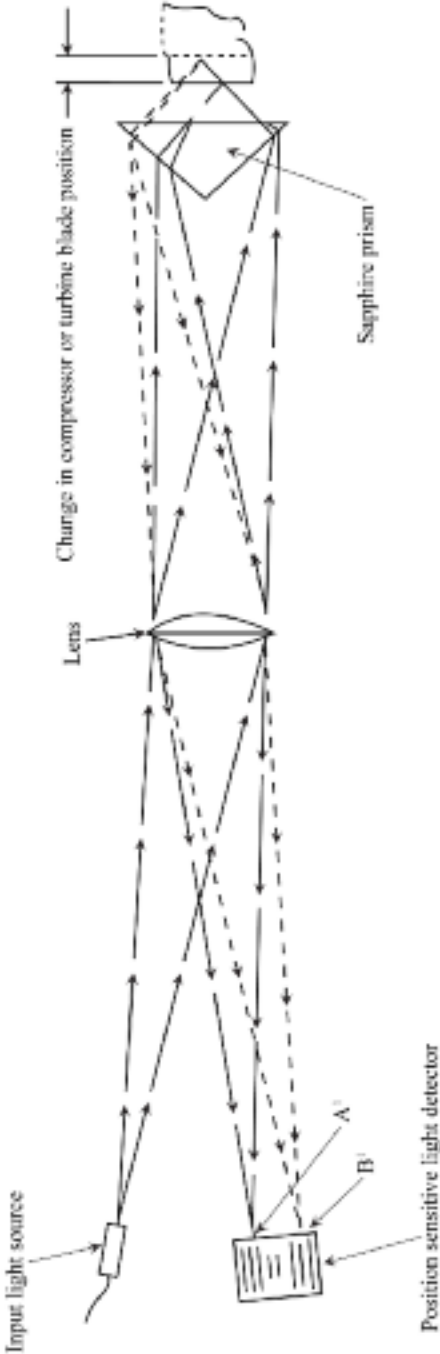


FIGURE 2.2. Folded optical triangulation probe.

In operation the wire is charged to 600 volts and moves towards the target. When the wire is within approximately 0.01 mm of the target, the voltage across the gap becomes sufficient for a spark-discharge to occur between the wire and the target. The measurement system's electromechanical arrangement then retracts the wire and immediately moves it back towards the target. In this way the wire oscillates above the target with amplitude of approximately 0.03 mm. A measure of displacement is achieved by counting the direct current motor's mechanical turns. The system's gearing is such that one complete direct current motor revolution causes the probe wire's linear displacement of exactly one thousandth of an inch. In this manner, the turns counter indicates displacement directly in thousandths of an inch.

Between 1980 and 1985 the incorporation of new technology gave the electro-mechanical clearance measurement technique, which Fenlow Ltd. first developed, a new lease of life. Despite many researchers considering it an obsolescent technique, Amsbury and Chivers (1978) at Rolls-Royce in England and Knoell *et al.* (1981) at MTU in Germany developed electromechanical clearance measurement systems that Rolls-Royce and MTU used in gas turbine development programmes. Davidson *et al.* (1983) further developed Amsbury and Chivers' (1978) electromechanical clearance measurement system. Although robust and reliable in service, Davidson *et al.*'s (1983) system was large enough to make it difficult to fit on successive stages of a gas turbine's compressor or turbine which limited its practical application.

However, all electromechanical-based measurement techniques suffer similar disadvantages when operated in a gas turbine environment. These are:

1. unreliability of the mechanical actuators in high-vibration/high-temperature environments;
2. complex, heavy and expensive measuring probes;
3. susceptibility of probes to damage due to intermittent contact with blade tips under casings/probe vibratory conditions or the rotor's eccentricity/orbiting;
4. indication only of clearance to the longest blade. Information on average or individual blade clearances is not available.

Researchers have developed fluidic-based displacement measurement techniques which were particularly popular during the 1960s and 70s in the power generation industry. This is due primarily to the technique's total immunity to magnetic or electrical disturbances. Belsterling (1970) comprehensively reviews a range of pneumatic back-pressure sensors and nozzle designs which researchers have developed and evaluated. Hall and Jones (1976) concentrate their efforts on one particular design, the 'cone-jet' sensor, which uses air as the working fluid as compared with Rubinshtein and Trubilov's (1958) earlier work which uses steam as the working fluid. Two problems, specific to the particular application, have emerged. These are:

1. The effective area of the target (the blade tips) presented to the jet of air is almost an order of magnitude less than the target area of a continuous surface such as a shaft or rotor disc. This small effective area results in a very weak measured back pressure versus clearance relationship.

2. The Mach number of the gas passing across the measuring nozzle affects the back pressure versus clearance relationship.

The cone-jet sensor initially appears very attractive due to its extended measuring range (when compared with the basic back pressure system), relative simplicity and potential robustness. Unfortunately, the above two problems effectively eliminate the technique as a viable gas turbine blade tip-to-casing clearance measuring system.

Researchers have developed various blade-tip clearance measuring systems which rely on the electrical capacitance formed between a casing-mounted insulated electrode and the rotor blade tips. Barranger (1978) describes improvements to a system in which the blade tip to electrode capacitance forms an element in a resonant LCR (inductance, capacitance and resistance) circuit. The resonant circuit's inductive component link is coupled via a 50 ohm impedance transmission line to a remote oscillator circuit. The oscillator output frequency is a function of the measured capacitance and hence the blade tip-to-casing clearance. However, the oscillator frequency is also a function of the resonant circuit's temperature in the measuring probe and the probe tip's temperature.

The capacitance to measure between an electrode and a blade tip is typically 1 to 10 pico-farads. However, the probe's total capacitance and connecting cable, which may be two orders of magnitude greater than the clearance-related capacitance, shunt this capacitance. Even relatively small temperature-induced changes in the probe and cable's standing capacitance will thus cause measurement errors which are many times greater than the distance-related capacitance. The system improvement which Barranger (1978) describes consists of switching a known complex impedance in parallel with the probe tuning elements whenever the system has stabilised at an operating temperature. Researchers observe the effect that switching a known complex impedance in parallel with the probe tuning elements has on the measurement and derive a correction factor for temperature-induced errors.

Knoell *et al.* (1981), in addition to considering the merit of electromechanical systems, describe a 'Coulomb-Probe', a direct-current polarised capacitance system. This system makes use of a guard electrode arrangement, similar in effect to that of the direct-current capacitance probe which Amsbury and Chivers (1978) described, in order to minimise temperature-induced changes in the probe and cable's capacitance and hence the errors in the tip clearance measurement. Although promising in compressor applications, direct-current polarised capacitance systems are unsuitable for turbine application. The combustion process results in ionised gas which passes through the turbine that in turn manifests itself as unwanted noise that reduces the measurement system's performance. Direct-current polarised capacitive systems are also unsuitable for application in large power generators due to direct current unipolar effects, and voltage offsets between rotor and stator in large machines which can disrupt direct-current capacitance clearance measurements.

Poppel (1979) has investigated a simple optical-based technique. The prime purpose of the research was to identify the technology base required to develop a compressor blade tip-to-casing clearance measuring technique which would provide

an input to a digital electronic gas turbine control system. The work showed that the measurement technique, although having a very limited range (less than 0.5 mm), would appear feasible in a compressor environment. However, the instability of such a long optical path length (approximately 150 mm) in a turbine environment due to refractive index variations, which extreme gas temperature and density gradients caused, would render the technique unusable.

TECHNIQUE EVALUATION AND SELECTION

Following the survey of previous work in the field of blade tip-to-casing clearance measurements, the author generated a short list of four techniques — two optical based, one microwave and one capacitive based. Chivers (1989) reports a complete analysis of the relative merits of the four techniques and concludes that a blade tip-to-casing clearance capacitive measurement was the most promising. Therefore, this chapter focuses on the development of the capacitive measurement technique.

The principle of this measuring technique is based upon the electrical capacitance variation which forms between an insulated electrode and the target rotor-blade tips. The survey of previous work described several partially successful systems based upon measurement of capacitance variation. We can consider the casing-mounted probe simply as a parallel plate capacitor. Neglecting the effects of fringing, the measured capacitance is related to the clearance by the relationship:

$$C = Er.Eo.A / d$$

where:

- C = capacitance in Farads;
- Er = relative permittivity of the dielectric between the electrodes;
- Eo = permittivity of free space in Farads/metre;
- A = electrode area in m^2 ;
- d = electrode separation in m.

We can determine the effective relationship between capacitance and displacement empirically. However, for the calibration to remain valid throughout the gas turbine operating envelope, the value of relative permittivity of the dielectric (air) must remain constant over a wide range of temperatures and pressures.

Alternatively, we must know the dielectric's relative permittivity at each gas turbine condition in order to apply a correction to the measured clearance. According to Kaye and Labey (1956), the relative permittivity of air minus one is proportional to density, assuming the constituents are non-polar permanent gases. We may express it as:

$(Er - 1)$ is proportional to pressure divided by the absolute temperature.

Table 2.1 gives the gas pressure/temperature relationships measured at eight locations through a gas turbine at sea level and on an ISA day for a civil gas turbine in the 220 kN (50,000 lbf) thrust class.

The author used this data to calculate the air’s relative permittivity at each of the eight gas turbine locations, Figure 2.3. The maximum value of permittivity of 1.00564 occurs at plane 4 (high-pressure compressor exit) and represents a permittivity deviation of 0.51% from the value at standard temperature and pressure (1.000536) and hence a maximum measurement error of 0.51% of reading. The minimum permittivity value of 1.00012 which occurs at plane 8 generates an error of less than 0.05% of reading when using a calibration derived at ambient temperatures and pressures. This performance is well within the target specification.

The considerations so far have assumed that the working fluid throughout the gas turbine has been air. We have not made allowance for fuel burning in the combustor, which affects the gas composition. Prior work in the field of combustion research has determined that a typical gas turbine exhaust from the hot nozzle contains the constituents by volume, Table 2.2 illustrates. The working fluid before and after combustion has taken place, practically, has an invariant value of electrical relative permittivity.

The simplicity of a capacitance based blade tip-to-casing clearance measuring system, combined with the capacitance sensor’s high operating temperature capability and the stability of the working fluid’s relative permittivity in a gas turbine context, makes this technique the preferred gas turbine blade tip-to-casing clearance measurement technique.

SYSTEM DESIGN CONSIDERATIONS

A frequency modulated oscillator offers the required necessary system characteristics, but only if it could incorporate a driven guard screen concept. Such a system could comprise the following elements:

Table 2.1. *Environmental conditions within a gas turbine at the critical locations engineers fit tip clearance measurement sensors.*

Location	Pressure (kPa)	Temperature (°C)
Fan entry	101	15
Fan exit	146	50
Intermediate-pressure compressor exit	693	253
High-pressure compressor exit	2856	536
High-pressure turbine entry	2696	1227
Intermediate-pressure turbine entry	1003	952
Low-pressure turbine entry	489	743
Low-pressure turbine exit	169	524

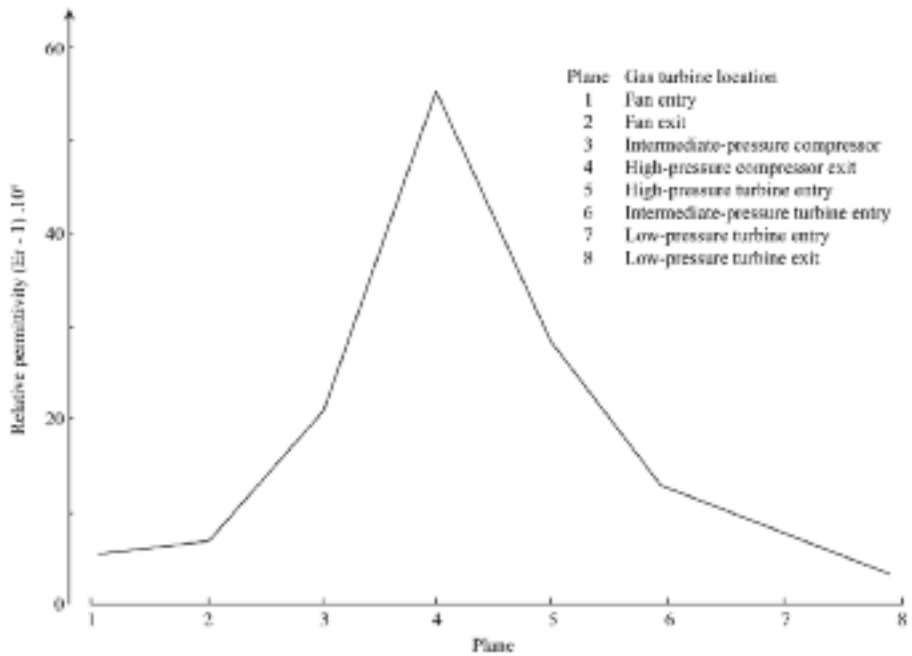


FIGURE 2.3. Variation of relative permittivity of air versus location through a gas turbine.

Table 2.2. *Combustion gas composition through a gas turbine's turbine.*

Gas	Composition (%)
Nitrogen	77
Oxygen	17
Carbon Dioxide	3
Water Vapour	2
Carbon dioxide, oxides of nitrogen and inert gasses	1
Total	100

1. A measuring probe which would be test-vehicle mounted and would contain the capacitance sensor and the oscillator, the frequency of which the capacitance variations and the circuitry necessary to drive the sensor guard screen would modulate.
2. A ground station remote from the test vehicle containing a demodulator, which would convert the oscillator's frequency variations into a varying analogue voltage, as well as circuitry for providing the oscillator's automatic frequency control.

3. An integrator to generate an electrical signal which would be a function of the measured compressor or turbine stage mean blade tip-to-casing clearance in the test vehicle.
4. A data collection and recording system capable of producing blade tip-to-casing clearance variation time history plots.

Figure 2.4 shows a schematic diagram of such a system. We now consider the factors affecting each system element's design, together with an examination of the system calibration requirements.

Measuring probe: sensor

The sensor electrode forms one plate of a variable capacitor, the value of which is the blade tip-to-casing clearance's required function. The rotor blade tips form the capacitor's second plate, which is of necessity electrically earthed to the test-vehicle

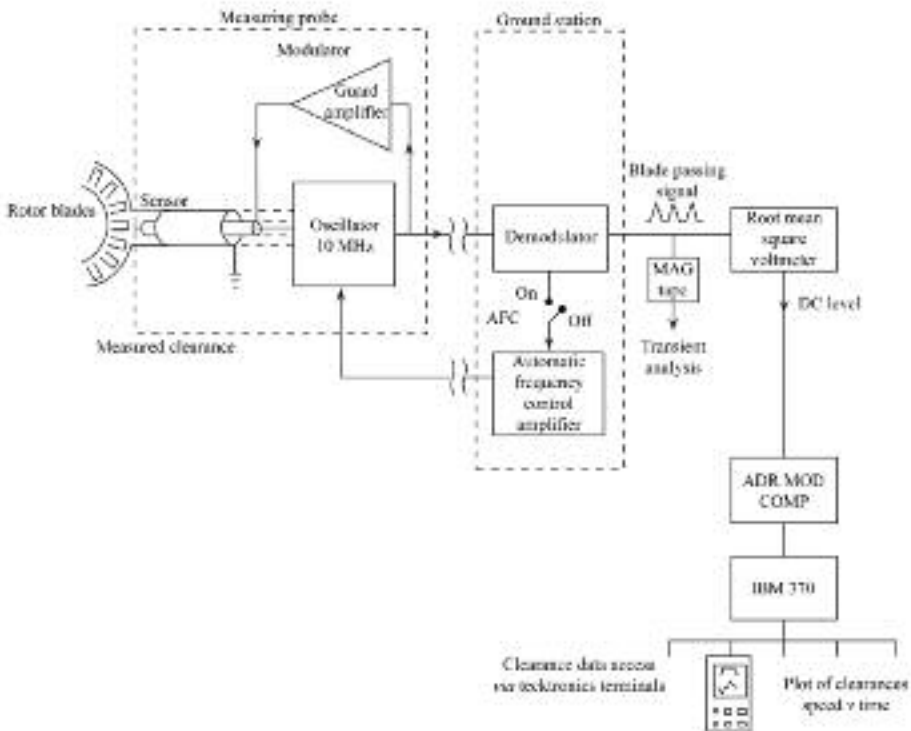


FIGURE 2.4. Frequency modulated driven guard capacitive clearance measurement system schematic block diagram.

casings via the bearings, seals and if present, gear trains. It is clear that the sensor electrode must be located in the compressor or turbine casing immediately above the rotor blades whose clearances we must measure. We must also electrically insulate the electrode from the casing in which it is mounted and must remain so under all temperatures and pressures which the test vehicle generates, assuming that we do not utilise slave cooling facilities (water or air from external sources). We can expect casing temperatures of typically 527°C and 827°C , respectively, in the gas turbine's high-pressure compressor and turbine.

Figure 2.5 shows a schematic diagram of a capacitance sensor. The proposed construction utilises an alumina bead insulator which is brazed into a metallic housing. An electrode is, in turn, brazed into the alumina insulator thus producing an all-brazed probe assembly with an electrode insulated from earth. The figure shows an alumina-insulated double-screened cable brazed into the probe tip assembly to connect the sensing electrode to the oscillator. The cable's outer screen is electrically earthed, but the inner screen is connected to the amplifier driving the guard circuitry.

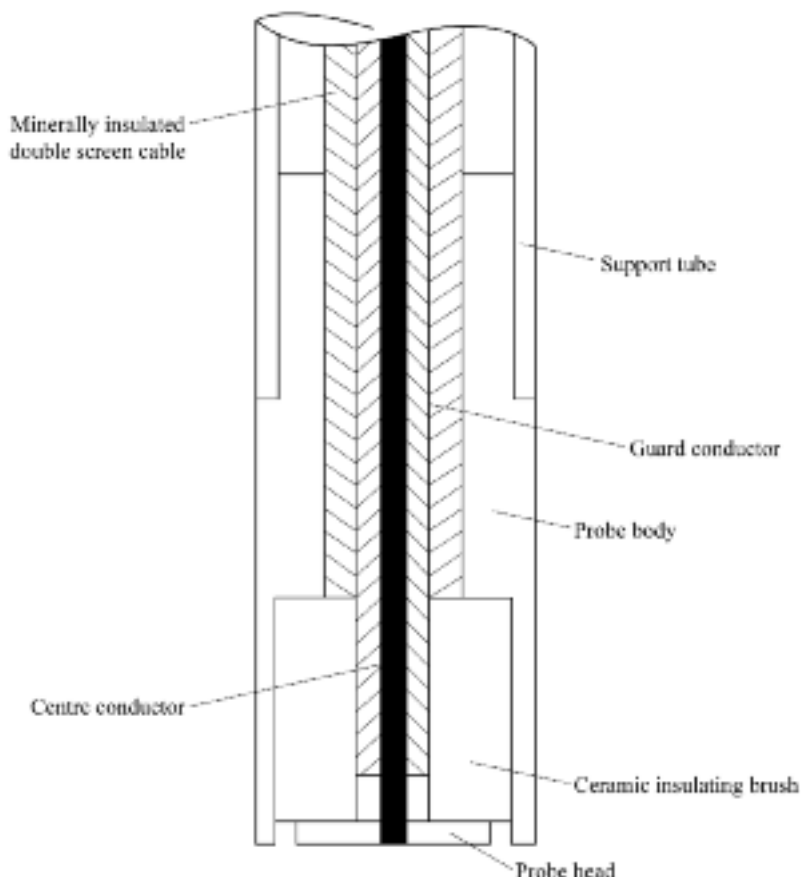


FIGURE 2.5. Capacitive clearance measurement system sensor schematic diagram.

The inner screen is terminated physically as close as practical to the sensing electrode, thus keeping to a minimum the value of non-varying shunt capacitance to earth.

Measuring probe: modulator

The measuring probe modulator comprises an oscillator and guard amplifier and is the most critical part of the blade tip-to-casing clearance measuring system. For this reason, we examine the modulator's behaviour in detail. The modulator's prime purpose is to transduce the capacitance variations which the sensing electrode detects as the rotor blades pass underneath, into a signal whose instantaneous frequency is a function of the instantaneous value of capacitance. Circuitry for powering the guard screen must form an integral part of the modulator circuitry if we are to realise the potential advantages of using a frequency-modulated transduction technique.

We must also incorporate additional circuitry for driving the oscillator signal along potentially long transmission lines in the modulator in addition to some form of voltage stabilisation to power the oscillator. The entire modulator will reside on the test vehicle and is thus subject to significant temperature transients. Thus, the modulator's thermal performance is of paramount importance.

THE OSCILLATOR

The oscillator circuit's function is to react to the capacitance variations which the rotor blades cause as they pass the sensing electrode. This reaction will take the form of the oscillator's change in frequency.

The author considered the suitability of various recognised oscillator designs for this application, including Colpitts, Hartley and Clapp. The author chose the Hartley design for development as the feedback network has only one capacitor which determines the oscillation frequency. Hence, in an application where only one capacitor is varied by a small amount, this circuit can have greater frequency sensitivity than any of the alternatives.

The author chose a 10 MHz frequency as optimum from consideration of the following combination of factors: sensitivity to capacitance changes, stability, circuit design layout and the ready availability of devices and circuitry to demodulate the frequency-modulated carrier containing the clearance data.

THE GUARD AMPLIFIER

Functionally, the guard amplifier must ensure that the instantaneous voltage between the sensing and guard electrodes is zero. Thus, the need is simply for a unity gain amplifier which is capable of powering a reactive load which the guard screen's total capacitance to earth represents.

The criteria for judging the amplifier design's efficiency were the voltage gain deviation and phase shift across the amplifier from values of 1 and 0 degrees, respectively. The amplifier needed an efficiency of at least 99% in order to reduce the probe's varying component shunt capacitance to a sufficiently small value (<2 pF), such that the automatic frequency control circuit can effectively maintain control of the carrier frequency. The author achieved this with a sensor design with a reactive load represented by a 180 pF capacitor at the previously chosen operating frequency of 10 MHz. When driving the reactive load at the operating frequency, the guard final amplifier design was able to achieve a voltage gain of 0.998 and a phase lag of 7 degrees. Effectively, in a driven screen configuration, the sensors 180 pF capacitive load reduced to only 1.8 pF. We can express the effective maximum reactive load of 180 pF in terms of a length of sensor alumina-insulated cable, typically 180 mm.

System calibration factors

The particular measuring probe/demodulator combination not only determines the absolute clearance versus system output voltage relationship (the system calibration), but is also a function of the application's geometry. The term 'geometry' includes the fundamental physical factors which affect the absolute value of capacitance measured, such as the rotor blade tips' measured thickness and the measuring probe sensor electrode area. However, less obviously, the blade tips' angle to the gas turbine axis, commonly called the blade stagger angle, and the relative spacing of the rotor's blades, affect the capacitance clearance measuring system's calibration.

The blade stagger angle and spacing do not affect the peak values of capacitance measured and hence the oscillator circuit's peak frequency deviation. However, in order to derive a mean value of clearance for a complete stage of rotor blades rather than individual blade clearances, as more generally required, a root mean square voltage converter averages the voltage pulses at the demodulator circuit's output. Hence, the demodulator output signal's form factor directly affects the measured root mean square value and therefore the system calibration. The demodulator's root mean square output was directly proportional to the blade pitch ratio's square root. Increasing the stagger angle effectively increases the blade pitch ratio by the angle's cosine.

The author went on to characterise the susceptibility of the oscillator and demodulator to changes in temperature. He also tested the first batch of measuring probes to quantify the effect of changing probe temperature on the measured blade tip-to-casing clearance. A hot air blower heated the probe electrode to a temperature of approximately 647°C whilst measuring a series of known clearances between the electrode and the blades on a model spinning rig. The heating of the electrode assembly had no measurable effect on the measurement of clearance.

However, heating of the modulator circuitry up to a maximum temperature of 97°C degrees by the same means produced an average reading error of -8% in measured full-scale clearance when the author did not activate the automatic frequency

control circuitry. Selection of the automatic frequency control restored and stabilised the oscillator's centre frequency and reduced the measurement error to an average value of less than -1.5% of full scale.

SYSTEM EVALUATION: COMPRESSOR

The author performed the first evaluation of the capacitive clearance measuring system in a real-world environment on a demonstrator gas turbine's high-pressure compressor. Although the measurement equipment was a prototype, there was an engineering need to obtain an understanding of the compressor's mechanical behaviour, particularly with respect to the relationship between surge margin and blade tip-to-casing clearance. As such, the first evaluation was also an application within which success with the prototype measurement system would provide a valuable insight into the compressor's mechanical behaviour. The objectives of the gas turbine test were as follows:

1. to validate the blade tip-to-casing clearance measurements which the capacitive clearance measurement system produced, and
2. if the measurement technique proved successful, to investigate the compressor blade tip-to-casing clearances and the casing movements which static displacement probes in conjunction with the other instrumentation measured for:
 - acceleration/deceleration manoeuvres;
 - hot re-slam (maximum acceleration from idle to take-off thrust rating);
 - casing distortions;
 - effect of 'A' frames (the structures through which the thrust of the gas turbine transmits to the aircraft); and
 - effect of fan out of balance.

The gas turbine compressor that the author instrumented was a six-stage axial flow design and initially the measurement requirement was to install clearance probes on the compressor's first and last stages. However, due to difficulties in physical access, the author reached a compromise with the development engineers and fitted four probes to stage 2 and fitted four probes to stage 5 of the compressor. The other instrumentation was required to measure metal temperatures, gas temperatures and displacements.

The stage 2 and stage 5 compressor tip clearance probe designs housed the modulator in an enclosure that is remote from the probe measuring electrode and connected to it by a 180 mm length of mineral-insulated cable, Figure 2.6. A fixing clamp mechanically locates the probe assembly as near as practical to the location of the rotor blade tip-to-casing clearance measurement. This minimises any measuring probe electrode movement relative to the casing to which it is attached.

Measuring probe electrode movement occurs as a consequence of material thermal expansion mismatches and thermal gradients. By mechanically locating the

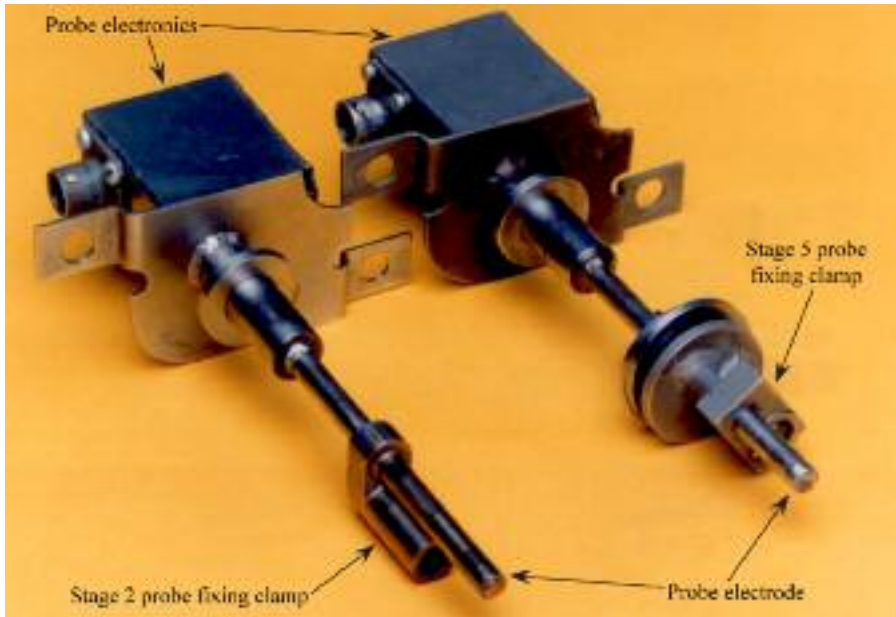


FIGURE 2.6. Prototype compressor stage 2 (left) and stage 5 (right) capacitive clearance measurement system probes.

probe assembly close to the probe electrode, the probe modulator is free to move both radially and axially in order to accommodate probe length changes with temperature and gas loading. This design feature is necessary as in a typical gas turbine installation the probe stem must pass through the compressor or turbine pressure casing that over the course of a gas turbine cycle does move relative to the probe electrode's location.

The measurement system's probes as designed had a measuring range of 2.5 mm. In order to obtain clearance measurements throughout the gas turbine operating envelope, it was essential that the cold static build clearance for each probe was set such that:

- the blade tips were at all times within the probes' operating range, and
- the minimum predicted probe to blade tip-to-casing clearance should be no less than 0.5 mm.

The above requirements resulted in a decision to mount the probes in the compressor casing with their sensing electrodes recessed into the abradable material which lined the casing over the rotor path. However, the engineers could not measure directly each probe's cold static build clearance once they fully assembled the compressor and fitted the capacitance probes to the casing. Consequently, it was not possible to measure the sensing electrodes recess into the abradable material. The author was able to measure the sensing electrodes recess indirectly by making a

series of drop-check measurements from nominated datum faces on the compressor casing to the blade tips of rotors 2 and 5 and to the probe mounting faces. Chivers (1989) describes the drop-check procedure in more detail. From these measurements, the author could calculate the absolute separation between each probe's sensing electrode and the rotor blades passing underneath and then calculate the sensing electrode recess.

The author assigned each measuring probe to a demodulator module to form a measurement system channel and then calibrated each channel to establish its particular clearance/voltage characteristic using the actual rotor blades as targets. He achieved this by mounting the bladed high-pressure compressor rotor, prior to its assembly into the compressor casing, in a framework referred to as a 'tip cropping fixture'.

For the purposes of calibrating the capacitance probes, the author simply used the fixture as a convenient means to spin the rotor whilst varying the distance between the probes and the blade tips. Subsequently, when engineers installed the probes in the compressor casing and used the calibration appropriate to the particular channel of probe/demodulator, the clearances as measured by the capacitance probes agreed closely (within 0.03 mm) with the physical drop-check measurements.

Test programme

Once the author confirmed the instrumentation operational, development engineers dry-cranked the gas turbine for 2 minutes, reaching approximately 25% speed (2500 revolutions per minute). This indicated that he had correctly located all probes and they were operational. The author noted the measured clearances as the datum values against which he compared all other measurements.

The next step in the test schedule was to supply fuel to the gas turbine, ignite it and reach a ground idle condition. Engineers achieved this with no further problems, after which they shut down the gas turbine and allowed it to cool. During a subsequent dry crank, the author repeated the datum tip clearance measurements.

Development engineers then took the gas turbine through an abbreviated version of a production pass-off schedule. This consisted of rapid accelerations, decelerations and hot re-slams. Throughout this testing the capacitance probes gave credible results. The next item on the test schedule consisted of operating the gas turbine through a number of simulated flight cycles. These consisted of setting the gas turbine sequentially at thrust levels consistent with those that pilots use for take-off, climb, cruise, descent, approach, landing, reverse thrust and idle.

The final test schedule items subjected the gas turbine to a series of soak-back tests, hot re-slam accelerations and fuel spike tests. The intention of the fuel spike testing was to determine the compressor's surge margin by progressively increasing the fuel volume injected into the gas turbine in a single shot. The probes all survived the surge shock. Development engineers de-rigged the gas turbine from the test bed with all probes fully operational after nearly 15 hours of gas turbine running time.

Discussion of results

Unfortunately, no experimental tip clearance data was available from previous tests against which the author could compare and validate the capacitance probe results. This exercise represented the first time that a researcher had attempted continuous measurement of tip clearances on a gas turbine compressor. The validation of the experimental data was thus confined to comparison of the test results with predictions of tip clearance variations for simple manoeuvres of which the author was highly confident.

The author examined simple gas turbine accelerations and decelerations between ground idle and maximum take off thrust for both compressor stages and calculated the constituent growths. The author assumed that if the experimentally obtained data was in close agreement with the theoretically derived data under these circumstances, the experimental data that he derived from manoeuvres which did not lend themselves to confident theoretical analysis would be accurate. The author used the gas turbine rotor path temperature measurements to evaluate approximate casing thermal growths.

The author obtained blade and disc centrifugal growth factors from a Rolls-Royce theoretical model and scaled by the rotor speed squared to give predicted centrifugal growths. The author also obtained blade and disc thermal growth curves from a second Rolls-Royce theoretical model and when combined with rotor centrifugal and casing thermal figures, he obtained a prediction of blade clearance variations against time. Figure 2.7 shows a plot of the four measured tip clearances against time for compressor stage 5 during a gas turbine deceleration from maximum take off thrust to ground idle. The dotted line shows the calculated predicted variation with time of tip clearance for the same manoeuvre. The agreement between prediction and measured results in this example and in all the other cases that the author examined was good.

This chapter does not present all the data that the author collected during the investigation as the majority of it is not relevant to the evaluation of the capacitive clearance measurement system. Various restricted internal Rolls-Royce reports contain the full presentation and analysis of the test data.

Figure 2.8 shows a typical plot of blade tip-to-casing clearance data and serves to show clearly the factors which affect it. The author obtained the data when the gas turbine operated through the simulated flight cycle. The top trace represents the gas turbine high-pressure rotor speed plotted against time on the x-axis. It identifies eight distinct phases: take-off, climb, cruise, descent, approach, landing, reverse-thrust and ground idle. The plots below the speed trace represent the tip clearances for stages 2 and 5 to the same time-base as the speed plot.

During the gas turbine's first acceleration, as the high-pressure rotor speed increases there is an initial reduction in tip clearances due to the rapid centrifugal growth of the discs and blades exceeding the casing's thermal growth. As the casing's thermal response is faster than that of the rotor, the tip clearances then increase, generally reaching values greater than the cold build clearances. At around

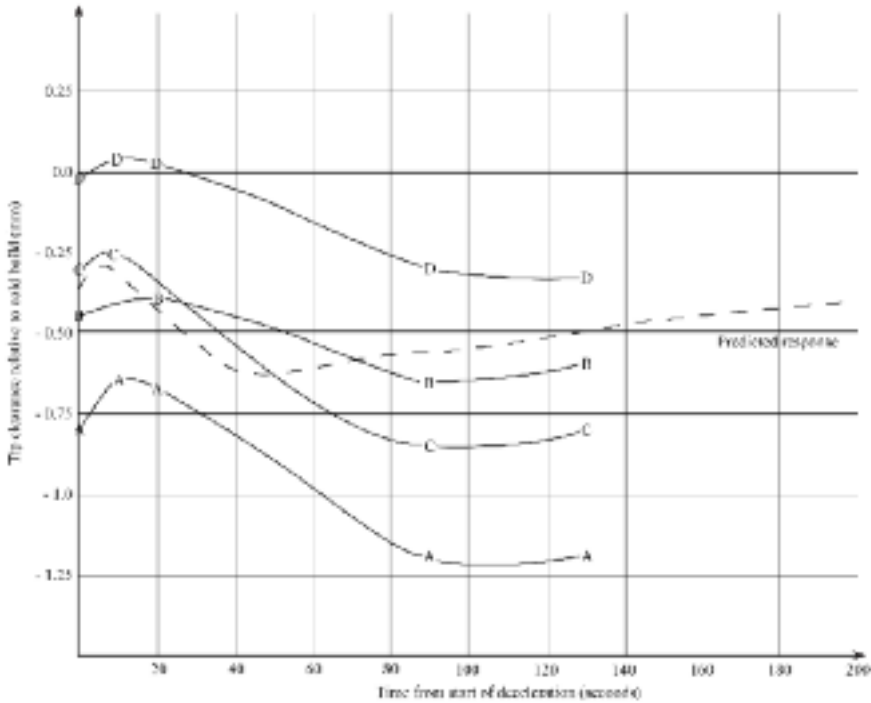


FIGURE 2.7. Comparison of compressor stage 5 predicted and measured blade tip-to-casing clearance.

40 seconds from the start of the acceleration, the rate of the disc bores' heating allows the disc rims to grow at a faster rate than the casing. After 60 seconds, the casing temperatures fully stabilise and the tip clearances gradually reduce as the bores reach stabilised conditions and allow full growth of the disc rims.

The tip clearances data which the author obtained during the gas turbine deceleration show the opposite effects. An initial increase in tip clearance as the centrifugal growth of the discs and blades reduces directly with speed. This is followed by a decrease in clearances as the casing cools and contracts faster than the rotor and, finally, a gradual increase in clearance again as the disc bores cool and restrain the disc rims.

The gas turbine's hot re-slam acceleration typically occurs on selection of reverse thrust on landing, resulting in the occurrence of minimum tip clearances due to a combination of hot rotor discs and cool casings.

During the gas turbine testing, whilst the author recorded root mean square output from each clearance measurement channel, the author also monitored the probe's blade passing signals at the demodulator output using an oscilloscope. At rotor speeds of less than 70%, the blade height profile was quite flat apart from the two cropped blades. At speeds above 70% gas turbine high-pressure rotor design speed

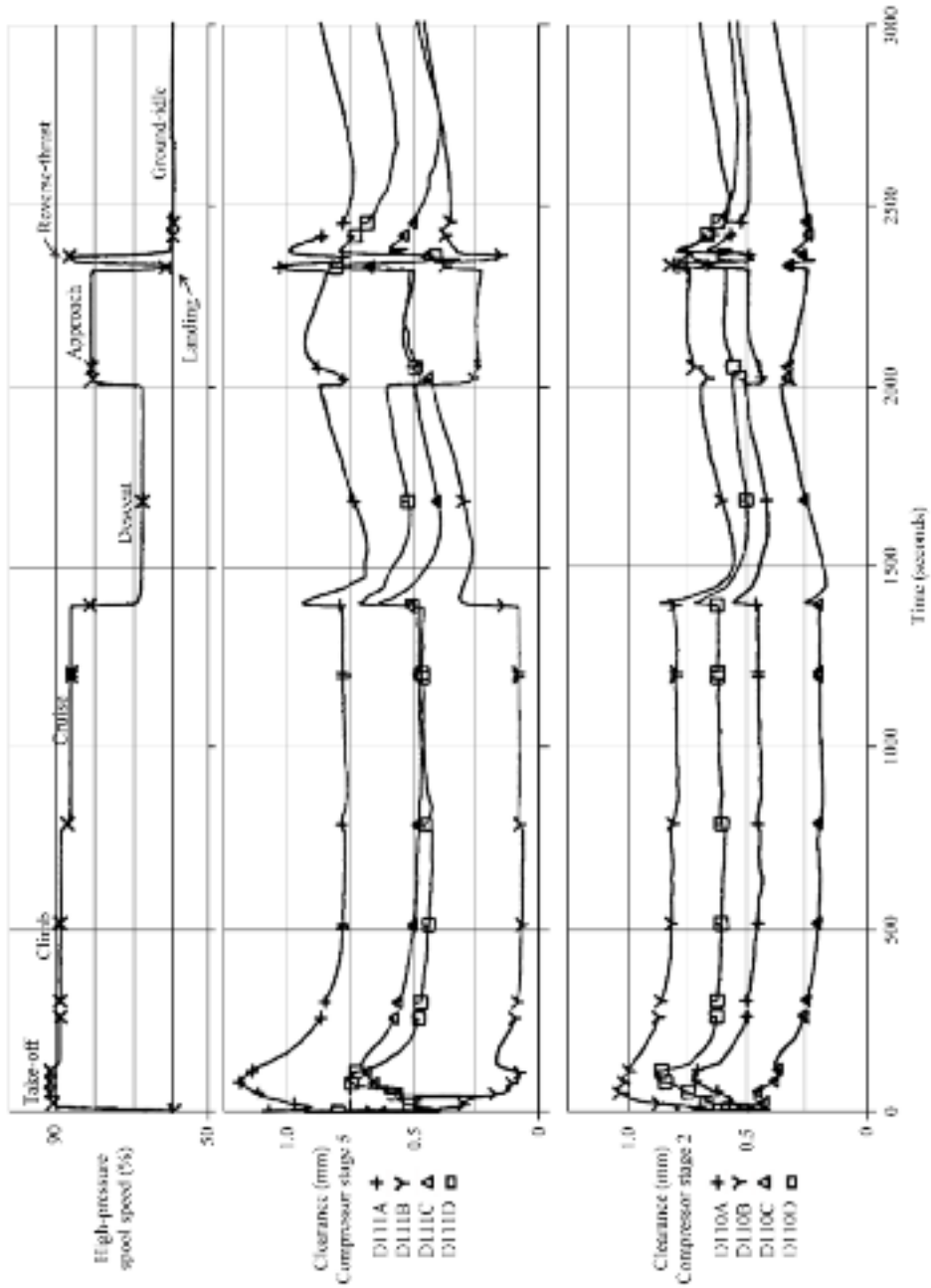


FIGURE 2.8. High-pressure compressor blade tip-to-casing clearance measurements obtained during a flight cycle.

during the gas turbine test, the blade height profile occasionally changed to a sinusoidal nature. This cyclic variation had two modes:

- the cyclic blade height profile was synchronous with high-pressure compressor speed and occurred at a rate of once per revolution. The profile thus appeared stationary when triggering the oscilloscope from the same point on the rotor;
- the cyclic blade height profile was still evident, but a lower frequency movement modulated it, approximately first order low-pressure rotor speed frequency or half high-pressure rotor speed frequency.

In all cases, the author estimated the blade height profiles' modulation amplitude as equivalent to a clearance variation of less than 0.15 mm.

SYSTEM EVALUATION: TURBINE

Following the successful use of the capacitive clearance measuring system on a gas turbine high-pressure compressor, the author moved on to make turbine blade tip-to-casing clearance measurements. This data would provide a method of verifying mathematical modelling of the turbine and shroud segment transient movements. The instrumentation specification required the radial and axial movement measurements of both the high-pressure and intermediate-pressure turbine blade tips. The author required axial tip movement measurements, in addition to the radial measurements, because the blade tips were not parallel to the gas turbine centreline.

In order to fully understand these axial and radial displacements, in addition to the tip clearance measurements, the experiment required the measurement of approximately 200 temperatures, of both metal and air, and the measurement of casing-to-compressor disc axial movement.

Both the high-pressure and intermediate-pressure turbine blades in the gas turbine under investigation were of a shrouded design. Each high-pressure blade has an aerodynamic feature, or 'fence', which provides, by chance, an almost perfect target for the capacitance probes, similar to the un-shrouded compressor blade tips.

The intermediate-pressure turbine blade tip design, however, is different in that the fence is missing and it substitutes three circumferential sealing fins. The adopted solution consisted of removing completely the central sealing fin from each blade tip and brazing in its place a fence-like plate.

The major consideration in the adaptation of the high-pressure compressor design of capacitance probe for use in a turbine environment was the higher temperatures. The two areas of concern were:

- The integrity of the measuring probe sensor. The author estimated the braze's maximum working temperature at 677°C, which he used to assemble the alumina bead insulator to the sensing electrode and the probe body. This

compares with expected casing metal temperatures of 827°C and gas temperatures of 1227°C.

- The author designed the measuring probe modulator circuitry to operate reliably up to a maximum temperature of 97°C. The under-cowl temperatures in the gas turbine's turbine region could be as high as 227°C.

The proposed solution to the anticipated temperature problems consisted of cooling the measuring probe sensor with high-pressure air which would surround the brazed assembly before venting into the turbine gas path. This cooling would have the additional benefit of protecting the insulating surface from possible contamination by combustion products. A jacket surrounding the modulator supplied with cold water cooled it. The requirement was for a total of ten radial tip clearance measurements, five from the high-pressure turbine and five from the intermediate-pressure turbine.

The final probe design was similar to that which the author used in the compressor testing, with the probe electrode connected to the probe electronics by 180 mm of mineral-insulated cable, Figure 2.9. Unlike the compressor probes, the turbine probes did not utilise a fixing clamp. The constraints imposed by the turbine environment made it impossible to fit a fixing clamp close to the probe electrode, and therefore the author needed an alternative method of facilitating thermal growth whilst locating the probe electrode against the turbine liner. The adopted solution was to install the probe in a water jacket, with a spring between the end of the probe and the water jacket. The spring force kept the probe located against its seating location on the turbine shroud segment with a force of 36 Kg. This arrangement allowed

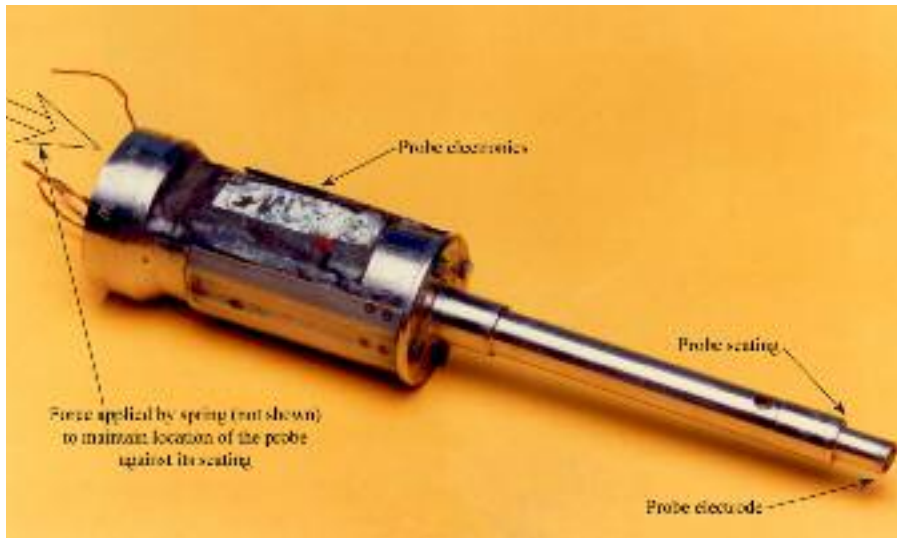


FIGURE 2.9. Prototype turbine capacitance probe, installed in both high-pressure and intermediate-pressure turbine stages.

for differential radial movements to occur between the turbine casing and the shroud segment.

As in the evaluation of the gas turbine compressor's system, the author had to calibrate the capacitance probes with the assigned demodulators against the particular target blades. Prior to completion of the gas turbine build the calibration of the five intermediate-pressure turbine capacitance probes was possible using the actual gas turbine intermediate-pressure turbine rotor as the target. Subsequent intermediate-pressure probe calibrations would have been impossible due to lack of access to the intermediate-pressure turbine. The design and manufacture of a dedicated capacitance probe calibration rig resolved the problem. The rig comprised a variable speed electric motor driving a shaft arrangement mounted in precision bearings. The author could attach a variety of aluminium discs to this shaft into the circumference of which were previously machined pseudo blade-tip profiles.

Before the author accepted the rig for the routine calibration of capacitance probes, he compared the calibrations derived from actual gas turbine rotor hardware with calibrations that he obtained using the purpose-made calibration discs. Without exception, the differences between the calibrations that he obtained using the two techniques were well within the calculated experimental error (less than 0.02 mm). Thus, he did not have to use the actual gas turbine hardware to calibrate the capacitance probes. This validated the introduction of a far more operationally acceptable calibration procedure using the calibration rig.

Before he fitted the capacitance probes to the gas turbine, the author performed dimensional drop-checks of a similar nature to those carried out on the compressor on the turbines. In order to generate signals from the capacitive clearance measurement system after probe installation in the gas turbine, the author needed to rotate both the high-pressure and intermediate-pressure turbines at a speed of approximately 60 revolutions per minute.

The spin checks demonstrated that the probes' radial movement measurement, achieved by the insertion of different thickness spacing washers, was accurate. These results indicated that the individual measuring probe calibrations were correct and that the absolute clearances that the measuring probes indicated were also correct. The generally undesirable non-linear clearance probe calibration characteristic proved very useful in this calibration validation exercise.

After the author had rigged the gas turbine on the test bed and connected the capacitance probes to the demodulators, he performed a number of dry cranks to confirm that all the instrumentation was fully operational. This was followed by starting the gas turbine and acquiring blade tip-to-casing clearance data from ground idle to maximum take off thrust to verify that both the gas turbine and the capacitive clearance measurement system were functioning as expected. The test schedule then put the gas turbine through square cycles (accelerations from ground idle to maximum take of thrust and back to ground idle) and simulated flight cycles as the author used in the gas turbine high-pressure compressor testing. Throughout this testing, the author continuously monitored the temperature of all the electronic modules in both the radial and axial movement measuring probes to ensure that overheating did not

occur. The maximum recorded temperature within any of the capacitance probes was 47°C, a figure which was sufficiently low to justify the choice of water as the cooling fluid as opposed to air.

Following the completion of the test schedule's blade tip-to-casing clearance measurement, the capacitance probes remained in the gas turbine for a further 59 hours of testing before the author finally stripped the gas turbine and removed the probes. All the capacitance probes were fully operational at this time.

Discussion of results

As with the testing of the capacitive clearance measurement system on the high-pressure compressor, the author recorded a substantial quantity of data. Figure 2.10 shows typical plots of capacitive clearance measurement system output for the high-pressure turbine.

During acceleration of the gas turbine to a stabilised maximum condition, the turbine radial blade tip-to casing clearances decrease very rapidly due to the rotor blades' and disc's centrifugal growth. The turbine casings then begin to heat up and increase in diameter at a faster rate than the turbine discs, so causing a temporary increase in clearance followed by a decrease to its stabilised condition. Deceleration of the gas turbine results in the opposite effects. Removal of the centrifugal loading causes a rapid increase in clearance as the blades and discs relax. The turbine casings have a lower thermal mass than the turbine discs and cool more quickly than the discs which causes a decrease in clearance followed by an increase back to the stabilised condition.

The author also analysed high-pressure and intermediate-pressure turbine blade tip-to-casing clearance data to show how the rotors' eccentricity in the casings varied with time and gas turbine condition. In so doing, the author was able to obtain a measure of the degree of casing roundness. The author used a computer program to obtain circle fits from the probe data. Using the rotor as a datum, the program then fitted the best circle through the shroud positions as indicated by the capacitive clearance measurement systems.

CONCLUSIONS

The author designed, developed and evaluated the capacitive clearance measurement system both in the laboratory and on two gas turbines. The data that he collected during the testing of the measurement technique on the gas turbines at Derby was of particular importance to Rolls-Royce. This is because it represented the first occasion on which experimental transient gas turbine blade tip-to-casing clearance data had been made available. The quantity and quality of data that the author obtained during the compressor and turbine testing demonstrated a significant advance both in experimental measurement techniques and the understanding of the gas turbine mechanical structures' transient behaviour.

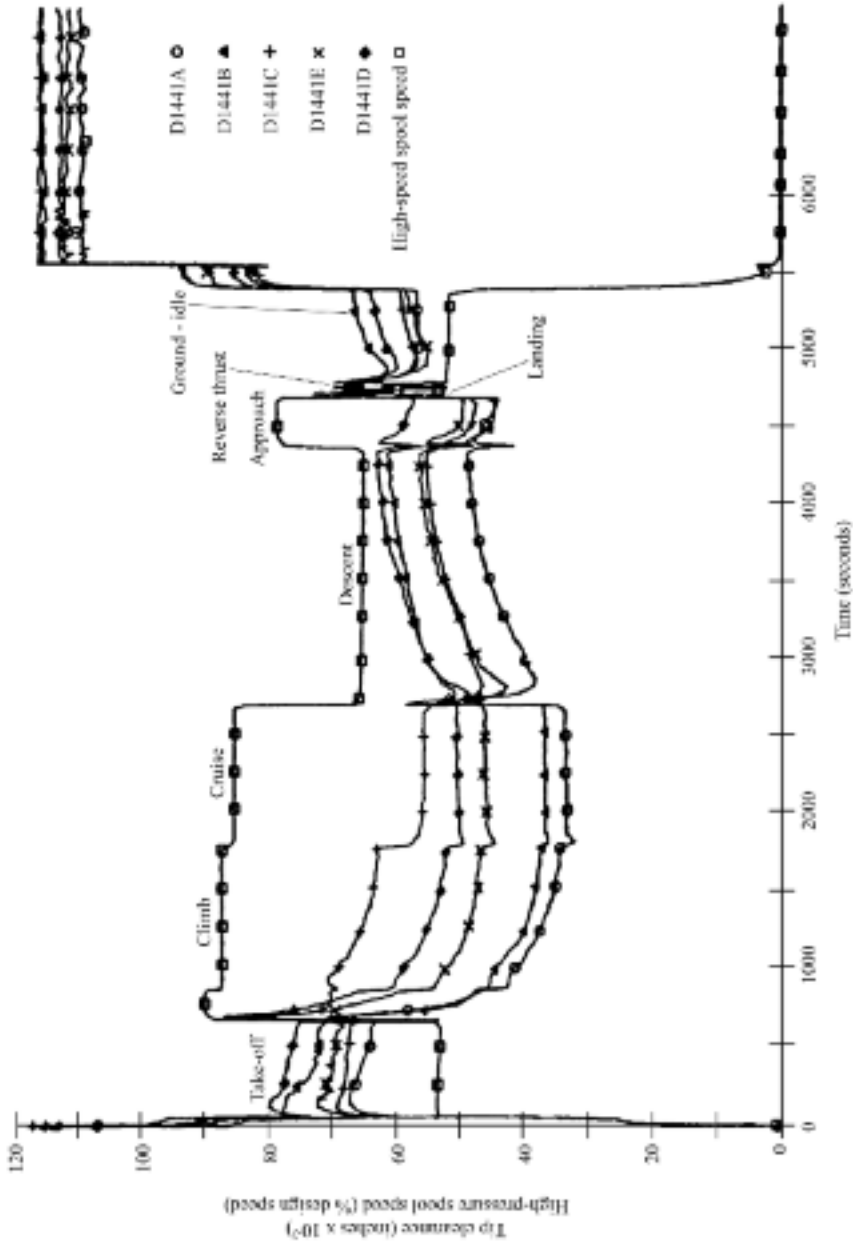


FIGURE 2.10. High-pressure turbine blade tip-to-casing clearance data obtained during a flight cycle.

The validation of the blade tip-to-casing clearance data that the capacitive clearance measurement system generated proved to be difficult as, at the time of the evaluation, there was no reliable alternative tip clearance measurement technique available against which the author could compare the results. However, by means of laboratory simulations, careful comparison of gas turbine build drop-check clearances with measured clearances, comparison of casing rub patterns visible on gas turbine strip with zero clearance indications during gas turbine testing and comparison of measured clearances with model predictions, it was possible to validate the measurement technique. The capacitive clearance measurement system's performance proved to have either equalled or bettered the original requirement specification in all cases. Rolls-Royce has subsequently adopted the capacitive clearance measurement system as the standard technique for blade tip-to-casing clearance measurement in compressors and uses it preferentially in turbines where the blade-tip geometry is suitable. The system has proved relatively inexpensive to manufacture and operate, particularly in comparison with some of the laser-based optical measurement techniques, and it is easy to operate and maintain.

REFERENCES

- Amsbury, C.R. & Chivers, J.W.H. (1978), 'System for the Measurement of Rotor Tip Clearance and Displacement in a Gas Turbine'. *AGARD Conference Proceedings, Seal Technology in Gas Turbine Engines*, vol. 234.
- Baker, L.C., Grady, G.E. & Mauch, H.R. (1978), 'Turbine Tip Clearance Measurement'. USARTL-TR-78-4.
- Barranger, J. (1978), 'An In-Place Recalibration Technique to Extend the Temperature Capability of Capacitance-Sensing Rotor Blade Tip Clearance Measuring Systems'. *Society of Automotive Engineers Aerospace Meeting*. San Diego, USA, Paper No. 781003.
- Barranger, J.P. & Ford, M.J. (1981), 'Laser Optical Blade Tip Clearance Measurement System'. *Transactions of the ASME, Journal of Engineering for Power*, vol. 103, pp. 457–60.
- Belsterling, C.A. (1970), 'Sensing with Air'. *25th ISA Conference*. Philadelphia, USA.
- Chivers, J.W.H. (1989), *A Technique for the Measurement of Blade Tip Clearance in a Gas Turbine*. PhD thesis, University of London.
- Davidson, D.P., De Rose, R.D. & Winnerstrom, A.J. (1983), 'Measurement of Turbomachinery Stator to Drum Running Clearances'. *Proceedings of the 28th American Society of Mechanical Engineers Gas Turbine and Aeroengine Congress*. Phoenix, Arizona, 27–31 March, Paper No. 83-GT-204.
- Drinkuth, W., Alwang, W.G. & House, R. (1974), 'Laser Proximity Probes for the Measurement of Turbine Blade Tip Running Clearances'. *Proceedings of the ISA Aerospace Instrumentation Symposium*. Paper No. 74228, pp. 133–40.
- Ford, M.J. (1980), 'Clearance Measurement System'. Report NASA CR 159402.
- Freeman, C. (1985), 'Effect of Tip Clearance Flow on Compressor Stability and Engine Performance'. *Von Karman Institute for Fluid Dynamics Lecture Series 1985–05, Tip Clearance Effects in Axial Turbomachines*.

- Hall, L.C. & Jones, B.E. (1976), 'An Investigation into the Use of a Cone-jet Sensor for Clearance and Eccentricity Measurement in Turbo Machinery'. *Proceedings of the Institution of Mechanical Engineers 1847-1982*, vol. 190, pp. 23-30.
- Hardy, H.D. (1972), 'Use of Laser-powered Optical Proximity Probe in Advanced Turbofan Engine Development'. *Symposium on Airbreathing Propulsion, Progress in Astronautics and Aeronautics*, vol. 34.
- Kaye, G.W.C. & Labey, T.H. (1956), *Tables of Physical and Chemical Constants*. Longman's Green & Co., London.
- Knoell, H., Schedl, K. & Kappler, G. (1981), 'Two Advanced Measuring Techniques for the Determination of Rotor Tip Clearance during Transient Operation'. *Fifth International Symposium on Airbreathing Engines*. Bangalore, India.
- Poppel, G.L. (1979), *Analysis and Preliminary Design of an Optical Digital Tip Clearance Sensor for Propulsion Control*. Report NASA-CR-159434.
- Rubinshtein, Ya.M. & Trubilov, M.A. (1958), 'A Steamjet Method for Measuring Clearance in Steam Turbines'. *Teplotenergetika*, vol. 5, pp. 68-74.
- White, S.D. (1977), 'Turbine Tip Clearance Measurement'. USARTL-TR-77-47.

Blade-by-blade Tip Clearance Measurement

A.G. Sheard

ABSTRACT

This chapter describes a capacitance-based tip clearance measurement system which engineers have used in the most demanding turbine test applications. The measurement system's probe has survived extended use in a major European gas turbine manufacturer's high temperature demonstrator unit, where it functioned reliably at a turbine entry temperature in excess of 1527°C. This chapter explores blade-by-blade tip clearance measurement techniques and examines probe performance under laboratory conditions in support of high temperature installations. The chapter outlines the blade-by-blade tip clearance measurement technique and describes the experimental facility which the author used to study tip clearance measurement. The chapter also fully describes calibration methods to ascertain measurement accuracy.

The chapter clarifies how the author overcame practical problems with measuring blade-by-blade tip clearance in both compressor and turbine environments. Since its initial development, gas turbine development programmes have routinely used the clearance measurement system. The system's inherent robustness has resulted in reliable blade tip-to-casing clearance in-service measurement in real-world applications.

INTRODUCTION

This chapter presents a study that the author initiated to demonstrate that a capacitance clearance measurement system utilising a frequency modulated driven guard operating mode can make accurate blade tip-to-casing clearance measurements over every blade in a compressor or turbine. Chivers (1989a) originally developed the capacitive clearance measurement system to measure average tip clearance over a gas turbine compressor and turbine's blades. This chapter reports the study results that established the accuracy with which Chivers' (1989a) capacitive clearance

This chapter is a revised and extended version of Sheard, A.G. (2011), 'Blade-by-blade Tip Clearance Measurement'. *International Journal of Rotating Machinery*, vol. 2011, Article ID 516128, pp 1-13.

measurement system could make a blade-by-blade measurement of blade tip-to-casing clearance in a laboratory environment.

Stringfellow *et al.* (1997) presented an enhanced version of Chivers (1989a) capacitive clearance measurement system. Müller *et al.* (1997) used the system to measure blade-by-blade tip-to-casing clearance in the compressor and turbine of a BR700 development gas turbine. BMW and Rolls-Royce plc developed the Rolls-Royce BR700 family of engines through the joint venture company BMW Rolls-Royce GmbH to power regional and corporate jets.

Müller *et al.* (1997) validated Stringfellow *et al.*'s (1997) capacitive clearance measurement system by analysing the blade-by-blade data and comparing it with a measurement of minimum tip clearance made using Sheard and Turner's (1992) electromechanical clearance measurement system. Müller *et al.* (1997) calculated the average blade tip-to-casing clearance and found it larger than the minimum clearance, Figure 3.1, a difference that they concluded was self consistent with the variation in the blade lengths that they recorded during the gas turbine build, plus the known bearing clearance.

Gill *et al.* (1997) evaluated Stringfellow *et al.* (1997) and Chivers (1989a) capacitive clearance measurement systems, fitting both to the stage-one turbine of the same General Electric MS6001FA industrial gas turbine. Despite commercial restrictions, Gill *et al.* (1997) observed that the MS6001FA firing temperature was 1288°C. Gill *et al.* (1997) concluded that Stringfellow *et al.*'s (1997) measurement system was both viable in larger industrial gas turbines, and more sensitive to clearance changes with better range than Chivers' (1989a) original measurement system.

Gill *et al.*'s (1997) aim was to utilise Stringfellow *et al.*'s (1997) capacitive clearance measurement system in an active blade tip-to-casing clearance control system utilising Sheard and Lawrence's (1998) capacitance probe design. The closed loop active clearance control system modulated cooling air to cool or heat the turbine casing, causing it to shrink or expand, thus maintaining a minimum safe gap between stage-one turbine blades and casing. Ramachandran and Conway (1996) noted that a critical casing design feature was the optimisation of 'thermal mass' size and location to minimise casing 'ovalisation' as it heats from ambient to running temperature, facilitating the active control of turbine blade tip clearance.

This chapter presents an extension of Chivers' (1989a) original capacitive clearance measurement system to first, facilitate the measurement of blade tip-to-casing clearance over every blade and second, establish the accuracy with which one can make a blade-by-blade measurement of clearance. The author conducted the experimental programme in a laboratory environment. The reader should, however, bear in mind that the author made no changes to the capacitance probe that would affect its ability to withstand the environment in the high-pressure turbine which Chivers (1989b) had already proven. Sheard (1989) characterised the high-pressure turbine environment and observed that a turbine entry temperature of 1200°C was representative of a large turbines' turbine entry temperature at the time Chivers (1989b) conducted his research.

Chivers (1989b) first studied the variation in average blade tip-to-casing clearances that occur as a consequence of internal gas turbine thermal effects using a

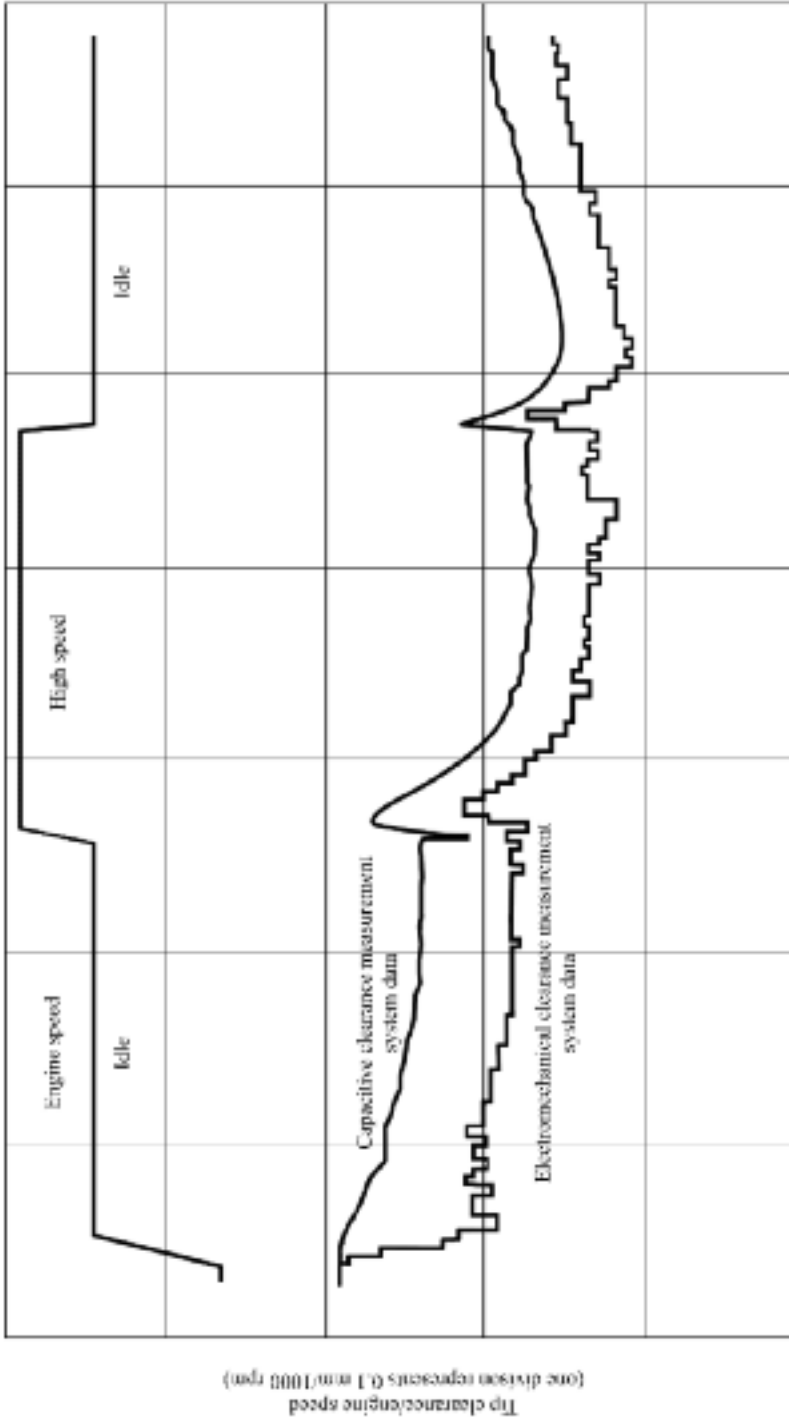


FIGURE 3.1. Trends in tip clearance. Measured by Müller *et al.* (1997) using an electromechanical clearance measurement system (Sheard and Turner, 1992) and capacitive clearance measurement system (Stringfellow *et al.*, 1997) in the high-pressure turbine of a BMW Rolls-Royce GmbH BR700 development gas turbine.

capacitive clearance measurement system. For the first time, Chivers (1989b) made continuous measurements of average blade tip-to-casing clearance on a gas turbine compressor and turbine. Chivers' (1989b) results indicated that average blade tip-to-casing clearance varied in two ways:

1. low frequency variations occurring over an entire gas turbine cycle due to thermal effects; and
2. high frequency sinusoidal variations.

Chivers (1989b) attributed the high frequency sinusoidal variations at the once per revolution frequency to bearing clearance. Chivers (1989b) was able to compensate for the effects of bearing clearance, identifying compressor disc and casing natural frequencies by fitting a total of four capacitance probes around a single compressor stage. By studying the phase relation between the outputs, he was able to identify disc and casing vibration modes. The maximum peak-to-peak variation of average tip clearance measured at 0.15 mm when the gas turbine encountered a compressor disc or casing natural frequency, which the capacitive clearance measurement system was able to resolve.

There is extensive published material available on blade tip-to-casing clearance measurement systems that can measure clearance over every blade in a compressor or turbine stage. The most commonly used technique is optical triangulation, as Drinkuth *et al.* (1974), White (1977), Baker *et al.* (1978), Barranger and Ford (1981) and Ford (1980) describe. Optical clearance measurement systems work reliably in a manufacturing environment (Sheard, 1993; Sheard *et al.*, 1994). However, the complexity and physical size of these systems has historically made them difficult to install and they have proven unreliable in high temperature and vibration environments such as those in a gas turbine.

The capacitance probe is an inherently rugged device, and therefore has been the subject of study in the past. Barranger (1978) described improvements to a frequency modulated type capacitive clearance measurement system, utilising the probe-to-blade-tip capacitance in a resonant inductance, capacitance and resistance circuit (an oscillator). The oscillator's output frequency was a function of measured capacitance. The principal drawback of Barranger's (1978) system was that the probe's connecting cable capacitance was typically two magnitude orders greater than the 1 to 10 pico-farad capacitance between probe and blade tip. Even relatively small temperature changes in the probe and connecting cable resulted in a change in the capacitance readings, making a reliable measurement of blade tip-to-casing clearance difficult.

Knoell *et al.* (1981) developed a direct-current (DC) polarised capacitance probe which used a guard electrode arrangement to minimise temperature effects. This system still suffered from temperature drift and additionally, was only suitable for use in a compressor due to its susceptibility to 'flame noise'. The combustion process ionises combustion products leaving the combustor. Ionised gases are attracted to the electrically charged plate that comprises the front face of a direct-current polarised capacitance probe. The ionised gases result is the sensor registering

an unsteady electrical signal that is not associated with any physical change in blade tip-to-casing clearance. The change in signal occurs as a consequence of the ionised combustion products, and constitutes unwanted noise, generally referred to as flame noise.

FM CAPACITANCE PROBE PRINCIPLE OF OPERATION

Chivers' (1989a) capacitive clearance measurement system, unlike Barranger's (1978) system, utilised a 'driven screen' to overcome the problem of probe and connecting cable capacitance. The frequency modulated capacitive clearance measurement system, Figure 3.2, comprises a probe that incorporates an oscillator and guard amplifier and a ground station that incorporates a demodulator and root mean square voltmeter. This root mean square voltmeter provides an output voltage that relates to average tip clearance via a calibration. Chivers (1989a) describes in detail the probe sensor, oscillator and guard amplifier, thus we will only touch upon them briefly here.

The probe sensor forms one plate of an oscillator's capacitor, connected to the other components in the oscillator via the centre wire of a tri-axial cable. The oscillator's function is to react to the change in capacitance that arises as a consequence

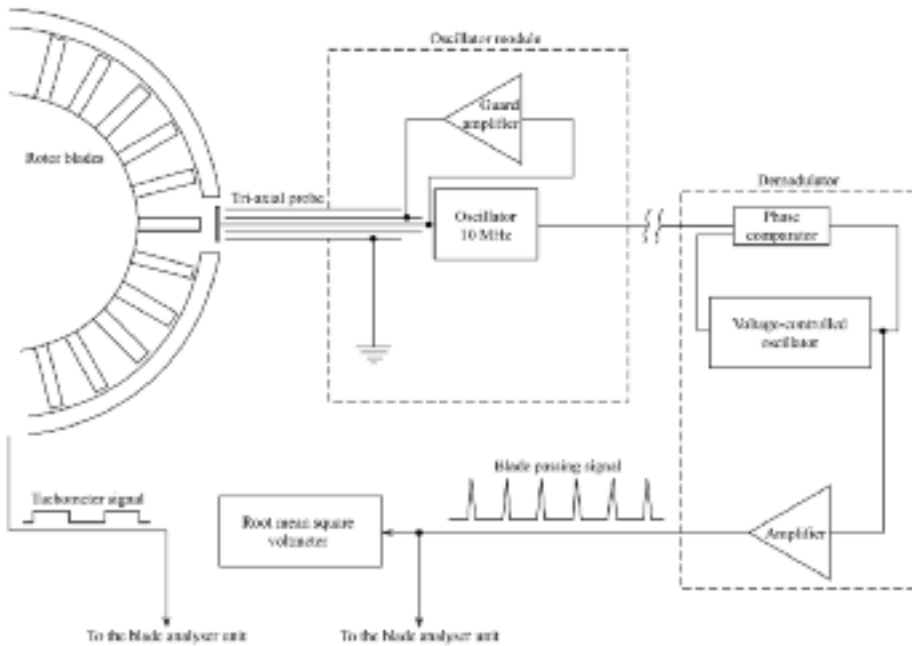


FIGURE 3.2. Frequency modulated driven guard capacitive clearance measurement system schematic block diagram.

of blade passing. The reaction takes the form of varying the oscillator output frequency so that it corresponds to the instantaneous capacitance measured at the probe tip. Chivers (1989a) chose a Hartly oscillator design operating at an optimum frequency of 10 MHz.

The guard amplifier's function is to ensure that the voltage between a tri-axial cable's inner screen and the centre wire is zero at all times, with the outer screen connected to ground. The reasoning is that in order for the inner screen to centre wire capacitor to charge, there must be a voltage difference between the two. By driving the tri-axial cable's inner screen to the same instantaneous voltage as the centre wire, the connecting cable capacitance is no longer a part of the measured capacitance between the probe sensor and blade tip. In practice, the guard amplifier comprises a unity gain amplifier capable of powering the reactive load which the guard screen's total capacitance represents to ground.

Chivers' (1989a) original guard amplifier design was current limited. The maximum capacitive reactive load it could drive was 180 pF at 10 MHz, equivalent to approximately 180 mm of mineral-insulated cable. In the driven screen configuration, Chivers (1989a) cited a reduction in apparent capacitance from 180 pF to 1.8 pF, with the capacitance between probe tip and blade varying from 1 pF to 10 pF. Using the capacitive clearance measurement system electronics and Stringfellow *et al.*'s (1997) mineral-insulated cable, Sheard *et al.* (1999) were able to develop Chivers' (1989a) original design, extending the maximum length of mineral-insulated cable that they could drive to 5 m.

The ground station incorporated a demodulator unit comprised of a voltage-controlled oscillator and a phase comparator. The output is an instantaneous voltage which is a function of frequency. Since the instantaneous value of frequency is a function of the capacitance between probe tip and blade, then the output voltage is a function of capacitance. The output from the demodulator unit is a pulse train, the peak height of each pulse a function of the capacitance between probe tip and each passing blade. During Chivers' (1989b) study, he fed the real-time pulse train to a root mean square voltmeter and an oscilloscope. He used the root mean square voltmeter to measure the average blade tip-to-casing clearance, and the oscilloscope to view the pulse train.

THE BLADE ANALYSER UNIT

The objective of the current study was to measure clearance over every blade. This method required measuring the height of each pulse from the demodulator. The author used a blade analyser unit (BAU), Figure 3.3, which Killeen *et al.* (1991) originally developed. It comprises the following sub-systems. The pulse train feeds into a peak detect, hold and reset circuit. This registers the height of the voltage peaks from the demodulator which then feed into an analogue to digital (A/D) converter. The pulse train and tachometer signal feed into a blade counter which registers the latest blade's number to pass. A dedicated micro-processor receives the output signals from the analogue to digital converter and the blade counter.

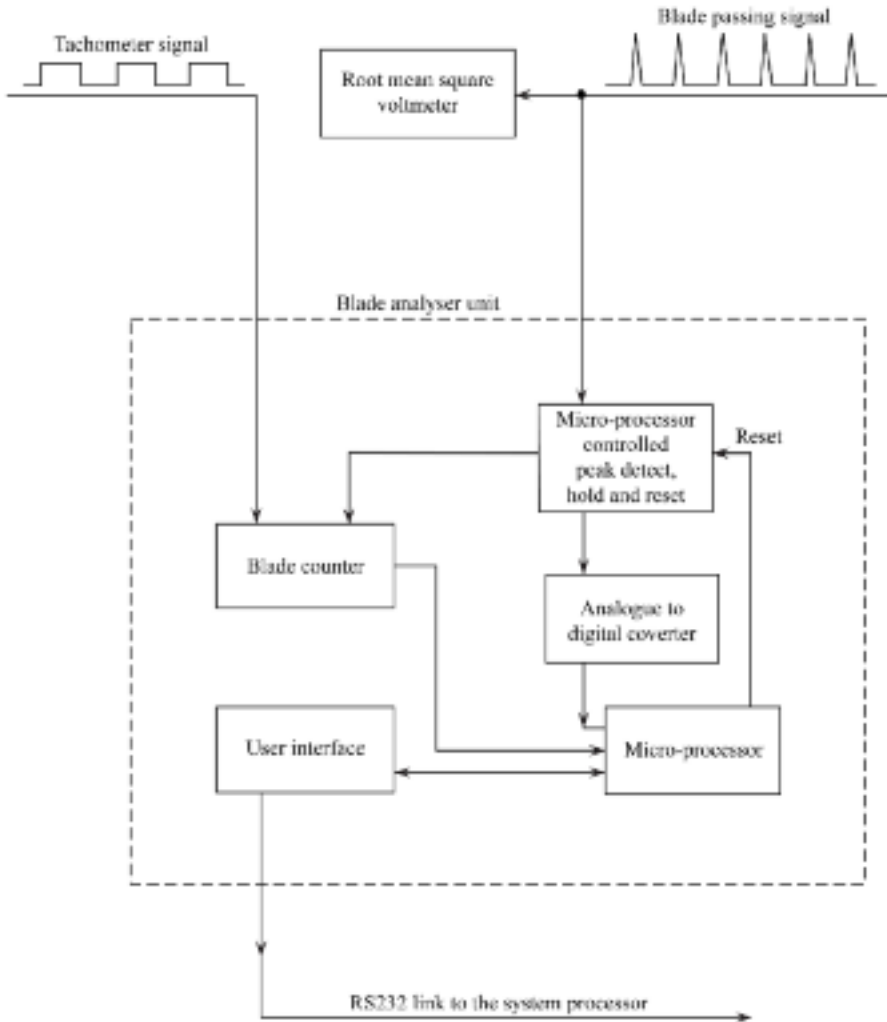


FIGURE 3.3. The blade analyser unit developed by Killeen *et al.* (1991) and used to measure individual pulse heights, schematic block diagram.

The micro-processor acquires pulse heights from the analogue to digital converter from one tachometer pulse to the next over one bladed disc's complete revolution. The micro-processor compares the number of pulses acquired with the known number of blades on the disc. If the two numbers are the same it assumes no missed pulses, and the pulse heights pass to a user interface where they are output in RS-232 format as a string of blade numbers versus pulse height.

During the current study, the RS-232 output from the user interface feeds into an 11-17 RS-232 to IEEE-488 converter to allow a Hewlett Packard computer,

Figure 3.4, to read the output. Killeen *et al.* (1991) wrote a software package to analyse the data from the blade analyser unit and the other inputs from the test facility.

FACILITY REQUIREMENTS

The addition of the blade analyser unit to capacitive clearance measurement system provided a method of measuring the peak voltage out of the demodulator. Since the height of each peak was a function of the blade tip-to-casing clearance between each blade and the probe tip, the pulse heights may be related to tip clearance over each blade. In order to evaluate the accuracy of the blade-by-blade clearance measurement, a method was necessary to determine the clearance over each blade around a disc independently of the capacitive clearance measurement system.

Second, there was a need for a calibration method for the capacitive clearance measurement system. During his work, Chivers (1989a) observed not only that the probe / demodulator combination determined absolute clearance versus system output, but was also a function of geometry. In this context, Chivers (1989a) defined 'geometry' effects as including fundamental physical factors which affect the absolute value of capacitance measured, such as rotor blade tip thickness and the measuring probe sensor electrode area. Additionally, Chivers (1989a) found the blade tips' angle to the engine axis (the stagger angle) and relative blade spacing (mark space ratio) to affect calibration.

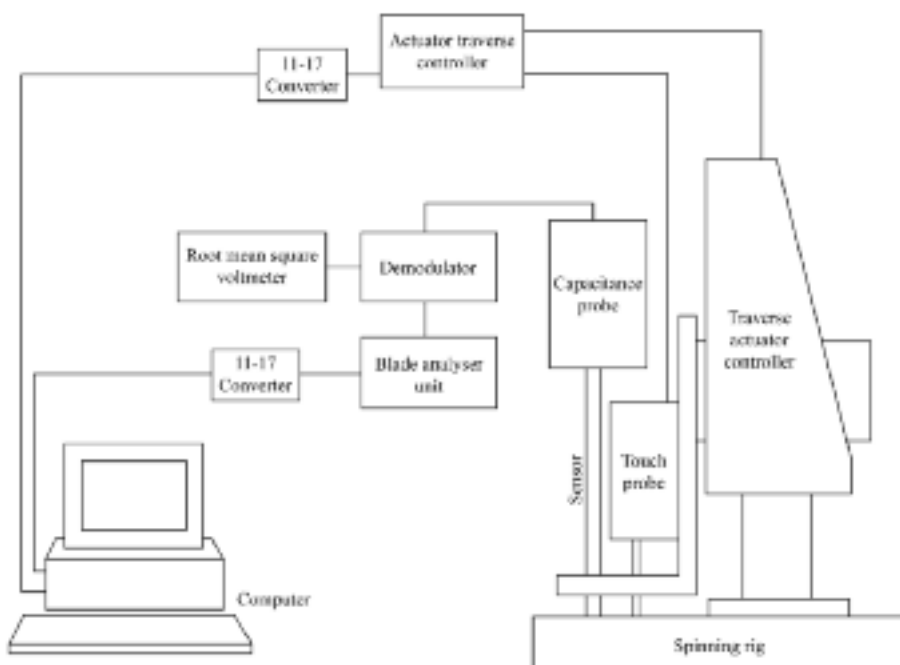


FIGURE 3.4. Layout diagram of the complete capacitive clearance measurement system used to measure blade tip-to-casing clearance over every blade.

The current study primarily establishes the absolute accuracy with which Chivers' (1989a) capacitive clearance measurement system could measure clearance over individual blades. In order to eliminate geometry and temperature effects, the facility design required an on-line calibration capability for the capacitive clearance measurement system, so that one could perform a calibration immediately prior to measuring blade tip-to-casing clearance.

FACILITY DESCRIPTION

A full compressor or turbine stage was not required for the capacitive clearance measurement system performance's laboratory study. The author designed a small spinning rig, Figure 3.5, which principally comprised an integral air motor and

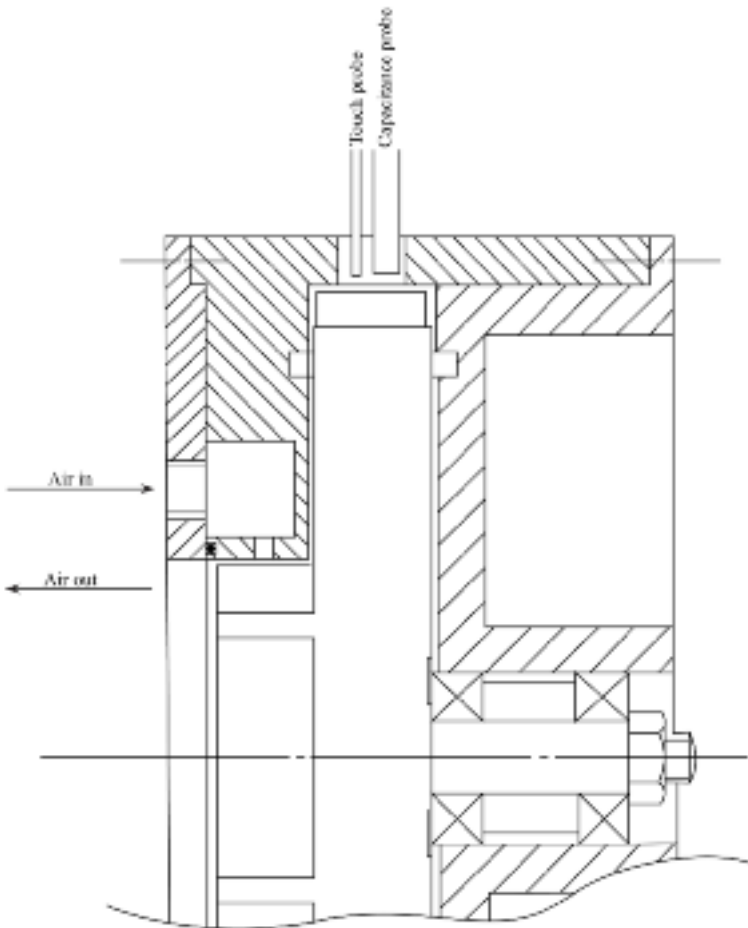


FIGURE 3.5. Spinning rig design used to evaluate the performance of Chivers' (1989a) capacitive clearance measurement system. The capacitance probe is fitted on a traverse actuator with touch probe to enable on-line calibration.

bladed wheel. The wheel geometry replicated that of a full scale compressor, whilst small enough for the available air supply to drive it, Table 3.1. Air motors are purely mechanical devices and do not generate the electrical noise one associates with a larger electric motor's rotating coils and magnets.

The author achieved capacitive clearance measurement system calibration and blade tip-to-casing measurement clearance over every blade using the alternative novel traverse-and-touch system method. Sheard *et al.* (1993) describe the traversing system in detail, as a platform on which to mount the capacitance probe. The traverse system comprises a precision stepper motor driven traverse actuator and active control system. Many others, notably Calvert *et al.* (1989), have used the traverse system. Ginder (1991) and Ginder *et al.* (1991) have used it to conduct area traverses behind every stator through a six-stage compressor at both design and off design conditions.

The ability to traverse the capacitance probe enables its position relative to the spinning rig's blades to vary by known amounts. The author cropped each blade's length on the wheel by known amounts relative to the longest blade, Table 3.2. In order to 'datum' the capacitance probe relative to the blades, it was necessary to

Table 3.1. *Spinning rig wheel geometry.*

Diameter	204 mm
Number of blades	24
Blade material	Aluminium
Blade passing frequency @ 10,000 rpm	4 KHz
Blade stagger angle	Zero
Mark space ratio	0.06
Blade tip velocity @ 10,000 rpm	107 m/s
Blade tip thickness	1.5 mm
Blade length	12 mm

Table 3.2. *Blade offset from the longest blade.*

Blade no.	Offset (mm)	Blade no.	Offset (mm)
1	0.0000	13	0.0334
2	0.6888	14	0.6616
3	0.0335	15	0.0827
4	0.6436	16	0.6051
5	0.1185	17	0.1289
6	0.5788	18	0.5154
7	0.1751	19	0.1706
8	0.5197	20	0.4611
9	0.2325	21	0.2347
10	0.4661	22	0.4127
11	0.3060	23	0.3076
12	0.3837	24	0.3409

establish its position relative to the longest blade. The author achieved this by mounting a touch detection wire alongside the capacitance probe. Sheard and Turner (1992) describe this method, so we will describe it only briefly here. One applies 400 volts to the wire which causes a discharge when the wire tip is within a small spark gap, typically a few microns. The touch occurs on the longest blade.

In the present study, the author mounted the touch wire 0.1 mm radially inward from the capacitance probe, Figure 3.6. When he detected a touch, the distance from the capacitance probe to the longest blade's tip was therefore 0.1 mm. This revealed each blade's length relative to the longest blade. Therefore, it facilitated calculation of the distance from the capacitance probe to every blade's tip. Further, when the traverse actuator stepped the capacitance probe back by a known amount, the author

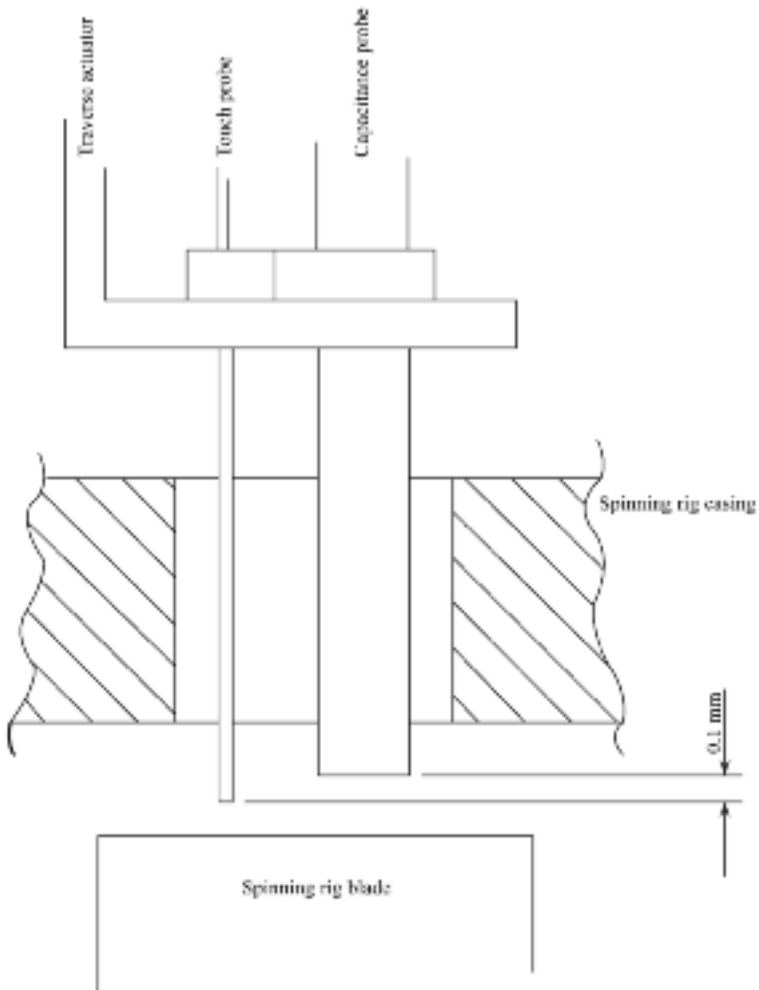


FIGURE 3.6. Capacitance probe and touch wire mounting arrangement on the traverse actuator carrier.

could still calculate the clearance between the capacitance probe and each blade. In this way it was possible to calculate the clearance between capacitance probe and blade tip at all positions, following the ‘datuming’ of the probe. The experimental programme used this process to derive the known blade tip-to-casing clearance.

The practical realisation of the spinning rig, Figure 3.7, vented the air motor exhaust directly into a soundproof test cell, with the traverse actuator mounted on top of the wheel housing. Figure 3.8 shows a close up of the capacitance and touch probes’ clamping arrangement on the traverse actuator carrier.

EXPERIMENTAL PROGRAMME

The experimental programme fell broadly into two phases: 1) commissioning of the spinning rig and blade analyser unit and 2) establishing the accuracy with which the capacitive clearance measurement system could measure clearance over individual blades.

The author commissioned the spinning rig and blade analyser unit at 10,000 rpm, the maximum speed at which continuous spinning rig operation was possible



FIGURE 3.7. The spinning rig used to evaluate performance of Chivers’ (1989a) capacitive clearance measurement system.



FIGURE 3.8. Close-up view of the traverse actuator mounting on the spinning rig housing showing the clamping arrangement of the capacitance probe and touch wire.

due to air supply limitations. The blade passing frequency at 10,000 rpm was 4 KHz, high enough to be representative of the typical compressor or turbine's blade passing frequency. The capacitance probe drove in towards the spinning rig blades until the wire registered a touch. The author then calculated the capacitance probe's position relative to every blade, and independently the author used the blade analyser unit to record the capacitive clearance measurement system output for each blade. The author then stepped back the capacitance probe 0.1 mm using the traverse actuator, and recorded the blade analyser unit output again. He repeated this procedure 20 times, increasing clearance over the shortest blade to 2.10 mm, plotting the known clearance over each blade against the capacitive clearance measurement system output, Figure 3.9.

The author used a least squares technique to fit a 'one over' distance curve through the data. The author determined the calibration error by subtracting known clearance from that which he obtained using the calibration which he plotted against

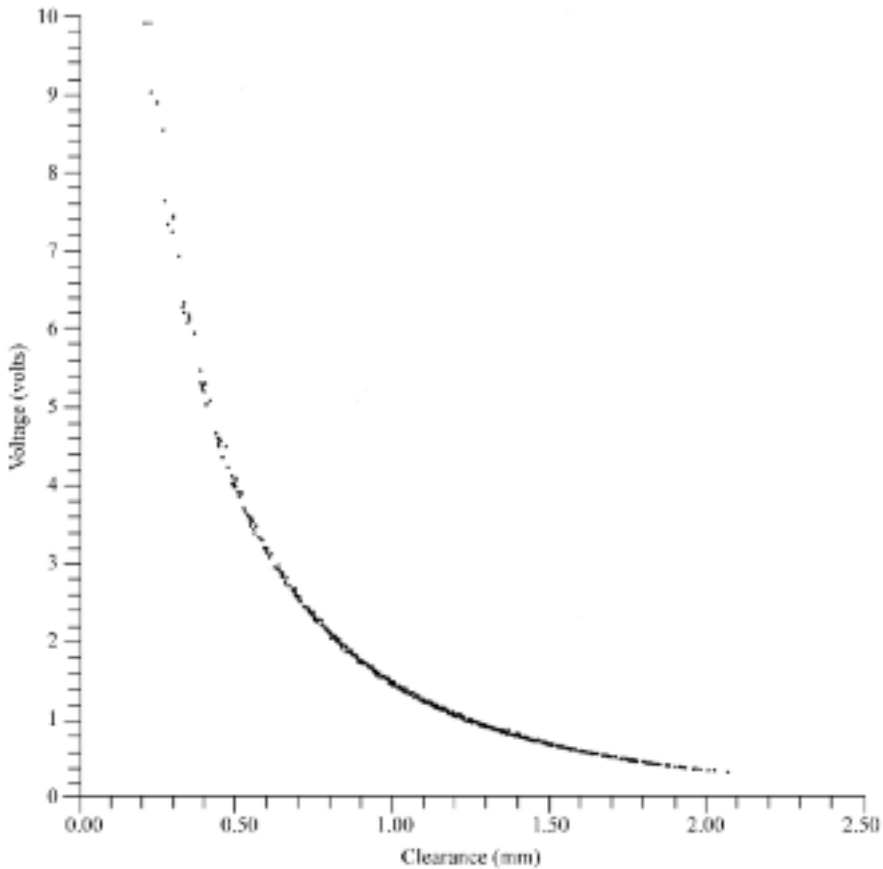


FIGURE 3.9. Capacitive clearance measurement system output plotted against known clearance illustrating the one over distance nature of the system output. Each dot on the graph is a single measurement made over a single blade.

clearance, Figure 3.10. The result indicated that the calibration gave clearance over each blade to an accuracy of ± 0.025 mm over a 2.0 mm range. Whilst this error was comparable to Chivers' (1989b) observations, the author hoped that datuming the capacitance probe against a wheel of known geometry would eliminate many of the factors that contributed to Chivers' (1989b) overall error.

At short range, measuring small clearances, the capacitance probe's sensitivity is high. As clearance increases sensitivity reduces, until at a range of 2.0 mm there is virtually no change in probe output with change in clearance. We might reasonably expect this phenomenon to give results of rising error with increasing clearance. The author did not see this result (see Figure 3.10). He re-plotted the error against the blade number as Figure 3.11 illustrates. There was a clear sinusoidal variation of the blade to blade results. The author checked the wheel with a dial gauge. The wheel was running ± 0.025 mm eccentrically in its bearings which was contributing to the capacitive clearance measurement system error.

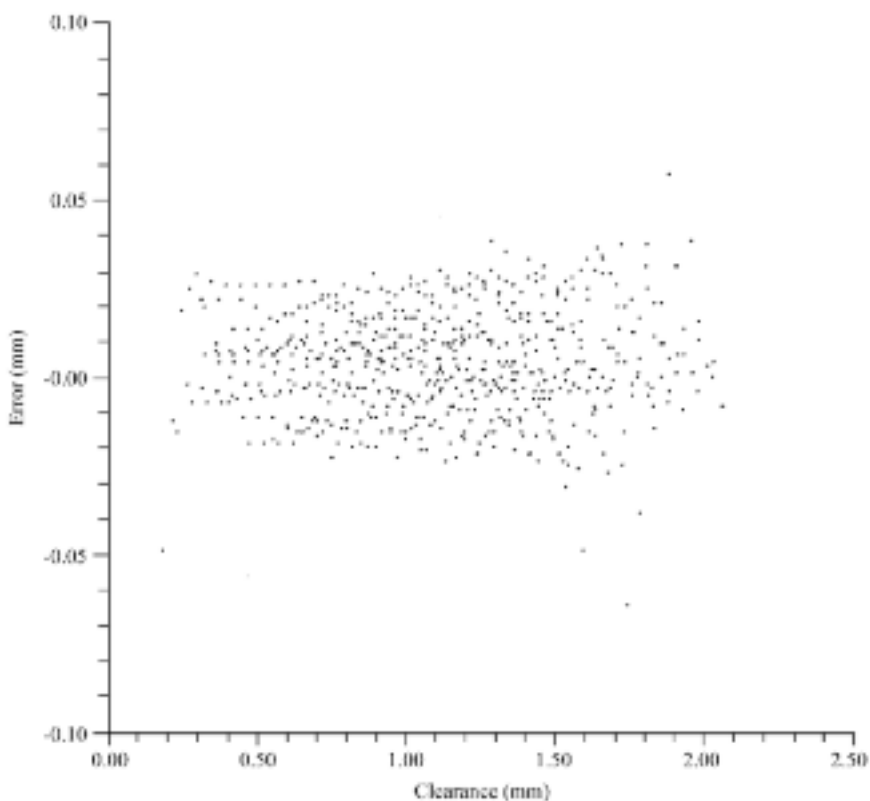


FIGURE 3.10. Error in capacitive clearance measurement system output, calculated by subtracting the known clearance between probe and blade tip from that obtained using the measurement system calibration for each blade.

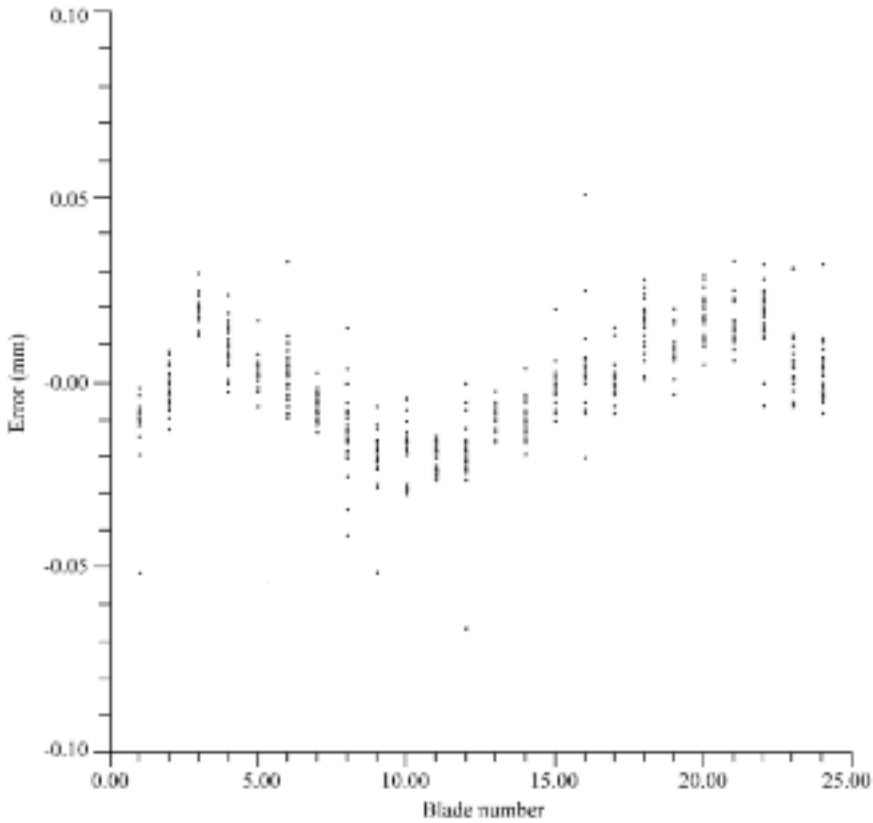


FIGURE 3.11. Error in capacitive clearance measurement system output plotted against blade number around the spinning rig wheel, illustrating a ± 0.025 mm variation in blade height due to shaft eccentricity.

The author modified the data reduction software to calculate each blade's offset due to bearing eccentricity. He subtracted the calculated offset from each measurement, which eliminated the bearings' effect from the error, Figure 3.12. He plotted the corrected clearance against known clearance, Figure 3.13, with noticeably less scatter. The author then re-plotted error against clearance, Figure 3.14, which exhibited the expected trend of increasing error with increasing clearance. The author concluded that the commissioning of the spinning rig and blade analyser unit was complete, and therefore he could commence the second phase of experimental work.

The primary difference between a gas turbine test and the spinning rig is that one does not know each blade's length relative to the longest blade. Second, dating of the capacitance probe with a touch wire assumes blade conductivity, which may not be the case with ceramic or thermal barrier coated blades. The author devised an experimental programme to calibrate the capacitive clearance measurement system, and then measure blade tip-to-casing clearance over each blade without touching the longest blade, or knowing each blade's length relative to it. The author

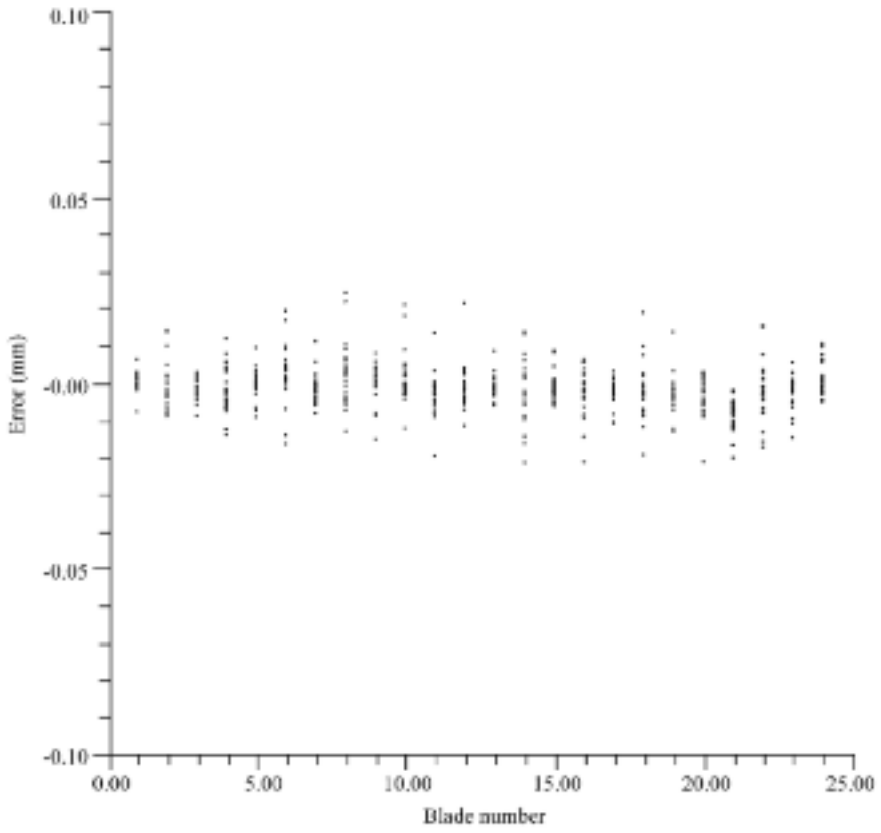


FIGURE 3.12. Error in capacitive clearance measurement system output plotted against blade number around the spinning rig wheel after compensating the error due to spinning rig shaft eccentricity.

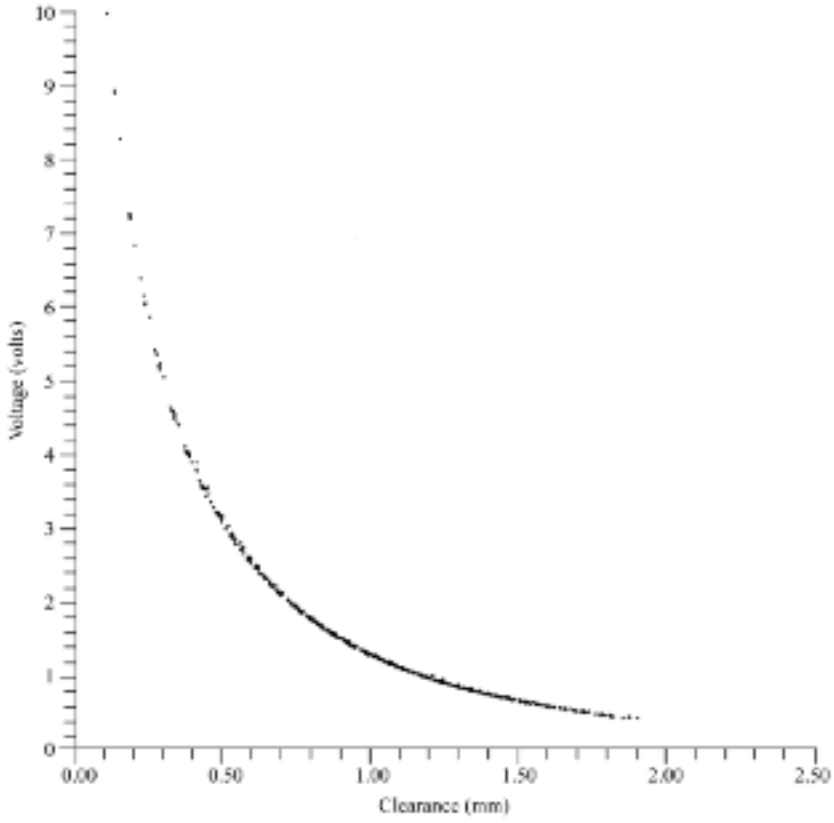


FIGURE 3.13. Capacitive clearance measurement system output plotted against known clearance after compensating for spinning rig shaft eccentricity.

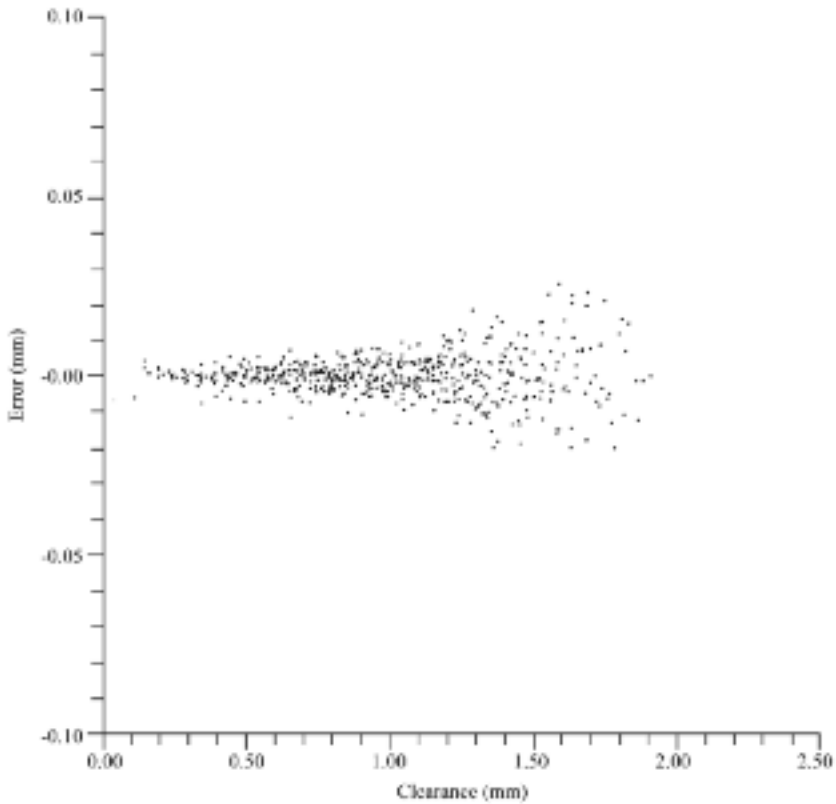


FIGURE 3.14. Error in capacitive clearance measurement system output, calculated after compensating for spinning rig shaft eccentricity.

used the following method. He stabilised the spinning rig speed at 10,000 rpm, and the traverse actuator moved in until the capacitance probe was close to the longest blade, but not touching. The author then recorded the reading from the blade analyser unit for the longest blade and used the traverse actuator to step the probe out 0.05 mm before repeating the data acquisition process. He then plotted the probe output against position, Figure 3.15, assuming zero clearance between capacitance probe and blade tip for the first data point.

The author used a least squares technique to fit a curve through the data in Figure 3.15, assuming the equation:

$$V = A_1 + A_2 / D$$

where A_1 and A_2 are constants determined by the curve fit, D is the distance between capacitance probe electrode and blade tip in millimetres and V is capacitance probe output in volts. The physics of a capacitor dictate that capacitance should approach infinity as the distance between the capacitor plates' approaches zero. In this case,

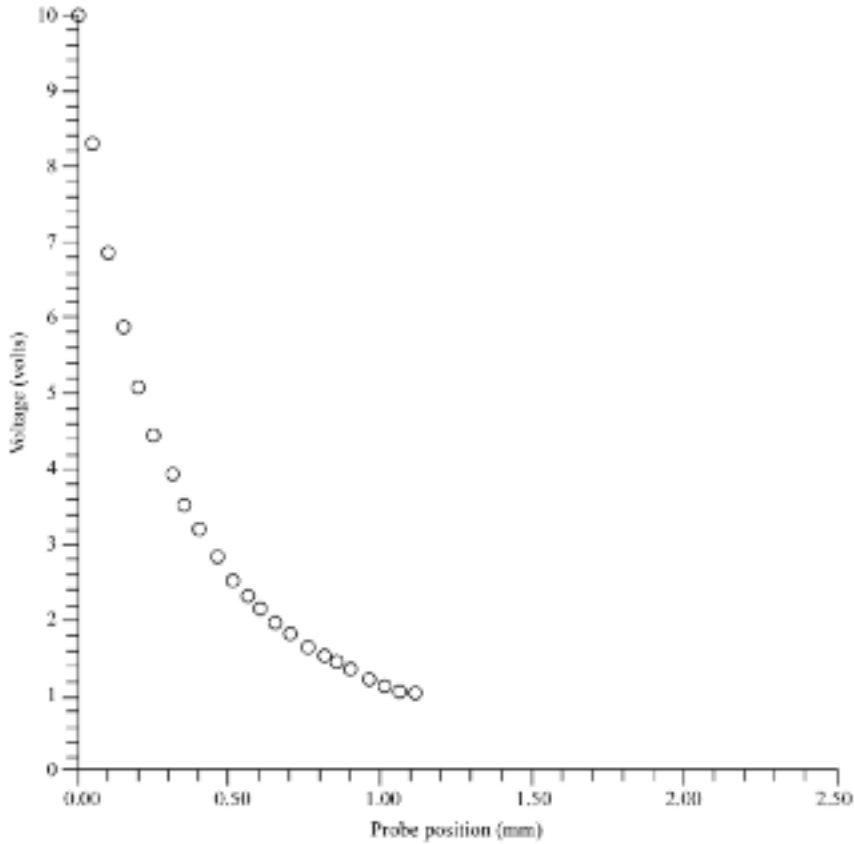


FIGURE 3.15. Capacitive clearance measurement system output for the longest blade of the spinning rig wheel plotted against position, which was changed using the traverse actuator.

because of the unknown actual clearance, the author placed the first data point in Figure 3.15 at zero. The author assumed the negative value at which the curve tended to infinity as the unknown clearance between the first data point and the longest blade. Therefore, he changed the constant A_1 sign from negative to positive to give the actual calibration.

By datuming the capacitance probe immediately following the experiment, the author found each data point's actual position. The actual data points match the calibration curve closely, Figure 3.16, giving confidence in the method that he used to calibrate the capacitive clearance measurement system without touching the longest blade, or knowing each blade's length relative to the longest blade.

Once the author obtained a calibration, he used the blade analyser unit to acquire probe output pulse height for every blade. Knowing each blade's length relative to the longest blade, it was once again possible to plot the known clearance over each blade against probe output, Figure 3.17. This figure shows known clearance

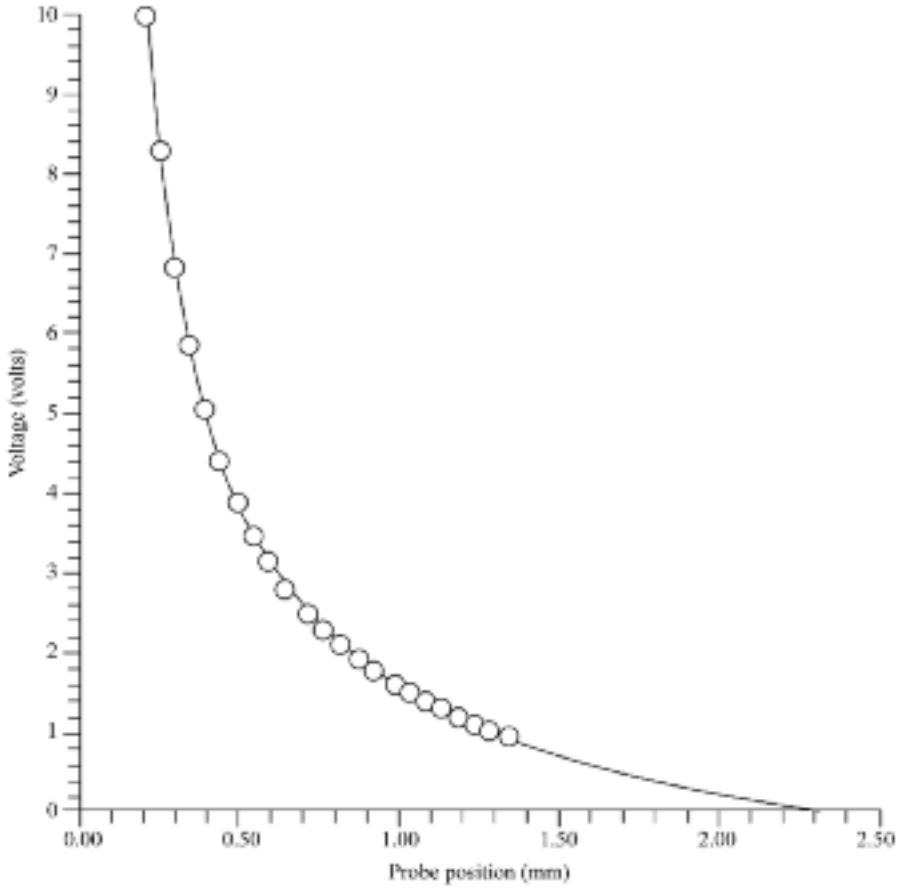


FIGURE 3.16. Capacitive clearance measurement system calibration obtained without datuming the probe or knowing the length of each blade relative to the longest blade. The figure also shows the actual position of the data points used in the calibration.

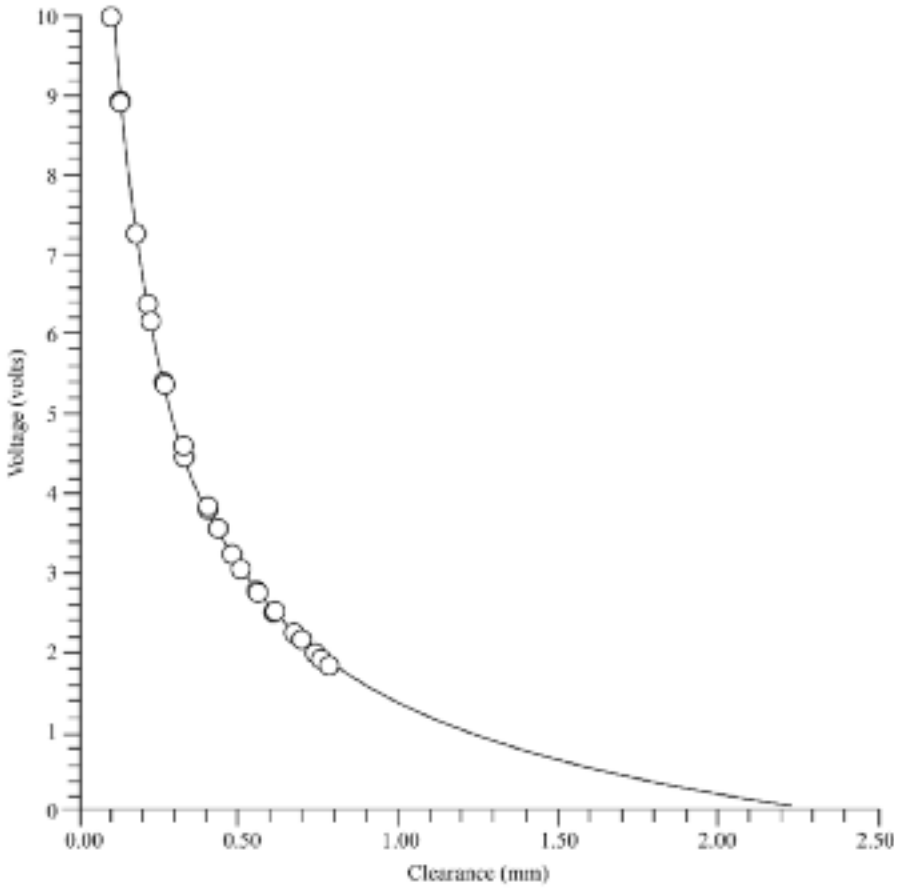


FIGURE 3.17. Capacitive clearance measurement system output for each blade of the spinning rig wheel plotted against known clearance, over-plotted with the recently acquired calibration.

plus the previously acquired calibration curve, illustrating the excellent agreement between the two. The author calculated the error by applying the calibration to probe output voltage, then subtracting known clearance. The resulting error plot, Figure 3.18, had only 24 points, each corresponding to the error in clearance over one of the spinning rig wheel blades. The author measured the clearance without knowledge of the probe's initial position relative to the longest blade, and without knowledge of each blade's length relative to the longest blade. The error of ± 0.025 mm, Figure 3.18, is sufficiently low for the approach to blade-by-blade clearance measurement to give useful data as part of a gas turbine development programme.

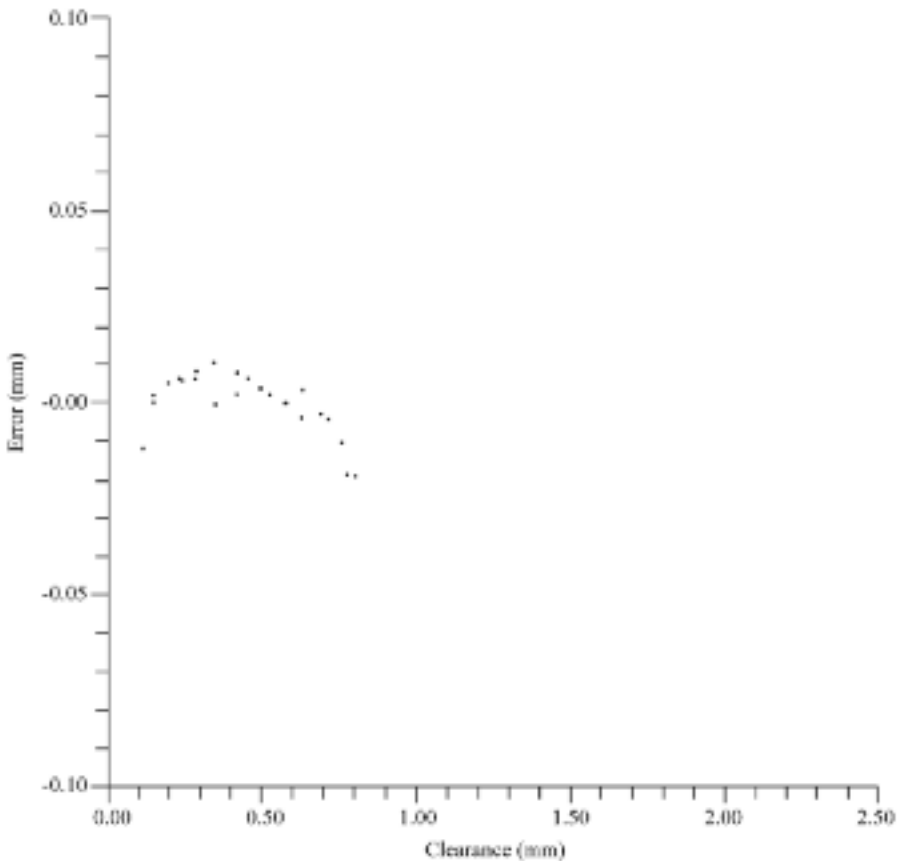


FIGURE 3.18. Error in capacitive clearance measurement system output over the 24 blades around the spinning rig wheel, calculated by subtracting the known clearance between probe and blade tip from that calculated from the measurement system calibration. The calibration was obtained without datuming the capacitance probe.

FURTHER DEVELOPMENT

Sheard *et al.* (1992) further refined the capacitive clearance measurement system calibration method that this chapter describes. Sheard and Killeen (1993) then combined the capacitance probe, touch probe and traverse actuator into a single hybrid unit, Figure 3.19, to develop a capacitive clearance measurement system that one can calibrate on-line. The prototype unit incorporates a 6 mm stroke traverse actuator.

Sheard and Killeen (1995) then evaluated the prototype unit in the C147 compressor at DRA Pystock, fitting Sheard and Killeen's (1993) prototype unit to the compressor's final stage. As with the work that this chapter reports, Sheard and Killeen (1995) identified that the rotor was running eccentric, in this case ± 0.050 mm, concluding that this level of eccentricity was self consistent with the 0.075 mm design clearance in the bearings. Sheard and Killeen (1995) successfully made a blade-by-blade tip-to-casing clearance measurement. They also measured the clearance over the longest blade around the compressor using Sheard and Turner's (1992) electromechanical clearance measurement system. The measurement was in close agreement to the measurement of blade tip-to-casing clearance over the longest blade made using Sheard and Killeen's (1993) prototype, and hence the author judged the blade-by-blade measurement system a success.

Although the blade-by-blade measurement system was successful, the reader should bear in mind that a capacitive approach to blade-by-blade clearance measurement is just one approach and has its limitations. As previously mentioned in this chapter, ionised combustion products leaving the combustor result in flame noise. Flame noise is an unsteady error source. A second limitation is the blades' axial thermal movement relative to the casing in which they run. Blades have an aerofoil shape and over the course of an engine cycle they move axially relative to their casing. A capacitance probe mounted in that casing, at different times during an engine cycle, will form a capacitive couple with a different part of the blade. Parts of the blade may have a different cross-sectional area as a consequence of blade geometry. A change in a probe's axial location relative to blades may therefore result in an apparent change in tip clearance which is a steady-state error source.

Engineers can avoid the above unsteady and steady-state error sources with optical clearance measurement systems, an approach that Kempe *et al.* (2003) and Haffner *et al.* (2008) favoured. In line with this chapter's focus, Kempe *et al.* (2003) and Haffner *et al.* (2008) identified the benefits of the measurement system's on-line calibration when making a blade-by-blade clearance measurement. Kempe *et al.* (2006) described initial laboratory validation of the optical clearance measurement system, and its application in an Alstom GT26 turbine's first stage behind each of the combustors. The GT26 utilises a sequential combustor system unique to the Alstom GT24 and GT26 gas turbines. The optical measurement system worked well initially; however, after 6 hours the signal to noise ratio fell too far to detect any blade tip-to-casing clearance. Kempe *et al.* (2006) attributed the degradation in signal to noise ratio to changes in the optical fibres' thermal behaviour within the casing and

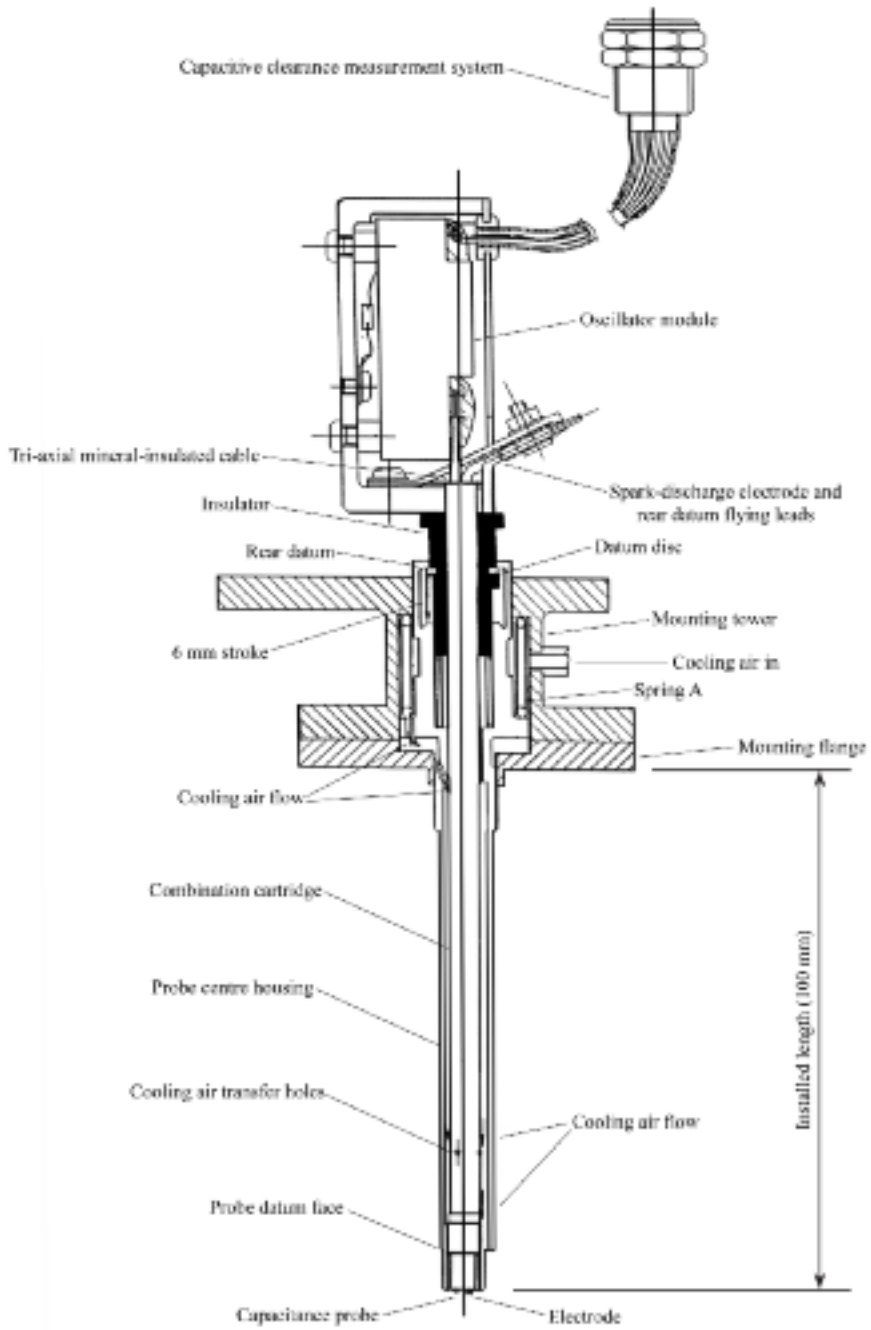


FIGURE 3.19. The hybrid probe developed by Sheard and Killeen (1993) and used by Sheard and Killeen (1995) to measure the blade-by-blade tip-to-casing clearance in the C147 compressor at DRA Pystock.

the turbine enclosure. As such, there is practical difficulty in reliably operating this optical clearance measurement system in the turbine environment.

Although the author anticipated finding the clearance measurement system to have wide spread application in a research environment where the blade-by-blade measurement of clearance was of primary interest, this was not the case. Some scholars used the capacitive clearance measurement system in research applications, notably Lawson (2003) and Lawson and Ivey (2005). They used the blade-by-blade measurement not to study tip clearance, but blade tip timing. The clearance measurement system, however, proved most valuable in development applications. Müller *et al.* (1997) utilised the clearance measurement system during the development of the BR700 gas turbine using capacitance probes positioned on opposite sides of the compressor casing to establish the magnitude of blade tip-to-casing clearance variation as changing engine speed caused the high-pressure compressor to pass through casing and rotating system natural frequencies. The primary value of the blade tip-to-casing clearance measurements that Müller *et al.* (1997) reported was, however, the resolution of transient changes in average blade tip-to-casing clearance that occurred as a consequence of step changes in engine speed. Müller *et al.* (1997) utilised this transient clearance measurement to establish the compressor casing's thermal time constants over each compressor stage.

The major achievement of the programme of work which this chapter describes is that it does overcome the practical problems of making a blade-by-blade measurement of tip-to-casing clearance in both compressor and turbine environments. As Kempe *et al.*'s work (2006) demonstrates, blade-by-blade tip clearance measurement in an actual turbine application is difficult. Since its initial development, engineers have used Stringfellow *et al.*'s (1997) clearance measurement system routinely in gas turbine development programmes. The inherent robustness of the Sheard and Lawrence (1998) sensor concept, coupled with Stringfellow *et al.*'s (1997) mineral-insulated cable and frequency modulated driven guard electronics system, have proven both robust and reliable in service. However, the inherent limitations of a capacitive measurement system remain. Those limitations are both known and predictable and therefore ultimately manageable in real-world applications.

CONCLUSIONS

The capacitive clearance measurement system in this study is capable of measuring blade tip-to-casing clearance over individual blades to an accuracy of ± 0.01 mm over a 0.0 to 1.0 mm range, and ± 0.025 mm over a 1.0 to 2.0 mm range.

The capacitive clearance measurement system measures clearance over individual blades to an accuracy of ± 0.025 mm when operated in a manner similar to that envisaged during operation in a gas turbine compressor or turbine installation.

The author has developed a method of calibrating the capacitive clearance measurement system which enables calibration *in situ* immediately prior to use. This overcomes the classical problems with capacitance probes of geometry induced errors, and drift with temperature.

A blade analyser unit (BAU) which Killeen *et al.* (1991) originally developed accurately measured the peak output voltage from the capacitive clearance measurement system demodulator. This enables one to use the capacitance probe to measure clearance over every blade, as opposed to only an average value for all blades.

The study gives confidence that engineers can use capacitance probes on a gas turbine to measure clearance over every blade in a compressor or turbine stage. This will facilitate the identification of casing and turbine vibration modes, allow a more accurate calculation of average tip clearance, and enable engineers to identify the change in longest blade length following a casing rub.

REFERENCES

- Baker, L.C., Grady, G.E. & Mauch, H.R. (1978), 'Turbine Tip Clearance Measurement'. USARTL-TR-78-4.
- Barranger, J. (1978), 'An In-Place Recalibration Technique to Extend the Temperature Capability of Capacitance-Sensing Rotor Blade Tip Clearance Measuring Systems'. *Society of Automotive Engineers Aerospace Meeting*. San Diego, USA, Paper No. 781003.
- Barranger, J.P. & Ford, M.J. (1981), 'Laser Optical Blade Tip Clearance Measurement System'. *Transactions of the ASME, Journal of Engineering for Power*, vol. 103, pp. 457–60.
- Calvert, W.J., Ginder, R.B., McKenzie, I.R.I. & Way, D.J. (1989), 'Performance of a Highly-Loaded HP Compressor'. *Proceedings of the 34th American Society of Mechanical Engineers Gas Turbine and Aeroengine Congress*. Toronto, Canada, 5–8 June, Paper No. 89-GT-24.
- Chivers, J.W.H. (1989a), *A Technique for the Measurement of Blade Tip Clearance in a Gas Turbine*. PhD thesis, University of London.
- Chivers, J.W.H. (1989b), 'A Technique for the Measurement of Blade Tip Clearance in a Gas Turbine'. AIAA Paper No. 89-2916.
- Drinkuth, W., Alwang, W.G. & House, R. (1974), 'Laser Proximity Probes for the Measurement of Turbine Blade Tip Running Clearances'. *Proceedings of the ISA Aerospace Instrumentation Symposium*. Paper No. 74228, pp. 133–40.
- Ford, M.J. (1980), 'Clearance Measurement Systems'. Report NASA CR 159402.
- Gill, S.J., Ingallinera, M.D. & Sheard, A.G. (1997), 'Turbine Tip Clearance Measurement System Evaluation in an Industrial Gas Turbine'. *Proceedings of the 42nd American Society of Mechanical Engineers Gas Turbine and Aeroengine Congress*. Orlando, Florida, USA, 2–5 June, Paper No. 97-GT-466.
- Ginder, R.B. (1991), 'Design and Performance of Advanced Blading for a High Speed HP Compressor'. *Proceedings of the 36th American Society of Mechanical Engineers Gas Turbine and Aeroengine Congress*. Orlando, Florida, USA, 3–6 June, Paper No. 91-GT-374.
- Ginder, R.B., Britton, A.J., Calvert, W.J., McKenzie, I.R.I. & Rarker, J.M. (1991), 'Design of Advanced Blading for a High Speed HP Compressor Using an S1-S2 Flow Calculation System'. *Proceedings of the IMechE Conference on Turbomachinery*, Paper No. 423/007.

- Haffner, K., Kempe, A., Rösgen, T. & Schlamp, S. (2008), 'Method and an Apparatus for Determining the Clearance Between a Turbine Casing and the Tip of a Moving Turbine Blade'. US Patent No. 7,400,418, 15 July.
- Kempe, A., Schlamp, S., Rösgen, T. & Haffner, K. (2003), 'Low-coherence Interferometric Tip-clearance Probe'. *Optics Letters*, vol. 28, pp. 1323–5.
- Kempe, A., Schlamp, S., Rösgen, T. & Haffner, K. (2006), 'Spatial and Temporal High-Resolution Optical Tip-Clearance Probe for Harsh Environments'. *Proceedings of the 13th International Symposium on Applications of Laser Techniques to Fluid Mechanics*. Lisbon, Portugal, 26–29 June.
- Killeen, B., Sheard, A.G. & Westerman, G.C. (1991), 'Blade-by-blade Tip Clearance Measurement in Aero and Industrial Turbomachinery'. *Proceedings of the 37th ISA International Instrumentation Symposium*. San Diego, California, USA, 5–9 May, pp. 429–47.
- Knoell, H., Schedl, K. & Kappler, G. (1981), 'Two Advanced Measuring Techniques for the Determination of Rotor Tip Clearance During Transient Operation'. *Fifth International Symposium on Airbreathing Engines*. Bangalore, India.
- Lawson, C.P. (2003), *Capacitance Tip Timing Techniques in Gas Turbines*. PhD thesis, Cranfield University.
- Lawson, C.P. & Ivey, P.C. (2005), 'Tubomachinery Blade Vibration Amplitude Measurement Through Tip Timing With Capacitance Tip Clearance Probes'. *Sensors and Actuators A: Physical*, vol. 118, pp. 14–24.
- Müller, D., Sheard, A.G., Mozumdar, S. & Johann, E. (1997), 'Capacitive Measurement of Compressor and Turbine Blade Tip-to-casing Running Clearance'. *Transactions of the ASME, Journal of Engineering for Gas Turbines & Power*, vol. 119, pp. 877–84.
- Ramachandran, J. & Conway, M.C. (1996), 'MS6001FA – An Advanced Technology 70-MW Class 50/60Hz Gas Turbine'. *39th GE Turbine State-of-the-Art Technology Seminar*, GER-3765B.
- Sheard, A.G. (1989), *Aerodynamic and Mechanical Performance of a High Pressure Turbine Stage in a Transient Wind Tunnel*. DPhil thesis, University of Oxford, <http://ora.ouls.ox.ac.uk/objects/uuid:73ecb15e-efde-474d-ae30-3f8f7e1d6f4e>
- Sheard, A.G. (1993), 'A System for Measuring Blade and Stator Radius During Compressor Build and Overhaul'. *Proceedings of the 9th International Turbomachinery Maintenance Congress*. Amsterdam, Netherlands, 18–22 October, pp. 1–12.
- Sheard, A.G. & Killeen, B. (1993), 'Hybrid System for High-Temperature Tip-Clearance Measurement'. *Proceedings of the 39th ISA International Instrumentation Symposium*. Albuquerque, New Mexico, USA, 2–6 May, pp. 379–94.
- Sheard, A.G. & Killeen, B. (1995), 'A Blade-by-blade Tip Clearance Measurement System for Gas Turbine Applications'. *Transactions of the ASME, Journal of Engineering for Gas Turbines & Power*, vol. 117, pp. 326–31.
- Sheard, A.G. & Lawrence, D.C. (1998), 'Gap Measurement Device'. US Patent No. 5,760,593, 2 June.
- Sheard, A.G. & Turner, S.R. (1992), 'An Electromechanical Measurement System for the Study of Blade Tip-to-casing Running Clearances'. *Proceedings of the 37th American Society of Mechanical Engineers Gas Turbine and Aeroengine Congress*. Cologne, Germany, 1–4 June, Paper No. 92-GT-50.

- Sheard, A.G., Westerman, G.C. & Killeen, B. (1992), 'An On-Line Calibration Technique for Improved Blade-by-blade Tip Clearance Measurement'. *Proceedings of the 38th ISA International Instrumentation Symposium*. Las Vegas, Nevada, USA, 26–30 April, pp. 32–51.
- Sheard, A.G., Killeen, B. & Palmer, A. (1993), 'A Miniature Traverse Actuator for Mapping the Flow Field between Gas Turbine Blade Rows'. *Proceedings of the IMechE Machine Actuators & Controls Seminar*. London, UK, 31 March, pp. 1–11.
- Sheard, A.G., Westerman, G.C., Killeen, B. & Fitzpatrick, M. (1994), 'A High-Speed Capacitance-Based System for Gauging Turbomachinery Blading Radius During the Tip-Grind Process'. *Transactions of the ASME, Journal of Engineering for Gas Turbines & Power*, vol. 116, pp. 243–9.
- Sheard, A.G., O'Donnell, S.G. & Stringfellow, J.F. (1999), 'High Temperature Proximity Measurement in Aero and Industrial Turbomachinery'. *Transactions of the ASME, Journal of Engineering for Gas Turbines & Power*, vol. 121, pp. 167–73.
- Stringfellow, J.F., Wayman, L. & Knox, B. (1997), 'Capacitance Transducer Apparatus and Cables'. Patent No. WO 97/28418, 7 August.
- White, S.D. (1977), 'Turbine Tip Clearance Measurement'. USARTL-TR-77-47.

An On-line Calibration Technique for Improved Blade-by-blade Tip Clearance Measurement

A.G. Sheard, G.C. Westerman and B. Killeen

ABSTRACT

This chapter describes a capacitive-based blade tip-to-casing clearance measurement system which integrates a novel technique for calibrating the capacitive clearance measurement system *in situ*. The on-line calibration system allows immediate capacitance probe calibration prior to use, giving operational advantages and maximum measurement accuracy.

The capacitance probe that forms the basis of the new capacitive clearance measurement system has been in regular use in gas turbine applications for a number of years. The spark-discharge and traverse systems required for on-line calibration have been in use for many years throughout the world for measuring minimum blade tip-to-casing clearances and traversing aerodynamic probes at elevated temperatures. Their addition to a proven capacitive clearance measurement system that measures clearance over individual blades, but needs calibration, is an ideal marriage of experienced partners.

This chapter provides a description of the prototype unit development. It considers the possible error sources when using it in service and describes the laboratory performance studies that the authors undertook to ascertain their magnitude.

INTRODUCTION

This chapter describes a programme of work which the authors undertook to produce a capacitive clearance measurement system which could calibrate *in situ* immediately prior to measurement. The 'on-line' calibration facility is a novel development of the basic capacitive clearance measurement system. This facility overcomes many of the classical problems that occur with capacitance probes, notably

This chapter is a revised and extended version of Sheard, A.G., Westerman, G.C. & Killeen, B. (1992), 'An On-Line Calibration Technique for Improved Blade-by-blade Tip Clearance Measurement'. *Proceedings of the 38th ISA International Instrumentation Symposium*. Las Vegas, Nevada, USA, 26–30 April, pp. 32–51.

calibration drift with temperature and errors between the calibration rig's geometry and the actual installation.

Chivers (1989) discussed capacitive clearance measurement system limitations and observed that the probe/ground station combination determined absolute clearance versus system output with output also a function of geometry. In this context, Chivers (1989) defined 'geometry' effects as including fundamental physical factors such as blade tip thickness, probe sensor electrode area, blade tip angle to the gas turbine axis (the stagger angle) and relative blade spacing (mark space ratio). Chivers (1989) found that all of these factors affected calibration.

Integrating electromechanical and capacitance probes into a single unit produces a hybrid system. The authors use the absolute measurement from the electromechanical system's internal datum to the longest blade around a disc in conjunction with the capacitance probe's blade-by-blade measurement of blade tip-to-casing clearance. They combine the two measurements to give an absolute value of clearance from the electromechanical system's internal datum to each blade tip. One can derive the distance from internal datum to outer annulus from the installation geometry, allowing one to relate this measurement of clearance to blade tip-to-casing clearance.

The Fenlow Company first introduced clearance measurement systems utilising the spark-discharge principle in the 1950s, but they typically suffered from thermal effects which limited their accuracy. Davidson *et al.* (1983) addressed and solved the problems of spark-discharge clearance system thermal susceptibility and developed a novel spring-loaded probe which they datumed within 25 mm of the probe tip. Sheard and Turner (1992) further developed their system and reduced its size by 82%, and incorporated numerous improvements to the basic design without changing the original concept.

The capacitance probe is an inherently rugged device and, therefore, is suitable for gas turbine applications. Barranger (1978) described improvements to a capacitance-based measurement system. He utilised the probe to blade tip capacitance in a resonant inductance, capacitance, resistance circuit (an oscillator). The circuit's output frequency was a function of measured capacitance giving a frequency modulated (FM) mode of operation. The principal drawback of Barranger's system was that the 1 to 10 pico Farad (pF) capacitance between probe and blade tip was shunted by the probe's total capacitance and connecting cable. This shunt capacitance was typically two orders of magnitude greater than that measured. Even relatively small temperature changes affected the capacitance readings due to blade passing.

Chivers (1989) developed a tri-axial frequency modulated capacitance probe which eliminated the shunt capacitance of Barranger's system. The shunt capacitance was the main contributor to the limited accuracy of Barranger's system. Sheard (2011) set about ascertaining the absolute accuracy with which Chiver's capacitance probe could measure clearance over individual blades. He concluded that a 3.0 mm diameter capacitance probe over 1.5 mm thick blades could measure clearance over individual blades to an accuracy of ± 0.01 mm over a 0.0 to 1.0 mm range, and ± 0.025 mm over a 1.0 to 2.0 mm range, with blade passing signals falling into the system noise floor at clearances above 3.0 mm. In order to achieve this accuracy it

was necessary to calibrate the capacitance probe immediately prior to use, thus eliminating target geometry and temperature induced errors.

Sheard's (2011) method for calibrating the capacitance probe was to relate probe output to known clearance. He used a least squares curve fit through the output versus clearance plot to provide the 'calibration', defining each measurement's deviation as 'error'. Whilst this work established capacitance probe performance, Sheard generated the 'calibration' from prior knowledge of the clearance over each blade. Therefore, he could not use it against a bladed disc of unknown geometry.

The development programme which this chapter describes falls broadly into two phases. The first phase is the integration of the capacitance probe and systems which calibrate it into a 'measurement head' and the separate electronic controller systems into a 'ground station'. The second phase is the development of calibration and error check routines to enable the probe calibration and use over bladed discs of unknown geometry.

FM CAPACITANCE PROBE PRINCIPLE OF OPERATION

Chiver's (1989) frequency modulated capacitance clearance measurement system comprises a probe assembly and demodulator, Figure 4.1. The probe assembly consists of a tri-axial probe, oscillator and guard amplifier. The tri-axial probe tip forms one plate of an oscillator's capacitor connected to the other components in the oscillator via the tri-axial cable's centre wire. The oscillator is a 10 MHz Hartly design. Its function is to react to the change in capacitance that arises as a consequence of blade passing. The reaction takes the form of varying the oscillator output frequency so that it corresponds to the measured instantaneous capacitance at the probe tip.

The guard amplifier's function is to ensure that the voltage between the inner screen of the tri-axial cable and the centre wire is zero at all times with the outer screen connected to ground. Maintaining a zero voltage between inner screen and centre wire cancels the cable's shunt capacitance and the oscillator only registers the probe tip's capacitance change.

In practice, the guard amplifier comprises a unity gain amplifier capable of powering the reactive load which the guard screen's total capacitance to ground represents. The maximum shunt capacitance it could drive out is 180 pF at 10 MHz, the equivalent to approximately 180 mm of mineral-insulated cable. In the driven screen configuration, Chivers (1989) cited a reduction in apparent capacitance from 180 to 1.8 pF, with the capacitance between probe tip and blade varying from 1 to 10 pF due to blade passing.

The oscillator's frequency modulated output feeds into a demodulator. The demodulator unit comprises a voltage-controlled oscillator and a phase comparator. The comparator output is an instantaneous voltage, which is a function of the instantaneous value of probe oscillator frequency. Since the frequency's instantaneous value is a function of the capacitance between probe tip and blade, the output voltage is a function of capacitance. The output from the demodulator unit is a pulse train, with the peak height of each pulse a function of capacitance between probe tip and each passing blade.

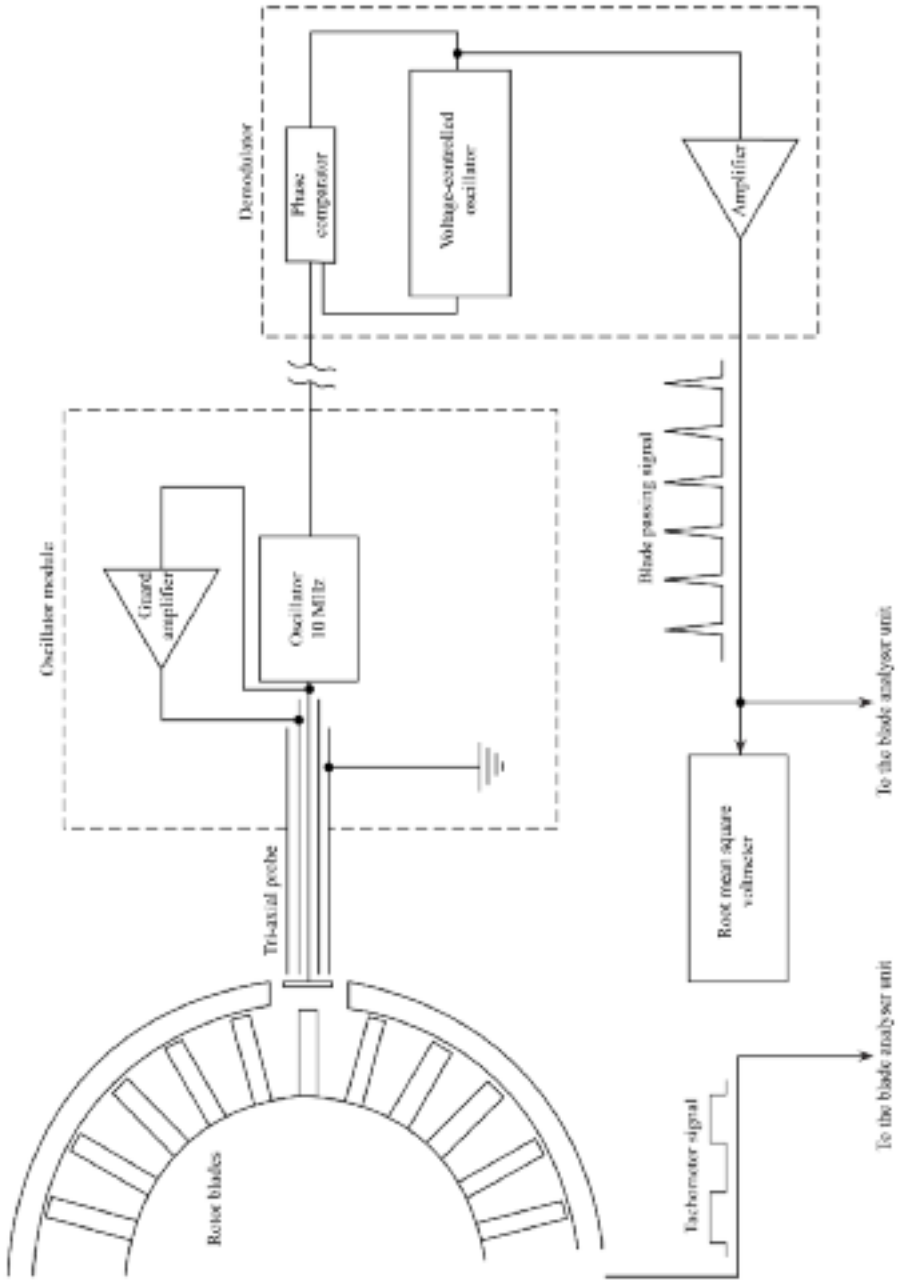


FIGURE 4.1. Capacitive clearance measurement system schematic block diagram.

THE BLADE ANALYSER UNIT

The authors used Killeen *et al.*'s (1991) blade analyser unit (BAU) to measure the height of each pulse from the demodulator. The pulse train feeds into the BAU's peak detect and reset circuit, Figure 4.2. This registers the voltage peaks' heights from the demodulator which then feed into an analogue to digital (A/D) converter. The blade analyser unit utilises a tachometer signal to reset a blade counter. The blade counter registers each blade as it passes. A dedicated microprocessor receives the output signal from the A/D converter and blade counter, partitioning each revolution of information into a data set.

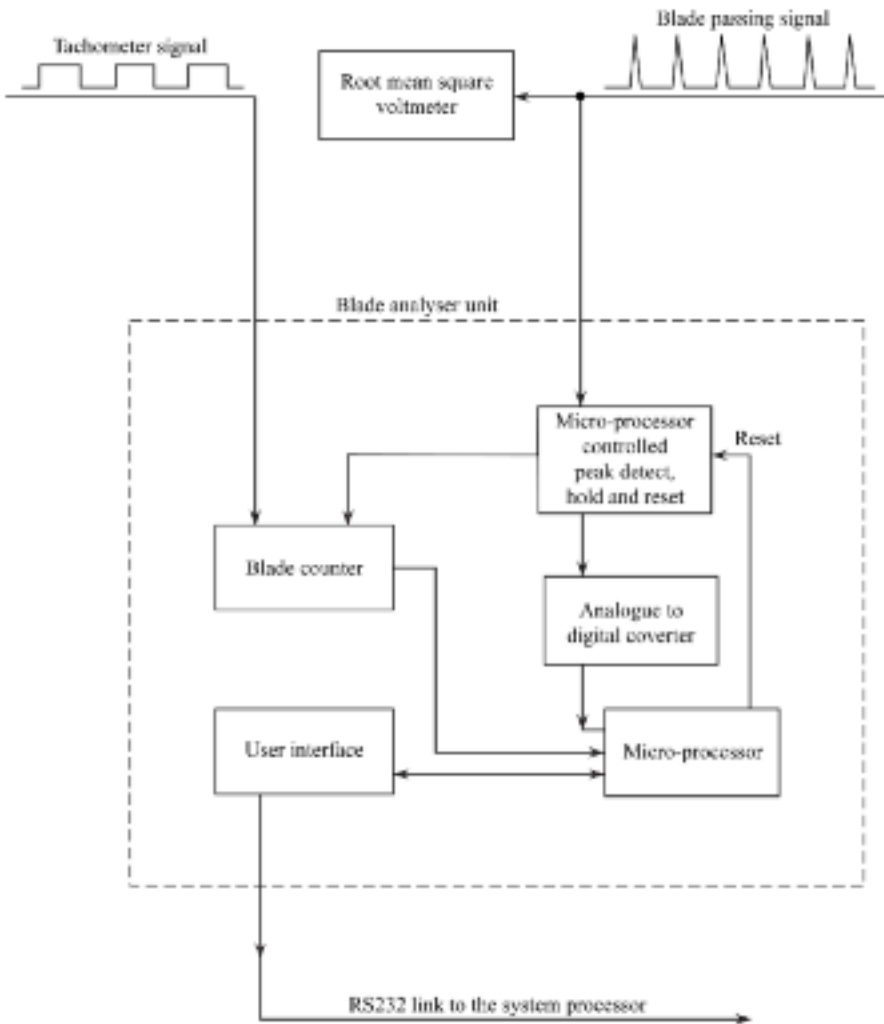


FIGURE 4.2. Blade analyser unit used to measure individual pulse heights, schematic block diagram.

The micro-processor acquires pulse heights from the A/D converter from one tachometer pulse to the next over one complete revolution of the bladed disc. The micro-processor compares the number of acquired pulses with the known number of blades on the disc. If the two numbers are the same it assumes that it did not miss any pulses during the data set acquisition. The authors averaged a number of successive data sets to suppress system noise.

THE PROTOTYPE MEASUREMENT HEAD

The authors recognised the requirement to produce a capacitance-based clearance measurement system which one could calibrate on-line and measure clearance over individual blades as challenging at an early stage in the system's development. The ultimate objective was to meet the requirements whilst retaining the capacitance probes' proven performance on development gas turbines and high-temperature demonstrator units. This required the new system to be physically small and able to withstand the 'shake and bake' of a high-pressure turbine environment.

The authors identified the first application of the new measurement system in the tip grind process of compressor manufacture, which Sheard *et al.* (1994) fully describe. Whilst the environment is not as harsh as a running turbomachine, the process is an ideal vehicle for system development and evaluation. In this application, bladed discs spin on a grinding machine to lock the blades centrifugally into their working position. The measurement head measures the bladed disc's radius over each blade during the grinding operation.

The measurement head's realised design, Figure 4.3, incorporates the spark-discharge electrode and capacitance probe into a single 8 mm probe, Figure 4.4, which mounts on a miniature traverse actuator. The probe assembly incorporates the tri-axial capacitance probe and electrode into its 8 mm diameter body. Both capacitance probe and electrode are insulated from the probe body, which independently earths following Morrison's (1991) recommendations to improve shielding of the capacitance probe. By taking care to ensure that the capacitance probe shielding extends flush with the probe tip, probe noise minimises and therefore range maximises. This design constitutes a re-packaging of Sheard's (2011) original system and is conceptually identical.

The authors based the traverse actuator that they used in the measurement head on one of Sheard *et al.*'s (1993) designs, Figure 4.5, intended for traversing aerodynamic probes between a turbine or compressor's blade rows. The actuator carriage carries a 'yaw module', with the carriage moving radially and the yaw module rotating the probe. The actuator carriage mounts between top and bottom blocks on guide bars, with a ball screw to move it. The carriage contains a split ball screw nut which spring loads into the ball screw, eliminating backlash.

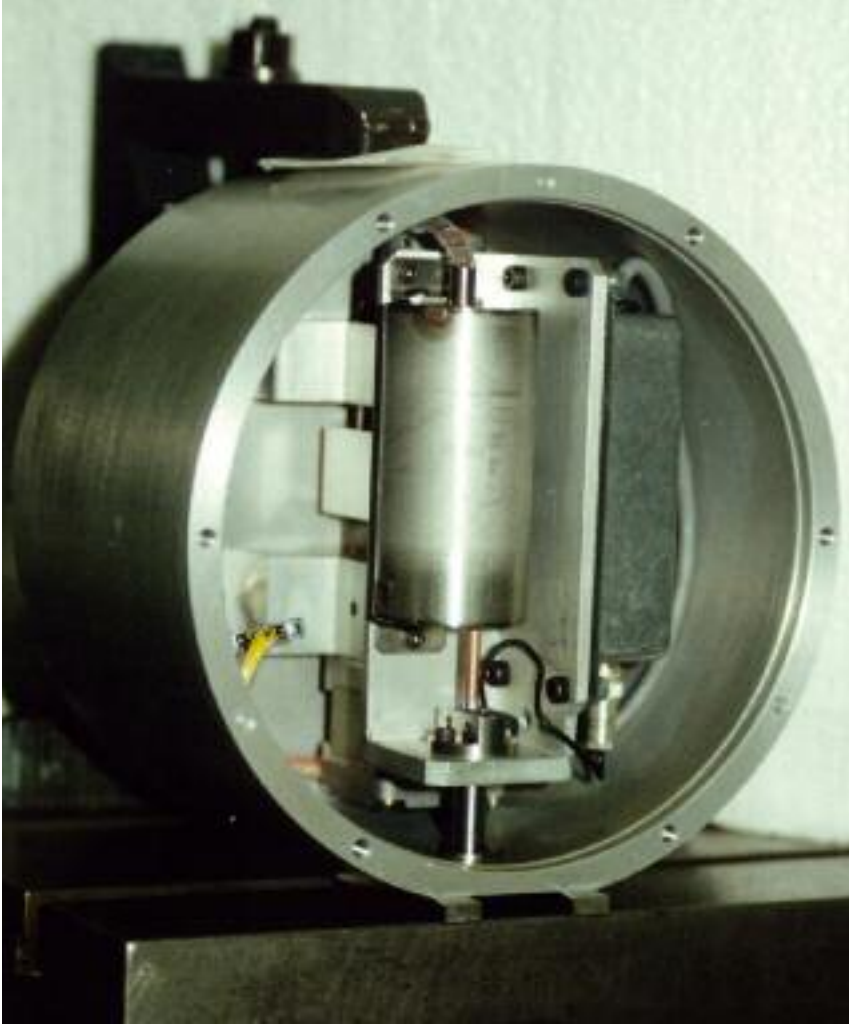


FIGURE 4.3. The prototype measurement head (without its cover), which integrates the capacitance probe, spark-discharge electrode and traverse actuator into a single unit.

A 400 pulse per revolution stepper motor drives the actuator ball screw. The ball screw has a 1 mm pitch, giving a step size of 2.5 microns. The authors fitted the top of the ball screw with a 400 pulse per revolution encoder, with the traverse controller generating the required number of stepper motor pulses, then interrogating the encoder to check that the stepper motor has actually executed them.

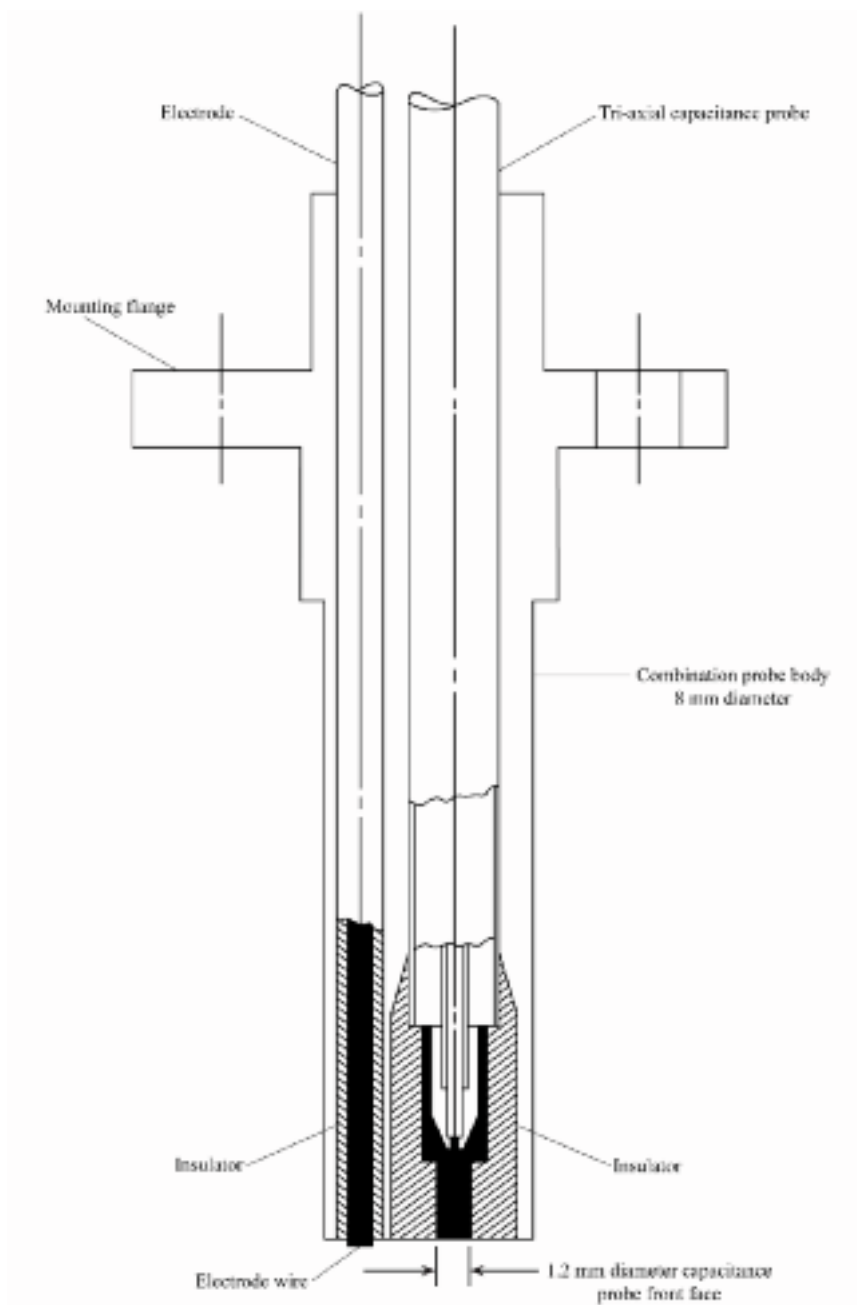


FIGURE 4.4. The 8 mm integrated probe with the adjustable electrode used in the prototype measurement head.

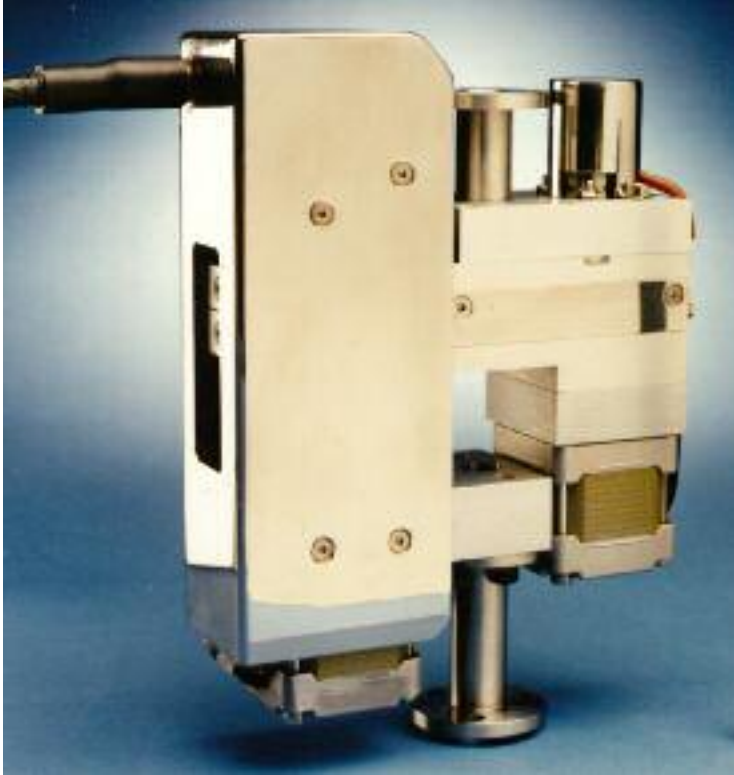


FIGURE 4.5. The original traverse actuator design, used for radial and angular positioning of aerodynamic probes in a gas turbine annulus. The radial transport mechanism was utilised in the prototype measurement head for positioning the capacitance probe and spark-discharge electrode.

In the prototype measurement head, the authors secured the traverse actuator top and bottom blocks to a back plate. The combination of guide bars and ball screw provides a rigid platform for the actuator carriage. The carriage itself forms a mounting point for the spark-discharge electronics module, capacitance oscillator module and probe assembly, Figure 4.6. Sheard and Turner (1992) and Chivers (1989), respectively, describe in detail the electronics module and oscillator module.

THE GROUND STATION

The authors' objective when designing the ground station was to combine all the electronics required to control the measurement head into a single unit. The authors wished to use existing subassemblies from Sheard's (2011) original control system where possible. This required a single RS232 link utilising simple ASCII commands to instruct the system processor. This in turn enabled the authors to interface the

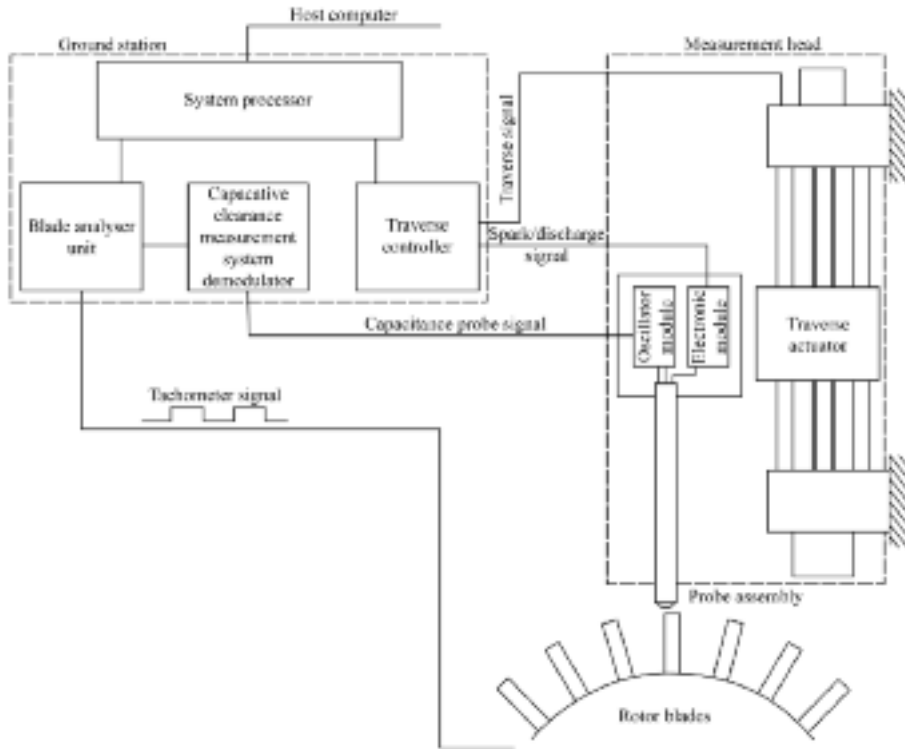


FIGURE 4.6. The inter-relationship between the ground station modules, measurement head and host computer illustrating the system processor's key role as an interface accepting input commands and then transparently orchestrating the action of other modules to act on them.

system processor with a data acquisition system. The ground station's principal elements are the traverse controller, capacitance probe demodulator, blade analyser unit and system processor, Figure 4.6. In Sheard's (2011) original control system these elements were separate, commercially available systems.

The authors' objective was to develop the system processor into an interface for the ground station which performed all internal communication within the ground station transparently to the user. During the programme of work the authors were developing all elements of the ground station, and the calibration and error check routines which they would store in the system processor EPROM. In the development system, the authors substituted an external computer for the single board micro-processor that would ultimately form the ground station's system processor. They used the external computer for developing the capacitance probe calibration and error check routines.

EXPERIMENTAL PROGRAMME

Following the measurement head and ground station design, the authors manufactured prototype units. The authors modified Sheard's (2011) calibration routines to run with the new hardware, with minor modifications to both hardware and software to achieve full functionality.

The authors selected a Pratt & Whitney JT8 stage 11 compressor for the experimental programme. This compressor disc incorporated small metal wedges under each blade to keep them locked out into their radial position to enable the authors to measure each blade's radius statically using conventional measurement techniques. This enabled them to measure clearance related to known geometry, therefore providing a method of establishing measurement error. They considered the JT8 stage 11 compressor typical of those over which gas turbine manufacturers routinely measure blade tip-to-casing clearance with a radius of approximately 300 mm and 70 blades of approximately 10 mm chord. The disc and blade set which the authors obtained were cycle scrapped components that had been gas turbine run. This was important as the actual variation in the disc's radius over each blade was typical of that which one would encounter in a gas turbine installation.

The authors fitted the measurement head and bladed disc to a computer numerically controlled (CNC) lathe, Figure 4.7. They mounted the measurement head on the lathes cross slide to enable it to move independently. In this way the bladed disc



FIGURE 4.7. The prototype measurement head fitted to a computer numerically controlled (CNC) lathe with a Pratt & Whitney JT8 stage 11 compressor disc and blade set.

could spin and the measurement head moved close enough to the blading to enable the authors to datum the capacitance probe.

CAPACITANCE PROBE CALIBRATION

The capacitance probe was able to make blade-by-blade measurements of clearance and, by utilising a once per revolution tachometer signal, the blade analyser unit could partition the results into single revolution data sets of clearance and blade number. Whilst clearance was unknown (as the probe was uncalibrated), the authors programmed the system processor to sort through a data set to identify the longest blade. The capacitance probe signal for each blade would change as the capacitance probe traversed to and from the blading. However, as the authors assumed that rotor geometry was constant, the longest blade would always give the largest signal in any one data set.

The authors spun the bladed disc at 1800 rpm, driving the capacitance probe in using the traverse actuator which stopped in close proximity to the longest blade using the spark-discharge probe. The authors then acquired a data set comprising capacitance probe output over a single revolution. They stepped back the capacitance probe from the blading and acquired a second data set. They repeated this process, Figure 4.8, until sufficient data sets were available to calibrate the capacitance probe.

Once the authors acquired the data sets, they compared the total distance traversed between the first and last data set to the difference in clearance between the shortest and longest blades. The authors considered that distance between the shortest and longest blade should be less than the distance between capacitance probe position when they acquired the first and last data sets. This was necessary to ensure that the authors could use the final calibration without extrapolating beyond the range of the data from which they generated it. Not extrapolating beyond the range of data from which one generates a calibration is important as, at extended range, capacitance probe signal approaches the system noise floor and, therefore, it becomes increasingly difficult to guarantee that the peak pulse heights that the authors recorded were blade passing pulses and not random peaks due to system noise.

The calibration criteria that the authors established were as follows. The initial traverse step size was 0.05 mm and they recorded successive data sets at 0.05 mm intervals. If it were not possible to acquire data with the correct number of blades, the authors assumed that blading was out of range and they abandoned their attempts to acquire data at that capacitance probe position.

The authors checked the number of data sets at different traverse positions. If there were less than six the authors reduced the traverse step size and repeated the procedure. They considered six data sets as the minimum to facilitate the calculation of measurement system calibration. If they acquired six or more data sets, they selected the minimum reading from the first data set (from the shortest blade) and maximum reading from the last data set (from the longest blade). If the longest blade reading from the last data set was smaller than the shortest blade reading from the

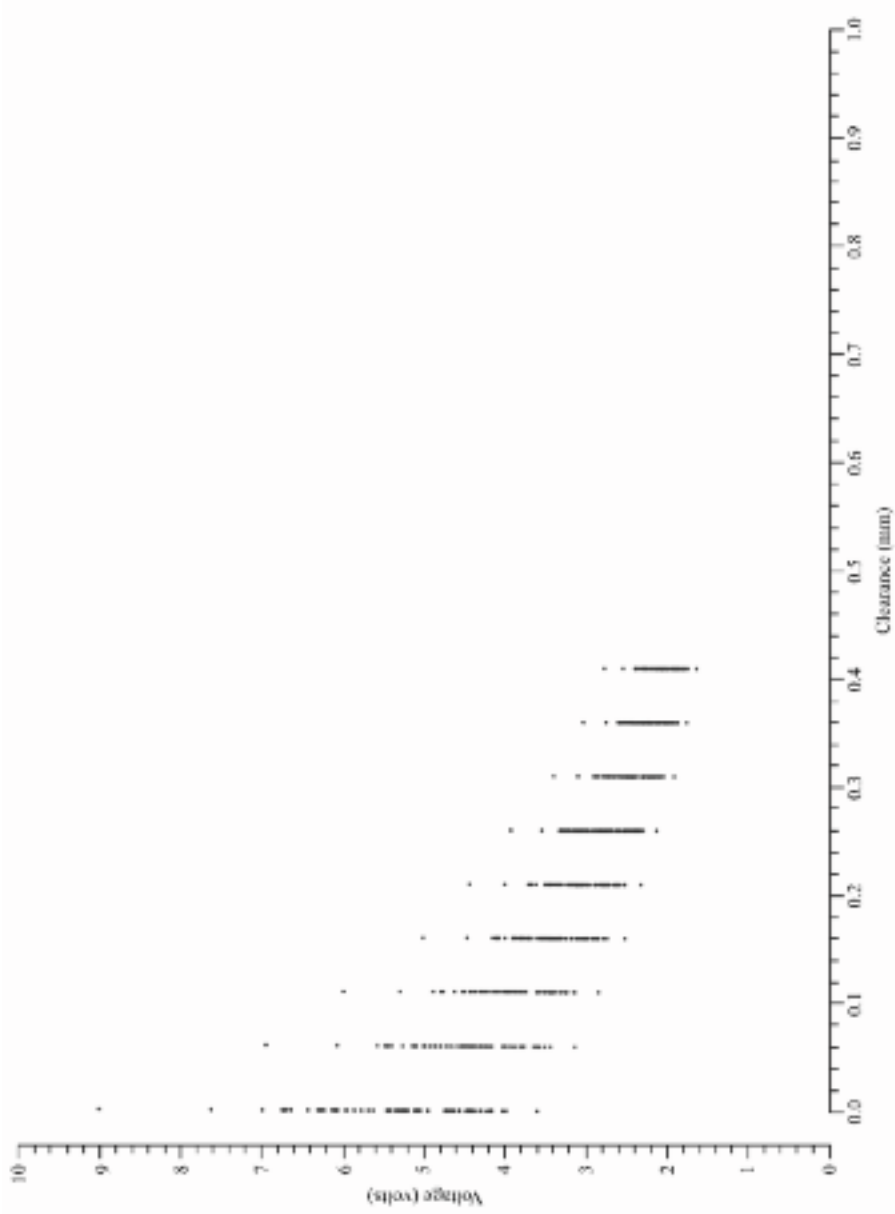


FIGURE 4-8. Seventy-point data sets acquired from the capacitance probe at nine different traverse actuator positions. Each dot on the graph is a single measurement over a single blade.

first data set, then the distance traversed between the two must be greater than the difference in clearance between them. Once the authors satisfied this condition, not only were there sufficient data sets available to enable them to calculate a calibration, there was confidence that they extended over an adequate range.

The authors acquired nine data sets over the JT8 stage 11 compressor with the system processor sorting through the data in each data set and selecting the signal corresponding to the longest blade, Figure 4.9. They used a least squares technique to fit a curve through the data, using the equation:

$$D = A_1 + A_2/V + A_3/V^2$$

where A_1 , A_2 and A_3 are constants determined by the curve fit, D is the distance between plates (the probe sensor electrode and blade tip) in mm and V is probe output in volts. The authors chose this form of the equation after extensively studying other possible forms.

The physics of a capacitor dictate that capacitance should approach infinity as the distance between the capacitor plates approaches zero. In this case, the authors assigned the first data point in Figure 4.9 a clearance of zero as the actual clearance was unknown. They made the assumption that the negative value at which the curve tended to infinity was the unknown clearance between the probe tip and the longest blade at the first data point. The authors set the constant A_1 to zero to give the actual calibration. They used the spark-discharge electrode to datum the capacitance probe prior to obtaining the first data set. They measured the distance from the capacitance probe sensor electrode to spark-discharge electrode tip. This enabled them to correctly position the data points on the axis of Figure 4.10. The accuracy with which the measured data points matched the calibration curve was excellent, with the calibration covering a range from zero to 0.65 mm.

The authors calculated the error that occurred with the developed on-line calibration technique using the following method. They recorded data sets of probe voltage which comprised 70 separate voltages, one for each blade, with nine data sets in all, one for each traverse position. Each data set formed one column of a 70×9 matrix $[V]$ of probe voltages:

$$[V] = [V_{b,t}]$$

where:

b = blade number;

t = traverse position.

The authors transformed the matrix $[V]$ into a 70×9 matrix of clearances $[C1]$ once a probe calibration was available:

$$[C1] = [C1_{b,t}]$$

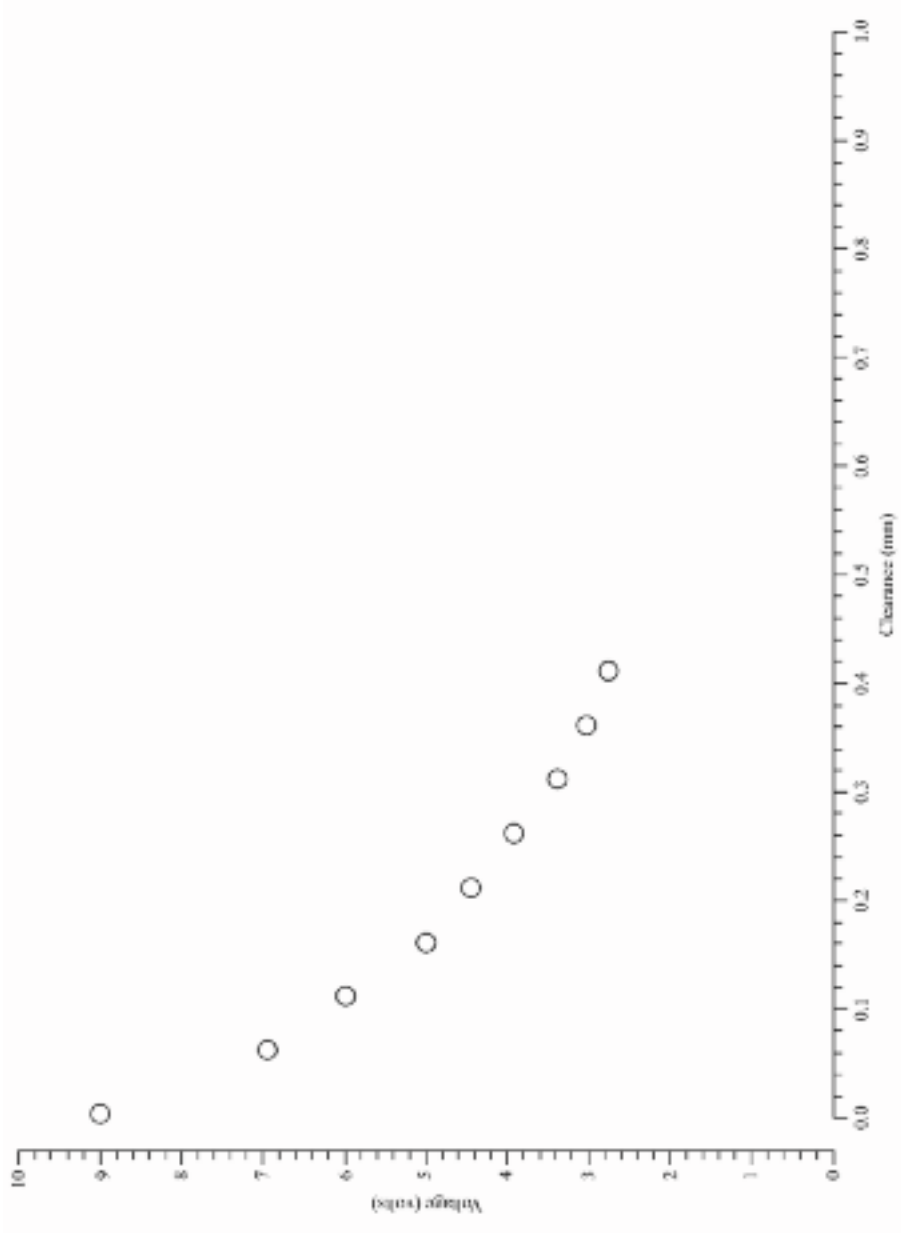


FIGURE 4.9. Capacitive clearance measurement system output for the longest blade of each data set plotted against known position, which was changed using the traverse actuator.

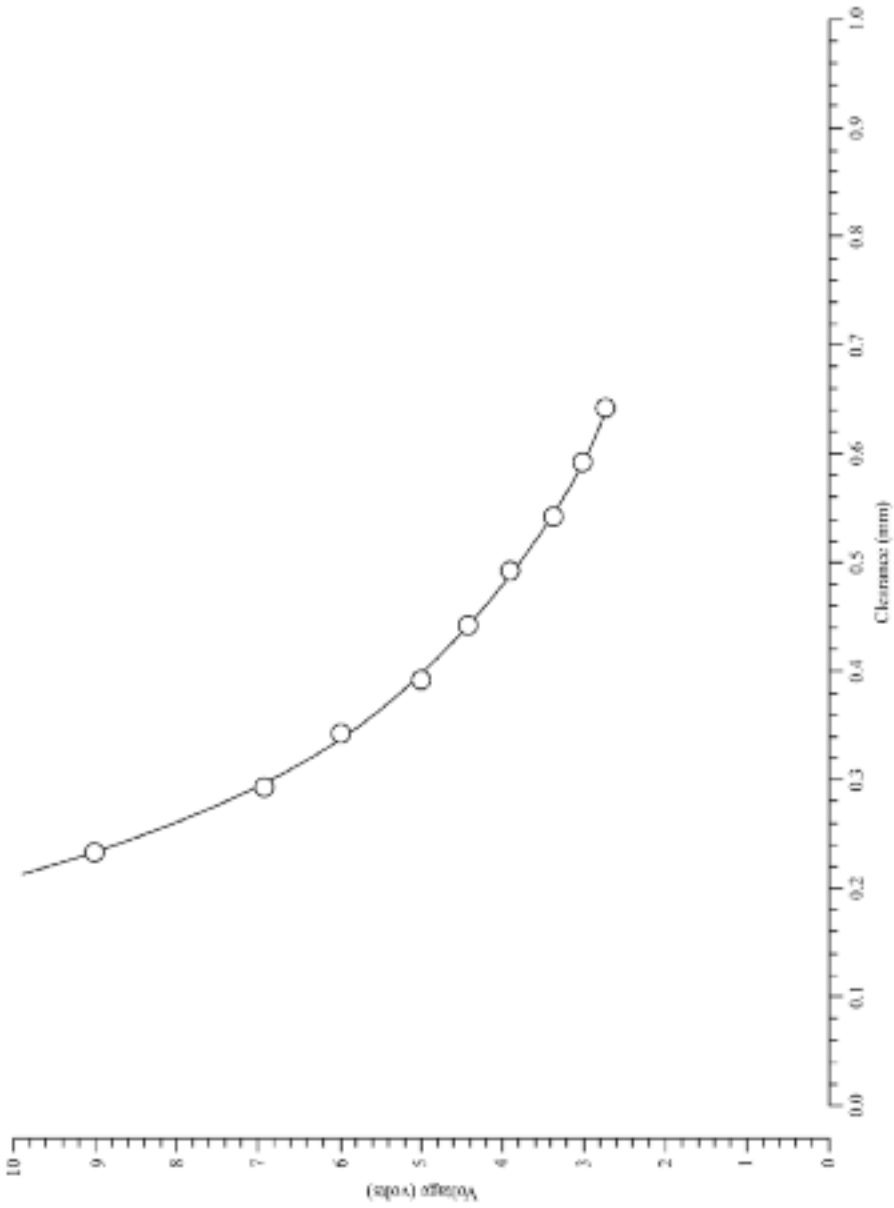


FIGURE 4.10. Capacitive clearance measurement system calibration obtained with no knowledge of relative blade heights or the distance from spark-discharge electrode to capacitance probe tip. The known positions of the data points used in the calibration are also shown.

The authors calculated each element of [C1] from the corresponding element in [V] using the calibration equation:

$$[C1_{b,t}] = \{A_1 A_2 A_3\} \begin{bmatrix} 1 \\ 1 / V_{b,t} \\ 1 / V_{b,t}^2 \end{bmatrix}$$

where:

$A_1 A_2 A_3$ = constants from the least squares curve fit;
 $V_{b,t}$ = probe voltage for blade b at traverse position t .

The form of the equation that the authors used for the curve fit included a squared term which introduced a turning point into the equation outside the range of the points which they used to generate the calibration. For this reason, the authors identified the location of all voltages in matrix [V] less than the smallest voltages that they used to generate the calibration, and set values of clearance in matrix [C1] in these locations to zero.

The authors defined a matrix of blade lengths, relative to the longest blade as:

$$[L] = [L_b]$$

They defined a matrix of probe distances between the probe and the longest blade as:

$$[P] = [P_t]$$

The authors defined a second matrix of clearance as:

$$[C2] = [C2_{b,t}] = [L_b] + [P_t]$$

As the clearance change between data sets was 0.05 mm, the authors could calculate clearance in a second way. They used the calibration coefficients to calculate clearances from the first column of [V], which gave clearance over every blade. They calculated the remaining columns by adding the appropriate multiple of 0.05 mm offset to the values in the first column generating a second clearance matrix [C2]. Again, the authors set all clearances calculated from voltages outside the calibration range to zero. They plotted clearance in matrix [C2] against capacitance probe output [V], Figure 4.11.

The authors calculated an error matrix:

$$[E] = [C2] - [C1]$$

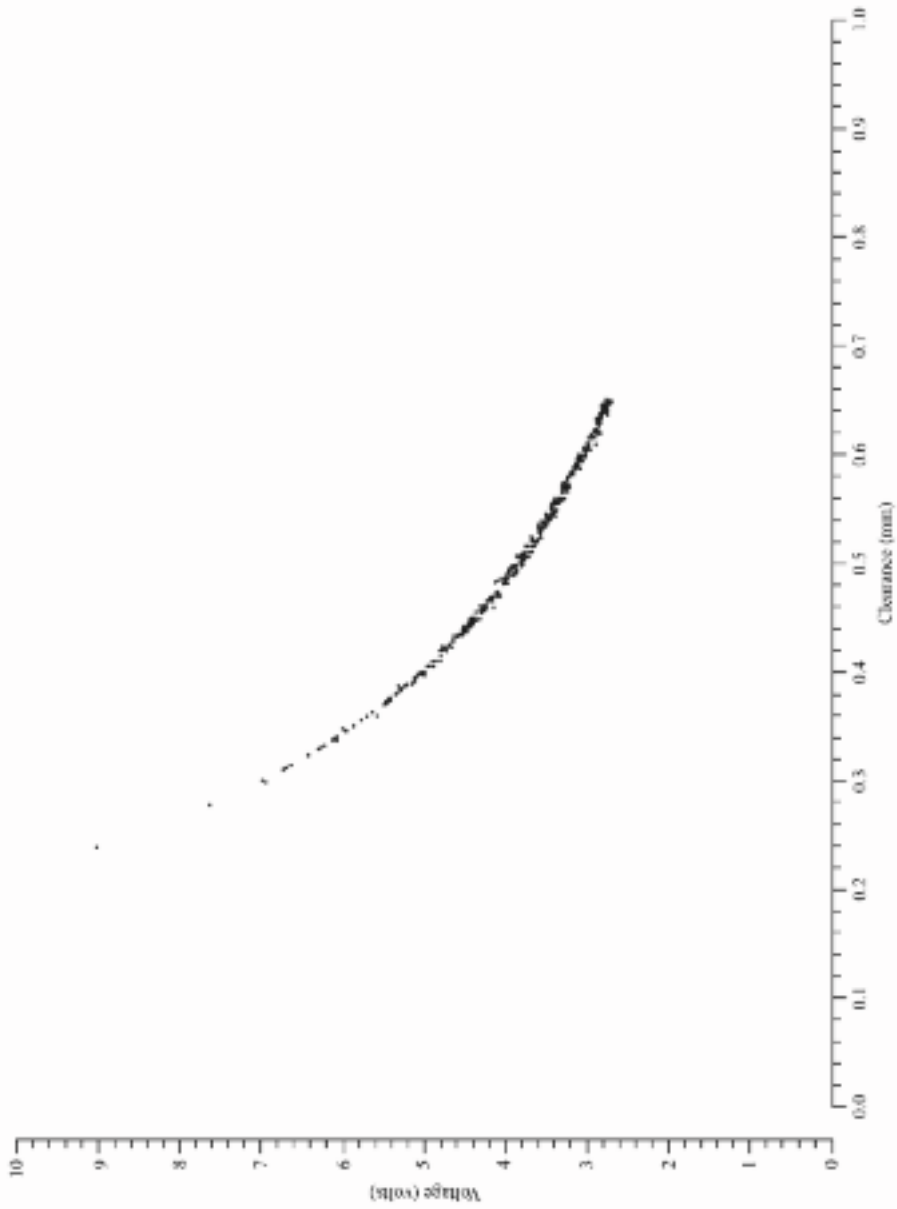


FIGURE 4.11. Capacitive clearance measurement system output plotted against clearance illustrating the one over distance nature of the system output.

The first columns of [C1] and [C2] were identical. The remaining columns would be identical if the calibration were perfectly accurate, but in practice it was not and small discrepancies arose. The authors quantified the discrepancies by subtracting [C1] from [C2] to generate error matrix [E]. The first column of [E] was zero, as were all locations which corresponded to out of calibration voltages in [V]. The authors plotted error in matrix [E] against [C2], Figure 4.12. The error plot exhibited the expected trend of increasing error with increasing clearance, but this scatter was approximately twice that which Sheard (2011) obtained over blading of known geometry.

CALIBRATION REFINEMENT

The calibration had been generated by performing a curve fit through the voltage from the longest blade in each data set. The finite values in error matrix [E] indicated that the calibration was not perfect. Each row of [E] corresponded to the error in clearance over one blade in each data set. Each column of [E] corresponded to the error in clearance over every blade in one data set.

The authors summed and averaged each row to generate a 1×70 matrix [F1].

$$[F1] = [F1_b] = \sum_{\frac{n=1}{T}}^{n=T} [E_{b,n}]$$

where:

T = total number of traverse positions.

The authors assumed actual errors in capacitance probe readings as random and Gaussian. The finite values in matrix [F1], therefore, corresponded to the error in clearance that arose due to the error in the original calibration.

The authors summed and averaged each column to generate a 70×1 matrix [F2].

$$[F2] = [F2_r] = \sum_{\frac{r=1}{B}}^{r=B} [E_{r,t}]$$

where:

B = total number of blades.

The finite values in matrix [F2] corresponded to the error in clearance that arose due to the error in traverse actuator positioning relative to its assumed position. The authors defined the limits to the errors contained in [F1] and [F2] that constituted an

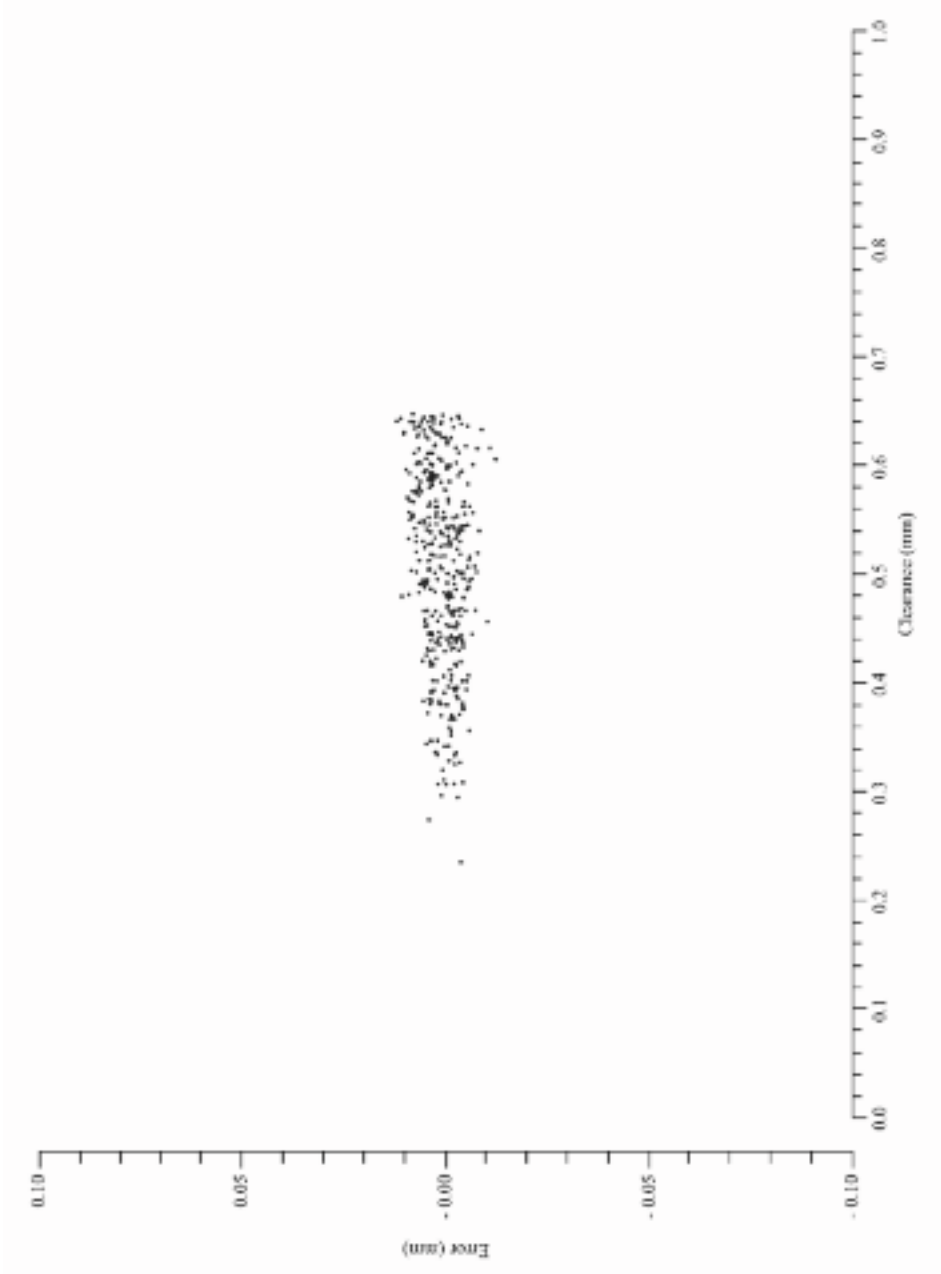


FIGURE 4.12. Error in capacitive clearance measurement system output, calculated by subtracting clearance obtained using system calibration from that obtained assuming no knowledge of traverse actuator position.

acceptable calibration. In this way the system processor was able to identify and reject corrupted capacitance probe calibration data.

We may refine matrix $[L]$ and matrix $[P]$ to give $[L2]$ and $[P2]$:

$$[L2] = [L] - [F1]$$

$$[P2] = [P] - [F2]$$

We can then define a matrix of refined clearances as:

$$[C3] = [C3_{b,t}] = [L2_b] + [P2_t]$$

We can use each element in $[V]$ and $[C3]$ in the least squares curve fit to give an improved set of calibration coefficients. The authors then used the coefficients to calculate a clearance matrix $[C4]$ from $[V]$ in the same way that they calculated $[C1]$ using the original coefficients.

The correction to the original clearance matrix $[C1]$ effectively utilised the other data that the authors acquired, but they did not use it to calculate the original calibration coefficients. They plotted capacitance probe output $[V]$ against corrected clearance $[C3]$, Figure 4.13, with noticeably less scatter. The authors calculated a second set of 'refined' coefficients by repeating the curve fitting exercise, this time using $[V]$ and $[C3]$.

The authors defined a self-consistency matrix as:

$$[H] = [C3] - [C4]$$

They then calculated refined clearances by applying the new calibration to $[V]$ to generate $[C4]$. The authors calculated the deviation of individual clearances from the refined calibration curve by subtracting $[C4]$ from $[C3]$ to give a self-consistency matrix $[H]$. Figure 4.14 illustrates the calibration's self-consistency as it plots $[C3]$ against $[H]$ with the scatter over the calibration range similar to that which Sheard (2011) obtained over blading of known geometry. The authors considered the outcome excellent.

CLEARANCE MEASUREMENT

Development of the capacitance probe calibration and error check routines focused on their self-consistency with no reference to the accuracy with which the authors actually could measure clearance. The authors considered this approach reasonable as the capacitance probe had no prior knowledge of the blading geometry. The ultimate test, however, of the capacitance probe calibration was its repeatability and accuracy when the authors used it to make absolute measurements of clearance.

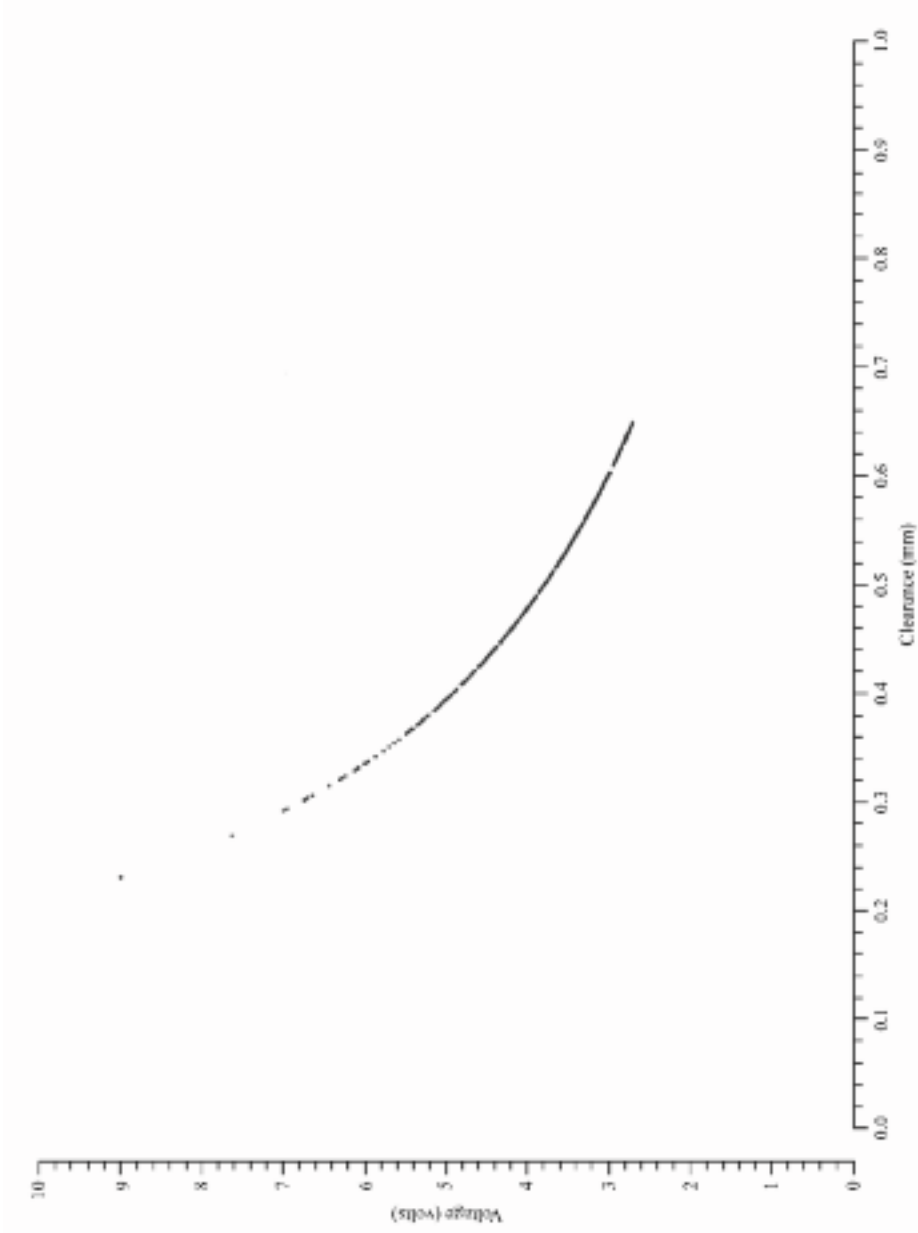


FIGURE 4.13. Capacitive clearance measurement system output plotted against corrected clearance illustrating that the data falls onto a curve with noticeably less scatter than before correction.



FIGURE 4.14. The deviation of capacitive clearance measurement system output from the refined calibration, illustrating an error of ± 0.005 mm. The error degrades at increasing range due to the capacitance probe's decreasing sensitivity.

The Pratt & Whitney stage 11 compressor disc exhibited a maximum blade-to-blade variation of radius 0.25 mm, which the authors assumed typical of compressor blading. They ascertained probe repeatability by calibrating, measuring then parking the measurement head six times, Figure 4.15. The scatter was ± 0.01 mm, which was a total system error for the lathe and measurement head over six completely independent measurements. The authors, therefore, considered the scatter consistent with the ± 0.005 mm error in the refined calibration. This gave confidence that the actual error in capacitance probe measurement was of that order.

The blades exhibited a $\pm 10\%$ tolerance on blade tip thickness, with thickness varying from 1.25 to 1.45 mm. The authors used a capacitance probe which was 1.2 mm diameter. Changes in blade thickness from 1.25 to 1.45 mm, therefore, should not change probe sensor electrode to blade tip overlap area and hence should not affect capacitance probe output. In order to verify that capacitance probe measurements were not influenced by the blade-to-blade variation in blade tip thickness, the authors machined all blades to the same radius within an estimated tolerance of ± 0.005 mm.

The authors calibrated the 1.2 mm probe and measured clearance and error from the known clearance over each blade, Figure 4.16. Over 95% of the measurements were within a ± 0.01 mm error. This was consistent with a ± 0.005 mm error in blade radius and ± 0.005 mm error in calibration self-consistency at the 0.25 mm range at which the authors measured. This gave confidence that the 1.2 mm diameter probe design was insensitive to changes in blade thicknesses. Second, the results were consistent with the accuracy which Sheard (2011) achieved over blading of known geometry. This indicated that the new calibration technique achieved the probe's full accuracy.

The results which the authors obtained with the JT8 stage 11 compressor gave confidence that the on-line calibration technique enabled them to measure clearance to ± 0.01 mm. The authors tested this confidence by arranging a 'back to back' test with a clearance measurement system utilising an optical triangulation operating principle, which Drinkuth *et al.* (1974) described. The laser-based optical system was capable of measuring clearance over individual blades with accuracy similar to that of the capacitance probe. The authors used a compressor with an operating point typical of modern high bypass ratio gas turbines for the back to back test. The compressor had 76 blades of 2 mm maximum thickness and the authors rotated it at 1800 rpm to ensure that the blades centrifugally loaded into their true working position. They then calibrated the capacitance probe and measured the clearance over each blade. They immediately calibrated the optical system and repeated the measurement of clearance. Clearance which the authors measured with the two systems, Figure 4.17, illustrates a 0.10 mm eccentricity of the rotor. The blade-by-blade measurements of clearance with the two systems are within 0.02 mm for over 90% of the blades. This is consistent with each system having an accuracy of ± 0.01 mm. Therefore, the authors considered the agreement between the two measurement techniques excellent.

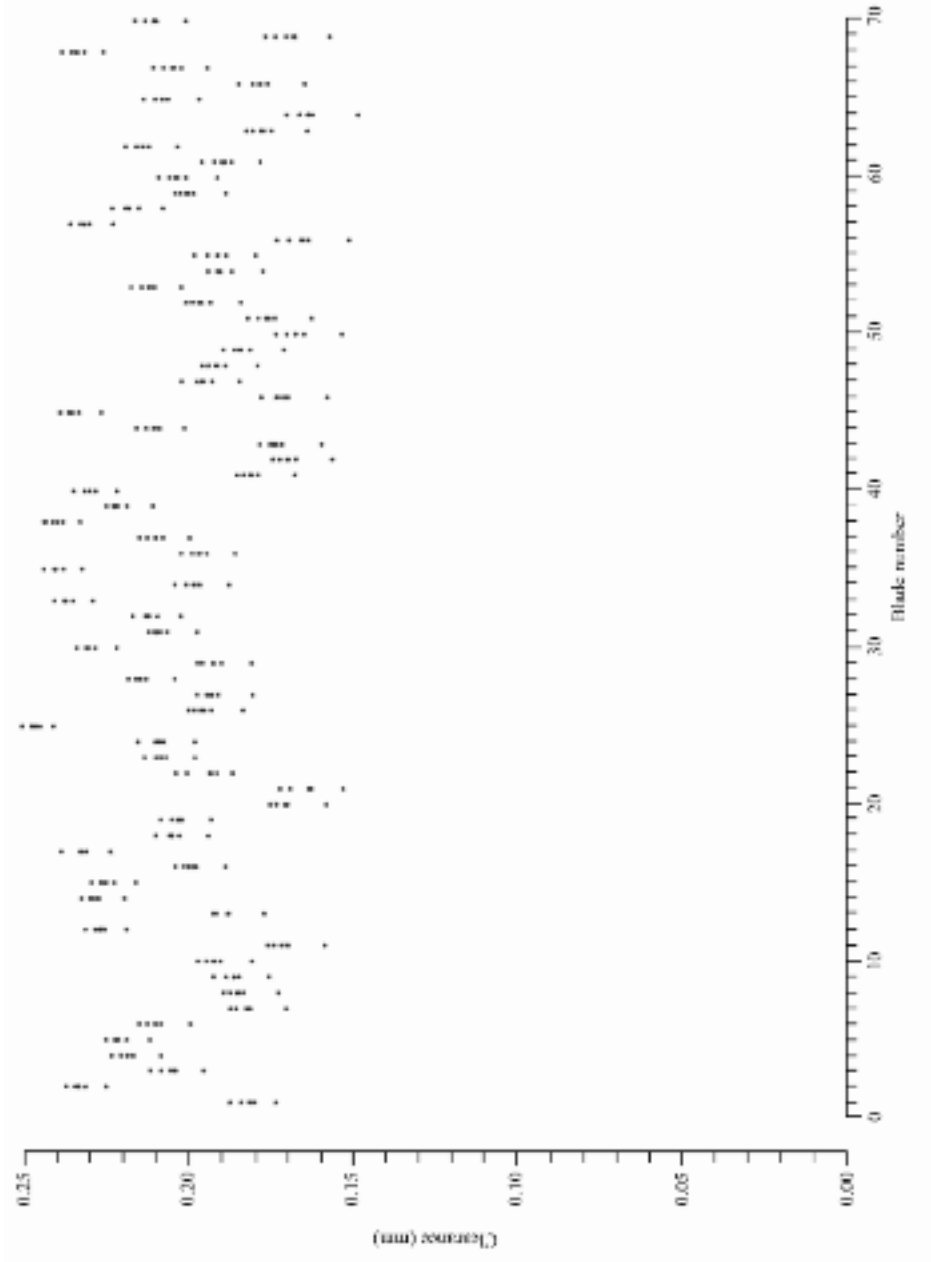


FIGURE 4.15. Clearance measured over each blade around the JT8 stage 11 compressor disc, measured six times, calibrating then parking the probe before and after each measurement.

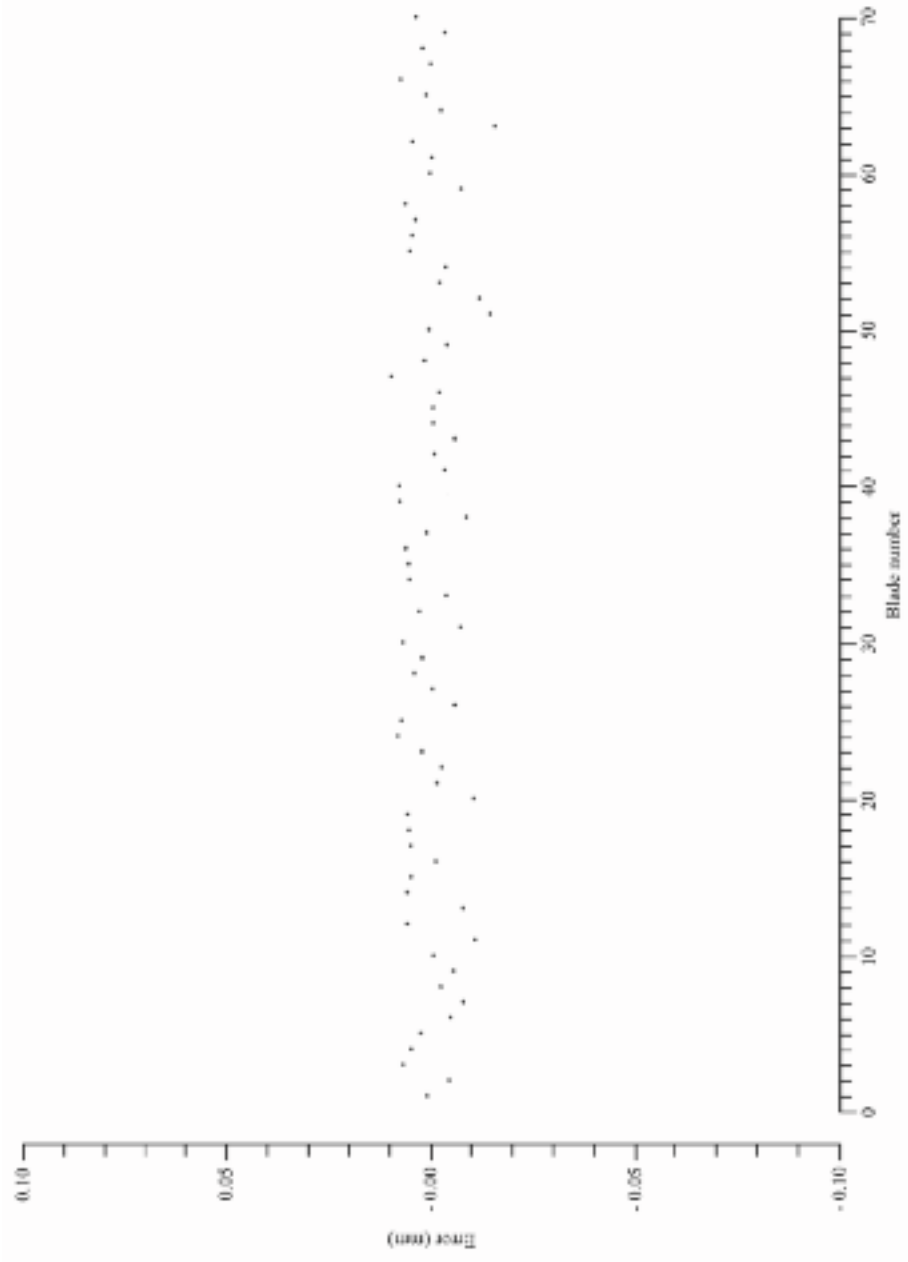


FIGURE 4.16. Error in measured clearance of each blade around the JT8 stage 11 compressor disc, measured with a 1.2 mm diameter capacitance probe at a probe range of 0.25 mm.

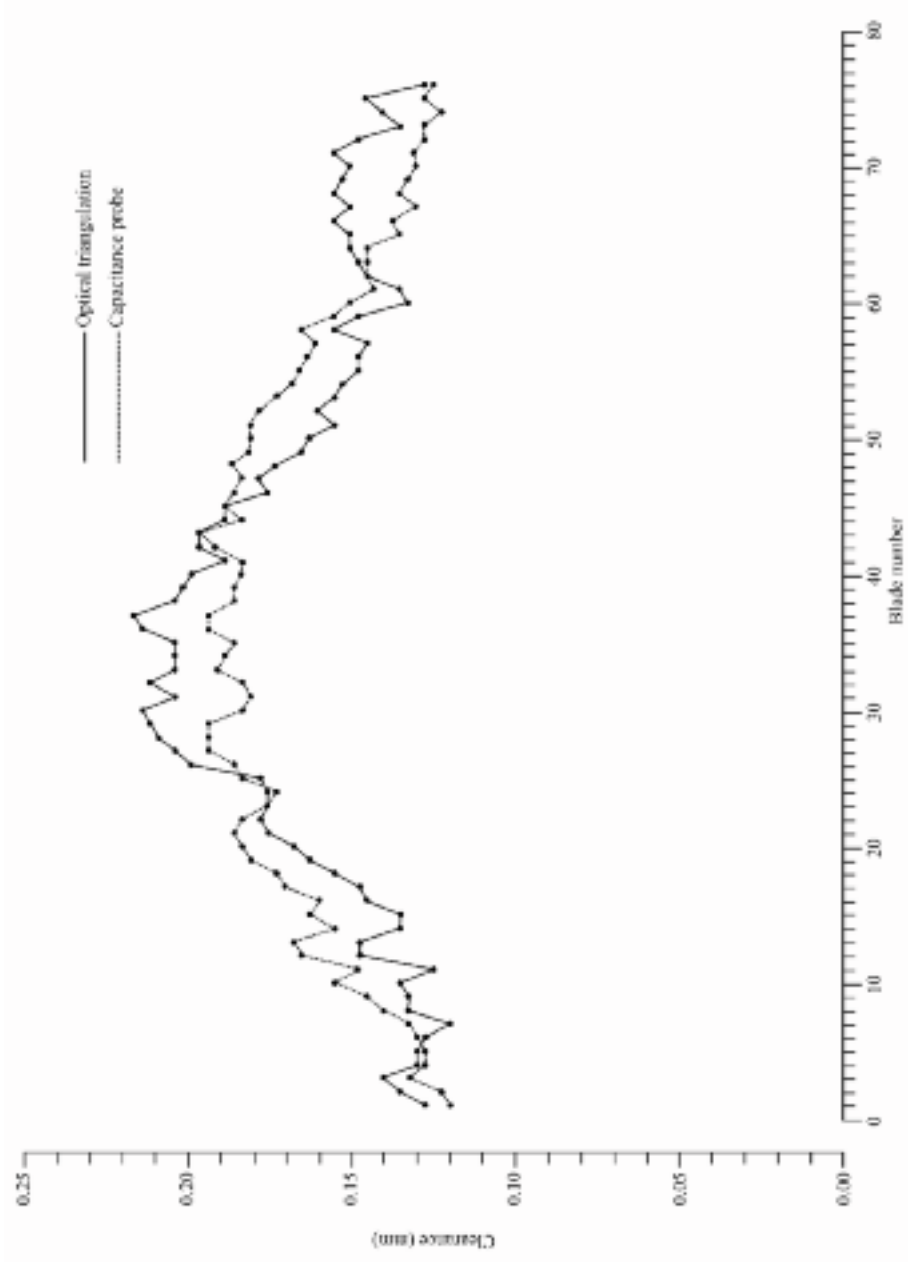


FIGURE 4.17. Clearance measured over each blade around the compressor disc, measured using an optical triangulation system and capacitive clearance measurement system following an on-line calibration.

The 1.2 mm diameter probe was able to measure over a range of 1.0 mm, 80% of its diameter. The authors considered this good for an unfiltered probe design capable of making measurements over individual blades. Whilst a range of 1.0 mm would not be acceptable for fixed capacitance probes, the authors programmed the system processor to 'track' the blading. In this way, they kept the capacitance probe less than 0.1 mm from the longest blade, therefore they utilised the capacitance probe range only to resolve the difference in clearance between longest and shortest blades. The cycle scrapped JT8 stage 11 compressor exhibited a maximum variation in blade length from longest to shortest of 0.25 mm. The range of a 1.2 mm capacitance probe was four times the 0.25 mm variations in tip clearance. With a demonstrated accuracy of ± 0.01 mm, the authors concluded that the new measurement system was suitable for making blade-by-blade measurements of clearance over typical gas turbine blading.

CONCLUSIONS

The authors developed a new capacitance-based clearance measurement system which incorporates all required elements for on-line calibration of the capacitance probe into a single measurement head and its associated controller. The authors established criteria for adequate capacitance probe calibration as a minimum of six sets of capacitance probe output covering the range over which they would use the probe to measure.

The authors developed algorithms to calibrate the capacitance probe by performing a least squares curve fit through the probe output for the longest blade, then they further refined the calibration using the probe output from the rest of the blades. The authors conceived and implemented error checking routines to enable them to establish the quality of a calibration prior to its use.

The 1.2 mm diameter capacitance probe proved insensitive to variations in blade tip thickness from 1.25 to 1.45 mm. Over typical compressor blading the probe's range was four times the variation in blade-to-blade clearance which the authors encountered in gas turbine run components.

The authors demonstrated that the studied capacitance probe is capable of measuring clearance over individual blades to an accuracy of ± 0.01 mm over the 0.25 mm blade-to-blade variation in clearance that occurs in gas turbine run components.

REFERENCES

- Barranger, J. (1978), 'An In-Place Recalibration Technique to Extend the Temperature Capability of Capacitance-Sensing Rotor Blade Tip Clearance Measuring Systems'. *Society of Automotive Engineers Aerospace Meeting*, San Diego, USA, Paper No. 781003.
- Chivers, J.W.H. (1989), *A Technique for the Measurement of Blade Tip Clearance in a Gas Turbine*. PhD thesis, University of London.

- Davidson, D.P., De Rose, R.D. & Winnerstrom, A.J. (1983), 'Measurement of Turbomachinery Stator to Drum Running Clearances'. *Proceedings of the 28th American Society of Mechanical Engineers Gas Turbine and Aeroengine Congress*. Phoenix, Arizona, 27–31 March, Paper No. 83-GT-204.
- Drinkuth, W., Alwang, W.G. & House, R. (1974), 'Laser Proximity Probes for the Measurement of Turbine Blade Tip Running Clearances'. *Proceedings of the ISA Aerospace Instrumentation Symposium*. Paper No. 74228, pp. 133–40.
- Killeen, B., Sheard, A.G. & Westerman, G.C. (1991), 'Blade-by-blade Tip Clearance Measurement in Aero and Industrial Turbo-Machinery'. *Proceedings of the 37th ISA International Symposium of Measurement Techniques*, pp. 429–47.
- Morrison, R. (1991), 'Grounding and Shielding in Instrumentation'. *Proceedings of the 37th ISA International Symposium of Measurement Techniques*, pp. 989–96.
- Sheard, A.G. (2011), 'Blade-by-blade Tip Clearance Measurement'. *International Journal of Rotating Machinery*, vol. 2011, Article ID 516128, pp. 1–13.
- Sheard, A.G. & Turner, S.R. (1992), 'An Electromechanical Measurement System for the Study of Blade Tip-to-casing Running Clearances'. *Proceedings of the 37th American Society of Mechanical Engineers Gas Turbine and Aeroengine Congress*. Cologne, Germany, 1–4 June, Paper No. 92-GT-50.
- Sheard, A.G., Killeen, B. & Palmer, A. (1993), 'A Miniature Traverse Actuator for Mapping the Flow Field between Gas Turbine Blade Rows'. *Proceedings of the IMechE: Machine Actuators & Controls Seminar*. London, UK, 31 March, pp. 1–11.
- Sheard, A.G., Westerman, G.C., Killeen, B. & Fitzpatrick, M. (1994), 'A High-Speed Capacitance-Based System for Gauging Turbomachinery Blading Radius During the Tip-Grind Process'. *Transactions of the ASME, Journal of Engineering for Gas Turbines & Power*, vol. 116, pp. 243–9.

A High-speed Capacitance-based System for Gauging Turbomachinery Blading Radius during the Tip Grind Process

A.G. Sheard, G.C. Westerman,
B. Killeen and M. Fitzpatrick

ABSTRACT

During the manufacturing and overhaul of gas turbines, it is necessary to ensure that all blades in a stage are of an equal and known length to minimise performance loss that arises as a consequence of the clearance between blade tips and gas turbine casings. Modern compressor and turbine blades are generally loose fitting in their root fixings and only adopt their true working position when running.

This chapter describes a new technique for measuring the rotor radius over individual blades. The measurement technique utilises a capacitance-based clearance measurement system which enables one to measure the rotor radius over each blade whilst spinning fast enough to ensure that the blades centrifugally load into their true working position. The chapter describes the measurement technique, and the method that the authors developed to calibrate and reduce measurement system output into a reading of radius over individual blades. The chapter presents the mechanical design of the 'measurement head' and describes the computer numerically controlled (CNC) lathe to which it interfaces. Finally, the chapter presents results of an experimental programme that utilised a fully bladed compressor disc, and in so doing, ascertained performance of the capacitance-based system when gauging blade radius during the tip grind process.

INTRODUCTION

The continuing effort by gas turbine manufacturers to improve the efficiency of their product has led to the use of computational fluid dynamic computer codes to assist design engineers in their efforts to minimise aerodynamic losses through the

This chapter is a revised and extended version of Sheard, A.G., Westerman, G.C., Killeen, B. & Fitzpatrick, M. (1994), 'A High-Speed Capacitance-Based System for Gauging Turbomachinery Blading Radius During the Tip-Grind Process'. *Transactions of the ASME, Journal of Engineering for Gas Turbines & Power*, vol. 116, pp. 243–9.

blading. This, in turn, has resulted in complex three-dimensional aerofoil designs which minimise the losses that occur with the various secondary flow mechanisms that develop through gas turbine blade rows. One source of aerodynamic loss occurs with leakage flow over the blade tip. Despite the small size of the blade tip-to-casing clearance, significant losses occur with the tip leakage vortex that develops as a consequence of the static pressure field across a blade passage. As design engineers progressively reduce other aerodynamic loss mechanisms, tip clearance related losses become an increasing proportion of what remains. Consequently, as blade design praxis improves it becomes correspondingly more important to reduce blade tip-to-casing clearance.

The use of an abradable material over rotating blading is common as it allows the blades to cut their own path when the gas turbine is new. Clearance is the result of blade tip-to-casing contact at some point during the gas turbine cycle and, therefore, the minimum that it may achieve. Active clearance control systems offer the potential to increase blade tip-to-casing clearance during transient conditions (to avoid blade tip-to-casing contact) and minimise clearance during stable operation (to maximise gas turbine efficiency). Irrespective of whether one employs an active clearance control system, one cannot completely eliminate the possibility of contact between blades and the casings within which they run. If one blade is significantly longer than the rest, the long blade will cut a path which will result in larger clearances over every other blade. At first sight the problem may seem trivial, simply ensuring that all blades are the same length. However, the design of modern blade root fixings in their disc is such that they are a loose fit and do not adopt their true working position until they centrifugally load.

In order to measure a bladed disc's radius over each blade, it is necessary to spin it fast enough to load each blade into its working position. The problems that occur when attempting to measure the bladed disc's radius whilst rotating are formidable and, until recently, researchers did not address them. This has, however, changed and the V2500¹, for example, now specifies in its build and overhaul procedures that manufacturers must machine each compressor and turbine stage as a bladed disc assembly. Gas turbine manufacturers have introduced the requirement to machine bladed discs as an assembly, as the previously used technique of grinding individual blades to a known length and then fitting them in a disc of known diameter is inadequate to meet required gas turbine compressor and turbine initial build tolerance.

This chapter presents two techniques for measuring the bladed disc's radius. The first of these techniques has been in service with gas turbine manufacturers and overhaul shops for over five years. The second utilises a new measurement system which is a development of the original technique which the authors produced in response to the changing needs of the gas turbine community.

¹ The V2500 gas turbine is manufactured by IAE International Aero Engines AG, a Zürich-registered joint venture manufacturing company formed in 1983.

RADIUS TO THE LONGEST BLADE

During the early 1970s, the desire to machine bladed discs became a need and the gas turbine community began to look for machine tools that could meet it. The problem was not one of machining because, although bladed disc machining does present problems, engineers can address them using those methods and techniques that the machine tool trade commonly utilises. The problem was one of measurement, when a blade does not adopt its true working position until it centrifugally loads by revolving at over 1000 rpm.

Measurement technique selection

Standard machine tool gauging techniques were simply never intended to measure the position of the discontinuous surface represented by the disc blades whilst rotating. It required some other technique. The gas turbine industry has developed techniques for measuring the clearance between compressor and turbine blading and the casings in which they run. Whilst this measurement is different to that required for the bladed disc measurement during machining, the authors recognised that blade tip-to-casing clearance measurement techniques developed for application in gas turbines might be more applicable to the bladed disc radius' measurement during machining than conventional machine tool techniques.

Davidson *et al.* (1983) originally developed an electromechanical clearance measurement system utilising a spark-discharge principle of operation for blade tip-to-casing clearance measurement in gas turbines. Sheard and Turner (1992) developed a miniaturised version of Davidson *et al.*'s (1983) measurement system and provide a detailed description of its principle of operation. Gas turbine development engineers have used Davidson *et al.*'s (1983) first generation electromechanical clearance measurement system since 1980 to measure blade tip-to-casing clearances, and since 1985 in tip-grinding applications. The system comprises a probe, actuator and electronic controller (Figure 5.1). In its original application, the probe inserted into a gas turbine and spring loaded onto an inner casing on a machined datum face.

The actuator, Figure 5.2, contains a stepper motor drive assembly and an electronics module. The electronics module generates 400 volts (V) which is applied to an insulated electrode running down the probe. The controller provides stepper motor drive pulses and interrogates the electronics module after each step. As the stepper motor drives the insulated electrode forward, the electrode pushes out of the probe tip towards the rotating blading. When the electrode comes within 3 to 4 microns of an electrically grounded target, such as a passing blade, there is a breakdown of the air in the gap and a spark jumps from the electrode to the blade.

The electromechanical system measures to the longest blade around a disc, as this is the first one it encounters. Whilst researchers recognised this as a limitation, after machining the blades should all be the same length. If the assumption that after machining all blades are the same length is accurate, the electromechanical system will provide an accurate measurement of the finished diameter.

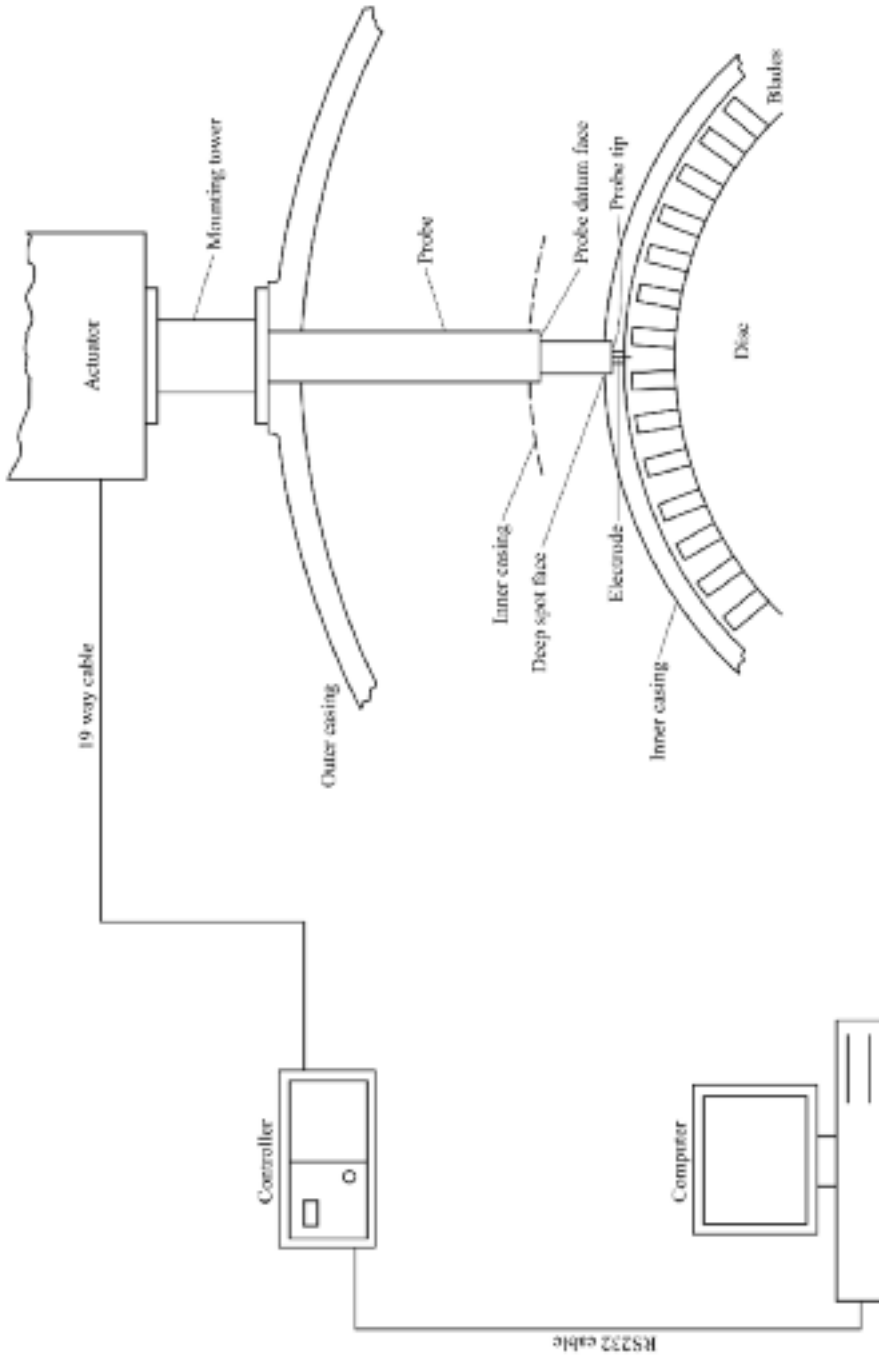


FIGURE 5.1. A schematic view of the electromechanical clearance measurement system probe and actuator mounted on a gas turbine, with the controller displaying distance from the probe's datum to the rotating blading.

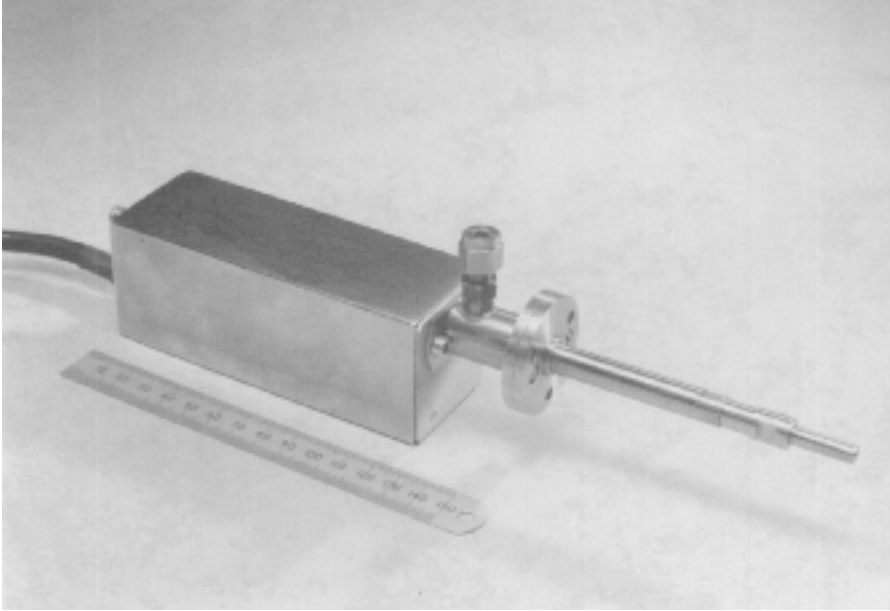


FIGURE 5.2. The electromechanical clearance measurement system actuator and probe cartridge. For tip-grind applications a bayonet-type probe cartridge with a soft copper tip facilitates rapid probe changes and prevents the probe electrode damaging the blading in the event that the electrode physically contacts the blade.

Operating procedure

All electromechanical measurement system tip-grind installations are fitted on manual grinding machines, with Figure 5.3 a typical example. Each machine has a different specification and, therefore, requires a different operating procedure when tip grinding. The operating procedure which we describe below is typical of those that the profession routinely uses.

The tooling that holds the compressor drum which requires machining incorporates a datum face and datum discs of known dimensions (Figure 5.4). After the machine operator mounts the compressor drum in the tip grinding machine, he or she checks the datum disc's concentricity against a compressor drum reference diameter, usually a bearing surface at the assembly's far end. Typically, to achieve build tolerance, the datum discs and compressor drum must be running concentrically to within ± 0.025 mm. The electromechanical actuator and probe mount on the grinding machine. In some installations the probe is free to move axially over the datum discs, blading and second reference diameter (Figure 5.5). In other installations it is fixed and the compressor drum moves relative to it. The probe is datumed against the axial datum face so we know its axial location.

The assembly rotates at between 1000 and 2000 rpm, depending on rotor diameter and the machine operator brings the measurement system up to the datum disc

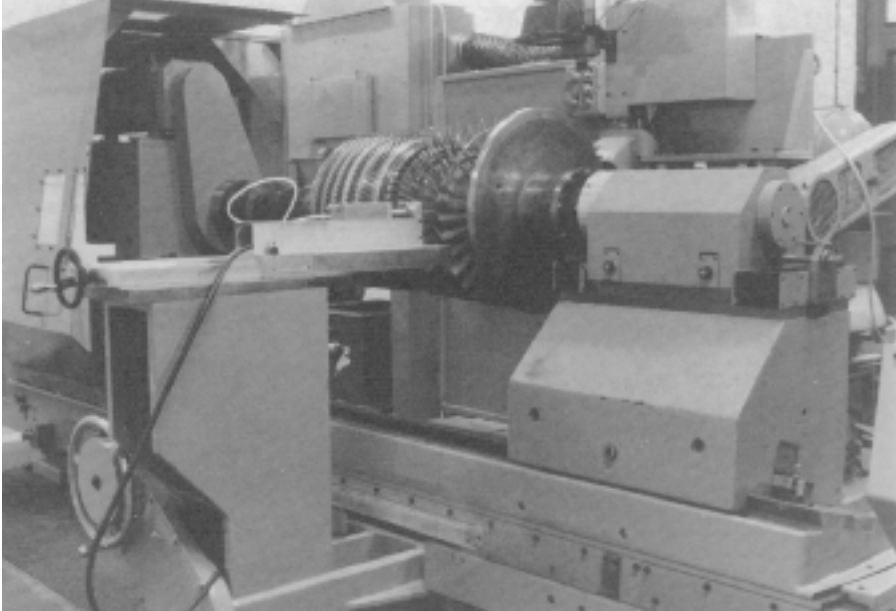


FIGURE 5.3. A typical tip-grind machine, based on a manual grinding machine fitted with three axis read out and the electromechanical measurement system developed by Davidson *et al.* (1983).

radial face and makes a measurement to the datum disc. The machine operator then moves the measurement system to the appropriate axial distance, Figure 5.4, over the first set of blades. The machine operator takes a second measurement, this time to the rotating blading. Knowing the datum disc diameter, the first and second measurements, the operator may calculate the bladed disc's radius. Once the machine operator knows the bladed disc's rotating radius, he or she can use the grinding wheel (Figure 5.5) to grind the blade to the required radius. The machine operator can then de-burr the blades with a wire wheel and repeat the measurement technique. If necessary, the operator can take further cuts.

The above procedure is a reliable and cost-effective solution to the problem of machining bladed disc assemblies when the blades are a loose fit in their root fixings. For many applications this is adequate, as the total accuracy that one may achieve on radius for a well set up rotor on a good grinding machine is ± 0.025 mm and typically no more than ± 0.05 mm on diameter.

RADIUS OVER EVERY BLADE

There are instances where there is a need to measure radius over every blade around a disc and in these cases, Davidson *et al.*'s (1983) electromechanical mea-

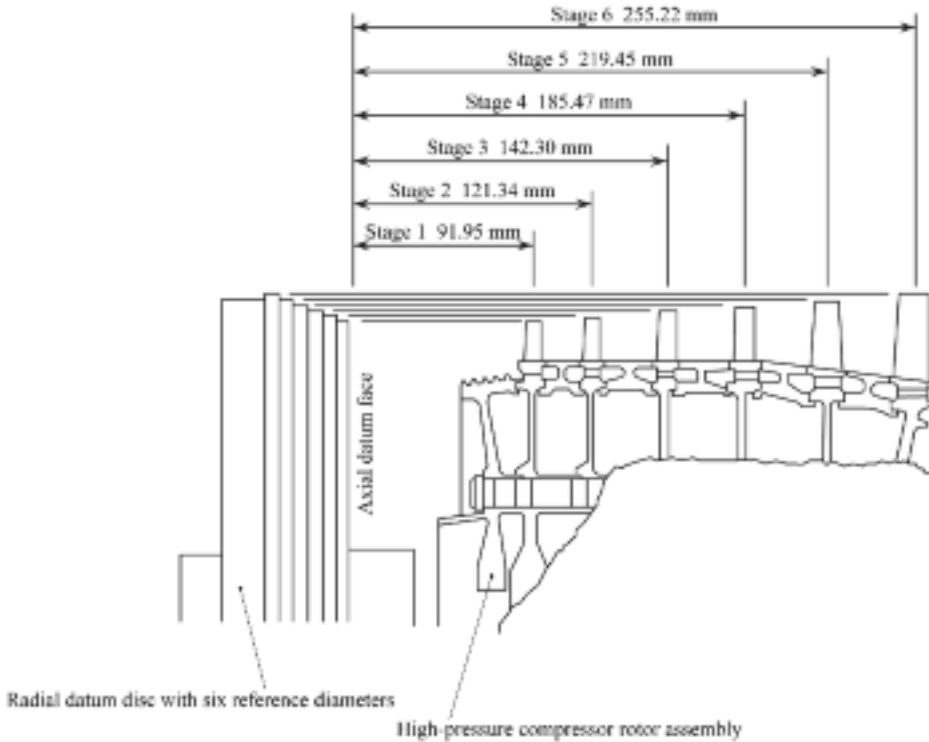


FIGURE 5.4. The blading of a typical compressor drum and the datum discs illustrating how the radial and axial datum faces enable machining of blades with a lead angle.

surement system is not suitable. Optical triangulation systems, such as that which Barranger and Ford (1981) describe, use a laser to measure clearance over individual blades. These systems are large, complex and inherently fragile. They are not ideal for use in a machine shop environment and therefore are not ideal for application in the tip-grinding process. Capacitance probes are small and rugged devices which engineers routinely use to measure blade tip-to-casing clearance in gas turbines. Chivers (1989) designed a capacitance-based clearance measurement system which Sheard (2011) developed. Sheard *et al.* (1992) further developed the system and designed a ‘measurement head’ able to measure clearance over individual blades to an accuracy of ± 0.01 mm. The measurement head was insensitive to variations in blade thickness, but was potentially susceptible to temperature-induced errors. Sheard *et al.* (1992) developed a technique to calibrate the measurement head on-line immediately prior to use, thus eliminating any errors due to temperature drift.

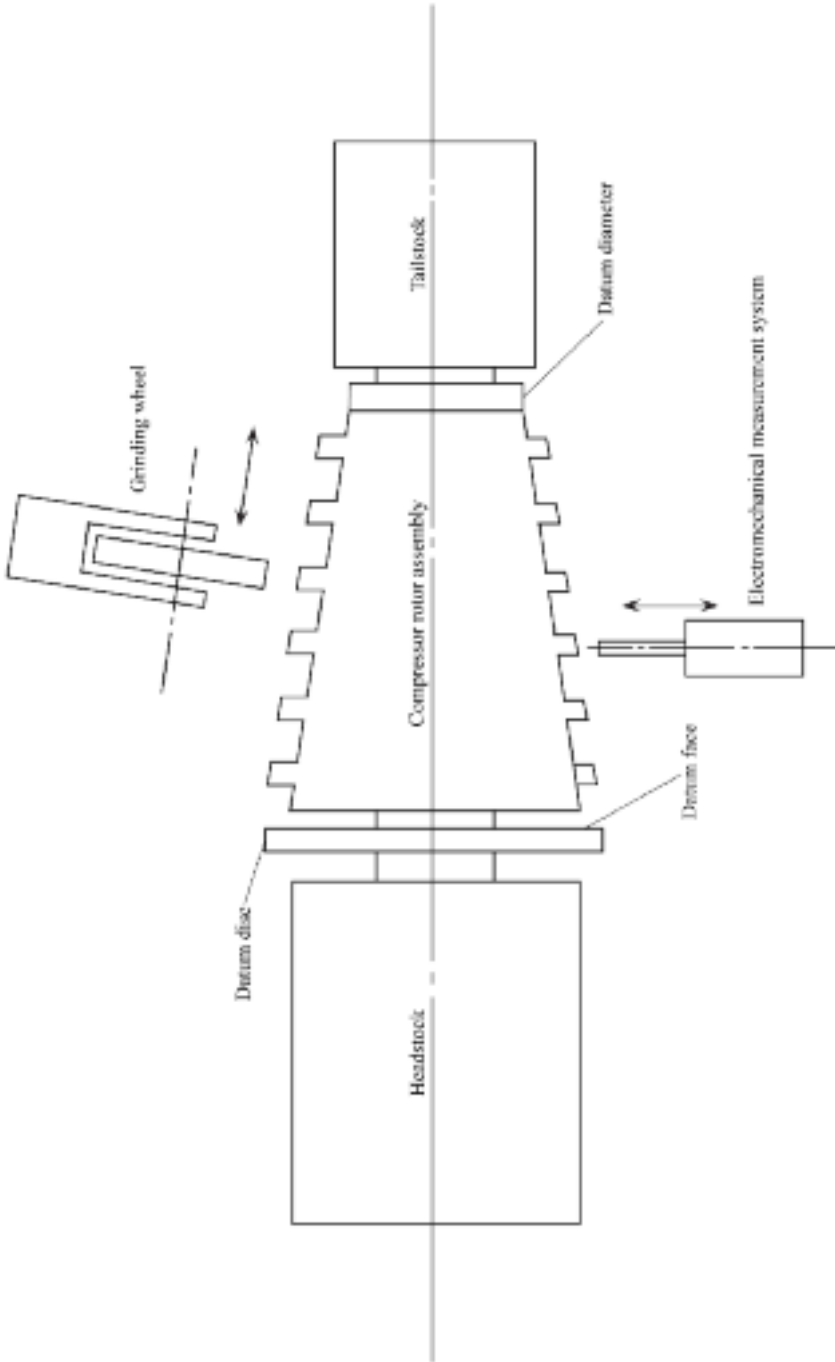


FIGURE 5.5. A schematic view of a bladed disc assembly fitted on a grinding machine with datum discs and an electromechanical measurement system.

A capacitance-based measurement system

The measurement head contains a traverse actuator, electronics module and capacitance probe oscillator (Figure 5.6). The compact design enables this to fit within a 195 mm diameter hermetically sealed case, which enables one to use it to measure internal stator blade radius down to a minimum stator internal diameter of 200 mm. The 8 mm diameter probe incorporates an insulated electrode and capacitance probe. The electronics module, oscillator and probe mount on a traverse actuator carriage and may step in towards the blading which facilitates probe calibration.

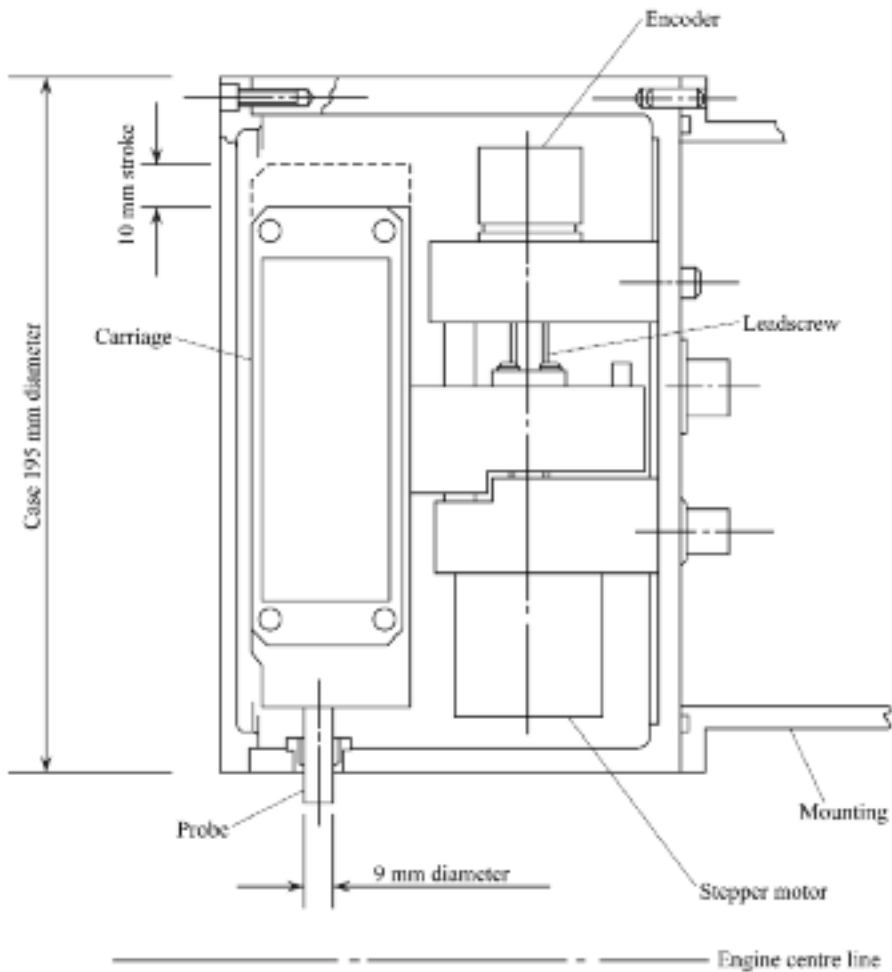


FIGURE 5.6. Layout of the measurement head designed for measuring radius of individual rotor and stator blades during their machining, developed by Sheard *et al.* (1992).

A capacitance probe utilises its own tip and a target as the capacitor's two plates. As capacitance is proportional to plate separation, so the capacitance measured as a blade passes is proportional to the blade's distance from the probe tip. The probe tip capacitance tunes an oscillator circuit. As the capacitance's value at the probe tip changes, the circuit's resonant frequency changes. The blade passing results in a modulation of the oscillator's natural frequency which is known as a frequency modulated (FM) mode of operation.

SYSTEM COMMISSIONING

In order to establish that Sheard *et al.*'s (1992) capacitive clearance measurement system could measure the bladed disc's radius during the tip grinding process, the authors undertook a two-stage commissioning exercise. They fitted a computer numerically controlled (CNC) lathe with a measurement head and grinding spindle. They acquired two cycle scrapped compressor discs, a Pratt & Whitney JT8 stages 7 and 11, each with a full blade set. These were typical of the disc type which gas turbine manufacturers and overhaul shops routinely grind to size. The authors then split the commissioning into two stages. The first stage utilised the stage 11 disc which has blades wedged out into their working position. This enabled the authors to measure the radius over individual blades using a dial gauge. Static radius measurement provided a useful benchmark against which to gauge the accuracy with which the measurement head could measure blade-tip radius under rotation. The second phase of the commissioning utilised the stage 7 disc, which had pin-fixed blades that did not adopt their true working position until centrifugally loaded.

Phase one commissioning

The authors manufactured suitable fittings and a datum disc to enable them to mount the stage 11 disc on a CNC lathe (Figure 5.7).

The authors spun the disc to 1800 rpm and brought the measurement head over the datum disc. The measurement head is driven in a similar manner to Davidson *et al.*'s (1983) electromechanical measurement system, with a measurement from its internal datum to the datum disc. The authors then repeated this procedure over the rotating blading, making a measurement from the electromechanical measurement system internal datum to the rotation blading. The difference between the distance from the electromechanical measurement system internal datum to the datum disc and rotating blading was the difference in diameter between the datum disc and rotating blading. In this way the authors were able to calculate the longest blade's radius.

The authors calibrated the capacitance probe on-line whilst making the measurement to the longest blade. Sheard *et al.* (1992) describe in detail the method that the authors used. The capacitance probe provides a measurement of the clearance over every blade relative to the capacitance probe tip. The authors used this in



FIGURE 5.7. The computer numerically controlled lathe fitted with a grinding spindle, prototype measurement head, datum disc and Pratt & Whitney JT8 stage 11 bladed compressor disc.

conjunction with the longest blade's measured radius to calculate the radius over each blade.

The authors measured the stage 11 disc radius over each blade using a dial gauge. They estimated dial gauge measurements as accurate to ± 0.01 mm. Sheard *et al.* (1992) concluded that the measurement head was also accurate to ± 0.01 mm. The authors plotted the dial gauge and measurement head radii against blade number and plotted the vertical axis as offset from the longest blade to enable them to expand the scale sufficiently for visibility of the ± 0.01 mm error bar (Figure 5.8). The two data sets' error bars show a high degree of overlap giving confidence in their accuracy. To facilitate comparison with results that the authors obtained during the measurement head grinding, the authors re-plotted the data against the radius (Figure 5.9).

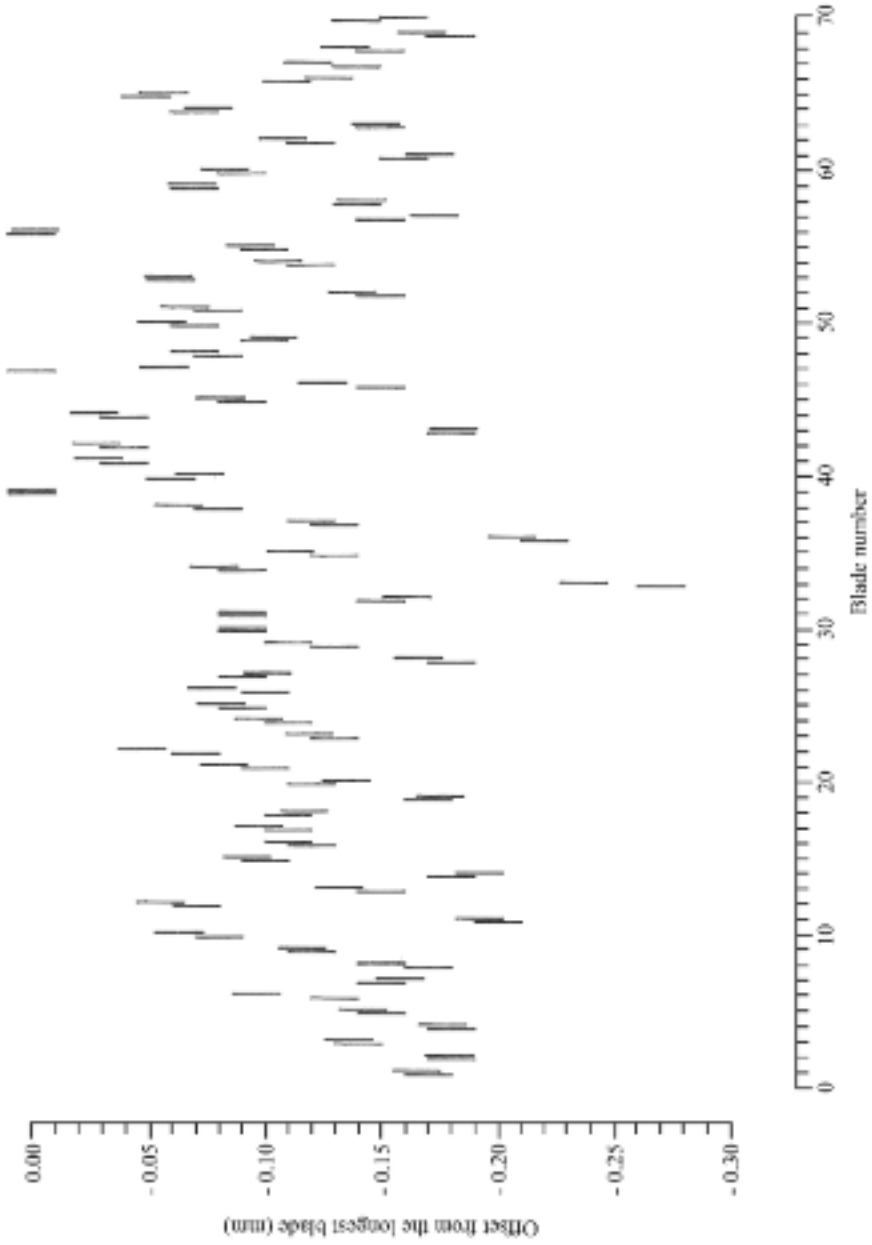


FIGURE 5.8. Offset of the JT8 stage 11 compressor blades from the longest blade, measured statically using a dial gauge and at 1800 rpm using the measurement head. Dial gauge measurements are offset to the left and measurement head measurements to the right for clarity.

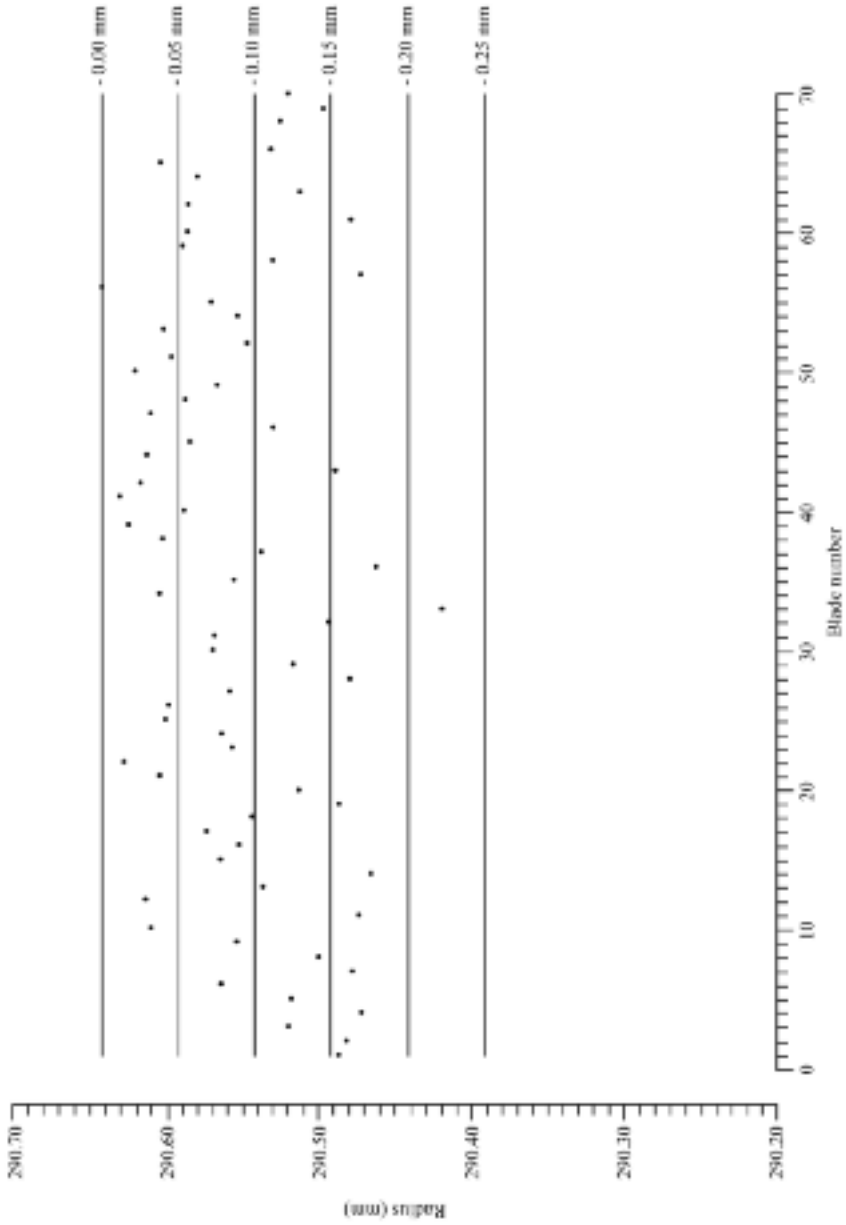


FIGURE 5.9. Radius of the JT8 stage 11 compressor blades prior to grinding, measured at 1800 rpm using the measurement head.

The authors used the grinding wheel to make a 0.05 mm cut (Figure 5.10). The authors considered the measured radius' repeatability for the blades before grinding (Figure 5.9) and after a 0.05 mm cut (Figure 5.10) excellent, with the exception of those blades which they had ground which were now correspondingly shorter. The authors repeated the process with a 0.10 mm cut (Figure 5.11), 0.15 mm cut (Figure 5.12), 0.20 mm cut (Figure 5.13), and finally a 0.25 mm cut (Figure 5.14). The authors clearly observed a progression to a finished diameter from one cut to the next. They used a dial gauge to check the finished radius, which was 290.39 mm, ± 0.01 mm, over each blade. The measurements that the authors made after the final cut exhibited a blade-to-blade variation in radius of 0.02 mm which compares well to the measured ± 0.01 mm variation in radius with the dial gauges.

The final check on measurement system performance utilised the measurement head to measure the radius over each blade six times. The authors moved the measurement head from its park to measure position and calibrated it to measure radius. The authors repeated this procedure six times. The repeatability of measurement, Figure 5.15, was ± 0.01 mm, which was in agreement with Sheard *et al.*'s (1992) ± 0.01 mm error, which the authors therefore considered excellent.

At this point, the authors considered phase one commissioning complete as the prototype measurement system had demonstrated that it could make reliable and repeatable measurements of radii over fixed blades whilst rotating.

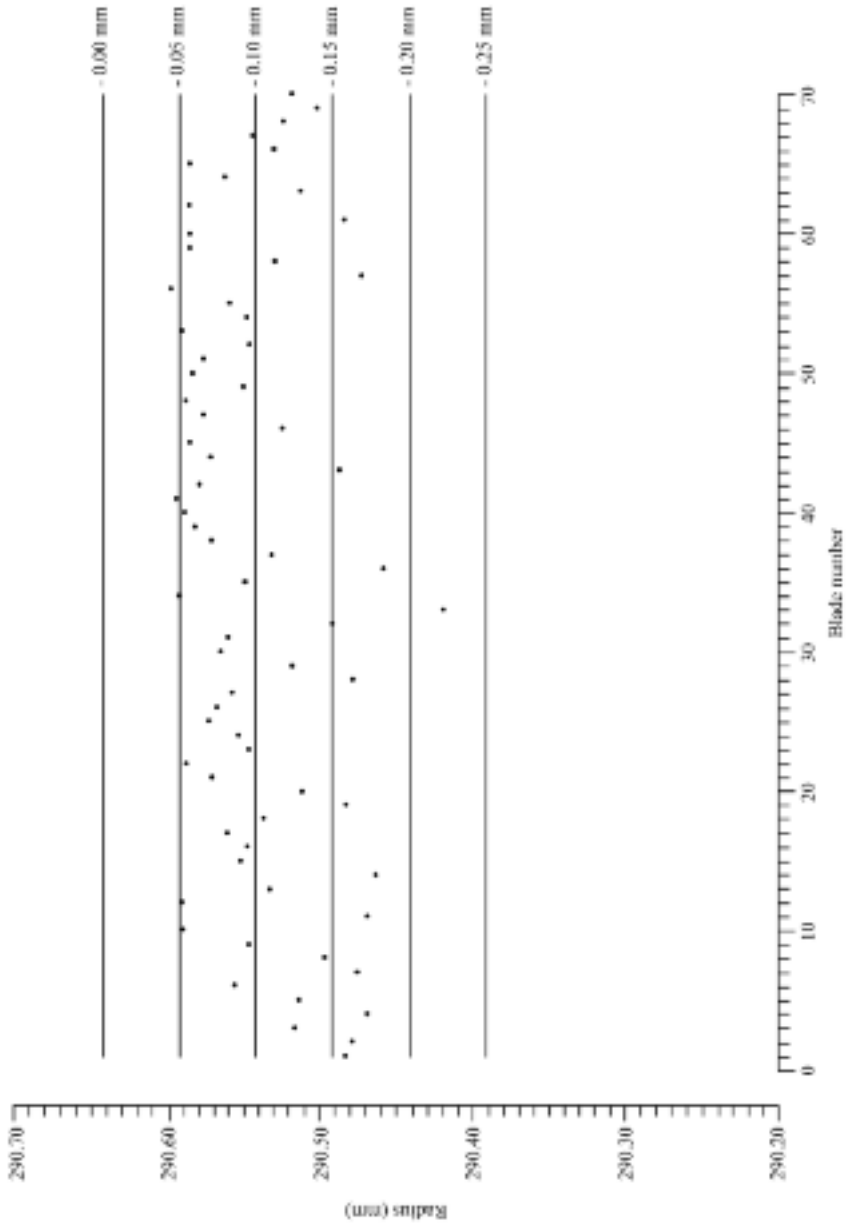


FIGURE 5.10. Radius of the JT8 stage 11 compressor blades after a 0.05 mm cut, measured at 1800 rpm using the measurement head.

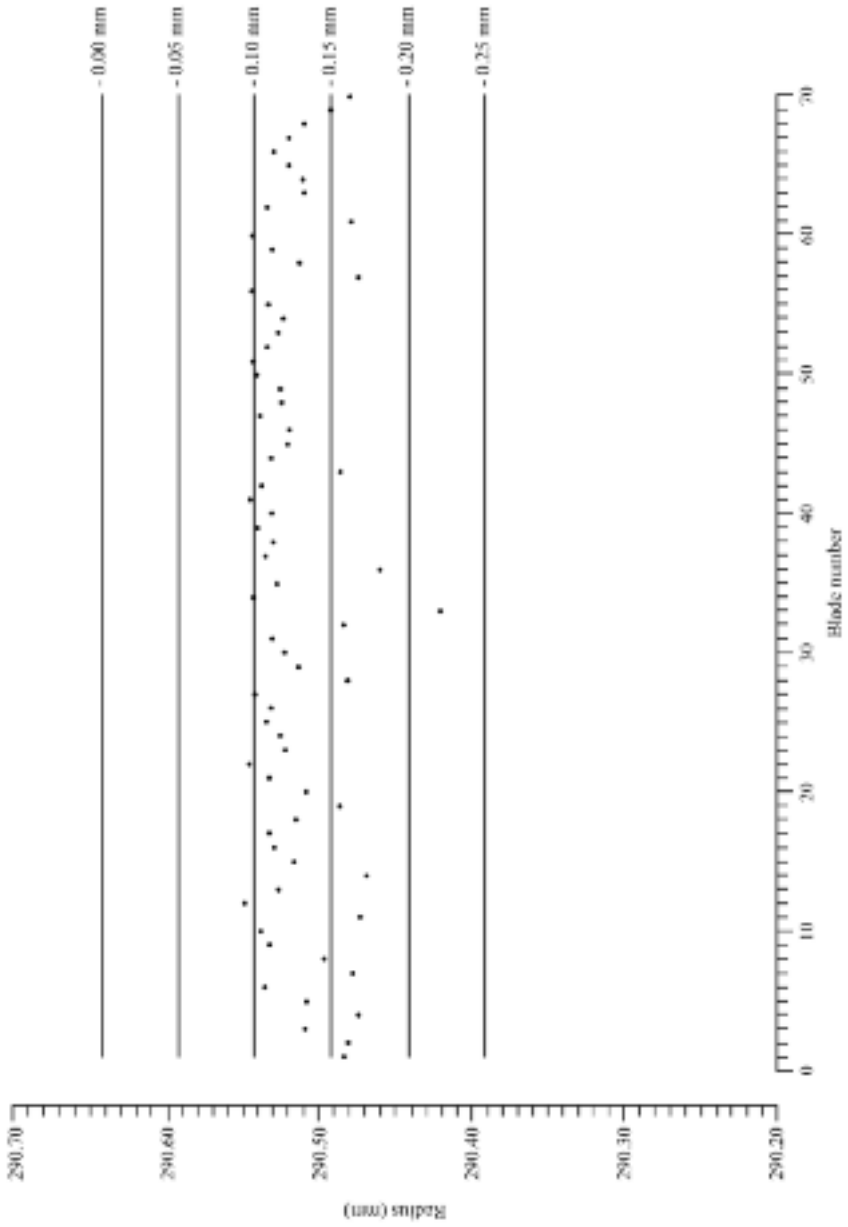


FIGURE 5.11. Radius of the JT8 stage 11 compressor blades after a 0.10 mm cut, measured at 1800 rpm using the measurement head.

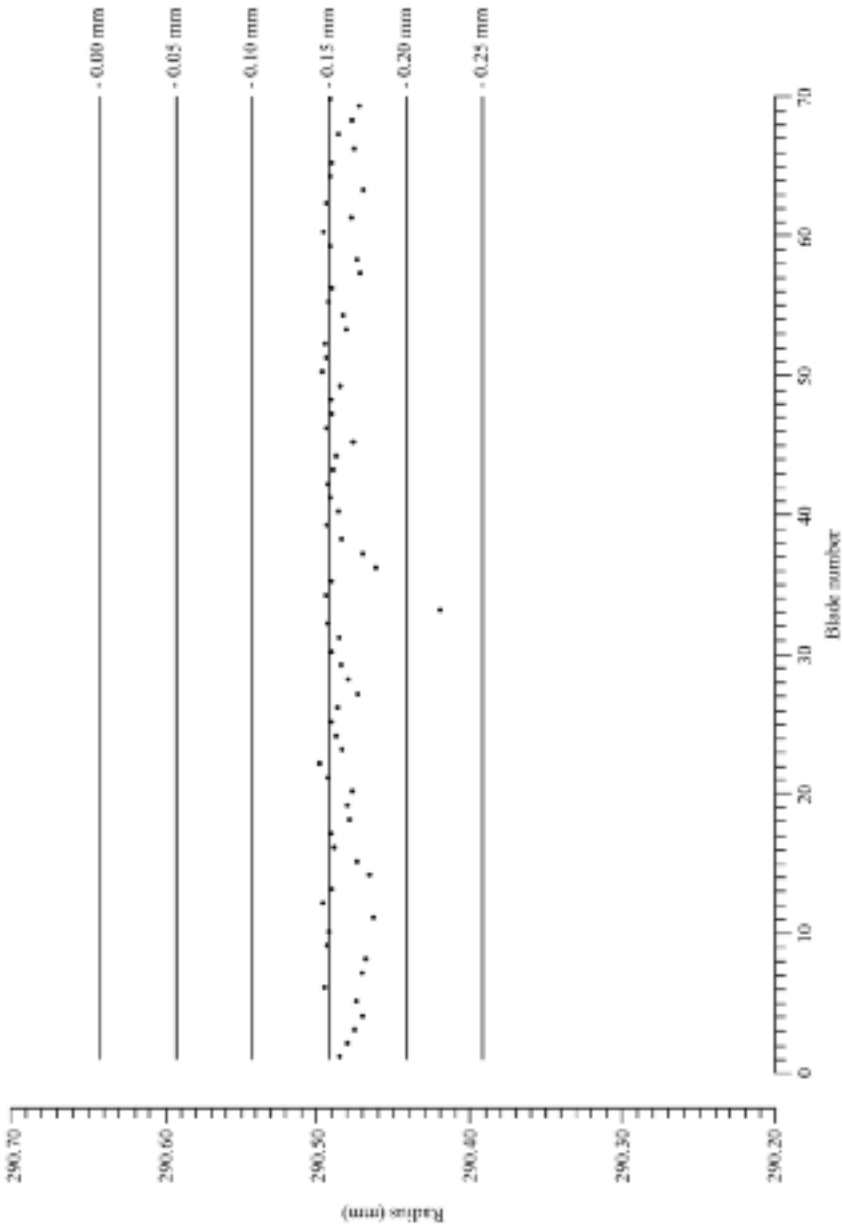


FIGURE 5.12. Radius of the JT8 stage 11 compressor blades after a 0.15 mm cut, measured at 1800 rpm using the measurement head.

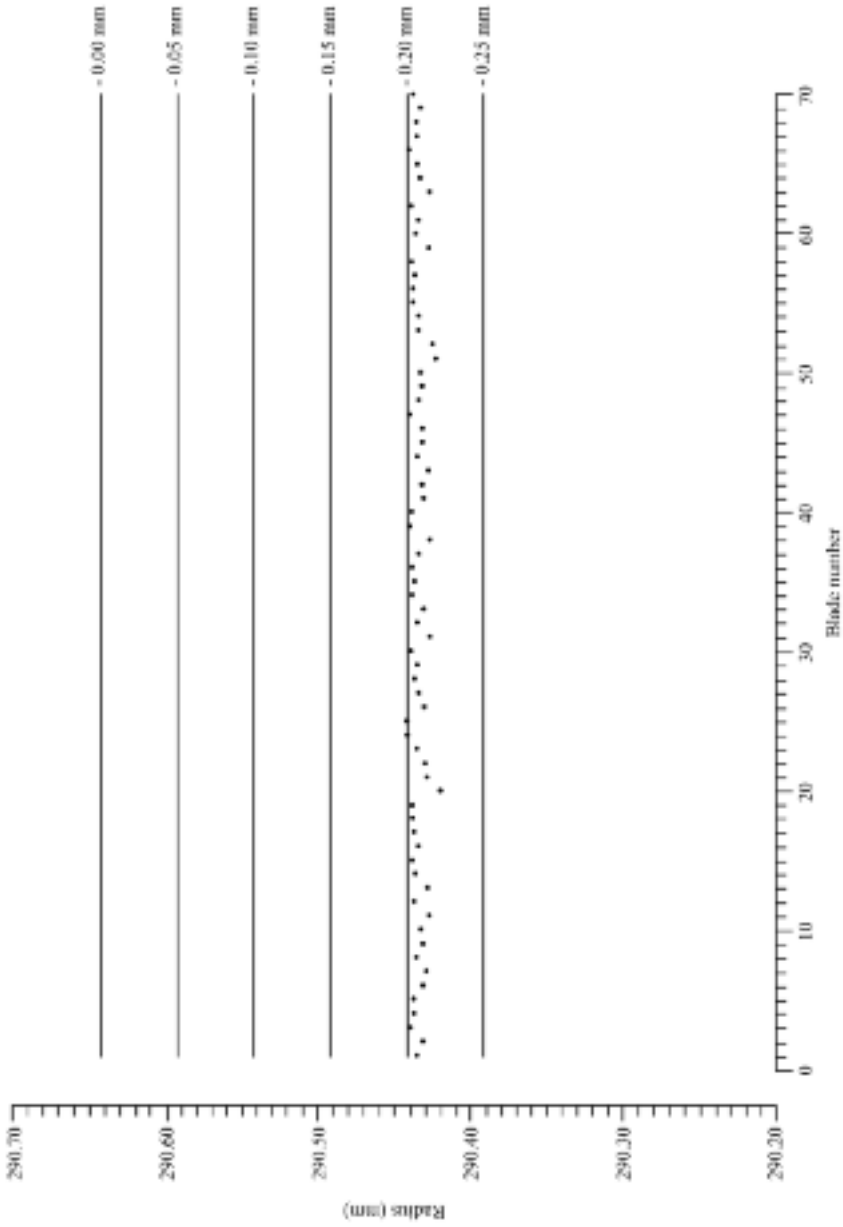


FIGURE 5.13. Radius of the JT8 stage 11 compressor blades after a 0.20 mm cut, measured at 1800 rpm using the measurement head.

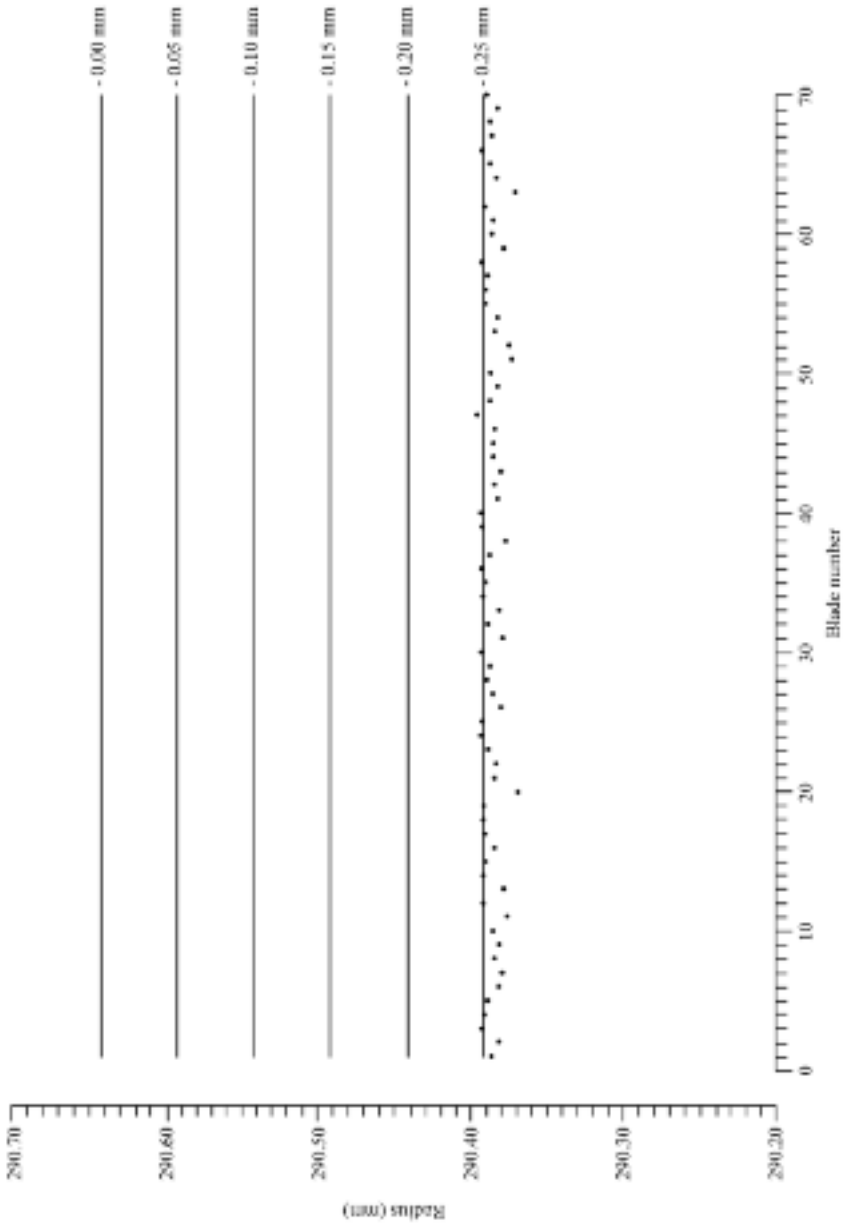


FIGURE 5.14. Radius of the JT8 stage 11 compressor blades after a 0.25 mm cut, measured at 1800 rpm using the measurement head.

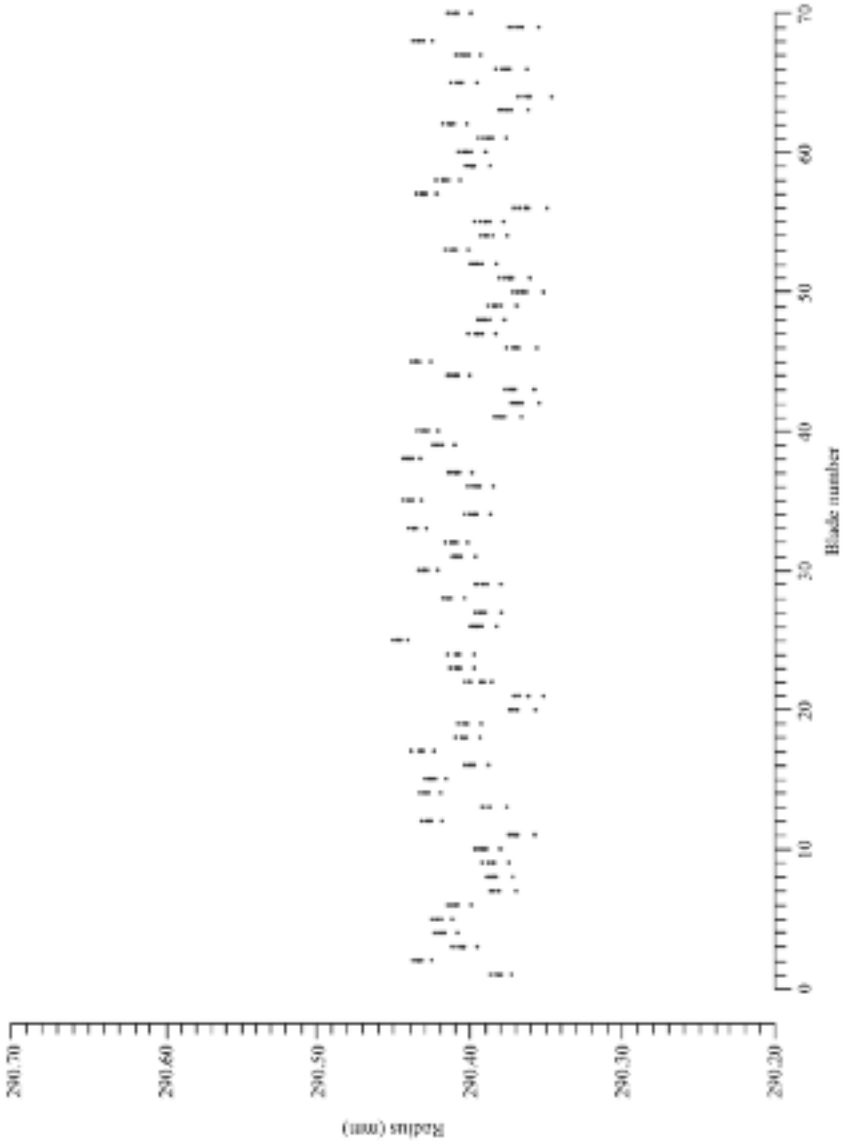


FIGURE 5.15. Repeatability test conducted on the Pratt & Whitney JT8 stage 11 bladed disc at 1800 rpm. The capacitance probe used in the measurement head was recalibrated prior to each of the six measurements of radius.

Phase two commissioning

The commissioning exercise continued with the Pratt & Whitney JT8 stage 7 disc. The blades in this disc are pin fixed, Figure 5.16, and therefore do not adopt their true working position until centrifugally loaded.

The authors used the prototype measurement head to measure the radius over individual blades, Figure 5.17, with the variation in blade heights typical of that which one would expect of gas turbine-run hardware. The authors repeated the same procedure of taking 0.05 mm cuts during phase one commissioning.

The authors remeasured radius after five 0.05 mm cuts radius (Figure 5.18). The results were disappointing as not only was the scatter in blade radius large compared to that achieved with fixed blades, but the radius had only reduced by an average of 0.15 mm, not the expected 0.25 mm.

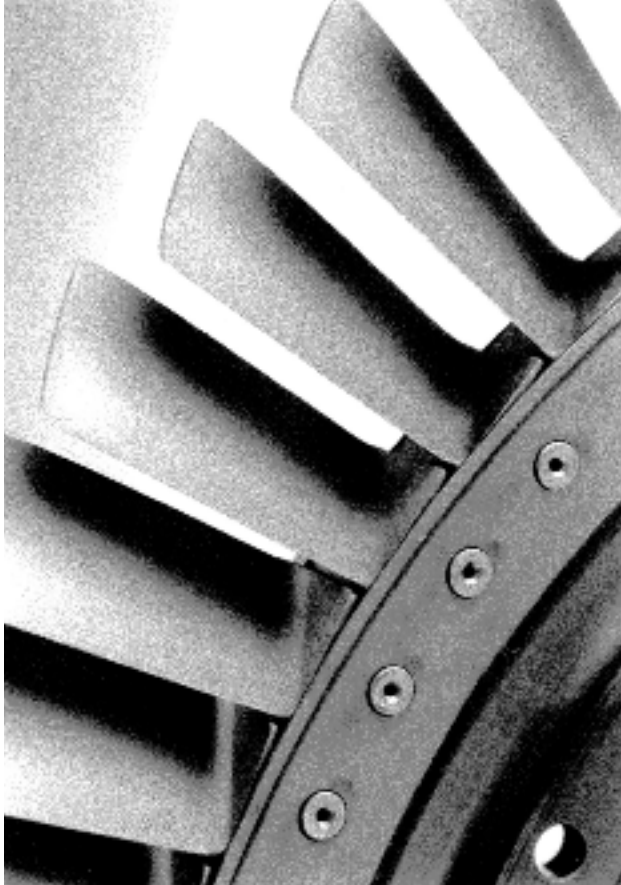


FIGURE 5.16. A close-up view of the pin-fixed blade root fixing arrangement of the Pratt & Whitney JT8 stage 7 blades.

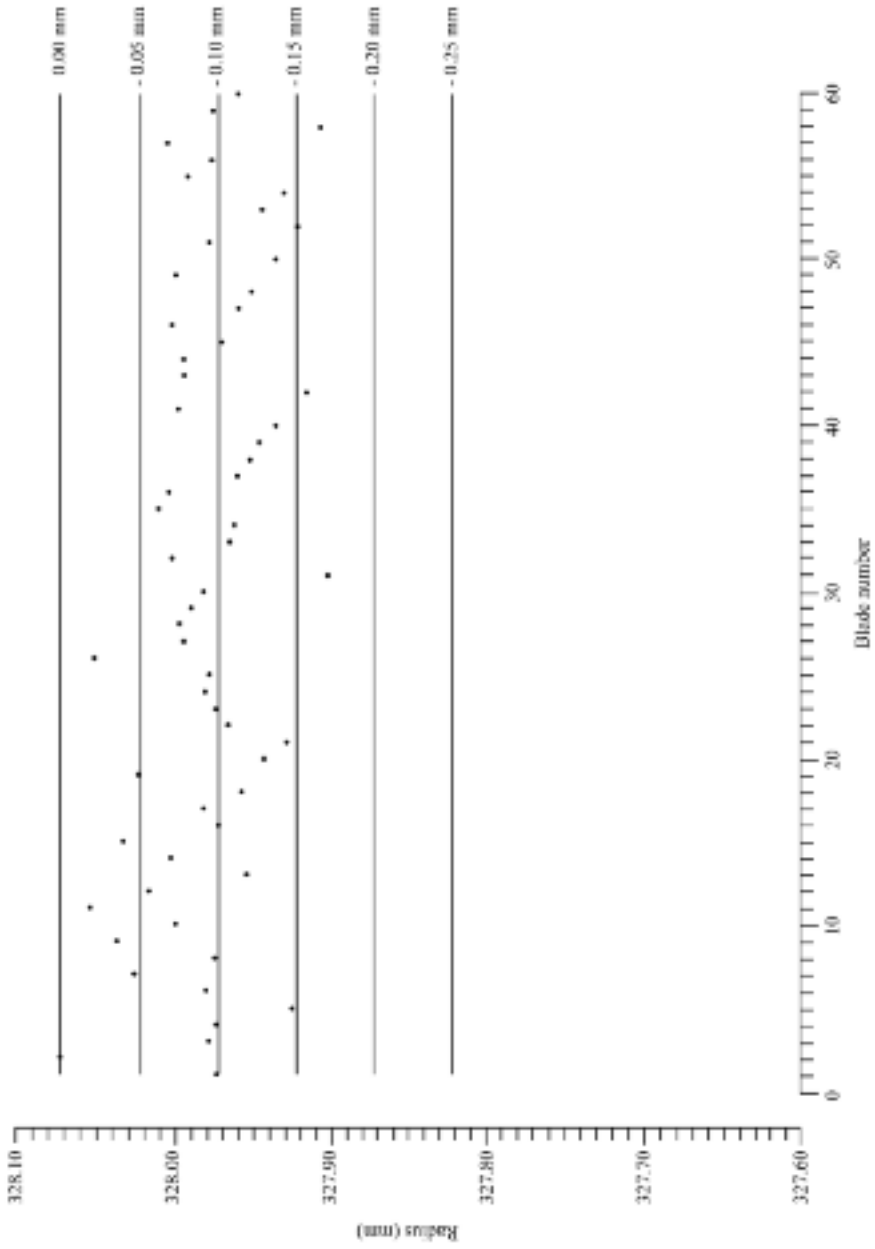


FIGURE 5.17. Radius of the JT8 stage 7 compressor blades prior the grinding, measured at 1800 rpm using the measurement head.

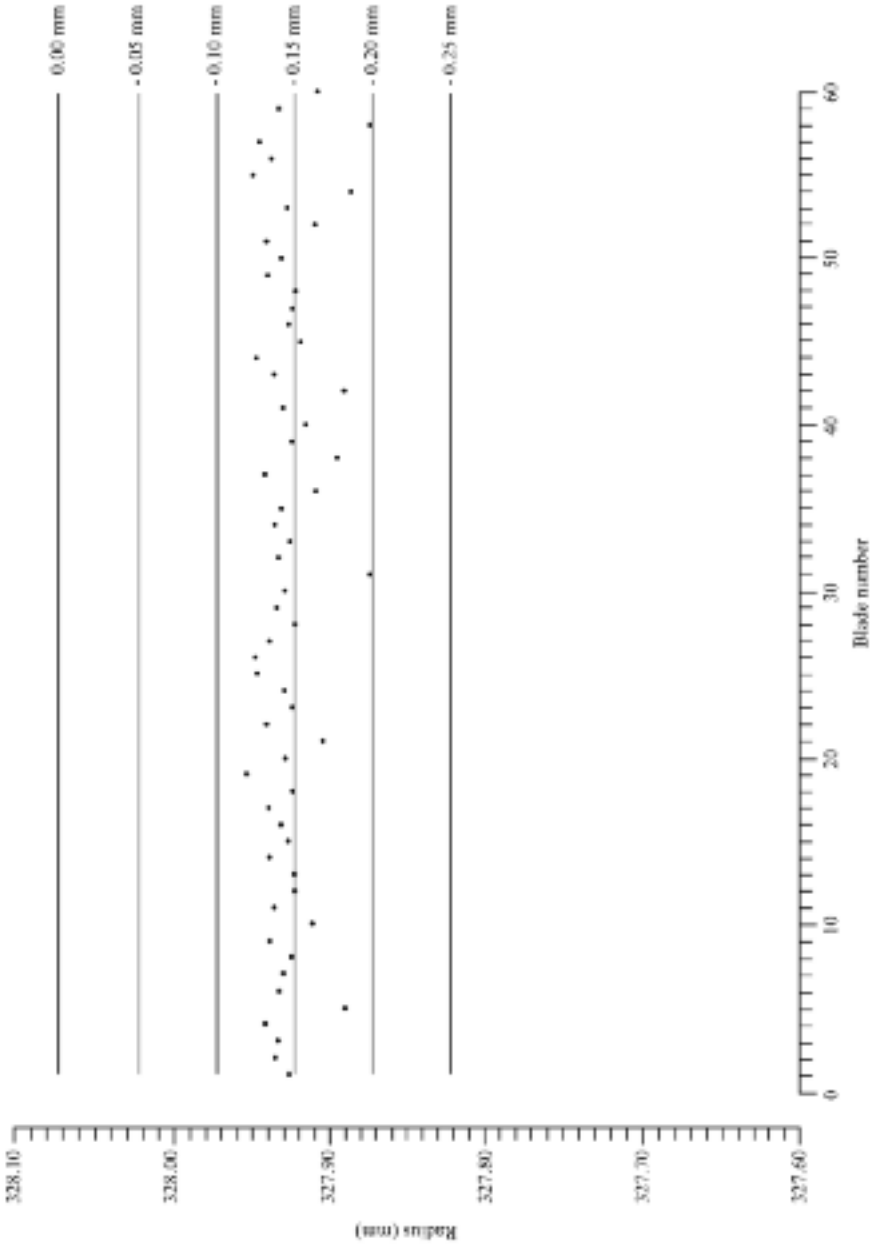


FIGURE 5.18. Radius of the JT8 stage 7 compressor blades after the final 0.25 mm cut, measured at 1800 rpm using the measurement head.

Sheard *et al.* (1992) and the authors during phase one commissioning established the measurement head's ability to measure radius to ± 0.01 mm. The authors, therefore, reasoned that the grinding technique which was satisfactory for fixed blades was not suitable for use with pin-fixed blades.

The accurate grinding of loose-bladed compressor drums to a specific radius is a specialised machining process. Those working in the field have established parameters critical to its success. Winfield's (1991) recommendations when grinding compressor drums with loose blades are as follows. Use a relatively soft grinding wheel which is dressed immediately prior to use. After completing the final cut, allow the grinding wheel to remain over the blading for several minutes. This minimises blading deflection due to cutting forces by allowing the blades to 'relax' back to their true radial location under the action of centrifugal force. With the grinding wheel still over the blading, this minimises blade-to-blade variation in radius. Lastly, measure the ground compressor after grinding without stopping the machine, as loose blades always re-seat in slightly different positions.

After implementing Winfield's recommendations, the authors ground the blades to the desired radius, Figure 5.19. The blade-to-blade variation in radius was 0.01 mm, which was an improvement over what they had achieved previously, Figure 5.18. This result confirmed that the discrepancy between the expected results and those that they initially obtained with loose blades was due to a grinding technique inappropriate to the compressor drum's machining with loose blading.

Once the authors achieved the required radius over each blade, they de-burred the blades by stopping the machine and manually removing the burr on each blade. They then spun the bladed disc back up to 1800 rpm and remeasured radius, Figure 5.20. De-burring the blades, combined with stopping and starting the machine, caused the blades to re-seat. This resulted in an increase in the blade-to-blade radius variation to 0.06 mm, of which the authors attributed 0.05 mm to the blade re-seating as blade-to-blade variation in radius had been 0.01 mm.

The variation in blade radius of 0.01 mm, Figure 5.19, is within the ± 0.01 mm error that occurs with the measurement head. This suggests that the grinding technique that the authors used achieved a final radius over each blade near the limiting accuracy with which they could machine blade lengths to a known diameter. The design of the blade root fixings appears to introduce a variation in blade seating of 0.05 mm, therefore grinding to a more accurate radius would not significantly improve the compressor's variation in blade-to-blade radius after the blades had re-seated.

The measurement head was able to measure radius to ± 0.01 mm, with a 0.06 mm variation in radius evident following the blade re-seating. The limiting accuracy with which one can machine radius over each blade to a specified value is, therefore, a function of blade root fixing design and not the ± 0.01 mm error inherent in the measurement technique. The authors concluded that the measurement head was, hence, suitable for measuring blade radius during the tip-grind process.

Commissioning concluded with an investigation of disc speed effects on measured blade radius. Changing wheel speed from 1400 rpm to 2200 rpm had no effect on the blades' relative heights. This was not unexpected as even at 1400 rpm the blades experience a centrifugal load of over 400 g so they should be seated in their

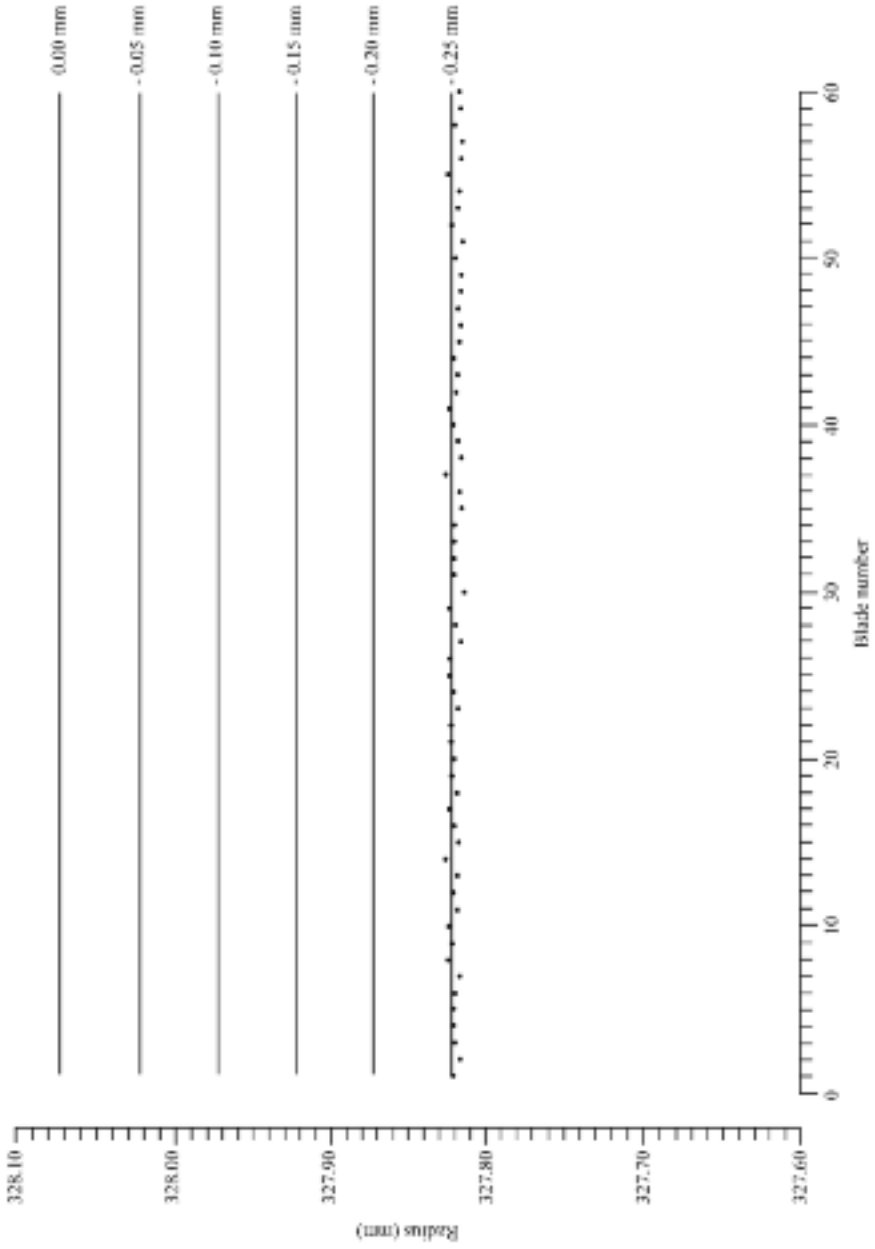


FIGURE 5.19. Radius of the JT8 stage 7 compressor blades after completing the 0.25 mm cut following Winfield's (1991) recommendation, measured at 1800 rpm using the measurement head.

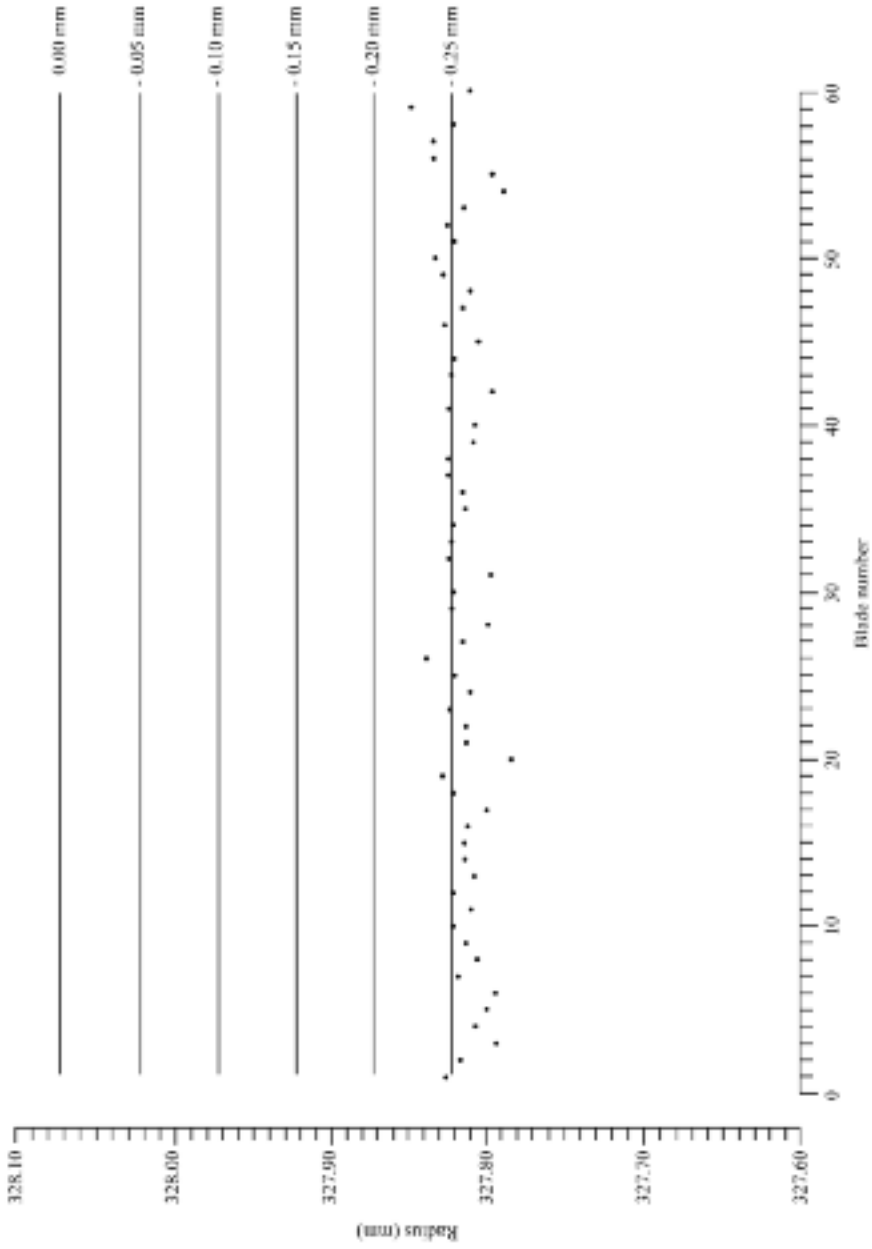


FIGURE 5.20. Radius of the JT8 stage 7 compressor blades after blade de-burring, measured at 1800 rpm using the measurement head.

root fixing. An important result, however, was that the measurement head remained unaffected by changes in blade passing frequency.

CONCLUSIONS

Manufacturers and machining shops have successfully used Davidson *et al.*'s (1983) first generation electromechanical measurement system since 1985 on manual grinding machines to enable them to machine bladed rotors to an accuracy of ± 0.025 mm on radius.

There are some situations where an inspection capability to enable measurement of the radius of the rotor over every blade is desirable to ascertain, for example, whether a previously run rotor requires re-blading.

The authors undertook a two-stage commissioning trial to verify the functionality of a capacitive measurement technique, using a computer numerically controlled lathe as a base. At the trial's conclusion, the authors determined that the measuring head could measure radius over individual blades to ± 0.01 mm.

De-burring rotor blades after the grinding operation combined with stopping and starting the grinding machine introduces a variation in the blades' radial seating in their root fixing of 0.05 mm. This indicates that the ± 0.01 mm measurement error is significantly less than the blade-to-blade variation of radius that it achieves after blading de-burring.

Increasing the accuracy with which the authors may measure blade radius beyond that which they achieved with the measurement head would not decrease the final blade-to-blade variation in radius because of the variation in blade seating.

The authors concluded that the accuracy, compact size, tolerance to blade width and blade passing frequency, plus the measurement head's inherent ruggedness, made it ideal for use during the tip grinding of rotor and stator blade sets.

REFERENCES

- Barranger, J.P. & Ford, M.J. (1981), 'Laser Optical Blade Tip Clearance Measurement System'. *Transactions of the ASME, Journal of Engineering for Power*, vol. 103, pp. 457–60.
- Chivers, J.W.H. (1989), 'A Technique for the Measurement of Blade Tip Clearance in a Gas Turbine.' AIAA Paper No. 89-2916.
- Davidson, D.P., De Rose, R.D. & Winnerstrom, A.J. (1983), 'Measurement of Turbomachinery Stator to Drum Running Clearances'. *Proceedings of the 28th American Society of Mechanical Engineers Gas Turbine and Aeroengine Congress*. Phoenix, Arizona, 27–31 March, Paper No. 83-GT-204.
- Sheard, A.G. (2011), 'Blade-by-blade Tip Clearance Measurement'. *International Journal of Rotating Machinery*, vol. 2011, Article ID 516128, pp. 1–13.

- Sheard, A.G. & Turner, S.R. (1992), 'An Electromechanical Measurement System for the Study of Blade Tip-to-casing Running Clearances'. *Proceedings of the 37th American Society of Mechanical Engineers Gas Turbine and Aeroengine Congress*. Cologne, Germany, 1–4 June, Paper No. 92-GT-50.
- Sheard, A.G., Westerman, G.C. & Killeen, B. (1992), 'An On-Line Calibration Technique for Improved Blade-by-blade Tip Clearance Measurement'. *Proceedings of the 38th ISA International Instrumentation Symposium*. Las Vegas, Nevada, USA, 26–30 April, pp. 32–51.
- Winfield, D.P. (1991), Private communication with Mr D.P. Winfield, Rolls-Royce plc, Product Engineering Manager Repair and Overhaul ATO.

A Blade-by-blade Tip Clearance Measurement System for Gas Turbine Applications

A.G. Sheard and B. Killeen

ABSTRACT

It is difficult to make a reliable measurement of blade tip-to-casing clearance in the hostile environment over a modern gas turbine's blading. When gas turbine development engineers require the measurement over every blade during live development tests, system reliability, ruggedness and ease of operation are of primary importance.

This chapter describes a blade tip-to-casing clearance measurement system that can measure clearance over every blade around a rotor. The chapter presents the measurement system concept and describes the system design in detail. The chapter next discusses the commissioning of the measurement system on a compressor test facility, and the results. The chapter concludes with an analysis of system performance during the commissioning trials.

INTRODUCTION

This chapter describes a programme of work that the authors undertook to develop and test a clearance measurement system that measures blade tip-to-casing clearance over individual blades around a rotor. The work's objective was to reduce the practical problems that occur with system operation, providing a 'plug in and play' measurement system that relatively unskilled operators could use. In principle, this enables a routine measurement of the blade tip-to-casing clearance on a blade-by-blade basis during those rig and gas turbine tests that constitute a new gas turbine's development.

The described measurement system is a third-generation electromechanical device. Davidson *et al.* (1983) and Sheard and Turner (1992) reported the first two

This chapter is a revised and extended version of Sheard, A.G. & Killeen, B. (1995), 'A Blade-by-blade Tip-Clearance Measurement System for Gas Turbine Applications'. *Transactions of the ASME, Journal of Engineering for Gas Turbines & Power*, vol. 117, pp. 326–31.

generations, respectively. Pavey (1993) utilised a first generation electromechanical clearance measurement system to measure clearance over the blading of a high-pressure turbine, Figure 6.1. The effect of applying turbine shroud cooling air clearly showed a 20% reduction in blade tip-to-casing clearance around the entire casing. Using Sheard *et al.*'s (1993) aerodynamic probe traversing system Pavey (1993) quantified the effect of reducing tip clearance on the turbine gas angle radial profile, as Figure 6.2 illustrates. Without shroud cooling, turbine gas angle departed from its design value by over ten degrees in the blade tip region. Pavey (1993) concluded that a 20% reduction in turbine blade tip-to-casing clearance significantly improved turbine performance.

The third-generation electromechanical clearance measurement system aimed to retain the ruggedness and ease of use of the first two generations. It utilises an electromechanical stepper motor-driven probe and a spark-discharge technique to ascertain the proximity of an electrically grounded target, typically a rotating compressor or turbine blade. This proximity measurement is to the longest blade around a rotor. A capacitive clearance measurement system, which Chivers (1989) described, had been incorporated into the 'blade-by-blade' electromechanical clearance measurement system, which provides a measure of the difference in each blade's length relative to the longest blade.

In the current programme of work, the authors focused on minimising complexity of operation, whilst providing a system that was completely self-calibrating over a wide range of temperatures and a 6 mm range. The authors decided to undertake this development programme after a thorough review of the gas turbine community's current and future clearance measurement requirements. Sheard and Killeen (1993) presented this review and went on to consider the available techniques for blade-by-blade tip-to-casing clearance measurement before proposing a third-generation electromechanical clearance measurement system.

CLEARANCE MEASUREMENT SYSTEM CONCEPT

The blade-by-blade electromechanical clearance measurement system integrates a capacitance probe and electrode into a single probe. When the blades are rotating and the probe comes within a few microns of the longest blade, a spark-discharge occurs. Each time a spark-discharge occurs, the controller retracts the probe by 0.1 mm, thus eliminating the possibility of the probe touching the blades during transient gas turbine operation. Whilst within range of the blading, the operator can log blade-by-blade clearance data using the capacitance probe up to 30 KHz.

The capacitance probe is recessed approximately 0.1 mm from the electrode, so it is close to the longest blade around the rotor when the spark-discharge occurs. The probe is retracted from the blading in 0.05 mm steps, with capacitance probe output for each blade at each recorded step. The algorithms that Sheard *et al.* (1992) developed utilise data from a series of steps to generate a capacitance probe calibration.

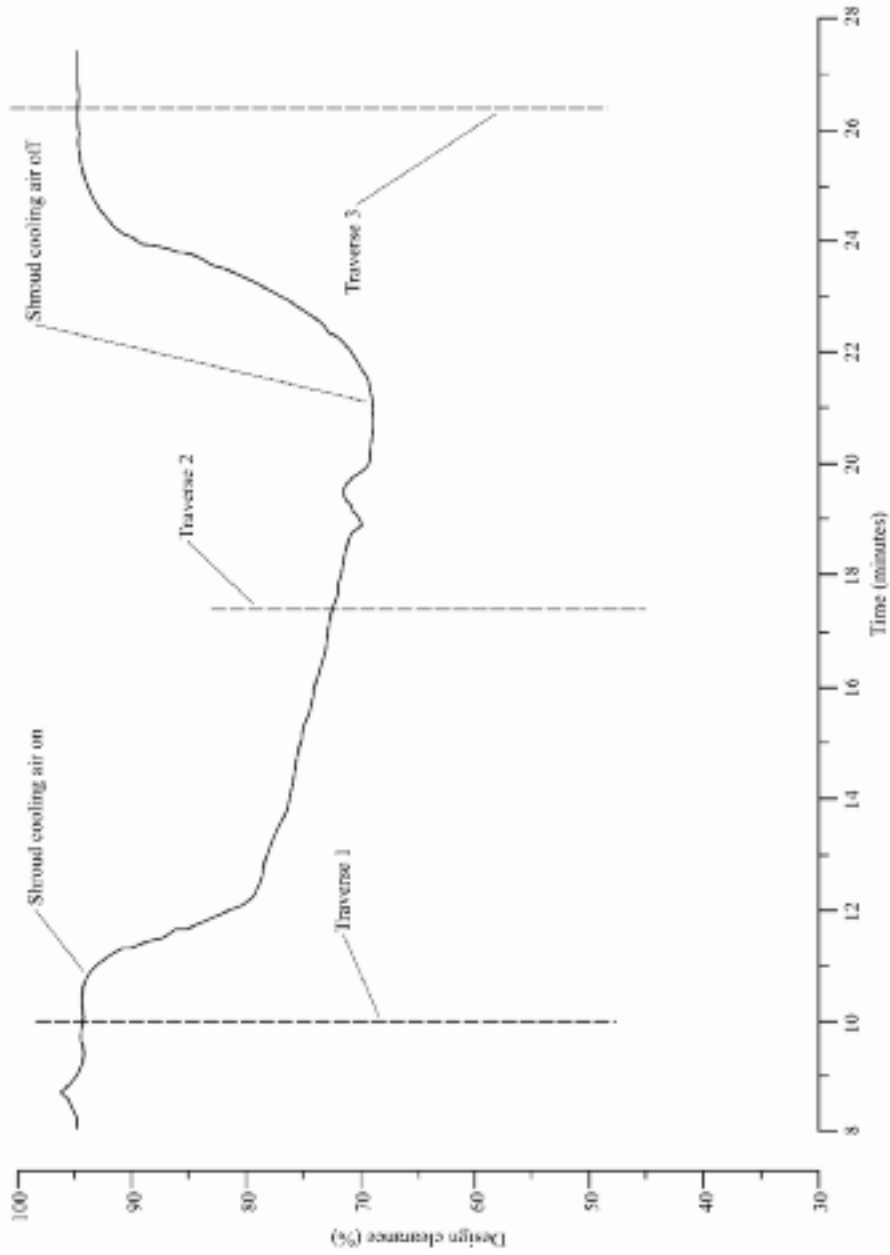


FIGURE 6.1. Clearance measured over the longest blade of a high-pressure turbine illustrating the 20% reduction in clearance achieved by applying shroud cooling air to the turbine casing.

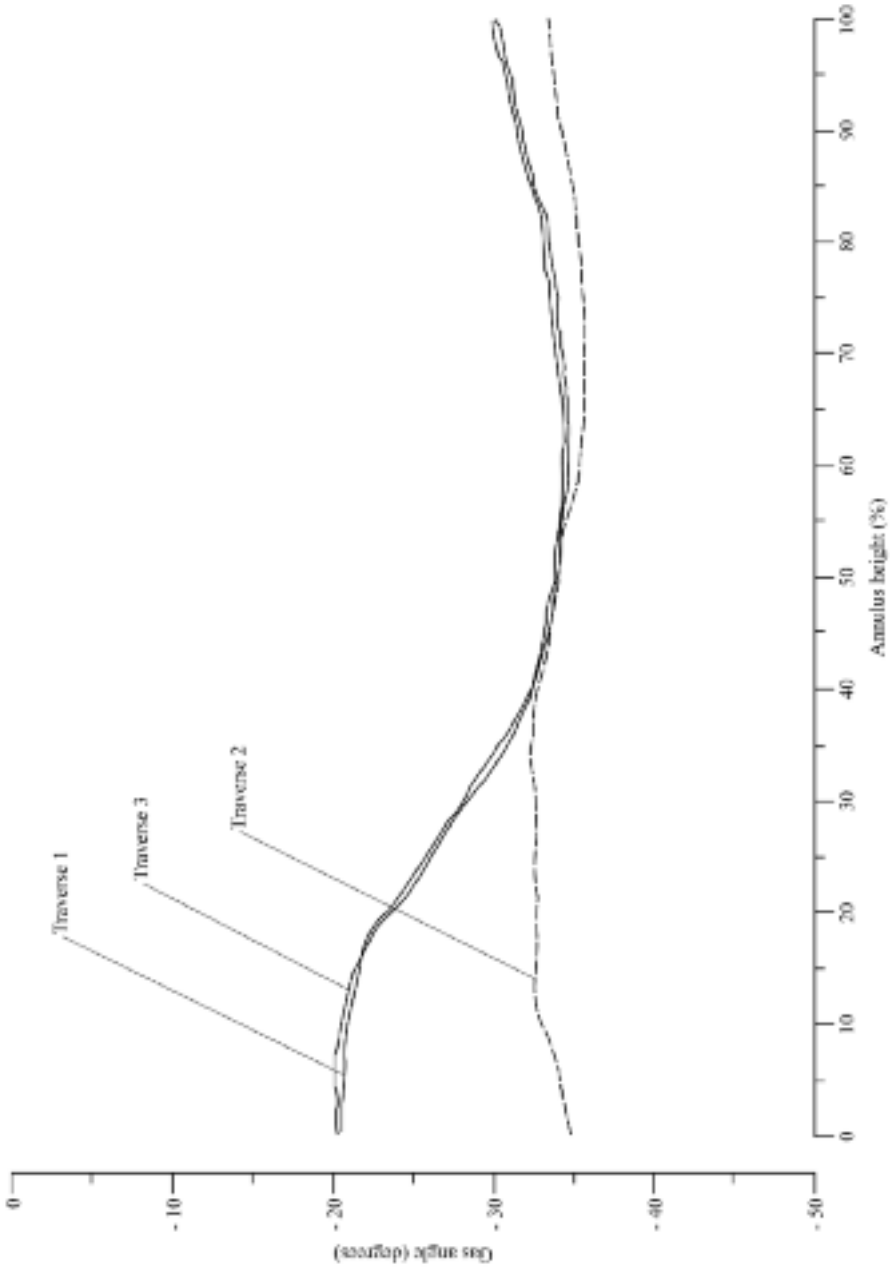


FIGURE 6.2. Turbine exit gas angle measured before applying shroud cooling air, with cooling air and after cooling air was removed, illustrating over ten degrees' change in gas angle in the blade tip region.

One can use two factors in blade tip-to-casing clearance calculation over the longest blade as Figure 6.3 illustrates. The first is distance, R , from the blade-by-blade electromechanical clearance measurement system electrode to the inner casing when the probe is against its rear datum. The second is stroke, S , of the probe when a spark-discharge occurs. We can define clearance over the longest blade as:

$$C_l = S - R$$

where:

C_l = clearance over the longest blade around the rotor.

Capacitance probe on-line calibration enables one to calculate the distance, c_n , between capacitance probe and each blade. The blade with the minimum clearance, c_l , between the capacitance probe and blade tip must be the longest blade, to which the electrode spark-discharge occurred. We can calculate the difference in clearance, A_{cn} , between the longest blade and every other as:

$$A_{cn} = c_n - c_l$$

where:

n = blade number.

We can calculate each blade's clearance, C_n , from the clearance over the longest blade, C_l , and the difference in clearance between the longest blade and every other blade:

$$C_n = C_l + A_{cn}$$

The above technique enables one to calibrate the capacitance probe after every spark-discharge, therefore ensuring the elimination of geometry effects and measurement system drift with temperature.

The capacitance probe is physically transported to the rotor blading. Capacitance probe range, therefore, only has to be large enough to measure from the electrode spark-discharge point to the shortest blade around the rotor. As the distance from the capacitance probe tip to the longest blade to which the spark-discharge occurred is typically only 0.1 mm, the capacitance probe is effectively only required to resolve the difference in clearance between different blades. The capacitance probe, therefore, requires only a short range. This permits the use of a capacitance probe of smaller diameter than the blade thickness, and so is insensitive to variations in blade thickness from blade to blade.

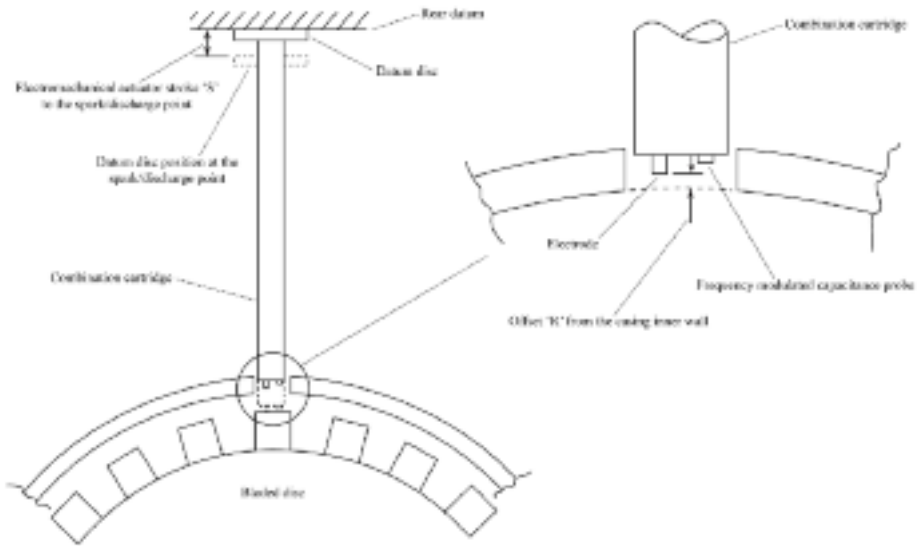


FIGURE 6.3. A schematic view of the probe installation illustrating the factors used to calculate blade tip-to-casing clearance over the longest blade.

The probe

The blade-by-blade electromechanical clearance measurement system contains a probe that combines an electrode and a capacitance probe into a single unit. Sheard and Killeen (1993) describe the probe in detail, therefore coverage in this chapter will be brief.

The probe, Figure 6.4, incorporates a datum disc that consists of a metal ring electrically charged to 400 volts. Mounted on an insulated disc, it electrically isolates from the probe body. During normal operation the probe is driven in until the 400 volts on the electrode has shorted to ground.

Once the electrode has shorted to ground it is retracted, following Sheard *et al.*'s (1992) method, the capacitance probe is calibrated, Figure 6.5. The distance travelled from spark-discharge on the rear datum to the spark-discharge to the longest blade and the capacitance probe output may be related to tip clearance over each blade.

The electromechanical actuator

The major design criteria when designing the electromechanical actuator was minimum overall size. The design, Figure 6.6, incorporates two principal components: the stepper motor drive assembly and an electronics module. Table 6.1 summarises the design specifications.

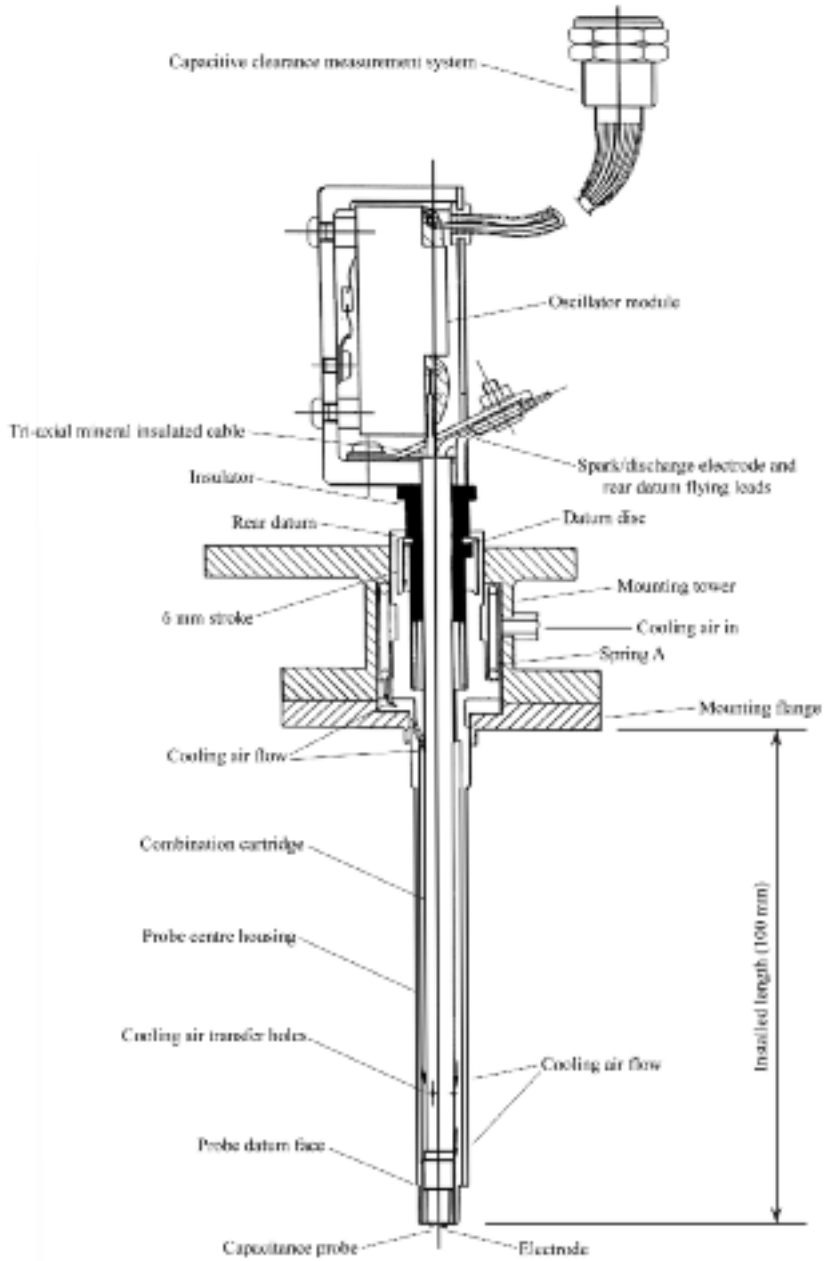


FIGURE 6.4. A 100 mm installed length, 6 mm stroke blade-by-blade electromechanical clearance measurement system probe.



FIGURE 6.5. A close-up view of a probe tip, with electrode (bottom), capacitance probe (top) and cooling holes (left and right).

Table 6.1. *Blade-by-blade electromechanical clearance measurement system specification.*

Range	6.0 mm
Resolution	2.5 microns
Repeatability	+/- 6 microns
Accuracy (ambient)	+/- 10 microns
Accuracy (627°C)	+/- 25 microns
Sample rate	30 KHz
Minimum target presentation time	2 micro seconds
Probe diameter at the tip	4.8 mm
Maximum un-cooled probe temperature	627°C
Maximum gas temperature	1527°C
Actuator dimensions	215 × 72 × 60 mm
Actuator weight	1.7 Kg
Actuator environmental temperature limits	50°C
Output from the controller	RS232

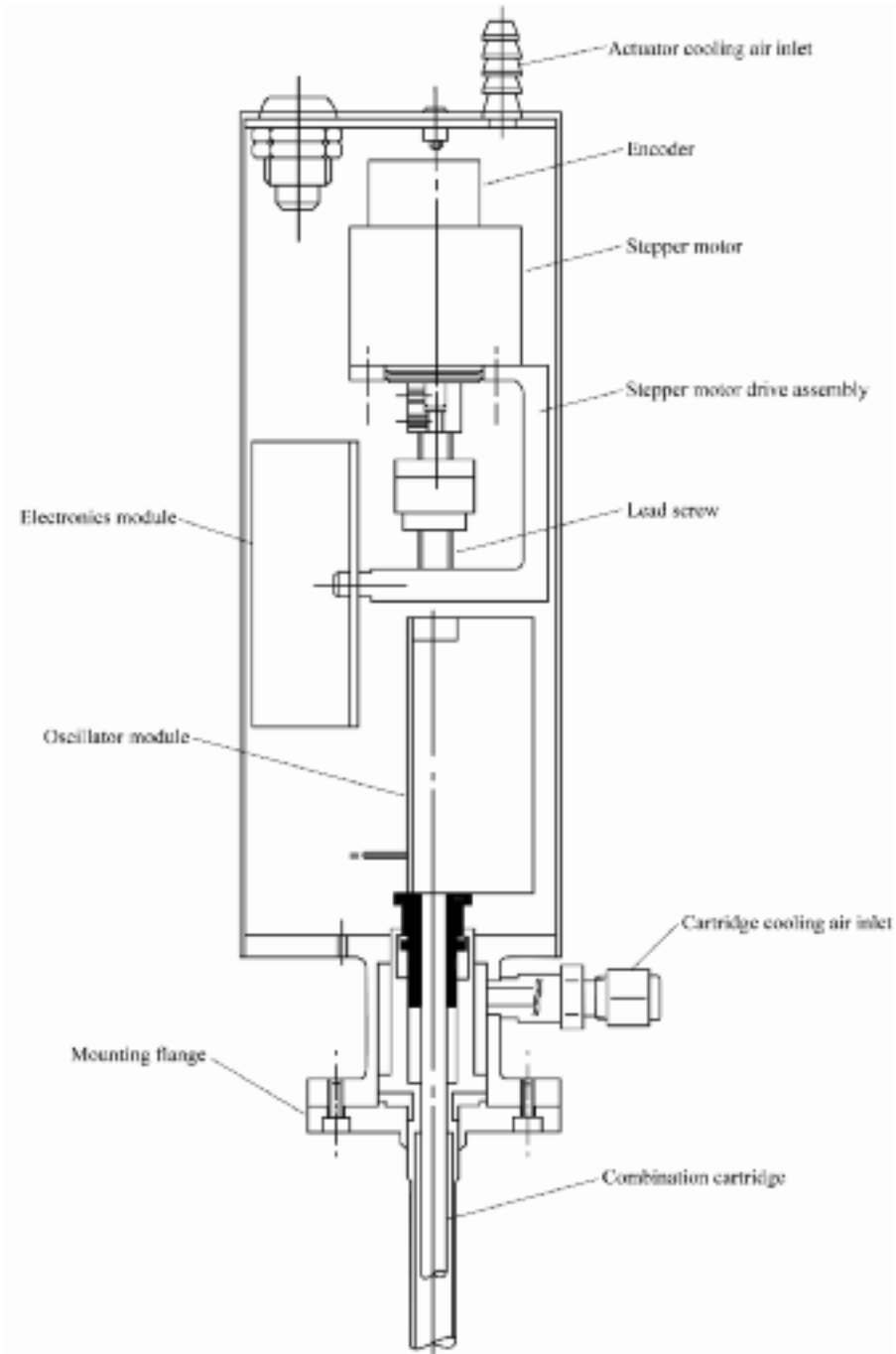


FIGURE 6.6. The blade-by-blade electromechanical clearance measurement system actuator and probe.

Sheard and Killeen (1993) describe the actuator in detail, therefore coverage in this chapter will be brief. The stepper motor drive assembly moves the probe to and from the blading in 2.5 micron steps. The electronics module generates the 400 volts that the operator applies to the datum disc and the electrode. The electronics module also senses the electrode or datum disc sparking, latches the event and cuts off the current with less than 2 pJ of energy transfer.

Cooling requirements

The authors designed the electromechanical actuator and probe for use in gas turbines where turbine entry temperature can exceed 1527°C; therefore, the actuator and probe require cooling techniques. A dry purge air supply cools the probe and actuator, Figure 6.7. During the initial commissioning trials, the authors used oxygen-free bottled nitrogen as the air supply. Later, they used standard ‘shop’ compressed air. In both cases, they filtered the purge air through a 0.5 micron filter immediately prior to entry into the probe. The purge air feeds into the mounting tower, Figure 6.6, and exits from the probe tip. The purge air also prevents contaminants from entering the probe from the gas path that could otherwise cause false short circuits from the electrode to ground.



FIGURE 6.7. The blade-by-blade electromechanical clearance measurement system actuator and probe illustrating the actuator and probe cooling air inlet locations. The actuator cooling air inlet is on the top of the actuator and the probe cooling inlet is located at the bottom, immediately above the mounting flange.

The electronic controller

A ground station drives the probe and actuator, Figure 6.8, which performs all functions necessary to generate data sets of clearance over each blade versus blade number. The ground station consists of four separate modules. A stepper motor drive module (SDM) generates all stepper motor drive signals, interrogates encoder output to verify the drive's correct motion and checks for a front or rear spark-discharge. The second module, a capacitance probe demodulator, converts the probe oscillators frequency modulated signal into a voltage pulse train. The third module is a blade analyser unit (BAU) which latches the height of each blade passing pulse and converts it from an analogue voltage peak to a digital number. A tachometer signal triggers the blade analyser unit's analogue to digital converter. The next tachometer signal triggers the data set of pulse heights to close and pass to the blade analyser unit's output stage.

The stepper motor drive module and blade analyser unit communicate with the fourth module, the system processor (SP), via RS232 links. The system processor is the ground station's interface between an external data acquisition system and the first three modules. The system processor firmware contains the algorithms which Sheard *et al.* (1992) developed to calibrate the capacitance probe on-line and calculate clearance over each blade. The output of the system processor is a stream of data sets, where each data set comprises a list of blade numbers versus blade tip-to-casing clearance in engineering units.

PC software

In order to acquire data from the ground station, the authors used an IBM-compatible computer as a host computer. The authors wrote a program to enable the downloading of setup information to the system processor. As the system processor performed all conversion of raw data to engineering units, it was not necessary for the program to perform any further calculations. In essence, the software provided only a pre-test setup facility, a test control facility and a data logging facility. The software was also able to display blade tip-to-casing clearance versus blade number as it was acquired. This facility made blade tip-to-casing clearance data interpretation possible as the program acquired it.

THE TEST FACILITY

The authors conducted the commissioning of the blade-by-blade electro-mechanical clearance measurement system on the C147 large scale, high-speed high-pressure research compressor at the Defence Research Agency (DRA) Pyestock, Figure 6.9. Table 6.2 provides the C147 compressor overall design parameters and Calvert *et al.* (1989) describe them. Table 6.3 gives the rig conditions local to the electromechanical clearance measurement system.

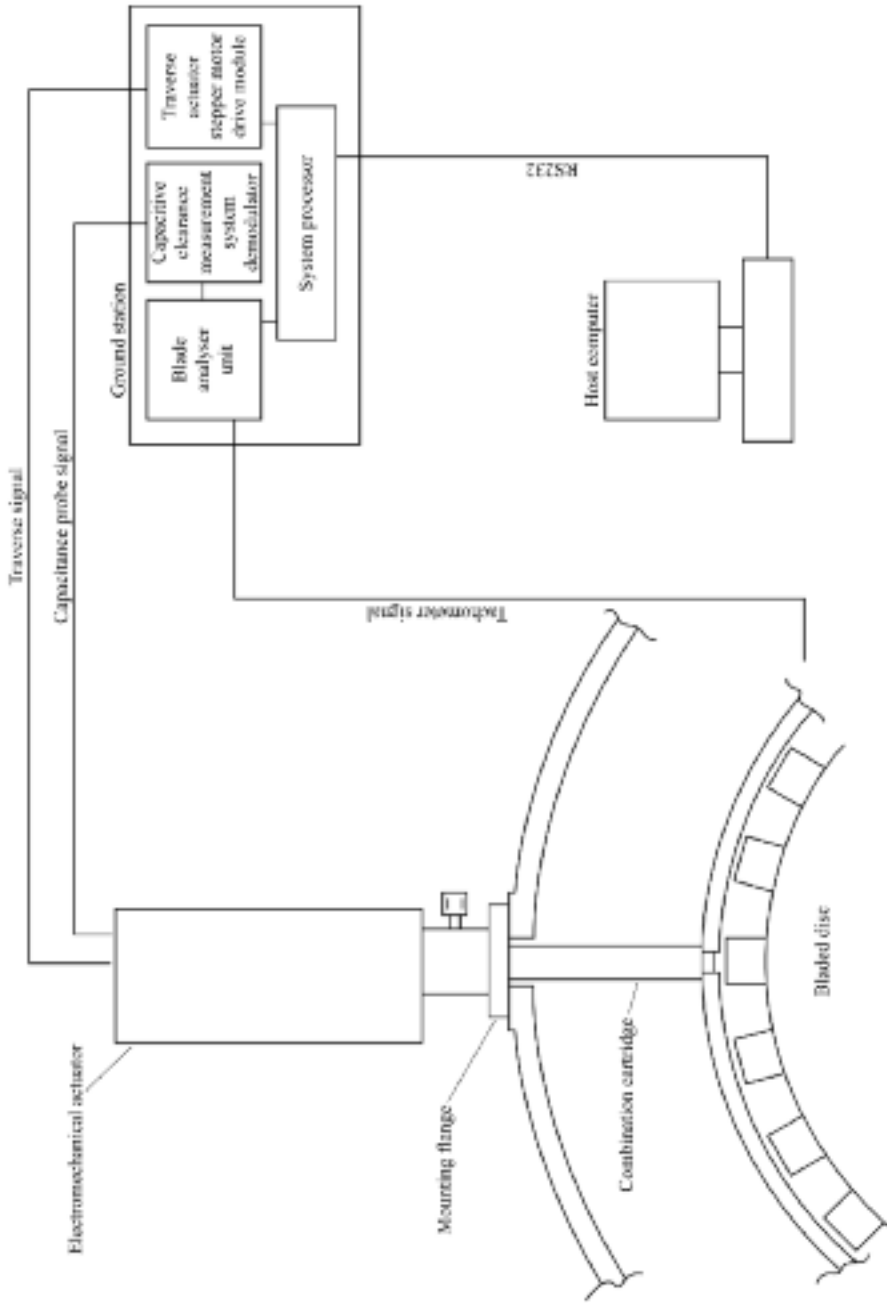


FIGURE 6.8. The interrelationship between ground station modules, electromechanical actuator and host computer.

Table 6.2. *The C147 compressor overall design parameters.*

Pressure ratio	6.4
Mass flow (at 15°C & atmospheric inlet pressure)	49.5 Kg/s
Rotational speed (at 15°C & atmospheric inlet pressure)	6894 rpm
Compressor stage-5 blade hub-to-tip ratio	0.912
Compressor stage-5 blade height	38.1 mm
Compressor stage-1 blade tip diameter	917 mm

Table 6.3. *Commissioning test vehicle conditions.*

Stage number	Last of 5
Number of blades	91
Rotational speed	6894 rpm
Gas path total temperature	234°C
Approximate ambient air temperature local to the electromechanical clearance measurement system actuators	20°C
Gas path total pressure	400 KPa absolute
Vibration	4 mm/s

The facility is extensively instrumented, Figure 6.9, with up to two area traverse mechanisms, five radial traverse mechanisms and five electromechanical clearance measurement systems for measuring clearance to the longest blade around each rotor. Figure 6.9 illustrates one radial and two area traverse mechanisms on top of the rig, but the facility cabling partially obscures them. Sheard *et al.* (1993) describe both radial and area traverse systems, and Davidson *et al.* (1983) describe the spark-discharge clearance measurement systems. The authors designed the blade-by-blade electromechanical measurement system to be interchangeable with Davidson *et al.*'s (1983) system, allowing one to fit it into the same mounting tower, Figure 6.10. The authors installed the blade-by-blade electromechanical measurement system without any modification to the facility. The only addition was a second cable from the actuator to carry the capacitance probe signal.

COMMISSIONING

The authors undertook commissioning on the final stage of the C147 compressor to demonstrate system ability to withstand the environment that exists when running turbomachinery. The ability of any system to operate in an ambient environment is no guide as to its likely performance when installed on an active compressor or turbine.

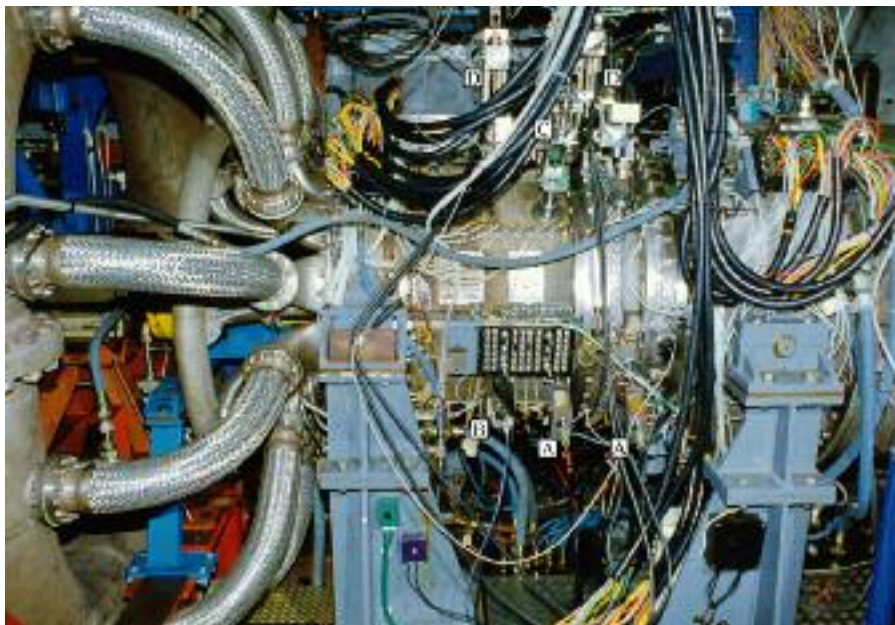


FIGURE 6.9. The C147 compressor at DRA Pyestock fitted with two of Davidson *et al.*'s (1983) electromechanical clearance measurement systems (A), a blade-by-blade electromechanical clearance measurement system (B), a radial traverse actuator (C) and two area traverse systems (D). Courtesy British Crown (1993).

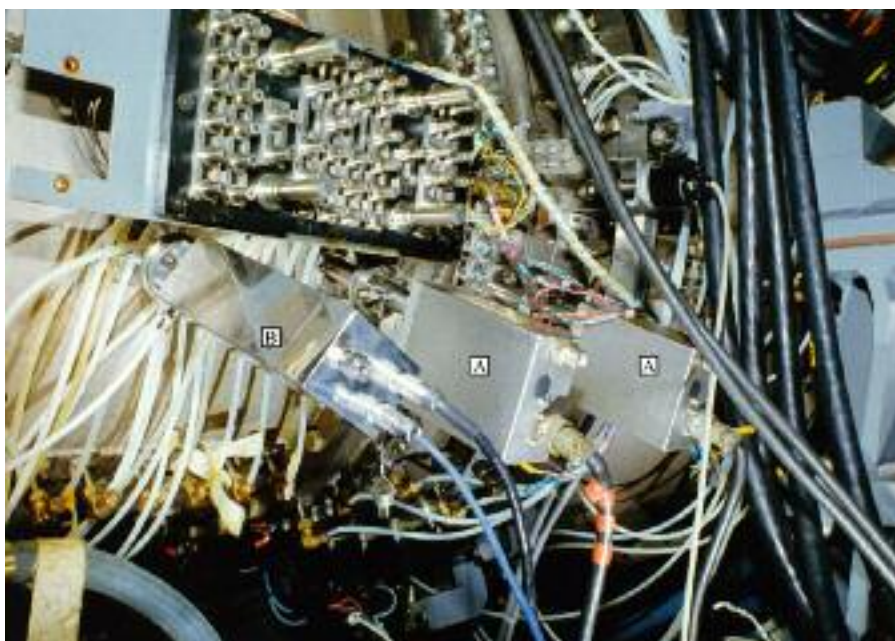


FIGURE 6.10. The C147 fitted with two of Davidson *et al.*'s (1983) electromechanical clearance measurement systems (A) and a blade-by-blade electromechanical clearance measurement system (B). Courtesy British Crown (1993).

The authors drove the compressor to 100% design speed and held that speed for 5 hours. They used the blade-by-blade electromechanical measurement system to measure clearance over each blade around the rotor every 15 minutes during the time spent at condition, to ascertain measurement system reliability and repeatability. The authors did not encounter operational problems with the radial transport and spark-discharge electronics, with the actuator and probe cooling system keeping both at near-ambient temperature. The authors therefore concluded system reliability as good on the C147 compressor and similar to that which Sheard and Killeen (1993) reported in the laboratory.

The drop from probe internal datum to the spark-discharge point on the longest blade increased by 0.04 mm over the first 15 minutes at design condition, then over the next 75 minutes decreased by 0.06 mm, Figure 6.11. The drop then remained constant for the remainder of the test. The authors drew two conclusions from the drop measurements at design condition. First, the facility took 1.5 hours to thermally stabilise after reaching the design point. Second, transport repeatability during the last 4 hours at design condition was excellent with no evidence of probe tip erosion.

The authors conducted the commissioning trial at the conclusion of a 400 hour test programme, during which they had utilised Davidson *et al.*'s (1983) electro-mechanical clearance measurement system extensively to measure clearance over the longest blade on the compressor's final stage. Using the blade-by-blade electro-mechanical clearance measurement system, the authors compared the clearance over the longest measured blade using Davidson *et al.*'s (1983) measurement system, Figure 6.12. The minimum and maximum clearances that they measured with the blade-by-blade electromechanical clearance measurement system were within the scatter of the previous results. First, the authors concluded that the blade-by-blade electromechanical clearance measurement system results were in excellent agreement with the earlier data. Second, the authors could attribute a significant contributor to the scatter of the earlier results to the compressor's thermal stabilising time.

The primary purpose of the commissioning programme was to measure blade tip-to-casing clearance over individual blades. The authors used a capacitance probe to measure blade-by-blade clearance over the 91 blades around the C147 compressor stage 5. A typical example of the capacitance probe raw output voltage, Figure 6.13, illustrates the voltage peak that occurred with each blade passing event. The raw output reduces to a data set of clearance over each blade versus blade number, where the authors defined blade 1 as the first blade to follow the falling edge of the once per revolution tachometer signal.

The data sets that the authors acquired during the last 4 hours at design condition showed a high degree of repeatability, with the clearance over individual blades varying randomly by approximately 0.025 mm. The authors acquired two data sets after 1 hour at design condition (run 1) and 3 hours at design condition (run 2). Figure 6.14 illustrates this point clearly.

The blading around a rotor is a loose fit in its root fixing, with Sheard *et al.* (1994) measuring a 0.05 mm variation in blade radius from one rotor cycle to the next. The authors speculated that the blading might move in its root fixing over a

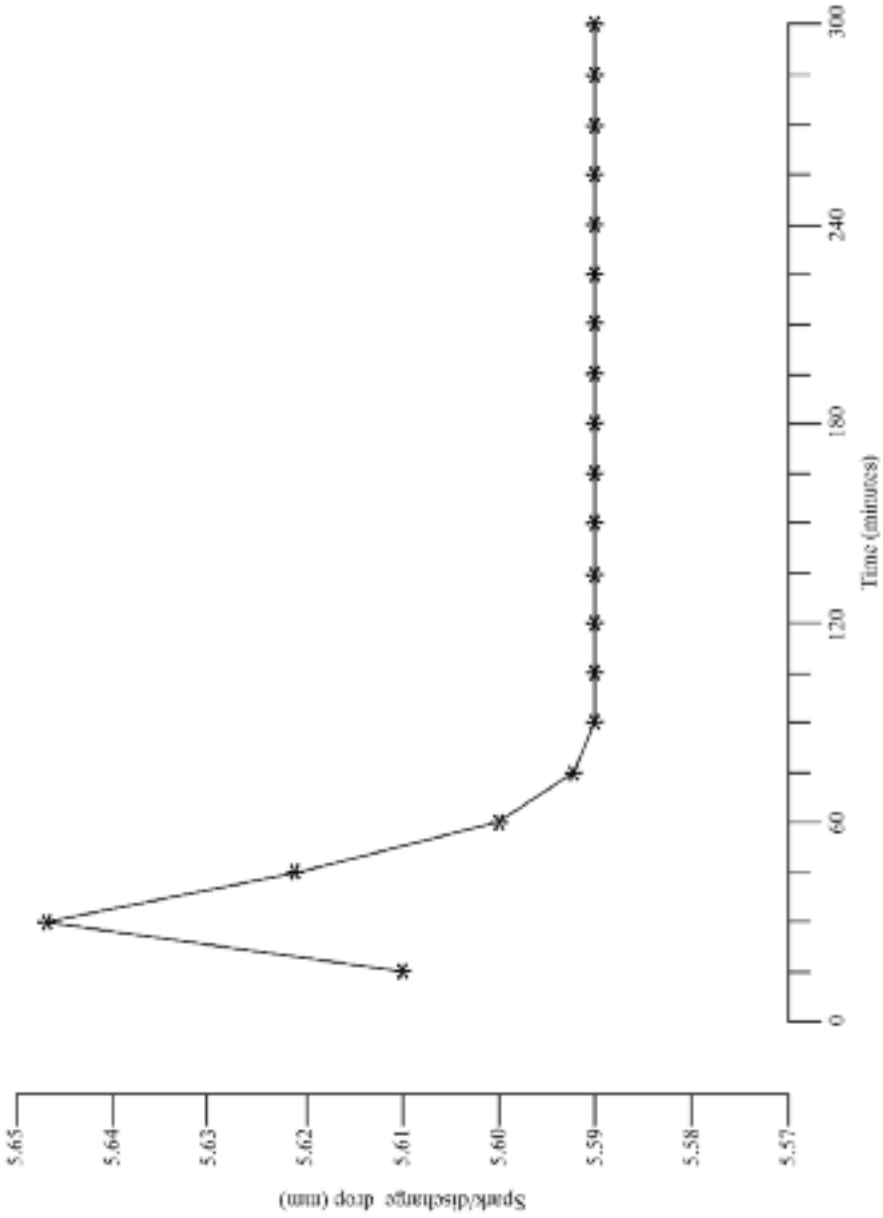


FIGURE 6.11. Measured distance from the blade-by-blade electromechanical clearance measurement system datum to the C147 compressor stage 5 longest blade during commissioning.

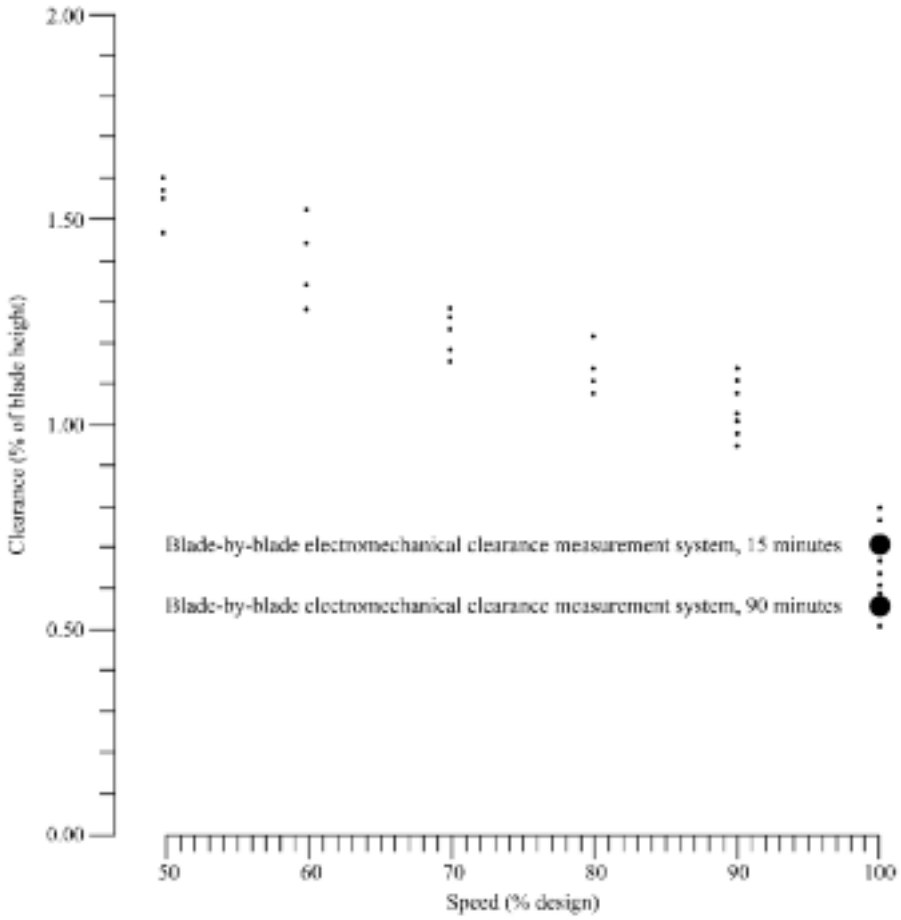


FIGURE 6.12. Measured C147 compressor stage 5 clearance from Davidson *et al.*'s (1983) electro-mechanical clearance measurement system and results from the blade-by-blade electromechanical clearance measurement system.

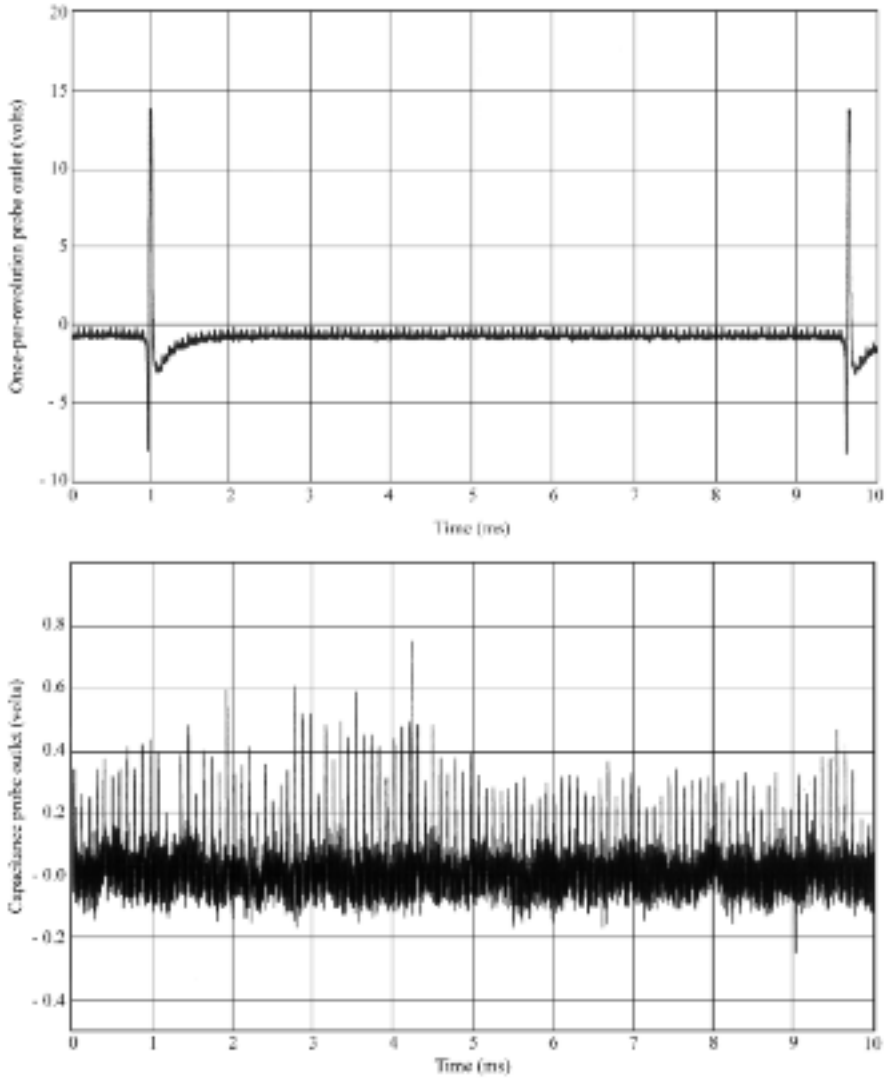


FIGURE 6.13. A typical capacitance probe output voltage signal after a spark-discharge to the longest blade (bottom) and tachometer signal (top).

period of time due to unsteady aerodynamic forces on the blading and the rig's mechanical vibration. These phenomena may explain the variation in clearance of 0.025 mm over individual blades from one data set to the next.

It appears that the C147 rotor assembly was running eccentric, a phenomenon that we can see by re-plotting the data in Figure 6.14 after subtracting the mean clearance and expanding the clearance axis, Figure 6.15. We can clearly see the rotor's once per revolution eccentricity as a ± 0.05 mm sinusoidal variation in tip clearance around the rotor. This level of eccentricity was self consistent with the 0.075 mm design clearance in the bearings, plus a small allowance on the rear bearing squeeze film. There was insufficient vibration data available to confirm that the once per revolution eccentricity was the rotor's synchronous unbalance response; however, the authors considered this most likely.

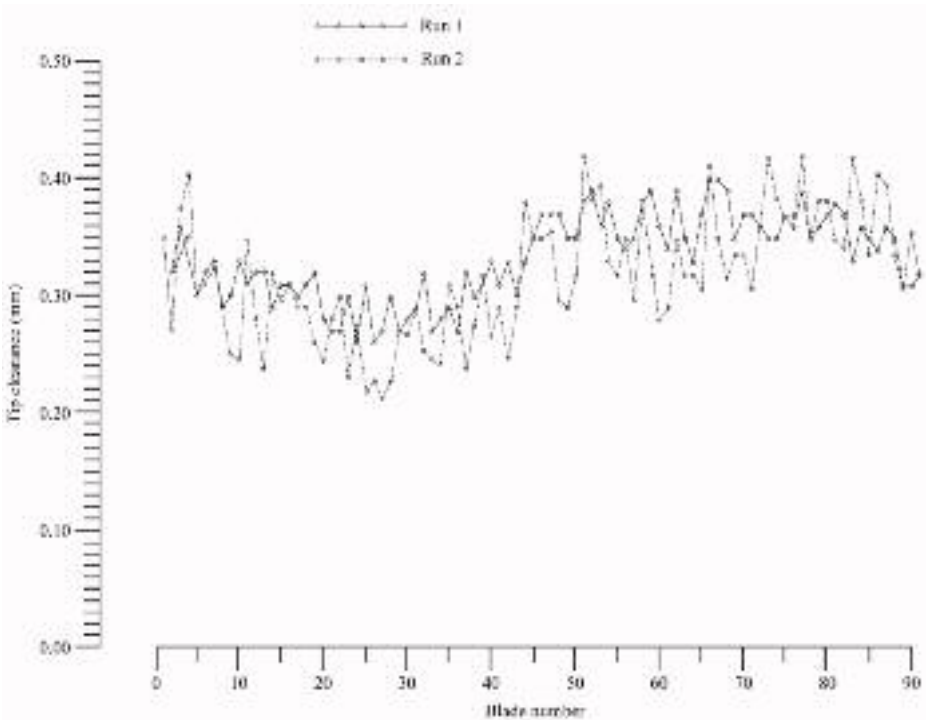


FIGURE 6.14. Two data sets of blade tip-to-casing clearance versus blade number data acquired after 1 and 3 hours at the compressor design point.

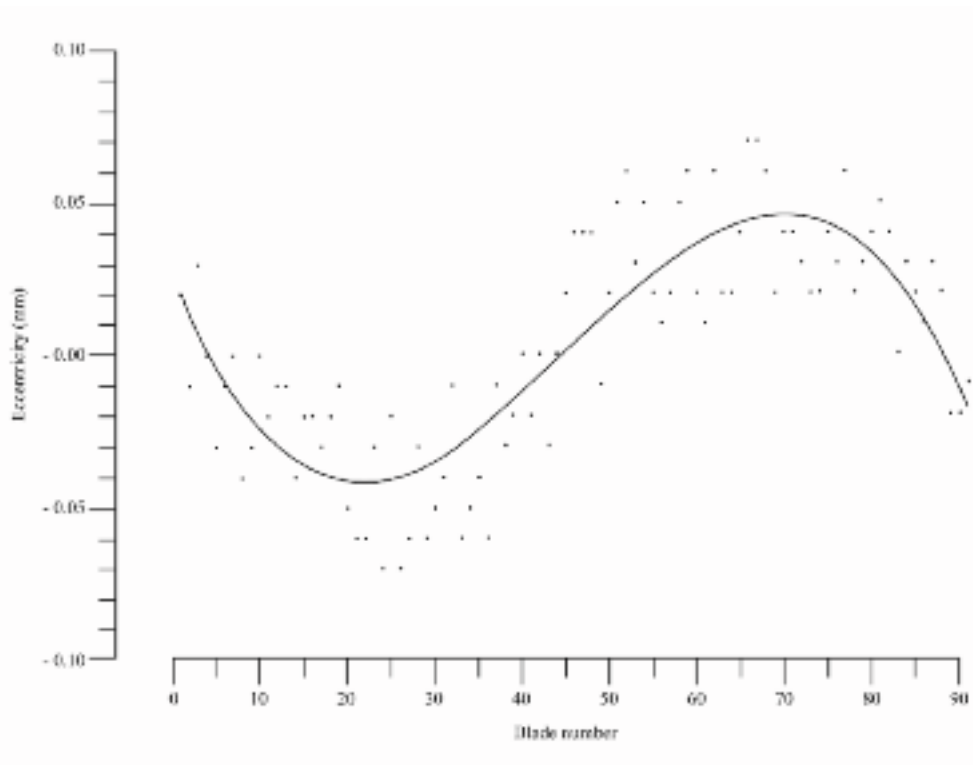


FIGURE 6.15. A clearance versus blade number data set, after subtracting the mean clearance.

CONCLUSIONS

The authors successfully used a blade-by-blade tip-to-casing clearance measurement system on a compressor under test to measure clearance over every blade around a rotor.

The blade-by-blade electromechanical measurement system has a similar geometry to Davidson *et al.*'s (1983) electromechanical measurement system, facilitating the free exchange of the two measurement systems in a gas turbine installation.

The blade-by-blade electromechanical clearance measurement system survived the commissioning trial, with no operational problems of the transport mechanism, the spark-discharge electronics or the cooling system. On completion of the trial, the authors inspected the actuator and probe which showed no sign of distress.

Clearance over the longest blade around the compressor final stage rotor measured using the blade-by-blade electromechanical measurement system and Davidson *et al.*'s (1983) electromechanical measurement system were in close agreement, giving confidence in the new measurement system.

The blade-by-blade electromechanical clearance measurement system revealed a ± 0.050 mm eccentricity of the rotor.

REFERENCES

- Calvert, W.J., Ginder, R.B., McKenzie, I.R.I. & Way, D.J. (1989), 'Performance of a Highly-Loaded HP Compressor'. *Proceedings of the 28th American Society of Mechanical Engineers Gas Turbine and Aeroengine Congress*. Toronto, Canada, USA, 5–8 June, Paper No. 89-GT-24.
- Chivers, J.W.H. (1989), 'A Technique for the Measurement of Blade Tip Clearance in a Gas Turbine'. AIAA Paper No. 89-2916.
- Davidson, D.P., DeRose, R.D. & Wennerstrom, A.J. (1983), 'The Measurement of Turbo-machinery Stator to Drum Running Clearances'. *Proceedings of the 28th American Society of Mechanical Engineers Gas Turbine and Aeroengine Congress*. Phoenix, USA, 27–31 March, Paper No. 83-GT-204.
- Killeen, B., Sheard, A.G. & Westerman, G.C. (1991), 'Blade-by-blade Tip-Clearance Measurement in Aero and Industrial Turbomachinery'. *Proceedings of the 37th ISA International Instrumentation Symposium*. San Diego, California, USA, 5–9 May, pp. 429–47.
- Pavey, P.G. (1993), Private communication with Mr. P.G. Pavey, Rolls-Royce plc, Engineering Manager Measurement and Test.
- Sheard, A.G. & Killeen, B.A. (1993), 'Hybrid System for High-Temperature Tip-Clearance Measurement'. *Proceedings of the 39th ISA International Instrumentation Symposium*. Albuquerque, New Mexico, USA, 2–6 May, pp. 379–94.
- Sheard, A.G. & Turner, S.R. (1992), 'An Electromechanical Measurement System for the Study of Blade Tip-to-casing Running Clearances'. *Proceedings of the 37th American Society of Mechanical Engineers Gas Turbine and Aeroengine Congress*. Cologne, Germany, 1–4 June, Paper No. 92-GT-50.

- Sheard, A.G., Westerman, G.C. & Killeen, B. (1992), 'An On-Line Calibration Technique for Improved Blade-by-blade Tip Clearance Measurement'. *Proceedings of the 38th ISA International Instrumentation Symposium*. Las Vegas, Nevada, USA, 26–30 April, pp. 32–51.
- Sheard, A.G., Killeen, B. & Palmer, A. (1993), 'A Miniature Traverse Actuator for Mapping the Flow Field between Gas Turbine Blade Rows'. *Proceedings of the IMechE: Machine Actuators & Controls Seminar*. London, UK, 31 March, pp. 1–11.
- Sheard, A.G., Westerman, G.C., Killeen, B. & Fitzpatrick, M. (1994), 'A High-Speed Capacitance-Based System for Gauging Turbomachinery Blading Radius During the Tip-Grind Process'. *Transactions of the ASME, Journal of Engineering for Gas Turbines & Power*, vol. 116, pp. 243–9.

Capacitive Measurement of Compressor and Turbine Blade Tip-to-casing Running Clearance

D. Müller, A.G. Sheard, S. Mozumdar and E. Johann

ABSTRACT

It is an established fact that the efficiency of a gas turbine has an inverse relationship with the clearance between the rotor blades and the casings within which they run. This 'tip clearance' is an essential measurement during development gas turbine testing. Whilst commercial tip clearance measurement systems are available, gas turbine size, geometry, physical accessibility and temperature distribution around the measurement region dictate their applicability to a gas turbine. This chapter describes a tip clearance measurement system's development based on the frequency modulated, driven guard capacitive measurement principle. The authors undertook the development programme to satisfy the application requirements of a specific class of gas turbines. The requirements included a relatively long and flexible cable to route the electrical signals out of the gas turbine. The authors successfully used a tip clearance measurement system during gas turbine development testing and obtained valuable data.

INTRODUCTION

Rotor blade tip-to-casing clearance (tip clearance) has a significant effect on a gas turbine's flow-field in the blade-tip region. In general, the larger the tip clearance, the larger is the tip-leakage with an associated loss of high-energy gas and, hence, the lower is the gas turbine's efficiency. Whilst computer models are available to predict the tip clearance for both compressors and turbines, engineers have to verify and fine-tune such predictions with test data. Thus, tip clearance is an essential measurement during a gas turbine's development programme.

This chapter is a revised and extended version of Müller, D., Sheard, A.G., Mozumdar, S. & Johann, E. (1997), 'Capacitive Measurement of Compressor and Turbine Blade Tip-to-casing Running Clearance'. *Transactions of the ASME, Journal of Engineering for Gas Turbines & Power*, vol. 119, pp. 877–84.

During the development of the family of BR700 gas turbines in the 65 to 110 kN thrust class (Kappler *et al.*, 1992), the design requirements called for a tip clearance measurement system with a 2.5 to 3.0 metre long flexible cable to measure blade tip-to-casing clearances accurately in the 0.0 to 2.0 mm range. No commercially available system could meet the installation and performance requirements for this application. The authors, therefore, decided to develop a new system based on the existing knowledge base of frequency modulated driven screen capacitive type tip clearance measurement systems which Chivers (1989a) originally developed. The authors chose the frequency modulated driven guard capacitive clearance measurement system because in contrast to a direct current system, a frequency modulated driven guard system is insensitive to gas ionisation effects. Insensitivity to ionisation effects enables engineers to use the system in turbine applications, immediately downstream of the combustion system that produces ionised combustion products.

Development of the system comprised separate but coordinated activities which, working in parallel, four different research groups pursued. Killeen *et al.* (1991), Sheard and Lawrence (1998) and Sheard (2000) undertook system integration, system calibration and probe development. Sheard *et al.* (1999) developed analogue electrical measurement system components. Stringfellow *et al.* (1997) developed mineral-insulated and flexible cables respectively to link the capacitive sensor to its oscillator and the oscillator to its demodulator. Through the programme of research which this chapter reports, BMW Rolls-Royce GmbH developed measurement system calibration procedures, planned system testing across a series of flight standard development gas turbines and evaluated measurement system data. Finally, the four research groups participated in their respective measurement system components' post-test analysis.

The following sections comparatively describe the system concept and validation with the blade tip-to-casing clearance data which the authors obtained using Sheard and Turner's (1992) electromechanical clearance measurement system. The chapter concludes with a presentation of clearance data that the authors obtained during flight standard development gas turbine testing.

SYSTEM CONCEPT

The capacitive clearance measurement system is based on a measurement of the capacitance between a probe and the blade tip. We can relate the measured capacitance to the blade tip-to-casing clearance using a predetermined calibration.

A probe fitted into the gas turbine casing over the blade tips represents one capacitor plate, the blade tip and the other plate. The resulting capacitance is a function of the plates' geometry, the distance between the plates and the material in between. If we assume that the geometry and material properties remain constant, the capacitor's value is a function only of distance between the plates from which we can derive blade tip-to-casing clearance.

The small overlap area between probe tip and blade of typically 5 mm², combined with the large distance between them of typically 1 mm, results in a very small capacitance of 0.04 pF. To measure this small capacitance accurately, Chivers (1989a) proposed integrating the capacitor into an oscillator. A change in the capacitor's value will result in a change in the oscillator's natural frequency. We can measure and relate this frequency shift to blade tip-to-casing clearance using a calibration.

System module description

Figure 7.1 shows the system's structure as a schematic block diagram. The probe-cable assembly and oscillator module are linked to a demodulator, which converts the change in frequency into a change in voltage. The authors used a lineariser to apply the system calibration, enabling it to output clearance in engineering units. In addition, the authors used a tachometer to generate an analogue speed signal and a once-per-revolution trigger, which they used for dynamic data analysis.

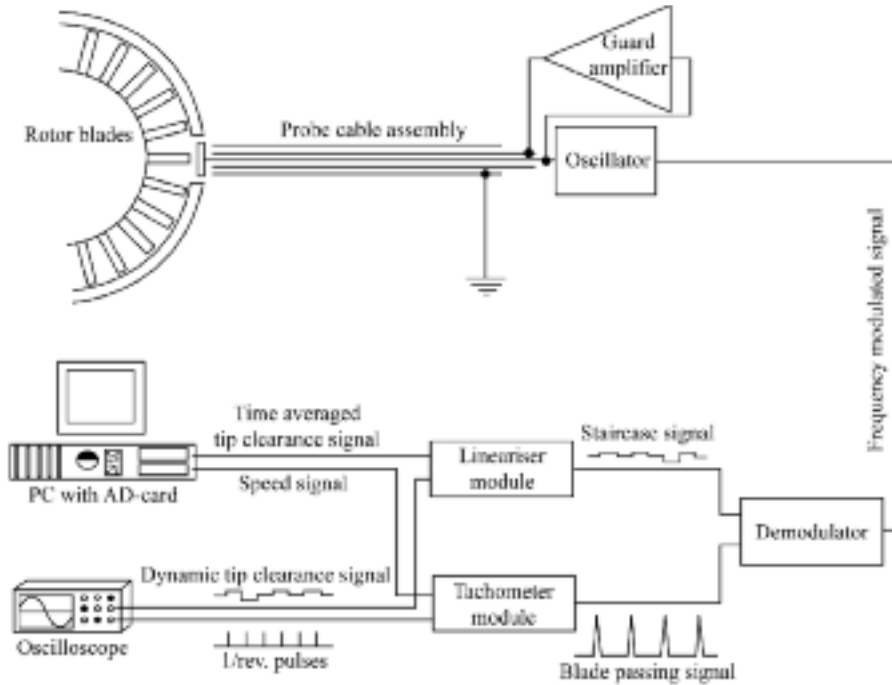


FIGURE 7.1. Capacitive clearance measurement system schematic block diagram.

Probe-cable assembly

The probe-cable assembly comprises the probe head and the cable, as Figure 7.1 and 7.2 illustrates. The authors designed the probe head for a maximum temperature of 800°C and a maximum probe front-face electrode temperature of 1000°C.

The cable capacitance of typically 300 pF forms a ‘shunt’ capacitance that is in series with the probe tip-to-blade capacitance. The shunt capacitance is approximately 1000 times greater than the capacitance which the authors measured at the probe tip. Very small changes in cable temperature and shape result in its capacitance changing by more than the value of the probe tip-to-blade capacitance.

To eliminate the shunt capacitance, Chivers (1989a) adopted a tri-axial probe cable that incorporated a conductor, inner screen and outer screen, Figure 7.1. The conductor connects the oscillator electronics to the probe tip. The outer screen connects to ground. A guard amplifier drives the inner screen to the same voltage as the conductor. By driving the inner screen to the same instantaneous voltage as the conductor, Chivers (1989a) was able to eliminate the effect of cable shunt capacitance. This enables the oscillator to connect to the probe tip without changes in cable capacitance resulting in a change in system output.

To accommodate the application requirements for gas turbine installations, Stringfellow *et al.* (1997) developed two different kinds of cable. The first is a mineral-insulated (MI) tri-axial cable for use in high-temperature applications. This cable type is made from a stainless steel outer screen and conductor with a nickel alloy inner screen, insulated with silicon oxide. The resulting cable is suitable for application with temperatures of up to 800°C. Stringfellow *et al.* (1997) used materials that resulted in a cable that is relatively stiff and inflexible, thus making it difficult to negotiate bends and corners when routing the cable in a gas turbine application.

The second cable is a flexible tri-axial cable for use in applications which require flexibility and where the environment is relatively cool. It can withstand temperatures of up to 200°C. The cable is made out of copper with poly-tetra-fluoroethylene (PTFE) as insulator. An external nickel braiding mechanically protects the cable. The authors were able to combine both cable types as needed up to a total cable length of 3 metres.

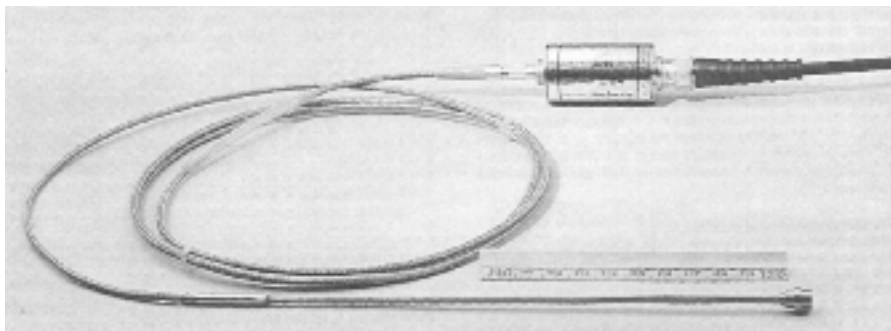


FIGURE 7.2. Capacitance probe, cable assembly and oscillator.

Oscillator and guard amplifier

The oscillator's function is to convert a change in capacitance that arises as a consequence of blade passing at the probe tip into a change in frequency. The oscillator includes a guard amplifier that drives the inner screen of the tri-axial probe cable. The voltage on the inner screen has to follow the oscillator frequency, amplitude and phase, to ensure a zero voltage difference between conductor and inner screen. The guard amplifier's current delivery capability limits the tri-axial cable's maximum inner screen to outer screen capacitance that the oscillator can drive, whilst maintaining the inner screen at the same instantaneous voltage as the conductor. The oscillator's current delivery capability therefore limits maximum cable length. In the present case, the cable properties and the amplifier characteristics allowed a cable length of up to 3 metres. With a tri-axial cable length of 3 metres between probe and oscillator, the sensitivity of Stringfellow *et al.*'s (1997) oscillator is 150 kHz/pF or approximately 6 kHz for a 1.0 mm thick blade passing the sensor at a 1.0 mm clearance.

The oscillator and guard amplifier electronics size were reduced by Stringfellow *et al.* (1997) to a cylinder 25 mm in diameter and 44 mm in length, see Figure 7.2. Chivers' (1989a) original oscillator design was significantly larger than Stringfellow *et al.*'s (1997) and required a multi-core cable to connect it with its respective demodulator. Stringfellow *et al.*'s (1997) oscillator operated at a frequency of 5 MHz, in contrast to Chivers' (1989a) design that operated at 10 MHz. In addition, Stringfellow *et al.*'s (1997) oscillator linked to its respective demodulator using a standard 50 ohm co-axial cable. The reduced operating frequency made possible the use of longer tri-axial cables between probe and oscillator, and the use of a standard 50 ohm co-axial cable to connect the oscillator to its respective demodulator made system installation in gas turbine test cells practical. In the research which this chapter reports, the authors used 50 ohm co-axial cable lengths of up to 150 metres.

Demodulator

The demodulator's primary function is to convert a change in oscillator frequency into a change in output voltage. The demodulator unit comprises a voltage-controlled oscillator (VCO) and a phase locked loop (PLL). The authors adjusted the VCO control voltage using the PLL to keep it in phase with the external oscillator to which they connected the probe. For this reason, the VCO control voltage is proportional to the external oscillator frequency. This VCO control voltage passes to an AC-coupled amplifier to yield the 'blade passing signal', Figure 7.3.

The authors calibrated the amplifier, and hence the demodulator, to give a 6 V peak-to-peak output for a 30 kHz change in the oscillator's nominal 5 MHz operating frequency. This corresponds to a typical clearance of 0.2 mm over a 1.0 mm thick blade. Because of this electronic arrangement, all calibrated demodulators behave identically and, therefore, are exchangeable. Engineers can calibrate probe and oscillator pairs with a single demodulator, and then use them with any demodulator without affecting system calibration.

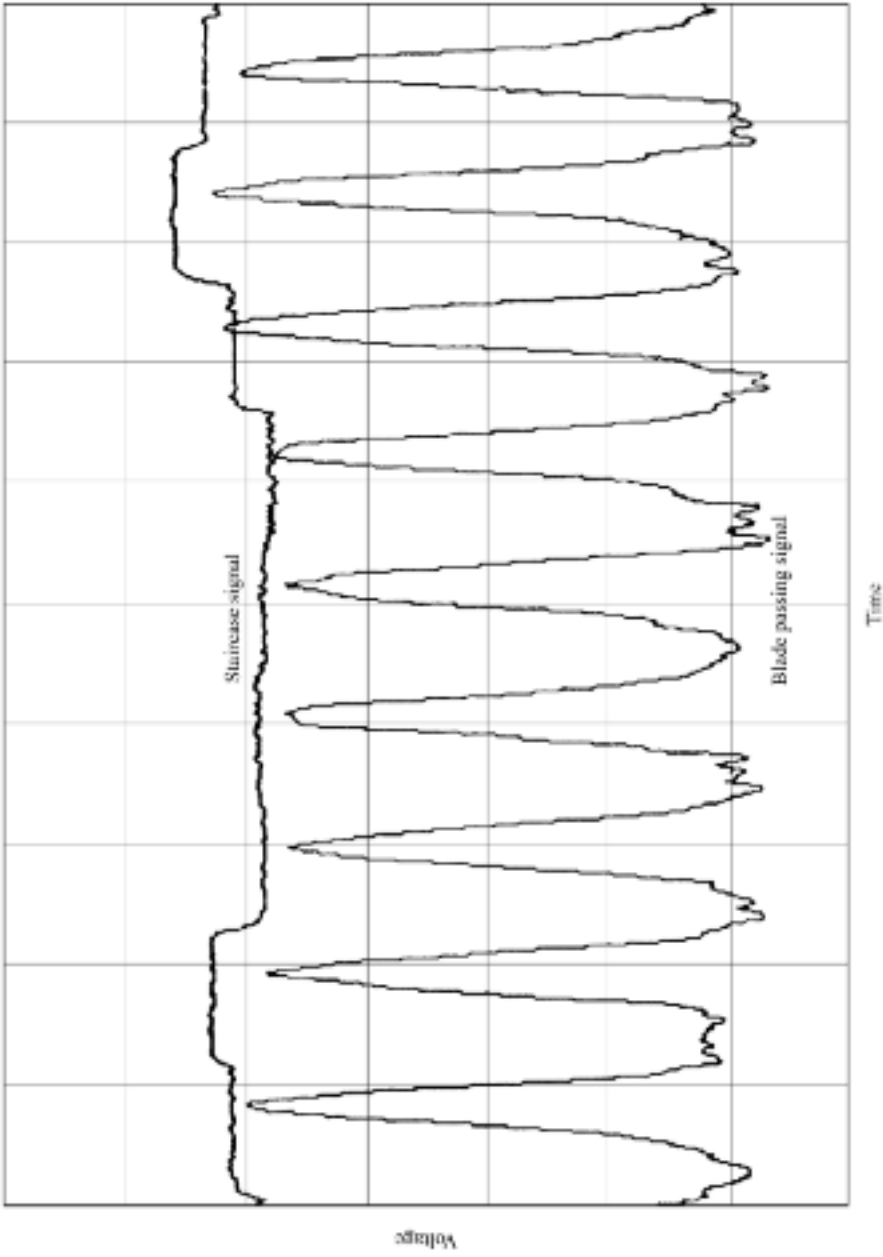


FIGURE 7.3. Blade passing and staircase signal, blade thickness > 1 mm, clearance > 1 mm (hardcopy from a digital oscilloscope used to monitor measurement system dynamic outputs).

The demodulator also incorporates a ‘staircase’ module. This module is a peak-to-trough picker and restores the blade passing output to a DC voltage. The voltage level corresponds to the height of the blade passing pulse, Figure 7.3. This output updates each time a new peak registers.

The staircase signal offers two advantages. The first advantage is that the staircase signal is insensitive to the blade passing signal’s base line modulation. Base line modulation can occur with probe cable exposure to high vibrations. The second advantage is that the staircase signal facilitates direct dynamic investigations of the blade-by-blade tip clearance signal.

Lineariser

The last module in the signal processing chain is the lineariser. The lineariser uses as input the demodulator’s staircase voltage, Figure 7.1. The lineariser converts this staircase signal into a blade tip-to-casing clearance measurement, updated each time a blade passes the probe, with an output in engineering units. The lineariser stores the required calibration data as a look-up table in an EPROM. The lineariser’s outputs are a dynamic staircase signal, and an averaged tip clearance signal, where the staircase signal is averaged over one second to suppress system noise. For both blade-by-blade and averaged outputs, one output volt is equivalent to 1.0 mm of tip clearance.

Speed module

The blade passing signal from one system channel feeds into a speed module, Figure 7.1. This module, with pre-stored information about the number of blades against channel, extracts speed information from the blade passing signal’s frequency. It then generates an output voltage proportional to the gas turbine speed. The speed module provides a once per revolution trigger, which the authors utilised during dynamic tip clearance data analysis.

System performance and specification

We can describe the system’s performance by considering its resolution and signal-to-noise ratio. Measurement uncertainty depends on calibration and installation effects which we discuss later in this chapter.

System resolution

The demodulator’s performance ultimately limits the system resolution. The minimum shift in frequency which the demodulator is able to detect is 50 Hz. The oscillator has a sensitivity of 150 kHz/pF. Therefore, the minimum detectable change in capacitance is 0.0003 pF. This is equivalent to a resolution of 0.01 mm at a 1.0 mm nominal clearance.

System signal-to-noise ratio

The staircase module picks the voltage between pulse peak and trough, and therefore is susceptible to noise. The major origin of noise within the capacitive clearance measurement system is in the demodulator. The demodulator's VCO control voltage hunts around the point at which the VCO and the external probe oscillator frequencies match. This hunting typically manifests itself in the form of 250 mV of noise superimposed on the peak-to-peak blade passing output voltage.

A typical output best illustrates the system signal-to-noise ratio (see Figure 7.3). The system noise is a function of the demodulator's amplification factor. The noise level relates to a signal height for a defined condition: a probe over 1.0 mm thick blades with a 5 mm diameter probe tip with a 0.2 mm clearance gives approximately a 6 V signal output. The signal-to-noise ratio is, therefore, typically 25.

A second noise source is the cross-talk between channels in a multichannel installation. During measurement system development the authors recognised the potentially negative consequences of system cross-talk. The authors therefore ensured that they avoided earth-loops and that they shielded and grounded system components. System tests have shown that the influence of cross-talk has no measurable effect on the system's uncertainty, and, therefore, the authors did not further consider system cross-talk.

To reduce the influence of noise, the authors averaged the staircase signal in the lineariser over one second and generated an output signal proportional to average clearance over all blades around a rotor. A small amount of noise manifests itself as an offset of approximately 30 mV on the averaged staircase signal. Due to the randomness of the noise, this offset is not constant and may fluctuate ± 10 mV over 30 mV.

System specification

Table 7.1 summarises the clearance measurement system specification. In Table 7.1 the minimum and the maximum blade-tip velocities define the minimum and the maximum gas turbine rotational speeds, respectively below or above which the system will not generate an output voltage. The velocities are valid for a 5.0 mm diameter probe and a blade thickness of 1.0 mm. The oscillator sensitivity describes the shift in oscillator frequency for a change in probe to blade tip capacitance of 1 pF. The demodulator sensitivity describes the change in staircase signal output voltage

Table 7.1. *Capacitive clearance measurement system specification.*

Operating frequency	5 MHz
Minimum blade passing velocity	1 m/s
Maximum blade passing velocity	500 m/s
Oscillator sensitivity	150 kHz per pF
Demodulator sensitivity	200 mV per kHz
Measurement range	2.5 mm typical
System resolution	0.01 mm
Signal to noise ratio	25 typically

for a 1 kHz frequency shift. The measurement range is typically 2.5 mm for a 5.0 mm probe and a blade thickness of 1.0 mm. A thicker blade or a larger probe will lead to a larger measurement range.

CALIBRATION AND SYSTEM UNCERTAINTY

Measurement system performance is limited by uncertainties that occur with its calibration procedure. Manufacturing tolerances that occur with differences between the actual gas turbine blade and casing geometry during system calibration also place a limit on the accuracy with which the system can measure blade tip-to-casing clearance.

Calibration procedure

Due to the variations in probe and oscillator electrical properties, it is necessary to calibrate probes and oscillators as a pair. Each probe and oscillator pair results in a unique relationship between system output voltage and blade tip-to-casing clearance. It is impractical in larger gas turbines to calibrate the probes directly over the actual rotor with which they will run. To overcome the impracticality of using the gas turbine itself, the authors used a calibration rig which Chivers (1989a) first developed, Figure 7.4. The authors produced calibration disks that replicated the blade-tip geometry for a specific gas turbine compressor or turbine stage.



FIGURE 7.4. Capacitance probe calibration rig, originally developed by Chivers (1989a).

To calibrate a probe and oscillator pair, the authors mounted the probe in a gas turbine casing replica, Figure 7.5. The casing replica is an aluminum block approximately 50 mm by 25 mm within which the probe itself is recessed. The authors could adjust the probe's position relative to the casing replica and in so doing set the probe's recess to match that of the recess in the actual gas turbine casing.

During the calibration process, the authors logged system output voltages for a set of known distances between a blade and the casing replica. In practice, due to the blades' manufacturing tolerances, the calibration disks will not represent the actual blade geometry exactly. To minimise the uncertainty introduced due to the difference between blade and calibration disc geometry, the authors corrected the calibration data using the blades' exact geometry with which they ran the probes. We can characterise the corrected calibration data using a least-squares curve fitting routine to calculate the polynomial's coefficients, Figure 7.6. This calibration curve downloads into the lineariser.



FIGURE 7.5. Capacitance probe mounted in the calibration rig. The capacitance probe is mounted on a traverse mechanism (right) with a reproduction of the gas turbine casing around the probe tip at the equivalent of 3 o'clock over the calibration disc blades.

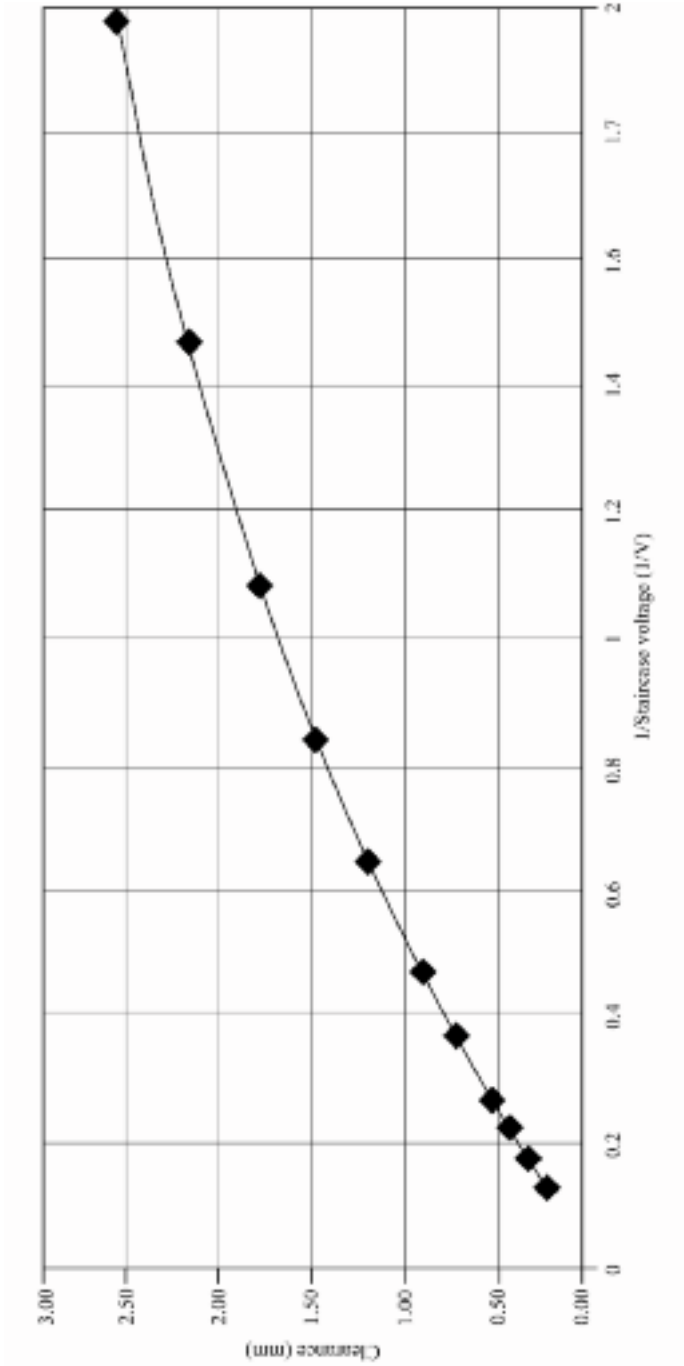


FIGURE 7.6. Typical calibration curve for a capacitive clearance measurement system probe and oscillator pair.

Uncertainty analysis

We can classify most of the uncertainties that occur with the capacitive clearance measurement system into three broad categories. The first originates within the measurement system itself (system uncertainty). The second category originates within the calibration. The third includes all effects related to the system's installation and operation. Table 7.2 quantifies uncertainty of those sources which are present in practice.

System uncertainty

To determine the measurement system uncertainty, the authors programmed the lineariser with a 1:1 calibration curve. The uncertainty is related to the system's staircase output voltage. System noise and cross talk each have a potentially major influence on system uncertainty. Minor uncertainties occur with the thermal stability of system electronic components. The uncertainty due to the analogue to digital and digital to analogue conversion within the lineariser is 10 mV. The analogue to digital card that the authors used in the data logging system had an uncertainty of 4 mV.

Table 7.2. *Capacitive clearance measurement system uncertainty analysis.*

System uncertainty	Uncertainty
System noise / cross talk	10 mV
Oscillator temperature coefficient	1.0 % of reading
Demodulator temperature coefficient	0.5% of reading
Lineariser uncertainty	10 mV
Data logger analogue to digital card uncertainty	4 mV
Root sum squared uncertainty typical at 1 mm clearance	< 0.02 mm
Calibration uncertainty	
Zero position uncertainty	0.005 mm
Clearance measurement uncertainty	0.005 mm
Data logger analogue to digital card uncertainty	4 mV
Curve fit uncertainty	0.010 mm
Influence of blade thickness variation	0.020 mm
Calibration of demodulator	0.005 mm
Root sum squared uncertainty typical at 1 mm clearance	< 0.03 mm
Installation and operation uncertainty	
Set back measurement uncertainty	0.020 mm
Uncertainty of probe head length measurement	0.020 mm
Uncertainty of installation of the probe head	0.020 mm
Thermal gas effects	1% of reading
Root sum squared uncertainty typical at 1 mm clearance	< 0.04 mm
Total root sum squared uncertainty typical at 1 mm clearance	< +/- 0.06 mm

Calibration uncertainty

The primary uncertainty in the calibration process is the deviation between the real gas turbine blade geometry and the calibration disk geometry. Correcting the calibration data minimised this uncertainty. The authors calibrated the demodulator separately and therefore had to consider the demodulator as a separate source of uncertainty. The probe's zero position is adjustable to an uncertainty of 0.005 mm. The authors measured the clearance relative to this zero position with an uncertainty of 0.005 mm.

Installation and operation uncertainty

Measurement of the probe recess in the gas turbine casing is the primary installation uncertainty. The authors found that this uncertainty can dominate the overall uncertainty. By introducing standard procedures within the gas turbine build process, the authors reduced this uncertainty to a minimum of 0.02 mm. It was a realisation of the potential for error when measuring probe recess in the gas turbine casing that inspired Sheard *et al.*'s (1999) research. Sheard *et al.* (1999) developed a direct current capacitive clearance measurement system that they could use to provide an independent measurement of probe recess during gas turbine assembly.

During the system's operation, changes in the gas composition and changes in gas properties due to thermal effects do introduce uncertainties which Chivers (1989a) characterised and concluded to be less than 1% of the measured capacitance in standard compressor and turbine applications.

SYSTEM INSTALLATION

The authors first installed the capacitive clearance measurement system in stage 4 of the high-pressure compressor (HPC) of a BR710 core gas turbine. The authors compared the data that they obtained from this test with data which they obtained using Sheard and Turner's (1992) electromechanical clearance measurement system.

They then installed and operated the system on two BR710 development gas turbines. They fitted probes to the HPC stages 6, 8 and 10. In each case they fitted four probes with approximately equal distribution around the casing's circumference. Using a similar arrangement, the authors fitted four probes around the casing of the high-pressure turbine second stage. They also fitted four probes to the high-pressure turbine second stage of a second development gas turbine.

Probe

The probe head incorporates a flange against which it sits in the compressor or turbine casing. The authors used a retaining ring and a clamping plate to fix the probe in the casing. The compressor casing incorporated a deep chamfer in the abrasible liner, which prevented the probe tip and casing forming a 'stray' capacitor.

To avoid damage to the probe in the event of a tip rub, the authors recessed probes approximately 0.5 mm (referred to as 'set back') within the casing. They measured the probe set back's exact value during the gas turbine build.

Cable

The probe tip to oscillator mineral-insulated and flexible cables are fragile due to their tri-axial design. The authors took care to avoid damage to the cables during installation and operation. They designed a cable routing scheme to avoid high-temperature and high-vibration locations. The preferred cable was mineral insulated, with the change to flexible cable coming only when flexibility was essential for routing purposes.

The authors optimised each probe's total cable length, resulting in the same overall length for each of the 12 compressor probes. This was to ensure that the cable just reached the oscillator enclosure on the outside of the gas turbine casing. The authors used a similar arrangement to optimise the cable length for the high-pressure turbine.

Oscillator

The authors designed an oscillator enclosure to contain 20 single oscillator modules. They mounted the oscillator enclosure on the outside of the gas turbine bypass duct, adjacent to the probe cables' exit port from the casing.

Ground station

All signal conditioning electronics were located in a cabinet, which the authors referred to as a 'ground station'. The ground station contained five electronic racks, Figure 7.7, with each rack containing the necessary electronics for four channels. In this way, the authors configured each rack for use with the four probes for a single stage.

The authors made the link between demodulators within the ground station and gas turbine-mounted oscillators using 50 ohm co-axial cables. These cables were test bed cables that were a permanent fixture of the test bed. An important system feature was its ability to utilise existing test bed wiring, with no special additional cables.

Data logging

The capacitive clearance measurement system's primary output is the lineariser mean output (time-averaged blade tip-to-casing clearance). This output gives average blade tip-to-casing clearance in engineering units. For the described measurements, the authors used a PC-based stand-alone data acquisition system to log blade tip-to-



FIGURE 7.7. A 20-channel capacitive clearance measurement system ground station.

casing clearance data. The authors scanned data at 1 Hz and stored it in an ASCII file format. In those instances where they required blade-by-blade tip-to-casing data, they recorded the system staircase output onto high-bandwidth magnetic tape.

OPERATING EXPERIENCE

The reported results from three gas turbine tests summarise experience with the system. On the first vehicle, a core gas turbine, the authors evaluated a two-channel system by comparing the blade tip-to-casing clearance data with that from Sheard and Turner's (1992) electromechanical clearance measurement system. On the second vehicle, a development gas turbine, the authors gained extensive experience with a 12-channel system on the high-pressure compressor and a four-channel system on the high-pressure turbine's second stage. On the third vehicle, a second development gas turbine, the authors made measurements with a four-channel system installed on the high-pressure turbine's second stage.

System evaluation on a core gas turbine

The authors evaluated a two-channel system on a BR710 core gas turbine. They fitted the probes to stage 4 of the high-pressure compressor. They simultaneously measured the blade tip-to-casing clearance with Sheard and Turner's (1992) electro-mechanical clearance measurement system which they fitted adjacent to the capacitance probes.

Figure 7.8 presents blade tip-to-casing clearance data which the authors obtained using the capacitive and electromechanical clearance measurement systems during a typical test run. Note that there is an important difference between the measurement principles of the two systems. The electromechanical clearance measurement system makes a measurement of clearance between the longest blade and the casing and, thus, measures the minimum clearance during each rotor revolution. In contrast, the capacitive clearance measurement system measures a time-averaged blade tip-to-casing clearance, which stores the blade tip-to-casing clearance for each blade, and it averages the stored data on a rolling basis over one second.

Figure 7.8 shows that at low speeds, the two systems measure nearly the same clearance. At idle and high speed, both measurements show the same trend. This gave confidence in the capacitive clearance measurement system's functional reliability. We can interpret the nearly constant deviation as rotor eccentricity, which the electromechanical clearance measurement system does not resolve. The capacitive clearance measurement system accounts for any rotor eccentricity during the averaging process, resulting in a larger average measure of blade tip-to-casing clearance compared to the electromechanical clearance measurement systems measurement of minimum blade tip-to-casing clearance. The authors also observed a similar phenomenon during gas turbine testing.

Measurement experience on development gas turbines

The core test results gave the authors confidence in the capacitive clearance measurement system's operational reliability. The authors therefore moved on and installed a 16-channel system in a development BR700 gas turbine. On this gas turbine, the authors configured stages 6, 8 and 10 of the high-pressure compressor each with four capacitance probes.

The authors also installed a set of four probes around the circumference of stage 2 of this gas turbine's high-pressure turbine, Figure 7.9. However, the data that the authors obtained from the high-pressure turbine probes were not reliable. The authors suspected, but were unable to prove conclusively, that there was a manufacturing error in the novel side-entry capacitance probes that they used in the stage 2 high-pressure turbine. The authors modified the manufacturing process that they utilised in the production of the turbine probes, and fitted new probes to a second development gas turbine. Once again the authors fitted four probes to the stage 2 high-pressure turbine where they went on to produce useful data. In the following analysis the authors combined the four individual blade tip-to-casing clearance measurements around the circumference into an arithmetic mean blade tip-to-casing clearance for

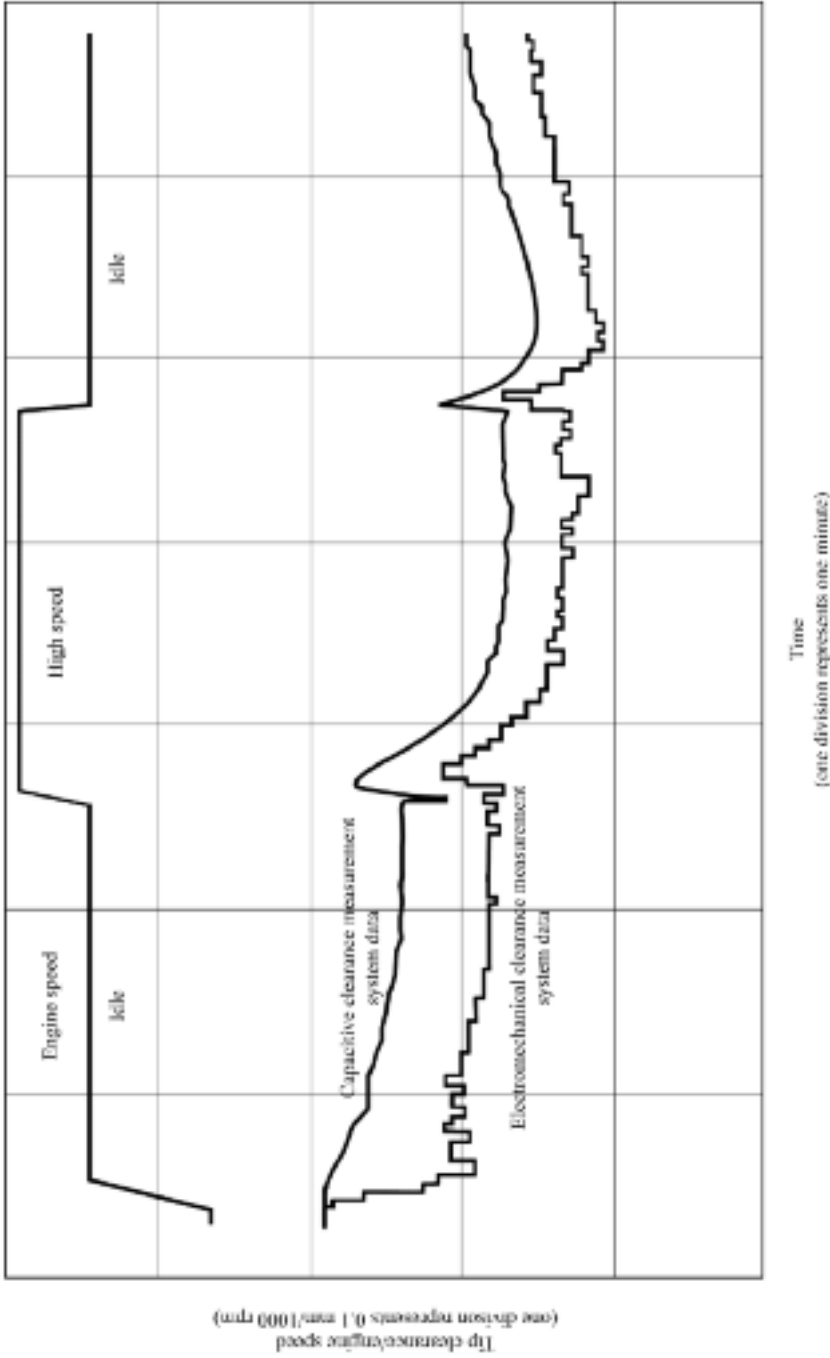


FIGURE 7.8. Blade tip-to-casing clearance data from Sheard and Turner's (1992) electromechanical clearance measurement system and a capacitive clearance measurement system.

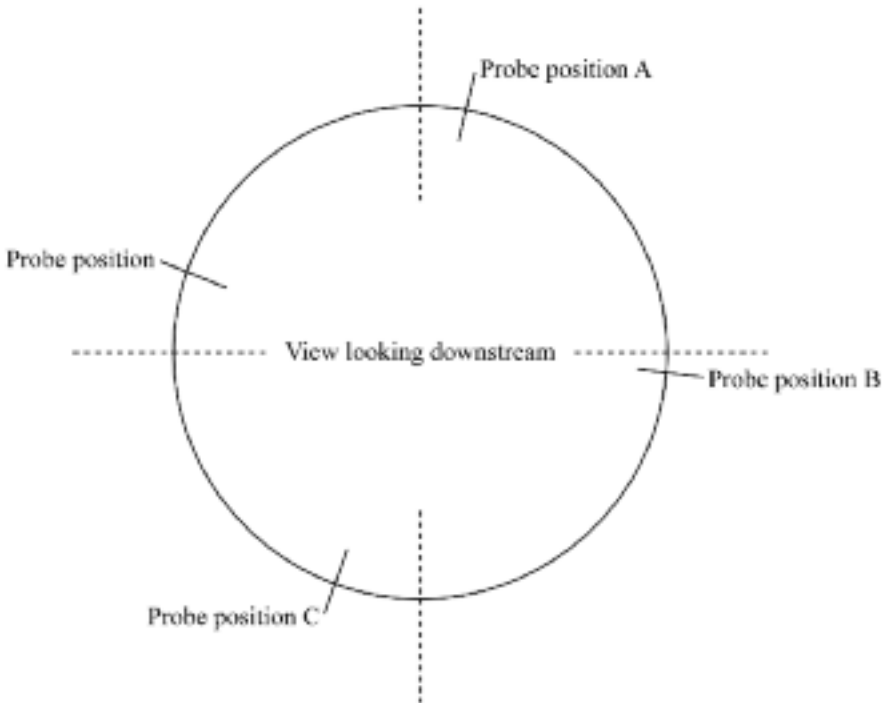


FIGURE 7.9. Typical circumferential probe positions around compressor stage 6, 8 and 10 plus high-pressure turbine stage 2.

each stage, referred to as ‘mean tip clearance’. The following sections describe specific tests and results.

Gas turbine cranks

The first tests with a newly built gas turbine are cranks under cold conditions. During the cranks, the authors measured blade tip-to-casing clearance and compared it to the cold build clearance (CBC) which they measured during gas turbine build. Ideally, the crank blade tip-to-casing clearance and the CBC should match exactly. Table 7.3 shows the deviation between crank blade tip-to-casing clearance and CBC. These initial measurements showed that the installed system’s uncertainty is within 5% of the total distance between probe and blade tip. This is within the uncertainty of the measurement.

Running in procedure

The gas turbine running in procedure incorporates a planned blade-tip rub, resulting in a defined ‘running clearance’. The manoeuvre that the authors performed to create a tip rub involves gas turbine stabilisation at its maximum thrust condition,

Table 7.3. Comparison between gas turbine crank clearance and cold build clearance.

Stage	Deviation between gas turbine crank clearance and cold build clearance
6	4%
8	4%
10	5%
Turbine, Rotor 2	3%

followed by a fast deceleration to idle and re-stabilise for a few seconds, followed by a rapid acceleration back to the maximum thrust condition. Figure 7.10 shows the corresponding gas turbine speed curve. The authors logged tip clearance throughout the manoeuvre. Figure 7.10 illustrates that for both the probes at location D on stages 8 and 10, the recorded blade tip-to-casing clearance went slightly negative, indicating a tip rub at these positions. An inspection of the gas turbine parts following a tear-down after the authors completed the test programme confirmed this. The authors found that the measured tip rub depth and that from the parts-inspection report were within the uncertainty of the measurements.

A comparison of the measured blade tip-to-casing clearance at the thermally stabilised condition before and after the tip rub, Figure 7.10, indicates an increase in the blade tip-to-casing clearance at both stages 8 and stage 10. We can relate this increase to a blade-tip rub during which the tips suffer wear, but it does not affect the abradable liner to the same extent.

Performance curve

The authors undertook a test programme to characterise the gas turbine performance. They increased the gas turbine speed in steps from idle condition to maximum take-off condition. Figure 7.11 presents the mean blade tip-to-casing clearance data.

The data in Figure 7.11 are typical of those logged, and provide insight into the physical effects that influence change in blade tip-to-casing clearance. For gas turbine acceleration, the blade tip-to-casing clearance first reduces due to centrifugal load. The light casing heats more quickly than the heavy rotor, resulting in the blade tip-to-casing clearance increasing, and then slowly reducing as the rotor heats up. The above observations are self consistent with those which Chivers (1989b) made. We can explain the difference in the trend for stage 6 by the difference of casing and rotor material combination for stage 6. An analytical thermal model predicted the behaviour of the individual stages.

Figure 7.12 presents the blade tip-to-casing clearance that the probes measured on stage 6. The four probes around stage 6 all show the same trends in clearance; however, it is clear that the blade tip-to-casing clearance characteristics at the four circumferential locations are different. Figure 7.13 presents a clearer representation of the data, where the difference between the mean blade tip-to-casing clearance and clearance at each circumferential location is plotted. The difference is set to zero for a thermally stabilised idle condition.

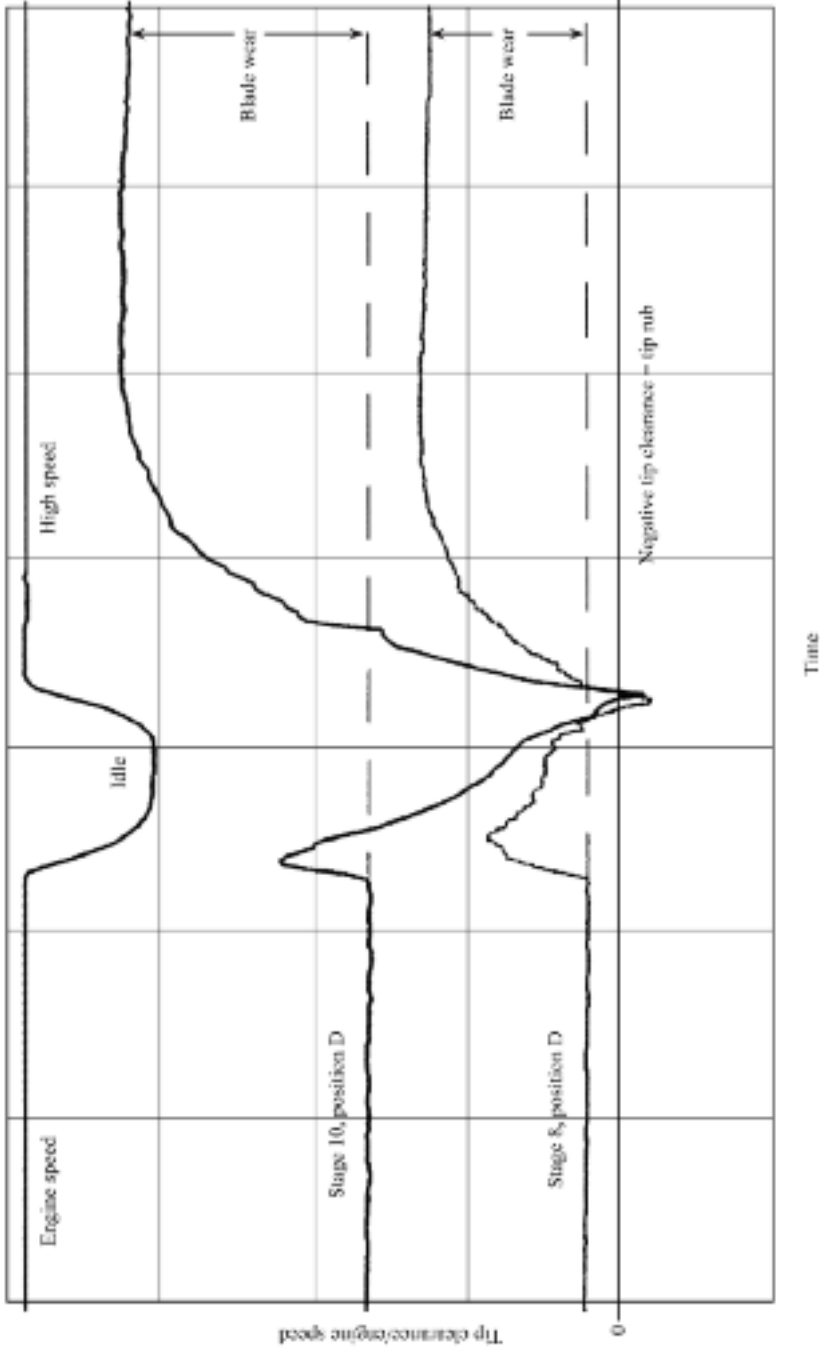


FIGURE 7.10. Capacitive clearance measurement system compressor tip-rub data acquired during the gas turbine running-in procedure.

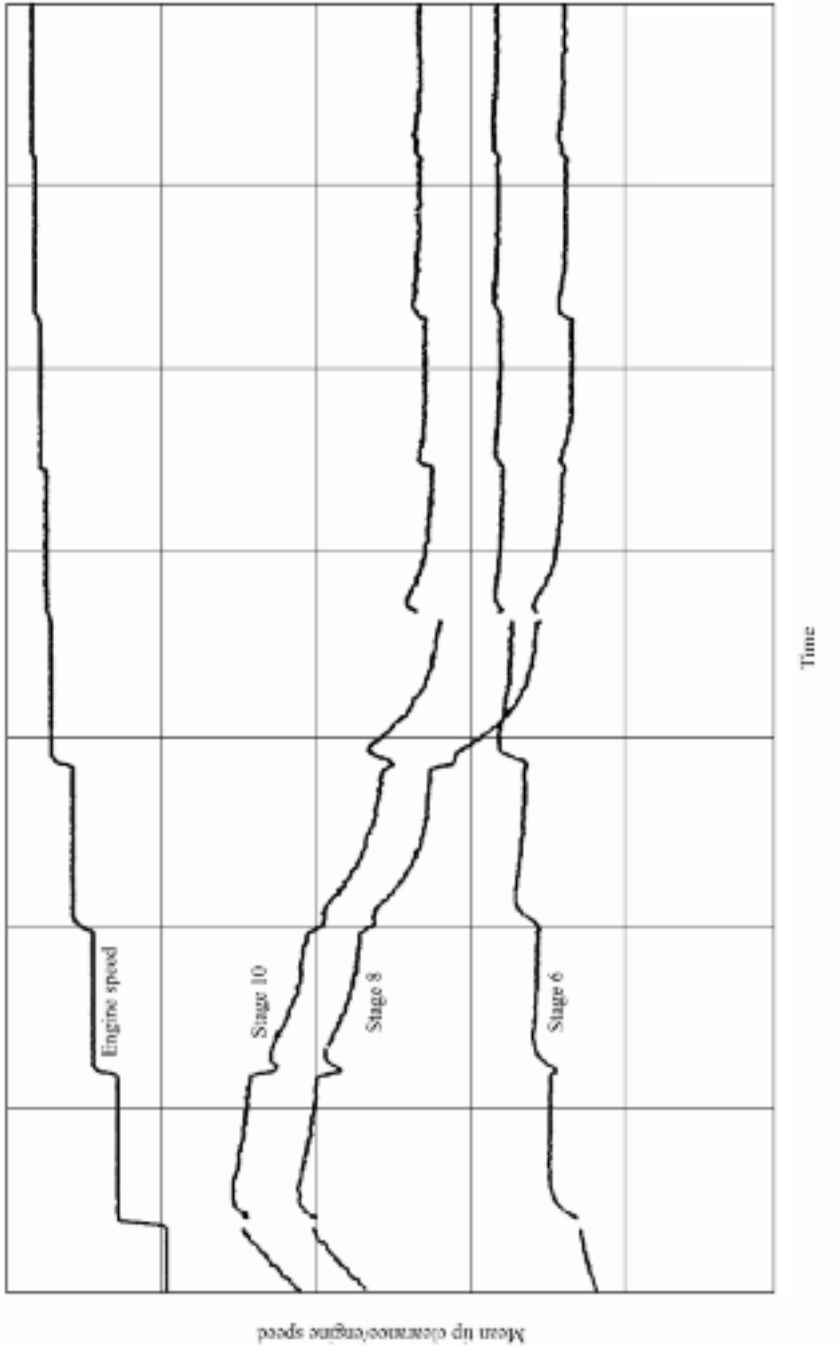


FIGURE 7.11. Capacitive clearance measurement system mean compressor blade tip-to-casing clearance data for a performance curve.

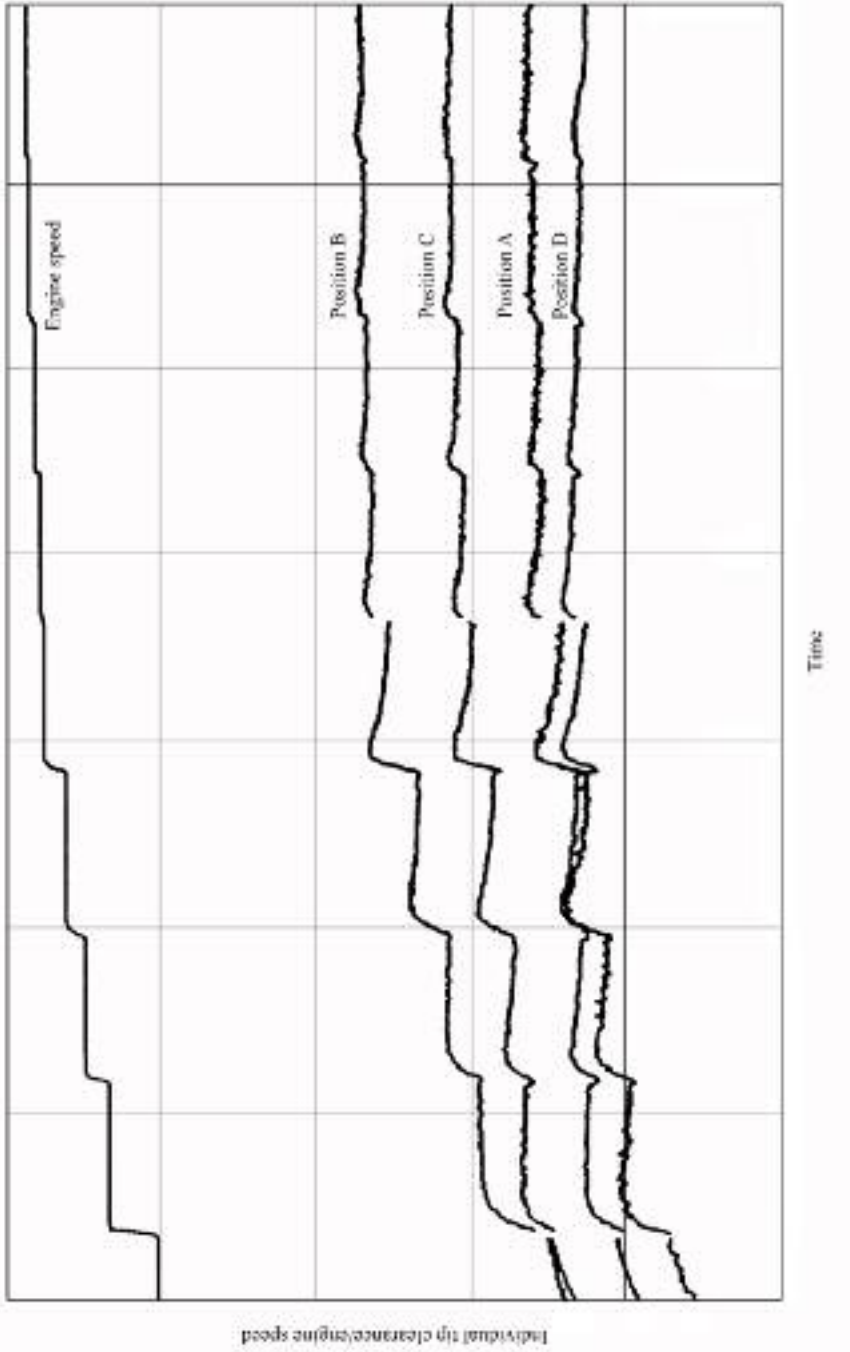


FIGURE 7.12. Individual blade tip-to-casing clearance data from four circumferential positions around compressor stage 6.

Figure 7.13 presents ‘difference’ curves comprising the same blade tip-to-casing clearance data as the authors previously showed, but as a deviation from the mean clearance which they calculated using data from all four probes around the stage. The difference curves diverge with speed. Probes positioned opposite each other give the highest and the lowest difference curves. A study of Figure 7.13 indicates that there was a relative radial shift between the casing and the rotor so that the blade tip-to-casing clearance at position B was the largest, and that at position D was the smallest of the four circumferential positions.

An analytical gas turbine performance model also predicted this effect, and the difference between the prediction and the measurement was within the uncertainty of the measurement. Note that this conclusion also correlates with the tip rub data. The authors observed a tip rub at position D only, where the blade tip-to-casing clearance was the smallest.

Turbine measurement

Figure 7.14 presents an example of blade tip-to-casing clearance data from the second development gas turbine which the authors obtained from stage 2 of the high-pressure turbine during a cold stabilisation test. This test determines the gas turbine’s transient thermal behaviour during a typical take-off manoeuvre. The gas turbine stabilises at idle before a fast acceleration to maximum take-off condition.

Whilst making measurement of blade tip-to-casing clearance using the turbine probes, the authors found that the high temperatures around the turbine at high-speed conditions affect the ceramic materials’ electrical properties within the probe-head. This led to a change in system sensitivity and, therefore, to a deviation between indicated and actual blade tip-to-casing clearance at high speeds. The authors developed a procedure to partially correct for this deviation and Figure 7.14 points to a corrected data point. The turbine capacitance probes utilised the same design as those of Chivers (1989b). Sheard *et al.* (1999) and Sheard and Lawrence (1998) reported the research programme that resulted in a ‘new technology’ probe that overcame the problems which they encountered during the development tests that form the basis of the research that this chapter presents.

Probe durability and long-term uncertainty

The development gas turbine configured with 12 compressor probes ran for approximately 100 hours. During this period the authors carried out intensive testing including several performance curves, cold stabilisation tests and fuel spiking tests. In the early testing phase, one probe failed due to a defective flexible cable. A second probe failed later in the test programme due to a broken conductor in the mineral-insulated cable. All other probes gave reliable data. Post-test inspection showed that the probe-heads were in good condition with no significant signs of mechanical damage.

The authors used the turbine probes over a period of 100 hours of rigorous testing. Post-test inspection of the probes showed no significant mechanical damage. The long-term sensitivity of the turbine probes proved stable. The measured blade

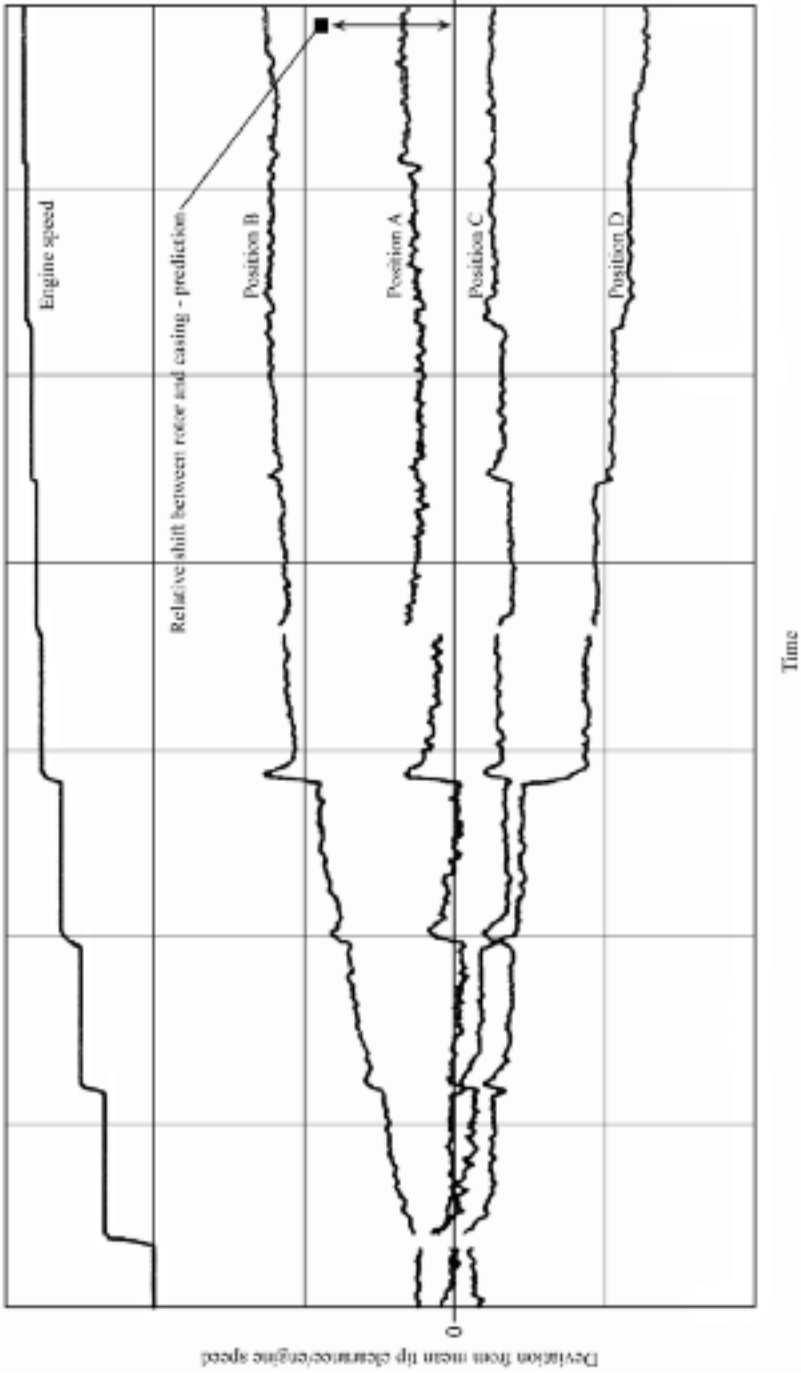


FIGURE 7.13. Deviation from mean blade tip-to-casing clearance for four circumferential probe positions around compressor stage 6.

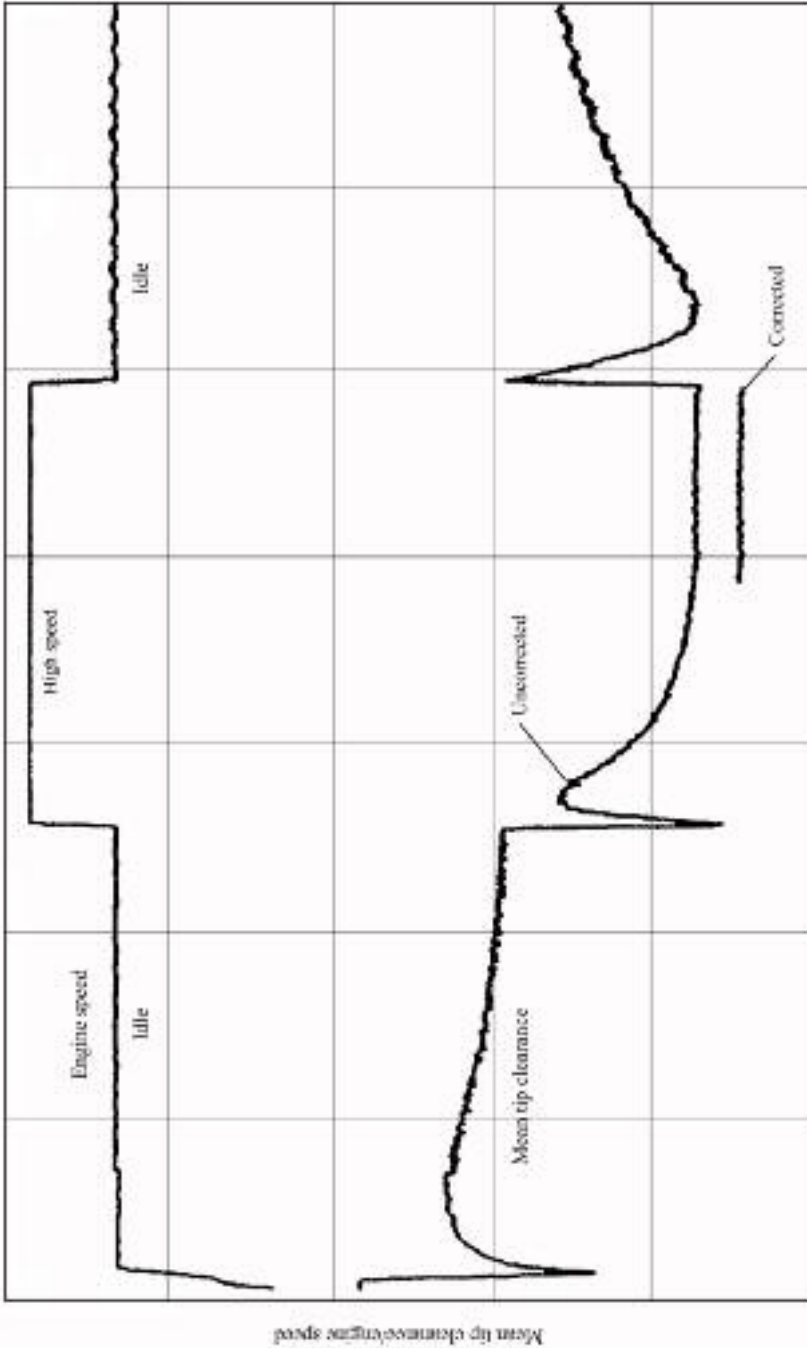


FIGURE 7.14. High-pressure turbine, stage 2 mean blade tip-to-casing clearance measured during a gas turbine cold stabilisation test.

tip-to-casing clearance for a defined gas turbine condition (20% speed, cold gas turbine) was constant throughout the entire test with maximum deviations within the measurement uncertainty.

Dynamic data analysis

The capacitive clearance measurement system incorporates a dynamic output, the staircase signal, which allows the study of rotor-dynamic effects. The authors logged and analysed the staircase signal on tape and monitored it in real time using a digital storage oscilloscope.

To analyse the staircase signal, the authors chose to suppress system noise. They operated a digital oscilloscope in its 'average mode' triggered by the once-per-revolution pulse which the speed module generated. In this mode the oscilloscope keeps a defined number of data sets in the memory and averages them. Since the once-per-revolution pulse triggered the oscilloscope, each dataset contained clearance information for the same number of blades in the same order. Overlaying and averaging the datasets suppressed the noise. Figure 7.15 presents the noise-filtered blade tip-to-casing clearance signals of two compressor probes positioned opposite to each other, locations B and D, recorded over approximately three rotor revolutions.

Figure 7.15 clearly indicates that the blade tip-to-casing clearance is modulated at the first engine order, and that the phase shift between the two signals is approximately 180 degrees. This indicates rotor eccentricity with reference to the casing. The authors found the magnitude of the eccentricity of the same order as that which they observed on the core, and can relate it to analytically predicted effects within the gas turbine's rotor-shaft support structure. Sheard and Killeen (1995) reported a similar effect.

CONCLUSIONS

The authors developed a capacitive frequency modulated driven guard tip clearance measurement system to satisfy the measurement and installation design requirements of a family of gas turbines. The authors successfully used the system to measure the blade tip-to-casing clearance in the gas turbine's compressor and turbine. The development programme has significantly advanced the state-of-the-art in blade tip-to-casing clearance measurement with the inclusion of a long (up to 3 metres) flexible cable and a lineariser to acquire data directly in engineering units. The following summarises the present work.

The capacitive clearance measurement system's uncertainty analysis predicted that one can measure blade tip-to-casing clearance within the gas turbine to an uncertainty better than ± 0.06 mm. Operational experience with the measurement system gave confidence that one can achieve this uncertainty in practice.

The capacitance clearance measurement system measures blade tip-to-casing clearance, consistent with measurements that the authors made with Sheard and Turner's (1992) electromechanical clearance measurement system.

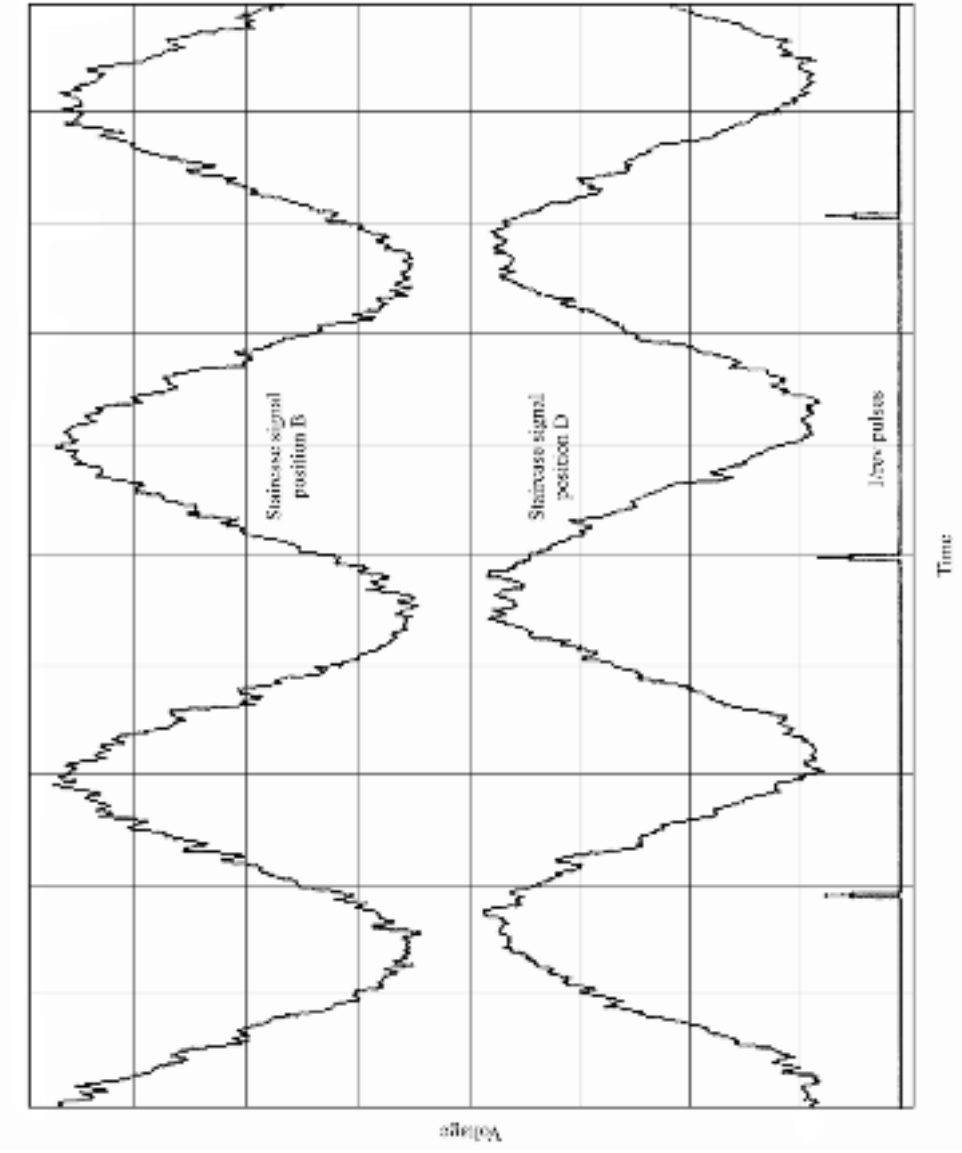


FIGURE 7.15. The capacitive clearance measurement system dynamic output of two circumferentially opposed capacitance probes.

Blade tip-to-casing clearance measurements which the authors took during cold gas turbine cranks matched cold build clearances that the authors measured during gas turbine assembly to within 5% of reading.

The authors identified the tip rub's time and depth using the capacitive clearance measurement system. By inspection following a gas turbine strip, the authors were able to confirm the tip rub's location and depth. The two measurements showed agreement within the capacitive clearance measurement system's uncertainty.

Clearance data from four probes around a stage showed a relative casing displacement with reference to the rotor. This displacement increased with rotor speed. An analytical model also predicted this effect. The difference between the measured and predicted displacement was within the measurement uncertainty.

The dynamic clearance data showed a blade tip-to-casing clearance signal modulation by a first engine order frequency. This modulation related to rotor eccentricity, which an analytical model predicted within the rotor-shaft support structure.

Inspection of both compressor and turbine capacitance probes showed no significant signs of mechanical damage after 100 hours of gas turbine operation.

REFERENCES

- Chivers, J.W.H. (1989a), *A Technique for the Measurement of Blade Tip Clearance in a Gas Turbine*. PhD thesis, University of London.
- Chivers, J.W.H. (1989b), 'A Technique for the Measurement of Blade Tip Clearance in a Gas Turbine'. AIAA Paper No. 89-2916.
- Kappler, G., Moore, R. & Hourmouziadis, J. (1992), 'Hochleistung-Turbo-Fan-Triebwerke ein Familienkonzept'. DGLR Paper No. 92-03-043.
- Killeen, B., Sheard, A.G. & Westerman, G.C. (1991), 'Blade-by-blade Tip-Clearance Measurement in Aero and Industrial Turbomachinery'. *Proceedings of the 37th ISA International Instrumentation Symposium*. San Diego, California, USA, 5–9 May, pp. 429–47.
- Sheard, A.G. (2000), 'Capacitive Gap Measurement Device'. Patent No. GB 2 325 305 B, 19 April.
- Sheard, A.G. & Killeen, B. (1995), 'A Blade-by-blade Tip Clearance Measurement System for Gas Turbine Applications'. *Transactions of the ASME, Journal of Engineering for Gas Turbines & Power*, vol. 117, pp. 326–31.
- Sheard, A.G. & Lawrence, D.C. (1998), 'Gap Measurement Device'. Patent No. US 5,760, 593, 2 June.
- Sheard, A.G. & Turner, S.R. (1992), 'An Electromechanical Measurement System for the Study of Blade Tip-to-casing Running Clearances'. *Proceedings of the 37th American Society of Mechanical Engineers Gas Turbine and Aeroengine Congress*. Cologne, Germany, 1–4 June, Paper No. 92-GT-50.
- Sheard, A.G., O'Donnell, S.G. & Stringfellow, J.F. (1999), 'High Temperature Proximity Measurement in Aero and Industrial Turbomachinery'. *Transactions of the ASME, Journal of Engineering for Gas Turbines & Power*, vol. 121, pp. 167–73.
- Stringfellow, J.F., Wayman, L. & Knox, B. (1997), 'Capacitance Transducer Apparatus and Cables'. Patent No. WO 97/28418, 7 August.

Turbine Tip Clearance Measurement System Evaluation on an Industrial Gas Turbine

S.J. Gill, M.D. Ingallinera and A.G. Sheard

ABSTRACT

The continuing development of industrial gas turbines is resulting in machines of increasing power and efficiency. The need to continue this trend is focusing attention on minimising all loss mechanisms within the gas turbine, including those that occur as a consequence of turbine blade tip-to-casing clearance.

In order to study tip clearance in the turbine, we require real-time measurement of clearance between turbine blades and the casing in which they run. Engineers do not routinely measure turbine blade tip-to-casing clearance in production gas turbines due to the turbine environment's harsh nature. On those occasions when engineers do measure turbine tip clearance, it is typically in development vehicles, often using cooled probes that are unsuitable for use in production applications.

In this chapter, the authors report a programme of work that they undertook with the purpose of identifying a promising turbine tip clearance measurement system that used the capacitive gap measurement technique. The chapter identifies and reports issues surrounding the application of three systems to the turbine section of a GE MS6001FA gas turbine. The chapter analyses the performance of the three evaluated systems.

INTRODUCTION

Rotor blade tip-to-casing clearance has a significant effect on the flow field in a gas turbines' blade tip region (Denton, 1993). Thermal transient effects within a gas turbine combine with centrifugal and vibration effects to make the tip clearance change significantly over the gas turbine's various operating conditions. Typically,

This chapter is a revised and extended version of Gill, S.J., Ingallinera, M.D. & Sheard, A.G. (1997), 'Turbine Tip Clearance Measurement System Evaluation in an Industrial Gas Turbine'. *Proceedings of the 42nd American Society of Mechanical Engineers Gas Turbine and Aeroengine Congress*. Orlando, Florida, USA, 2-5 June, Paper No. 97-GT-466.

gas turbines experience a 'pinch' point during their operating cycle, when a combination of effects at one point in the cycle results in a minimum gap size between blades and the casing within which they run. One possible practice is to set the clearance to zero at the pinch point.

Changes in gap size during an industrial gas turbine's start-up, stabilisation and shutdown cycle can be greater than 2.5 mm. No passive mechanism is currently available to reduce these clearances. The gap size can therefore be relatively large even at the gas turbine's design operating point. Denton and Cumpsty (1987) found large tip clearances to reduce the gas turbine's efficiency. Denton and Johnson (1976) and Bindon (1986), respectively, studied shrouded and unshrouded blades with both showing stage-by-stage efficiency loss as a significant function of the tip clearance.

Sheard and Killeen (1993) showed that the application of cooling air to the shroud of a high-pressure turbine in an aero application can reduce clearance over the blades by 20% at the design point. Sheard and Killeen's (1993) work also indicated that a relatively small reduction in tip clearance at design point can have a dramatic impact on stage performance.

The use of computational design methods over the last 20 years has systematically reduced blade profile and secondary loss mechanisms. Tip clearance losses occur with a physical gap, and therefore are not amenable to reduction using aerodynamic design methods. Dring and Joslyn (1981) considered the consequence of clearance related effects. They concluded that the largest single aerodynamic loss mechanism within the rotating blade row now occurs as a consequence of 'lost' flow over the blade tip.

Müller *et al.* (1997) have presented the results from complex thermal transient models to accurately model the change in tip clearance over a gas turbine cycle. Such models, however, cannot eliminate the purely mechanical issue of different rotor and casing thermal time constants, which lead to the varying clearances. Ideally, development engineers would minimise tip clearances across a gas turbine's full operating range, with particular focus on base load operation. Base load efficiency gains would yield the most significant fuel savings.

The ability to actively control turbine blade tip-to-casing clearance is required to minimise tip clearance over the full operating range. Minimising blade tip-to-casing clearance is not just necessary for base load gas turbines, but also for peaking units going through significant thermal transients on a daily start-stop cycle. One could configure an active clearance control system to deliberately increase turbine blade tip-to-casing clearance during those transients that would otherwise result in the blades making contact with the casing within which they run. At base load when the gas turbine has thermally stabilised, one would use the active clearance control system to reduce clearance, and in so doing maximise turbine efficiency.

The routine and long-term measurement of turbine tip clearance is the first step towards developing an active clearance control system for use in production applications. At the time of writing (1997) no commercially available turbine tip clearance measurement system has fully demonstrated an ability to operate routinely and reliably for extended periods of time in a turbine environment.

The purpose of the evaluation in this chapter was to determine if one could apply capacitance tip clearance measurement techniques in an industrial gas turbine. A secondary objective was to identify potential high-quality blade tip-to-casing clearance measurement system suppliers for future production gas turbine applications.

SYSTEM CONCEPT

GE Power Systems has performed tip clearance measurements in compressor and turbine applications during prototype testing using various clearance measurement systems. Most recently, they used Sheard and Turner's (1992) electromechanical system in a 12-channel configuration.

Although reliable in operation, Sheard and Turner's (1992) electromechanical system proved labour intensive to operate in comparison to other instrumentation. Engineers judged the level of support that the system required as only tolerable during prototype testing. They judged production applications to require a simpler and easier turbine tip clearance monitoring system. Ideally, an industrial gas turbine manufacturer would install and monitor the clearance system in a similar fashion to other standard instrumentation. However, before moving into a production application, engineers at General Electric judged that it was first necessary to demonstrate successful tip clearance measurement system operation during prototype testing on an industrial gas turbine. Only a successful demonstration during a prototype test would provide the confidence to go on and use the tip clearance measurement system to continuously monitor turbine tip clearance in production applications.

Evaluation systems

Burr *et al.* (1994) evaluated various high-temperature gap measurement techniques in a gas turbine environment. They reviewed the available measurement operating principles, including electromechanical, optical, capacitive, eddy current, microwave and fluidic. Burr *et al.* (1994) concluded that the capacitive blade tip-to-casing measurement technique was the most promising for use in the gas turbine's hot sections.

The authors identified three potentially suitable commercially available measurement systems for evaluation, each using a capacitive measurement technique. System 1 used Stringfellow *et al.*'s (1997) frequency modulated, driven guard capacitive measurement system concept. Stringfellow *et al.*'s (1997) measurement system concept constituted a developed form of Chivers' (1989) original. System 2 constituted a commercialised version of Chivers' (1989) original design. System 3 used sensors based on a direct-current capacitive measurement system concept which Foster (1989) described. It augmented Foster's (1989) original system with additional proprietary enhancements to improve system frequency response. Hughes (1995) discussed the frequency modulated and direct-current capacitive clearance measurement system concepts and provides a general review of capacitive gap measurement system operating principles.

Evaluation systems' prior experience

Müller *et al.* (1997) evaluated System 1 and concluded that its performance was satisfactory up to approximately 800°C, above which drift in the probe electrical properties caused the system to stop functioning. Sheard and Lawrence (1997) presented a 'new technology' probe design that addressed the shortcoming in probe design which Müller *et al.* (1997) encountered. Sheard *et al.* (1999) described the new technology probe. The new design performed up to 1100°C with no significant thermal drift.

Rolls-Royce plc has used System 2 in turbine applications as Pavey (1993) describes. The sensors operated for a limited time in a Rolls-Royce military high-pressure turbine demonstrator unit. Engineers ran the probes in a cooled configuration, which eventually caused cracking in the probe ceramic components.

General Electric unsuccessfully applied System 3 on a GE MS6001B turbine test in 1994. Issues with capacitive balance limited the useful data which they collected from the test. The supplier produced solutions intended to address the earlier problems and incorporated them into the new electronic system for the MS6001FA test.

System requirements

From an industrial or flight gas turbine manufacturers' prospective, the ideal turbine tip clearance measurement system would run with uncooled probes. It would also have a range that covers the gas turbine's entire operating envelope. Finally, the ideal system would include high-temperature cable long enough to enable the location of measurement system electronics far enough from the turbine to enable the electronics to operate without cooling, and in so doing eliminate all measurement system cooling requirements. Initially, the authors developed a set of specifications for the systems which they considered aggressive, but achievable. The authors specified shorter cable lengths than ideal, as probe range improved with reduced probe-to-electronics cable length. Table 8.1 provides a summary of the initial requirements and the initial predicted system specifications.

Table 8.1. Vendor provided generic system requirements and system specifications.

	Required	System 1	System 2	System 3
Probe body max. temperature	700°C	800°C *	600°C	1000°C
Cable max. temperature	400°C	600°C	600°C	600°C
Max. range	6.4 mm	4 mm	4 mm	2.5 mm
Total cable length	8 metres	2 metres **	1 metre	2 metres **
Operating life	500 hours			

*Calibration error induced above 600°C.

**Can be provided in longer lengths, but 2 metres chosen to maximise range and facilitate comparison between measurement systems.

The authors designed the probe external envelope to fit within existing turbine hardware, Figure 8.1. Based on the manufacturer's preliminary probe tip diameter-to-range ratio estimates, the authors selected a 9.5 mm probe tip diameter.

The authors decided to evaluate the three different capacitive measurement systems based on their ability to produce an output corresponding to mean turbine tip clearance. The three systems each produce a blade passing output, from which it would be possible to derive clearance over every blade as it passed the probe tip. The authors decided to evaluate the systems' ability to produce a mean turbine tip clearance because this requires minimal signal conditioning and the methods of determining minimum and maximum clearance vary significantly between the three systems. The authors recognised that they would require minimum tip clearance for active clearance control applications. However, the required signal conditioning to produce a minimum tip clearance output from a blade passing signal does not impact the basic system functionality. As the evaluation was focused on basic system functionality, the authors considered a mean turbine tip clearance measurement as acceptable.

TURBINE EVALUATION

It is possible to simulate some of the factors that contribute to the harsh turbine environment. However, laboratory simulations and testing cannot substitute for running instrumentation on an actual test vehicle.

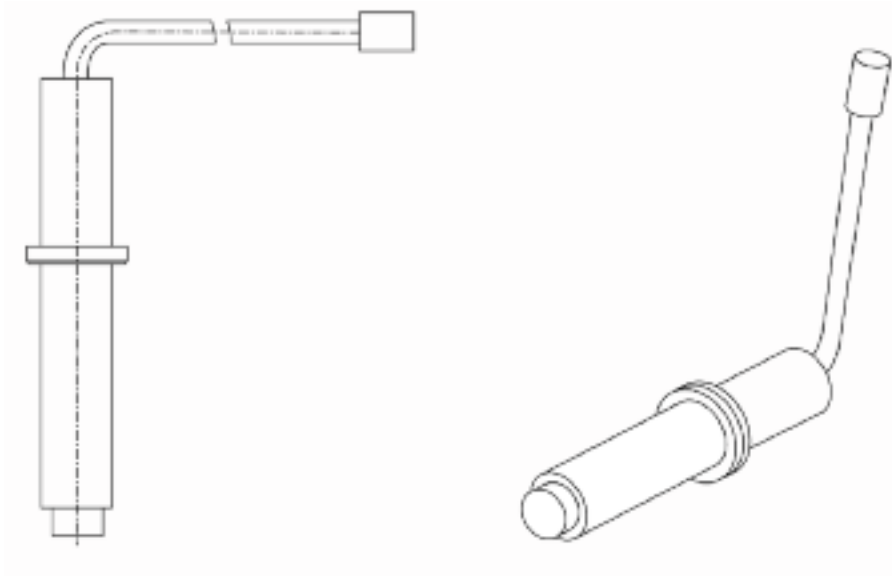


FIGURE 8.1. General Electric MS6001FA stage 1 turbine capacitance probe.

The MS6001FA gas turbine is a 70 MW class industrial gas turbine for both 50 and 60 Hz operation, Figure 8.2. It operates with a rated firing temperature of 1288°C, and an exhaust temperature of 597°C. Ramachandran and Conway (1996) describe the MS6001FA design and background. This MS6001FA is an extension of GE's FA product line that has recently passed 500,000 operating hours. Thus, the authors considered this gas turbine a suitable vehicle for testing a new turbine tip clearance measurement system. For this evaluation, the authors fitted 16 tip clearance probes around the Stage 1 turbine, Figure 8.3. They arranged the probes to facilitate comparisons between the three systems.

MS6001FA installation

Turbine component temperatures within the gas turbine under consideration are proprietary, but we may consider them state-of-the-art. Sheard *et al.* (1999) reported capacitance probe temperatures which were consistent with the MS6001FA capacitance probes' required operating temperature ranges.

The MS6001FA casing and shroud designs which the authors used in this evaluation are typical of F-class industrial gas turbines. The casing contains shroud segments which comprise outer and inner shrouds. The inner shrouds are exposed to the turbine flow around the Stage 1 turbine blades' circumference.

The authors designed the tip clearance probes as an integral component of the shroud, Figure 8.4. They designed the probe tip to fit through a small hole on the inner shroud, with a setback of 0.4–0.5 mm. The authors determined this setback for each probe using a depth micrometre, and included it in the respective calculation of blade tip-to-casing clearance.

The authors spring-loaded each probe into position and used caps to hold them in place, Figure 8.4. This design is based on a successful probe-mounting design for Sheard and Turner's (1992) electromechanical clearance measurement system. The probe installation design is a robust configuration that has a fixed locating point near the probe's tip. It also facilitated shroud assembly by allowing the authors to insert the clearance probe last, after they assembled various shroud components.

Target geometry

The Stage 1 turbine blade is an unshrouded design with a hollow tip to accommodate cooling holes that exit from serpentine cooling passages in the blade. Brandt and Wesorick (1994) describe the GE approach to turbine blade design. The resulting geometry is a 'fence' around the blades tip, Figure 8.5. For reference, Figure 8.5 shows the capacitance probe tip size, cold and hot locations relative to the turbine blade.

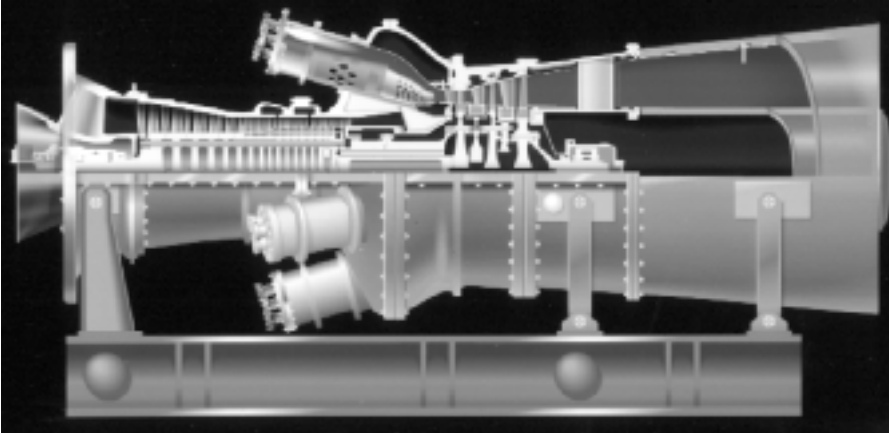


FIGURE 8.2. General Electric MS6001FA gas turbine cross section. Photo courtesy of General Electric Company.

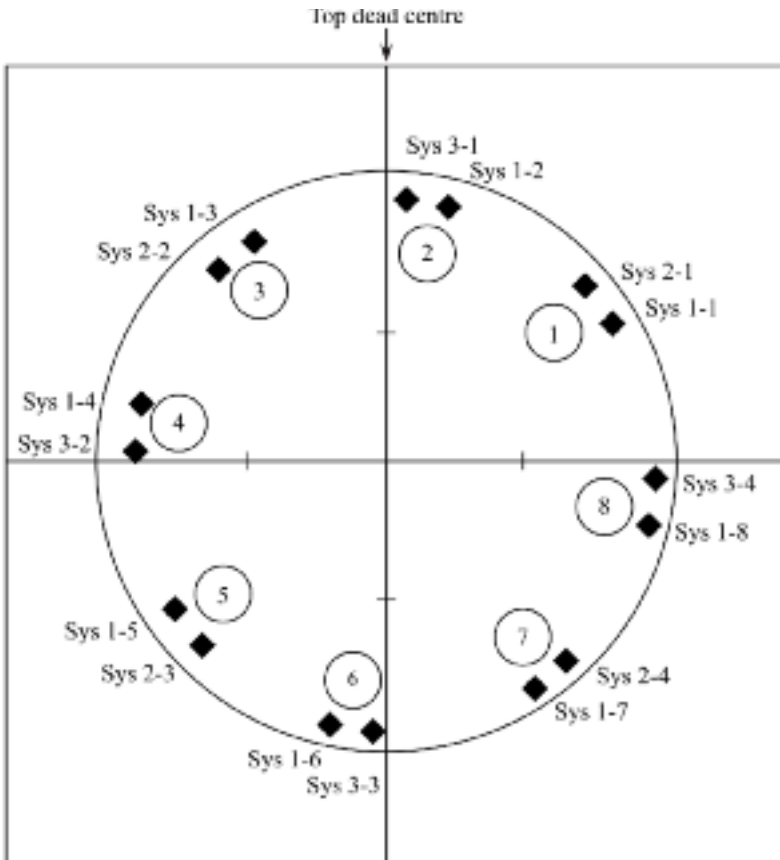


FIGURE 8.3. Schematic of the 16 evaluation probe location around the Stage 1 turbine: view looking downstream.

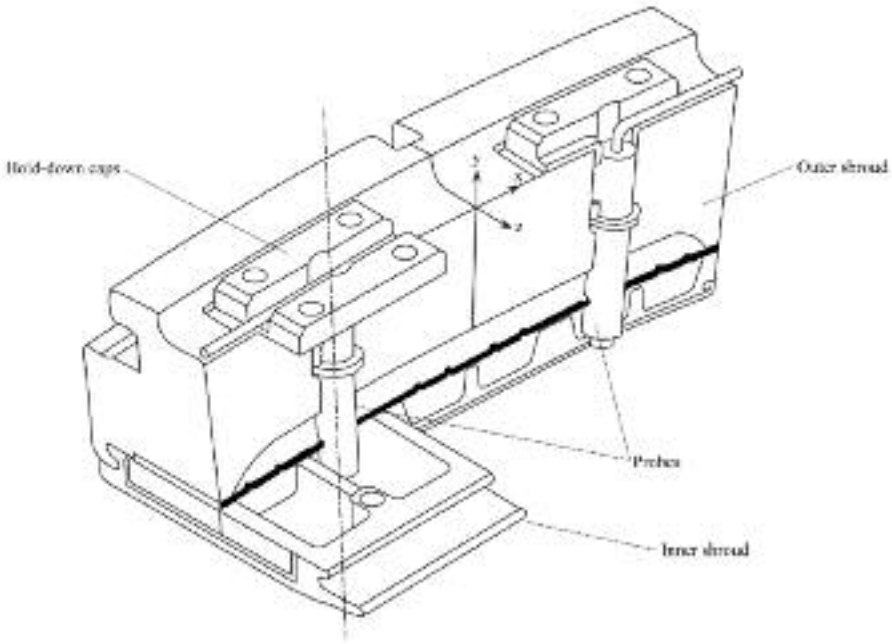


FIGURE 8.4. Isometric view of tip clearance probes in the turbine Stage 1 shroud.

CALIBRATION, INITIAL EVALUATION AND UNCERTAINTY ANALYSIS

The authors performed the System 1 and 2 calibrations in accordance with Müller *et al.*'s (1997) recommendations. They mounted the sensor over a calibration disc, and logged the output at known clearances between the sensor and blades. They designed the calibration disc to replicate the turbine blade tip's geometry. They used system output voltage and known clearance data to generate calibration coefficients that would in turn allow conversion of the non-linear system output voltage into turbine blade tip-to-casing clearance in engineering units.

Ideally, one should always calibrate a sensor over the bladed rotor against which it is to run in service. This eliminates any uncertainty introduced into the system calibration as a consequence of differences between calibration rig geometry and actual gas turbine geometry. However, this is difficult because in practice one would have to make provisions in the gas turbine balance facility for probe mounting. Although possible in theory, calibrating capacitance clearance probes during rotor balancing was not practical. However, the authors were able to measure actual blade tip fence thickness.

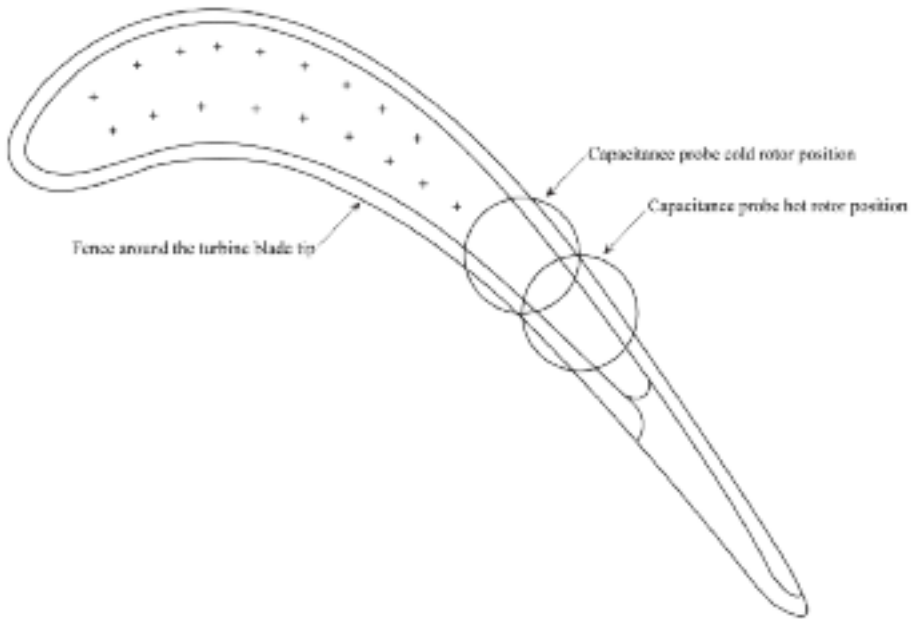


FIGURE 8.5. General Electric MS6001FA Stage 1 turbine blade tip geometry, and position of the capacitance probe used to measure blade tip-to-casing clearance relative to it.

An advantage of System 3 is the ability to calibrate over a non-rotating blade. This allows one to use an actual blade in a static setup fixture instead of the rotating rotor assembly. The ability to make a measurement of clearance to a stationary blade is a feature of direct-current capacitive clearance measurement systems. Recognising the potential usefulness of a static or low-speed measurement of clearance, Sheard *et al.* (1999) developed a direct-current capacitive clearance measurement system that they could use in combination with Sheard and Lawrence's (1998) 'new technology' probes. This facilitated more accurate calibration of capacitive clearance measurement probes when installed in an industrial or aero gas turbine.

Evaluation system calibration

All suppliers calibrated their respective systems independently. Each probe had the same external envelope, so we can attribute calibration curve variations to differences in probe internal design and electronic system performance. The authors produced calibration curves for each probe type giving mean clearance from each system, Figure 8.6. System 3 has an effective range of only 2.5 mm and therefore, the curve stops at that point.

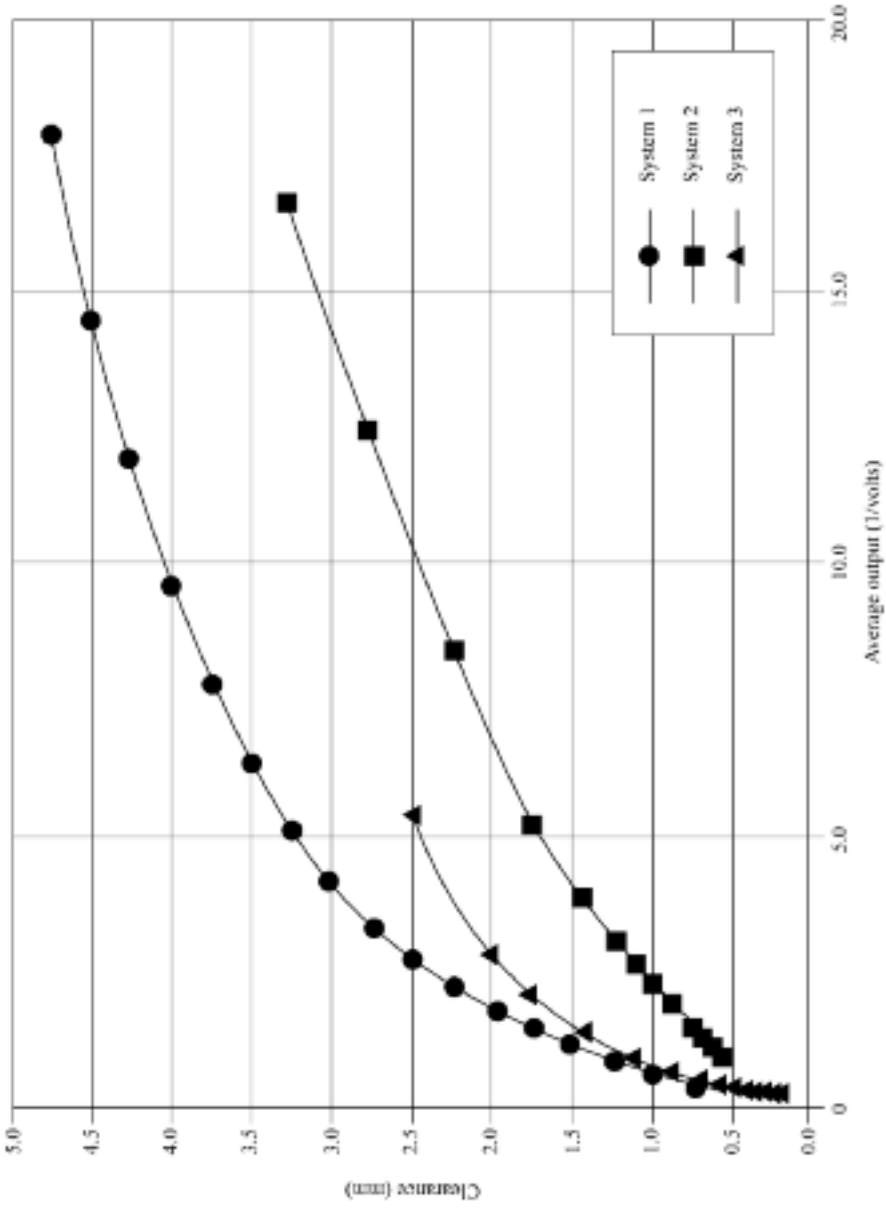


FIGURE 8.6. Calibration curves for average blade tip-to-casing clearance from Systems 1, 2 and 3.

Temperature dependency/limitations

The authors performed calibrations at room temperature and assumed no variation in calibration with change in temperature from ambient to turbine operating temperatures. However, Müller *et al.* (1997) observed that System 1 stopped functioning above 800°C, with temperature-induced calibration error above 600°C. Another temperature-related issue is that System 2 had a specific problem with the MS6001FA probes that resulted in a dramatic increase in system background noise level above 600°C. The manufacturers have since addressed both of these problems. Although System 3 does not have documented experience at turbine temperatures, the rated maximum probe temperature is 1000°C.

The manufacturers of System 2 and System 3 need to address the above temperature effects as Sheard *et al.* (1999) and Sheard and Lawrence (1998) have for System 1. This is an essential requirement for any tip clearance system in a turbine application. Capacitance probes must be able to perform in a turbine application at elevated temperature without suffering temperature induced errors in measured blade tip-to-casing clearance.

Error analysis

Müller *et al.* (1997) discuss uncertainty analysis for capacitive measurement systems. Following Müller *et al.*'s (1997) method, the authors identified eight error sources that contributed to the overall uncertainty of blade tip-to-casing clearance measurement, Table 8.2.

The dominant error source was a variation between the production blade and the calibration disc geometry. The authors based the calibration disc geometry on nominal blade tip fence thickness. They measured the actual fence thickness for a representative GE production gas turbine blade set to determine the manufacturing

Table 8.2. Generic system uncertainty analysis results at 2.5 mm (0.100") clearance.

Uncertainty source (at 2.5 mm)	Uncertainty	Calculated error (at a 2.5 mm range)
Calibration disc vs. actual geometry	3.3%	0.084 mm
Curve fit variation	3.0%	0.076 mm
Cold rotor using hot calibration	2.6%	0.025 mm
Oscillator temperature coefficient	1.0%	0.025 mm
Thermal gas effects	1.0%	0.025 mm
A/D card uncertainty	+/- 2.5 mV	0.025 mm
Demodulator temperature coefficient	0.5%	0.013 mm
Set back measurement		0.013 mm
Total RRS error @ 2.5 mm		0.142 mm

tolerance, Figure 8.7. Fence thickness is not a critical-to-quality characteristic of the blade design, and so GE does not closely control it during the blade manufacturing process. The variation in fence thickness resulted in a 3.3% variation in the blade tip-to-casing clearance measurement. The authors calculated the average blade fence thickness from the measured values for a set of production blades.

The ratio between calibration disc nominal fence thickness and average production blade fence thickness constituted a first order correction factor that the authors were able to use to correct the capacitive clearance measurement system calibration. The corrected calibration better matched the actual geometry, and was accurate enough not to require the manufacturing of calibration discs matched to actual production blade geometry.

A second potentially dominant error source occurred with the difference between the measurement system calibration at the cold and hot rotor position. As the gas turbine thermally stabilises, the rotor's axial position relative to the casing within which it runs shifts from a 'cold' position to a 'hot' position, Figure 8.5. This relative movement is due to the difference in thermal growth between the rotor and casing. This, in turn, changes the blade tip's geometry under the capacitance probe. The authors evaluated the error in hot clearance measurement when applying a cold capacitance clearance measurement system calibration to a capacitance probe in the hot position. The error was less than the authors had anticipated, although the total

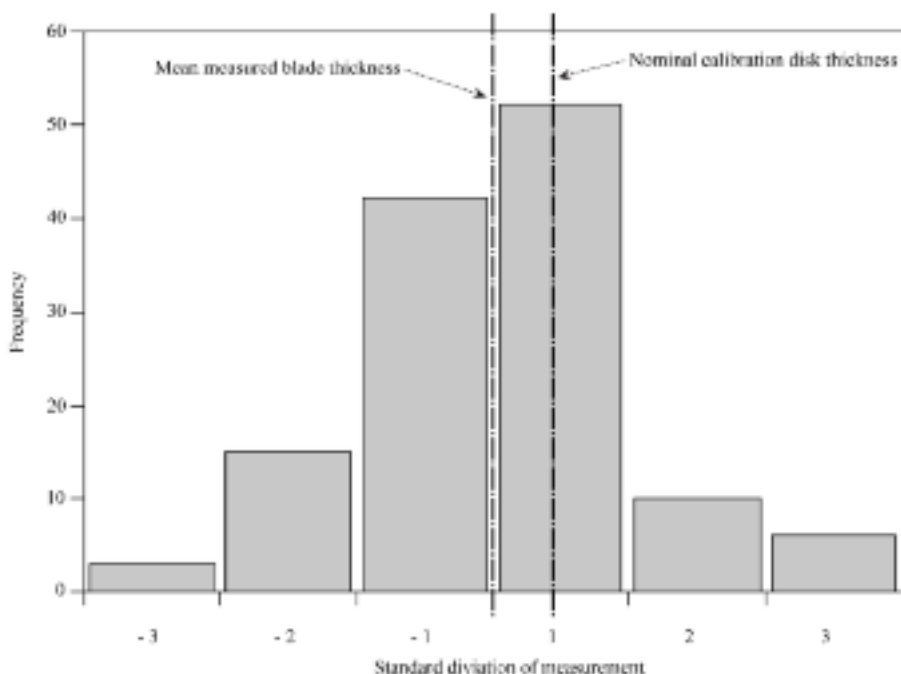


FIGURE 8.7. Histogram of measured blade fence thickness versus the nominal blade fence thickness used to specify the geometry of the capacitive clearance measurement system calibration disc.

blade-to-probe overlap area changed significantly from the cold to hot positions. However, the overlap area that occurred with the blade fences did not. As a consequence of the blade design incorporating tip fences, the capacitance probe's shift from cold to hot position produced a maximum error of 0.07 mm.

OPERATING EXPERIENCE

The authors ran the three measurement systems on the MS6001FA stage 1 turbine, during a full-speed no-load test at the GE facility in Greenville, South Carolina. They mounted all signal conditioning electronics in the test bed control room, Figure 8.8. The authors mounted oscillators for the two frequency modulated systems and 'DSP's' for the direct-current system close to the turbine. This necessitated cooling air to keep the signal conditioning electronics as the ambient temperature reached upwards of 120°C. Systems 2 and 3 included provisions for cooling built into their signal conditioning electronics. The System 1 oscillators had no provision for cooling, and so the authors fitted them into small boxes that could receive cooling air. The authors used filtered shop air for all cooling.

The authors fed the blade passing signal from each measurement system to a set of oscilloscopes. They used the blade passing signals to determine if the probes were functioning, and to qualitatively assess each measurement system's signal-to-noise ratio. The noise level superimposed on the blade passing signal can be indicative of cable vibration, broken cable conductors, overheated oscillators or moisture problems with the probe.

In addition to the blade passing signal, the signal conditioning equipment generated voltages proportional to the average blade tip-to-casing clearance. The authors logged these voltages in two ways: they used a laptop computer running LabVIEW® data acquisition software, and an HP1000 data system. The HP1000 was the test bed data logging system, with post-test analysis of the tip clearance data and comparison with other logged data during the test. The laptop computer was limited to monitoring the average clearance data from the measurement systems under evaluation in combination with a 16-channel PCMCIA data acquisition card. Although limited in its capability, the LabVIEW® application enabled real-time evaluation of the logged data. The authors stored the LabVIEW® data in an ASCII format for transfer to spreadsheet programs and post-test analysis.

Measurement system installed performance

Installation problems with System 3 electronics prevented it from performing during the limited test time on the MS6001FA gas turbine. This reduced the total number of available probes from 16 to 12. Systems 1 and 2 were functional, with blade passing outputs evident up to and beyond the capacitance probes' calibrated range.

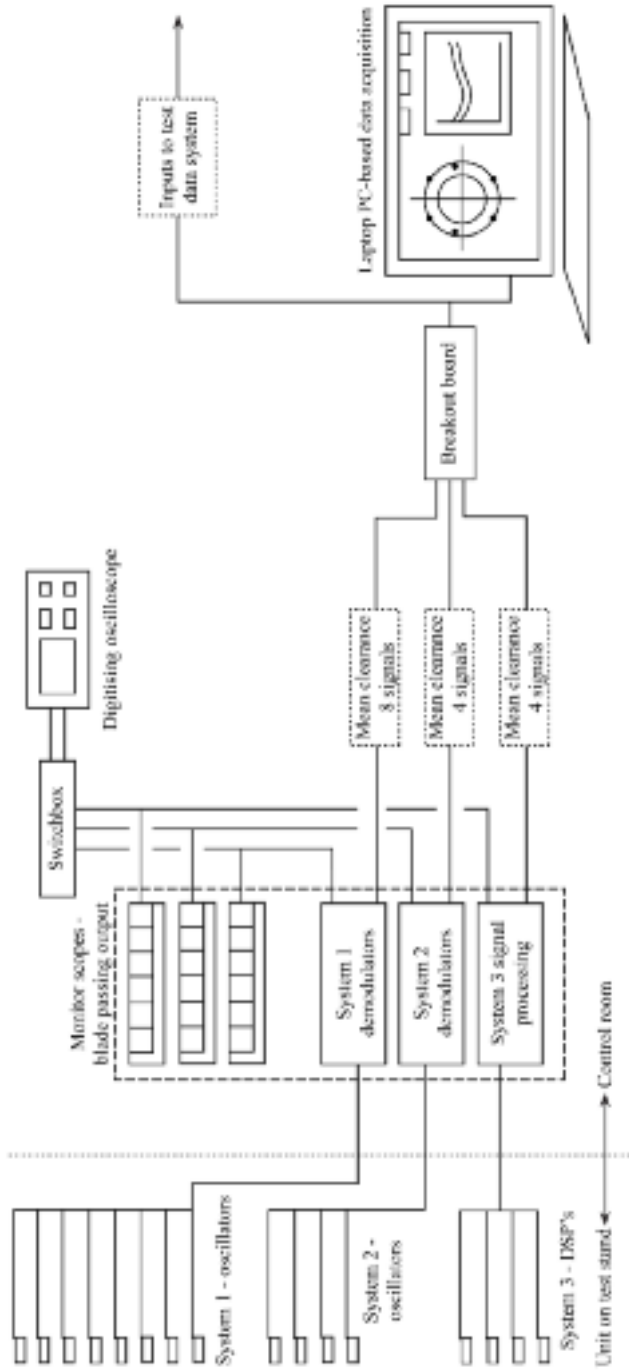


FIGURE 8.8. Configuration of the capacitance probes, electronics, signal conditioning electronics and data acquisition system.

A useful check of a capacitance probe's installation and measurement system calibration accuracy is to use the probe to measure clearance when the gas turbine rotor is 'cold-rolled' at low speed. At a blade passing frequency of approximately 1 kHz System 1 and System 2 measurement system signal conditioning electronics begin to register the presence of blades as they pass the probe. One can then compare these cold-roll clearances to cold-build clearances and make an initial probe installation and calibration accuracy check. The authors were not able to perform a cold-roll check on the MS6001FA installation as the cold clearance was large compared to both measurement systems' range, and so the MS6001FA blades were out of range during the cold-roll. The capacitance probe configuration around the stage 1 turbine shrouds allowed direct comparison between data from System 1 and System 2 during the MS6001FA full-speed no-load test. The authors fitted the System 1 and System 2 probes as pairs approximately 10 degrees apart, making possible a direct comparison of measured blade tip-to-casing clearance.

Test results

The authors monitored System 1 and System 2 outputs as MS6001FA gas turbine testing commenced. Figure 8.9 shows blade passing outputs from Systems 1 and 2 at the full-speed no-load test conditions. As mentioned previously, System 3 was not functioning during the gas turbine test.

Figure 8.10 presents data from start to the full-speed no-load condition for the MS6001FA gas turbine. The two blade tip-to-casing clearance signals are from System 1 and System 2 capacitive clearance measurement systems at location 1, Figure 8.3. The System 1 signal is low-pass filtered at 1 Hz, whilst the System 2 signal filters at 50 Hz, per the manufacturers' recommendations. The data in Figure 8.10 illustrates a correlation between the two systems' output at location 1 that is within the measurement's uncertainty. The agreement between the two system measurements of average blade tip-to-casing clearance gives confidence in the accuracy and consistency of the gas turbine build procedures, and the accuracy of the individual measurement system calibrations.

The trend in average blade tip-to-casing clearance, Figure 8.10, is as the authors expected for an industrial gas turbine. Clearance first decreases as speed increases due to centrifugal loading. The rotor and blades then heat up and expand faster than the casing, resulting in a 'pinch point' at approximately 3:30, Figure 8.10. Clearance then increases slowly as the heavy casing heats and expands away from the rotor.

The effect of a planned over-speed trip on the average blade tip-to-casing clearance at location 7, Figure 8.3, was dramatic, as Figure 8.11 illustrates. As anticipated, the additional centrifugal loading at the higher speed resulted in a decrease in clearance. From this we can compare clearance changes to calculated centrifugal loading to verify the clearance measurement's relative accuracy. As the unit trips, the sudden decrease in centrifugal loading caused average blade tip-to-casing clearance to increase beyond capacitance probe range.

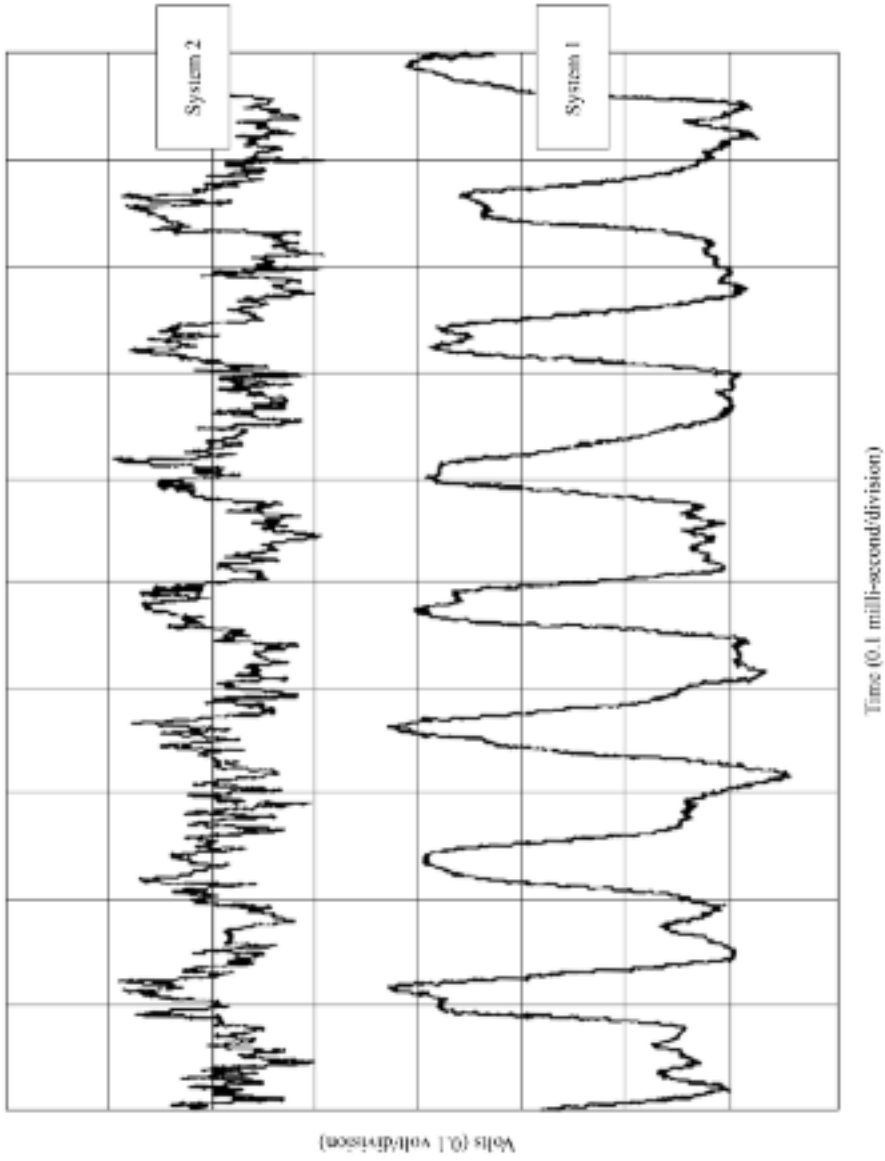


FIGURE 8.9. Blade passing outputs from Systems 1 and 2 at the full-speed no-load conditions.

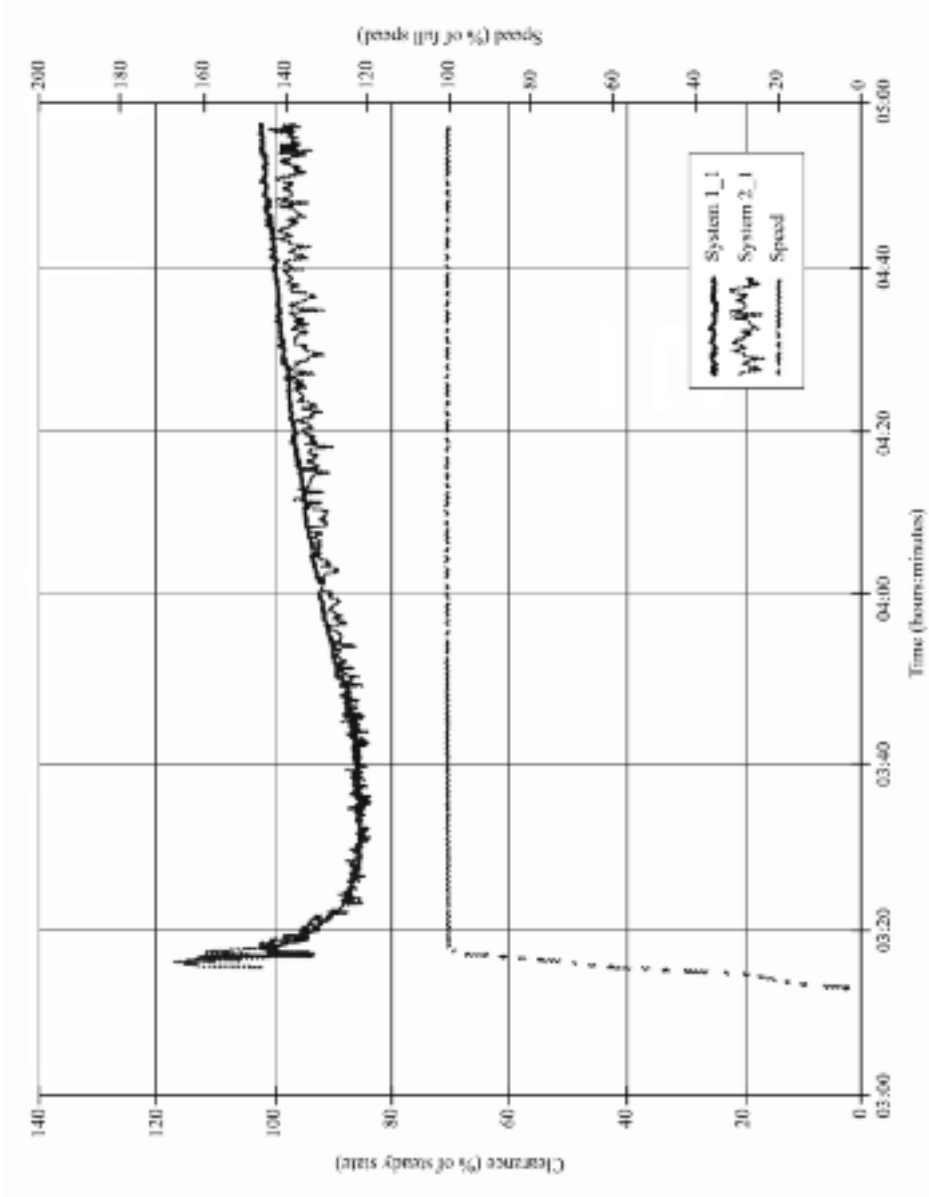


FIGURE 8.10. Plot of blade tip-to-casing clearance and speed versus time for Systems 1 and 2 positioned at location 1 on MS600 IFA Stage 1 turbine.

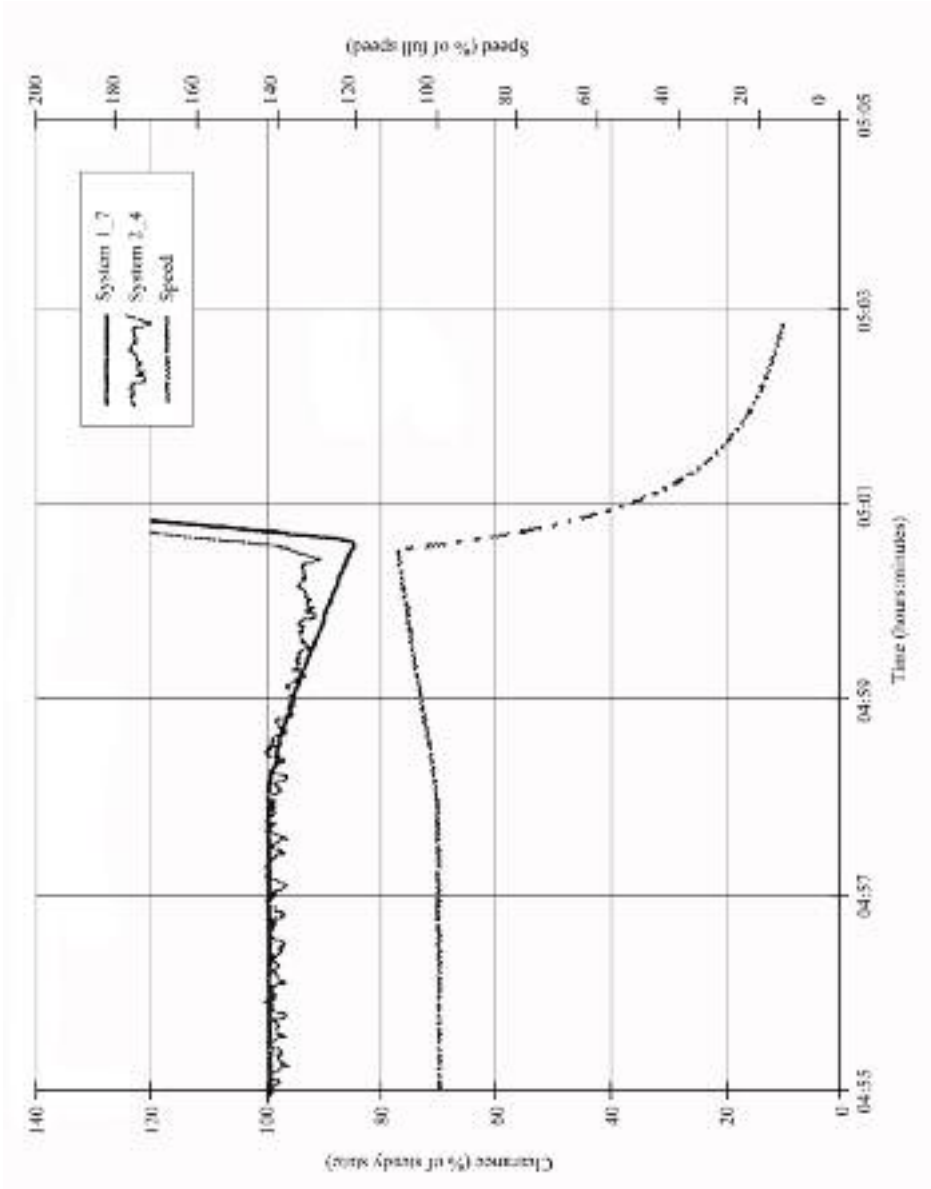


FIGURE 8.11. Average blade tip-to-casing clearance at location 7 on MS6001FA Stage 1 turbines during planned over-speed trip.

Analysing the output from diametrically opposed capacitance probes provides insight into the extent of casing ovalisation. Ramachandran and Conway (1996) discussed the MS6001FA casing design, and how the casing is kept round using thermal masses. These thermal masses are located around the casing and are thermally equivalent to the flanges at the turbine split line, Figure 8.12. The use of thermal masses facilitates a smaller design turbine blade tip-to-casing clearance. When the authors reviewed turbine capacitance probe data, it indicated that the thermal masses were effective in keeping the casing round.

Monitoring and diagnostics of probes and electronics

The authors developed monitoring and diagnostic tools in conjunction with the capacitive clearance measurement system manufacturers. The authors' primary objective was to assess system performance in a turbine application. Consequently, evaluation of signal conditioning techniques was not a priority. The authors recognised the potential value of maximum, minimum and blade-by-blade tip-to-casing clearance measurements; however, they did not focus on signal conditioning in the programme of work which this chapter discusses.

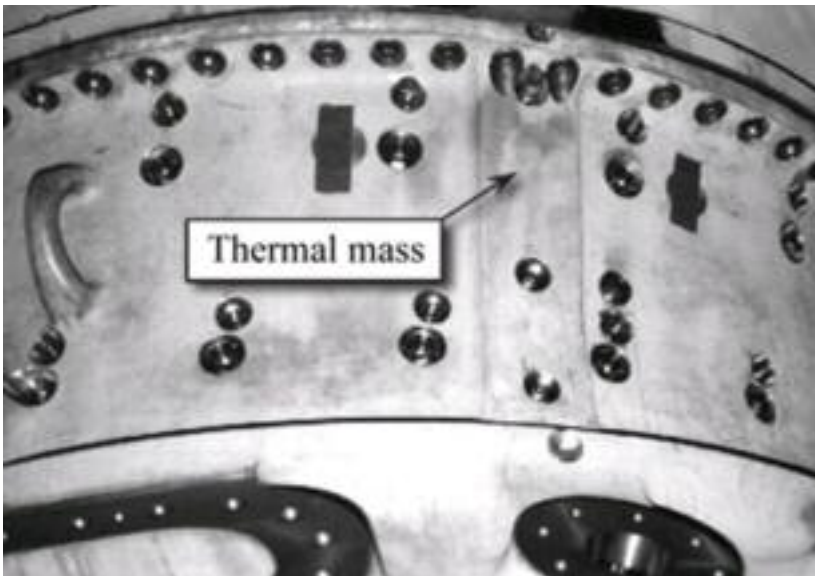


FIGURE 8.12. Typical equivalent 'thermal mass' to flanges at horizontal joint (Ramachandran and Conway, 1996). Photo courtesy of General Electric Company.

At all times during testing, the authors used oscilloscopes to display the blade passing outputs from System 1 and System 2. This enabled a real-time assessment of probe functionality, and changing gas turbine operating conditions. Systems 1 and 2 have a frequency modulated driven guard operating principle. Monitoring the carrier frequency can provide insight into probe and oscillator functionality. For example, the blade passing signal from one of the System 1 capacitance probes appeared inverted. A check of the carrier frequency indicated that it had become unstable. The authors checked the oscillator cooling system and found it had failed, resulting in the oscillators overheating. Restoring the cooling resolved the problem.

Future applications/potential improvements

To use capacitance probes in production applications, the authors considered two improvements which they incorporated into System 1:

1. Improved range using Sheard and Lawrence's (1998) new technology capacitance probes. The overall probe range increased to 75% of the probe diameter, from approximately 40% on the MS6001FA test and;
2. Sheard and Lawrence's (1998) higher temperature capability, new technology capacitance probes. These have a front-face temperature capability of 1100°C, as Sheard *et al.* (1999) documented, which is 300°C higher than the System 1 probes that they fitted to the MS6001FA test and 500°C higher than the System 2 probes.

The authors fitted four System 1 capacitive clearance measurement systems to a GE MS9001EC (9EC) industrial gas turbines that they tested in January 1997. They fitted these with Sheard *et al.*'s (1999) new technology capacitance probes. The MS9001EC (9EC) had a peak capacitance probe electrode temperature above 1200°C. Although the measured data was necessarily confidential, the measurement system operated successfully on the GE MS9001EC (9EC) stage 1 turbine. At the conclusion of the test the authors observed that the test constituted a successful demonstration of the capacitive clearance measurement system's ability to provide a reliable input to a clearance control system. The test therefore constitutes a step towards continuous, long-term blade tip-to-casing clearance monitoring and control in the turbine environment.

Capacitance probes for production turbine applications will be required to function for the full, standard inspection interval of industrial gas turbine hot gas path components. As such, the demonstration of sensor technology that can provide the future clearance control system's closed-loop input does not constitute development of a production clearance control system.

CONCLUSIONS

The authors have successfully applied capacitance probes into the stage 1 turbine of a MS6001FA industrial gas turbine during full-speed no-load testing. They assessed the performance of three manufacturer's capacitive clearance measurement systems on a single stage 1 turbine with successful operation of two out of the three installed systems.

System 1 had the greatest sensitivity and the largest range; however, neither System 1 nor 2 measured clearances during start-up as a consequence of their limited range. System 1 was able to resolve clearance up to 4.75 mm and System 2 was able to resolve clearance up to 3.25 mm. The authors determined measurement uncertainty at a nominal clearance of 2.5 mm as 0.14 mm. System 3 did not perform during gas turbine testing due to electronics problems.

Successful application of Sheard *et al.*'s (1999) new technology capacitance probes on the MS9001EC (9EC) stage 1 turbine opens up the possibility that the System 1 capacitive clearance measurement system technology will go on to form part of a future closed-loop clearance control system. A closed-loop clearance control system offers the possibility to minimise blade tip-to-casing clearance in future generations of industrial gas turbines, and contribute to their efficiency.

REFERENCES

- Bindon, J.P. (1986), 'Visualization of Axial Turbine Tip Clearance Flow Using a Linear Cascade'. Cambridge University Engineering Department Report CUED/a-Turbo/TR 122.
- Brandt, D.E. & Wesorick, R.R. (1994), 'GE Gas Turbine Design Philosophy'. *GER3434D, 38th GE Turbine State-of-the-Art Technology Seminar*.
- Burr, R. (1994), 'Sensor Comparison'. *Proceedings of the 1st P&W International Clearance Sensor Workshop*.
- Chivers, J.W.H. (1989), *A Technique for the Measurement of Blade Tip Clearance in a Gas Turbine*. PhD thesis, University of London.
- Denton, J.D. (1993), 'Loss Mechanisms in Turbomachines'. *Transactions of the ASME, Journal of Turbomachinery*, vol. 115, pp. 621–56.
- Denton, J.D. & Cumpsty, N.A. (1987), 'Loss Mechanisms in Turbomachinery'. *Proceedings of the IMechE International Turbomachinery Conference*. Robinson College, Cambridge, UK, 1–3 September, Paper No. C260/87.
- Denton, J.D. & Johnson, C.G. (1976), 'An Experimental Study of the Tip Leakage Flow around Shrouded Turbine Blades'. CEGB Report RIM1N848.
- Dring, R.P. & Joslyn, H.D. (1981), 'Measurement of Turbine Rotor Blade Flows'. *Transactions of the ASME, Journal of Engineering and Power*, vol. 103, pp. 400–5.
- Foster, R.L. (1989), 'Linear Capacitive Reactance Sensors for Industrial Applications'. *SAE 40th Annual Earthmoving Industry Conference*. Peoria, Illinois, USA, Paper No. 890974.

- Hughes, S.T. (1995), 'Sensors for Road Vehicles Based Upon Capacitance Variation'. *Proceedings of the IMechE Sensors — Autotech 95 Seminar*. Birmingham, UK, 7–9 November, Paper No. C498121/214.
- Müller, D., Sheard, A.G., Mozumdar, S. & Johann, E. (1997), 'Capacitive Measurement of Compressor and Turbine Blade Tip-to-casing Running Clearance'. *Transactions of the ASME, Journal of Engineering for Gas Turbines & Power*, vol. 119, pp. 877–84.
- Pavey, P.G. (1993), Private Communication with Mr. P.G. Pavey, Rolls-Royce plc, Engineering Manager Measurement and Test.
- Ramachandran, J. & Conway, M.C. (1996), 'MS6001FA — An Advanced Technology 70-MW Class 50/60 Hz Gas Turbine'. *GER-3765B, 39th GE Turbine State-of-the-Art Technology Seminar*.
- Sheard, A.G. & Killeen, B.A. (1993), 'Hybrid System for High-Temperature Tip-Clearance Measurement'. *Proceedings of the 39th ISA International Instrumentation Symposium*. Albuquerque, New Mexico, USA, 2–6 May, pp. 379–94.
- Sheard, A.G. & Lawrence, D.C. (1998), 'Gap Measurement Device'. Patent No. US 5,760, 593, 2 June.
- Sheard, A.G. & Turner, S.R. (1992), 'An Electromechanical Measurement System for the Study of Blade Tip-to-casing Running Clearances'. *Proceedings of the 37th American Society of Mechanical Engineers Gas Turbine and Aeroengine Congress*. Cologne, Germany, 1–4 June, Paper No. 92-GT-50.
- Sheard, A.G., O'Donnell, S.G. & Stringfellow, J.F. (1999), 'High Temperature Proximity Measurement in Aero and Industrial Turbomachinery'. *Transactions of the ASME, Journal of Engineering for Gas Turbines & Power*, vol. 121, pp. 167–73.
- Stringfellow, J.F., Wayman, L. & Knox, B. (1997), 'Capacitance Transducer Apparatus and Cables'. Patent No. WO 97/28418, 7 August.

High-temperature Proximity Measurement in Aero and Industrial Turbomachinery

A.G. Sheard, S.G. O'Donnell and J.F. Stringfellow

ABSTRACT

Engineers and researchers have measured disc and shaft displacement for many years as part of the development, commissioning and monitoring of all classes of turbomachinery. They have traditionally measured using sensors that cannot operate above the Curie point of rare earth magnets.

This chapter describes a programme of work that the authors undertook to develop a measurement system that could make a measurement of proximity between a sensor and target in a high-temperature environment. The specific objectives were first, to measure turbine disc axial movement and shaft motion in the gas turbine core, close to the combustion chamber or turbine; and second, to measure blade tip-to-casing clearance over shrouded turbine rotors.

INTRODUCTION

The measurement of proximity from a sensor to a continuous target, such as a disc or shaft, is routine within all classes of turbomachinery. The most common measurement principle is the eddy current sensor, which Sutcliffe (1977) describes. Two factors classically limit the practical application of these sensors. First, they operate only to the Curie point of rare earth magnets, typically 200°C¹. Second, target material property variations effect measurement system calibration. Hastings and Jensen

This chapter is a revised and extended version of Sheard, A.G., O'Donnell, S.G. & Stringfellow, J.F. (1999), 'High Temperature Proximity Measurement in Aero and Industrial Turbomachinery'. *Transactions of the ASME, Journal of Engineering for Gas Turbines & Power*, vol. 121, pp. 167–73.

¹ The paper that forms the basis of this chapter was originally drafted in 1996, at which time the Curie point of rare earth magnets was limited to approximately 200°C. At the time this edited volume was produced, rare earth magnets have been developed with a Curie point in excess of 800°C. However, practical applications above 200°C remain relatively uncommon as a consequence of the cost of high-temperature rare earth magnets.

(1996) reported improvements to the basic concept, which largely eliminate the susceptibility to target material property variations, but do not address the issue of limited temperature capability.

The measurement of clearance between a sensor and a discontinuous target, such as the blades around a compressor or turbine disc, is also routine within all classes of turbomachinery. Burr (1994) considered the possible operating principles for a high-temperature blade tip-to-casing clearance measurement system, Table 9.1. Burr (1994) concluded that optical and capacitive systems were the most mature, capacitive systems were least complex and that capacitive and microwave systems were most durable.

Barranger and Ford (1981) studied the use of lasers, but found them bulky and expensive in practice. Researchers such as Grzybowski *et al.* (1996) developed microwave sensors which show potential. However, practical sensor implementations are as yet unavailable. Sheard and Turner (1992) have successfully employed electromechanical techniques, but again they are bulky.

The use of capacitive sensors is common within the turbomachinery community (Müller *et al.*, 1997), where engineers classically use them to measure the clearance between a gas turbine casing and the blades that run within it. The automotive industry routinely uses capacitive sensors (Grice *et al.*, 1990; Hughes, 1995) to measure proximity to solid surfaces. The small size, low cost and insensitivity to target material properties made the capacitance sensor a logical operating principle to apply to high-temperature proximity measurement.

This chapter reports a programme of work that the authors undertook to develop a high-temperature proximity measurement system, based on the principle of measuring the capacitance between sensor and target. It describes the design and performance of proximity measurement signal conditioning. The chapter also presents the design and laboratory testing of a sensor suitable for use with the developed proximity measurement signal conditioning and blade tip-to-casing clearance measurement signal conditioning. In so doing, the chapter presents a sensor concept that engineers can use for high-temperature proximity measurement to a solid surface and high-temperature clearance measurement to a discontinuous target.

Table 9.1. Clearance sensor comparison of capability in gas turbine applications, compiled from data contained in Burr (1994).

Sensor	Resolution	Temperature limit (current state of the art)	Target geometry dependent	Size comparison	Cost per sensor
Electromechanical	0.05 mm	1200°C (purged)	No	Large	High
Optical	0.05 mm	1550°C (purged)	No	Large	Very high
Capacitive	5% of range	1100°C	Yes	Very small	Low
Eddy current	5% of range	650°C	Yes	Small	Low
Microwave	0.1 mm	1200°C	No	Medium	Medium
Fluidic	0.25 mm	1400°C	Yes	Small	Low

PRINCIPLE OF OPERATION

The proximity measurement system comprises three components. The first is a sensor, Figure 9.1, which Sheard and Lawrence (1998) describe in detail. The second is a gas turbine mounted oscillator, amplifier and filter, collectively named the capacitive displacement transducer (CDT) amplifier. The third is a rack-mounted receiver that links to the CDT amplifier via standard test bed 50 ohm co-axial cables, Figure 9.2. The CDT amplifier and capacitive displacement transducer amplifier and receiver constitute the proximity measurement system electronics.

The sensor is a tri-axial device, with the centre wire connected to the sensor tip. A guard surrounds the centre wire and sensor tip, and an outer screen surrounds the guard. The use of a guard allows cancellation of the cable capacitance's effect. This results in the registration of only the capacitance between the sensor tip and target.

Sensor

Grice *et al.* (1990) described the design of a co-axial capacitive proximity sensor. The co-axial proximity sensor is isolated from its surroundings using high-temperature plastic. This plastic is limited to approximately the same working



FIGURE 9.1. Traditional tri-axial capacitive sensor (top) originally developed by Chivers (1989a) and the new technology (NT) capacitive sensor (bottom) originally developed by Sheard and Lawrence (1998). This example of the new technology capacitive sensor was designed with side entry cable.

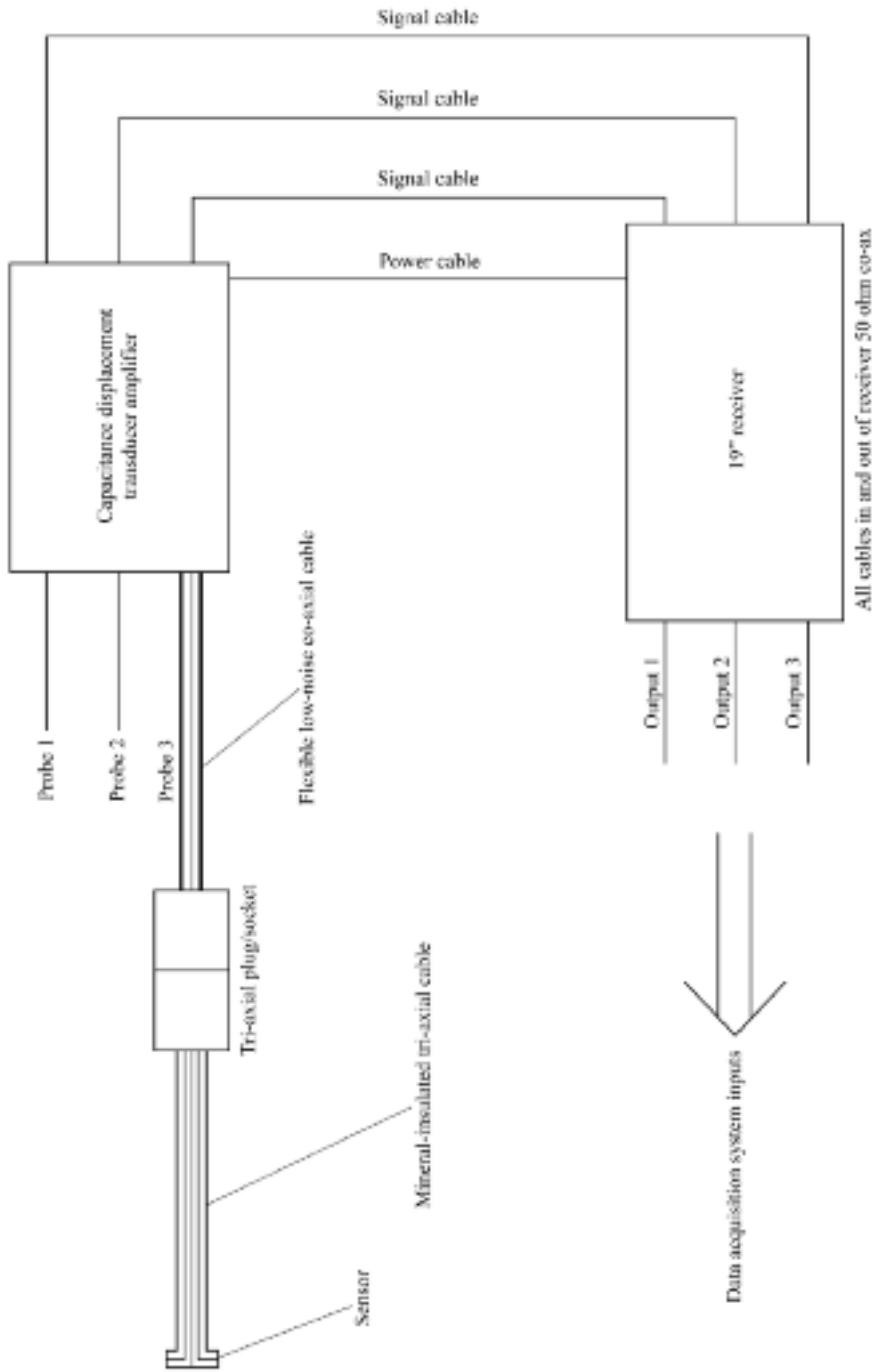


FIGURE 9.2. Proximity measurement system component parts and cable configuration.

temperature as the rare earth magnets within an eddy current sensor. The co-axial capacitance sensor, therefore, offers no better high-temperature capability than an eddy current sensor.

In order to produce a higher temperature proximity sensor, it was necessary to eliminate all plastic components, replacing them with materials resistant to higher temperatures. The adopted approach isolated Grice *et al.*'s (1990) co-axial sensor from its environment by encapsulating it in a third layer. The authors' developed form of the capacitive proximity sensor, therefore, became a tri-axial device. The authors took the same approach with the cable.

The authors employed the tri-axial sensor construction only to provide a high-temperature electrical isolation of the centre wire and guard from the environment. Once the environmental temperature falls below 200°C, the cable between sensor and oscillator can change to a low noise poly-tetra-fluoro-ethylene (PTFE) coated co-axial cable, Figure 9.2.

Gas turbine-mounted CDT amplifier

The authors developed the gas turbine mounted capacitive displacement transducer amplifier from the amplifier which Grice *et al.* (1990) first described. It drives the guard at 16 kHz and constant amplitude, Figure 9.3. It is insensitive to low-speed thermal changes in cable capacitance, keeping amplitude constant irrespective of cable capacitance. This induces an identical sinusoidal oscillation in the centre wire that is immune from changes in cable capacitance. As soon as a target comes into the sensor tip's range, the additional capacitive couple between sensor tip and target results in a change in the induced voltage on the centre wire. This manifests itself as a reduced centre wire voltage relative to that on the guard.

The capacitive displacement transducer amplifier contains a very high gain and high bandwidth product differential amplifier, with both the reference guard voltage and the induced centre wire voltage feeding into it. The differential amplifier output is a 16 kHz sine wave, the amplitude of which is proportional to the difference between reference and induced inputs.

Signal conditioning

The gas turbine mounted capacitive displacement transducer amplifier output feeds through a 50 ohm drive stage to enable linkage to a distant receiver module using a standard test bed 50 ohm co-axial cable, Figure 9.4. In making blade tip-to-casing clearance measurements, Müller *et al.* (1997) used 150 metre cable lengths in practical gas turbine test-bed installations.

Within the receiver module the 16 kHz sine wave synchronously rectifies to eliminate quadrature errors. The signal then passes through a three-pole low pass filter with a 3 db point at 5 kHz. The DC voltage output then scales to give 0–10 volts output proportional to sensor tip to target capacitance over the sensor working range. Table 9.2 summarises the drive electronic specification.

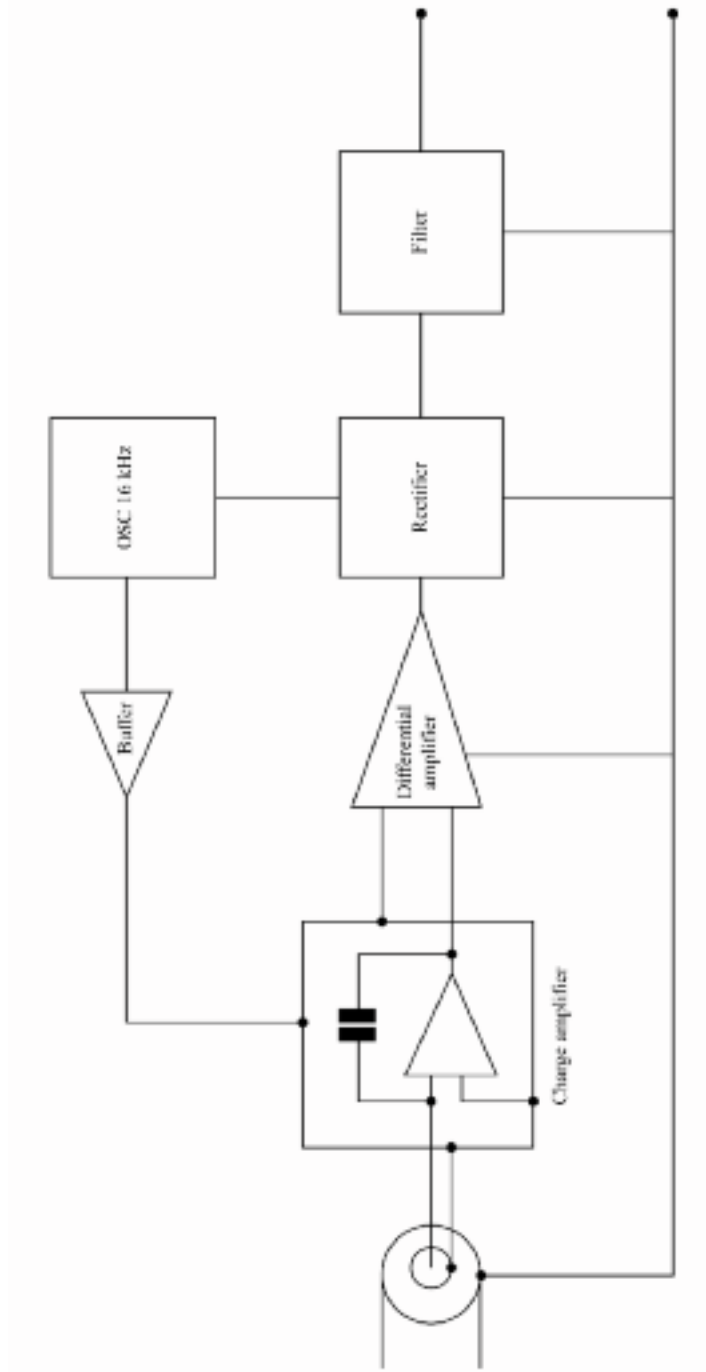


FIGURE 9.3. Schematic diagram of the gas turbine-mounted capacitive displacement transducer (CDT) amplifier.

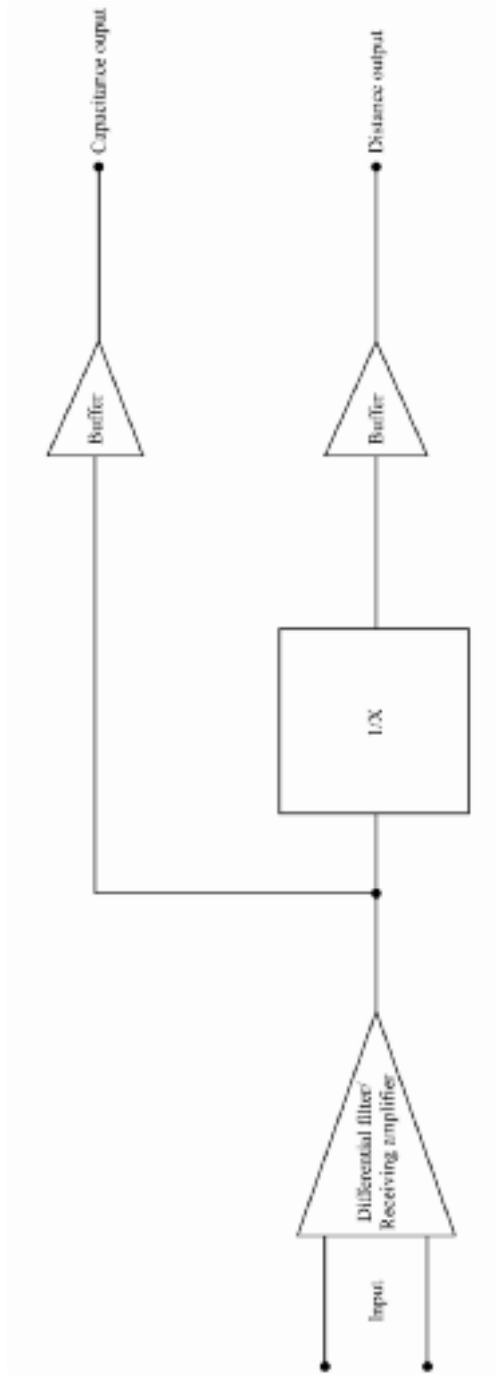


FIGURE 9.4. Schematic diagram of the proximity measurement system 19" rack mount receiver.

SENSOR DEVELOPMENT

The authors set sensor design objectives as representative of the turbine environments in current generation gas turbines. Atkinson (1994) considered the next generation of gas turbines with predicted combustor flame temperatures of 1773°C and a requirement for instrumentation capable of operating at 1500°C. The authors considered and then rejected this design objective. The authors reasoned that the turbine inlet temperature of gas turbines currently under development required a lower operating temperature. As such, they could fabricate the sensor from ferrous and nickel-based alloys. Sensor operation at 1500°C would necessitate a shift to platinum-based alloys. Fabrication of tri-axial cable and sensors from platinum-based alloys presents its own challenges, and it is therefore prudent to develop and prove the cable and sensor technology using more conventional materials. Table 9.3 presents the specification which the authors adopted. The following sections describe the programme of work that the authors undertook to achieve the specification.

Table 9.2. *Drive electronic specification.*

Oscillator	
Frequency	16 kHz
Level	Preset 10 Volts pk-pk
Distortion	< 0.5% harmonic distortion
Amplitude stability	< 100 ppm/C
Amplifier	
Target capacitance	(1) 1.500 pF to 0.150 pF (2) 0.750 pF to 0.075 pF (3) 0.375 pF to 0.0375 pF
Rectifier	Synchronous
Filter type	3 pole Butterworth
Cut off frequency	1 kHz typical, 5 kHz max.
Output	+/- 10 Volts @ 2 mA
Stability	< 0.1 %/C

Table 9.3. *Sensor specification.*

Front face peak operating temperature	1100°C
Sensor body temperature	800°C
Mineral-insulated cable temperature	600°C
Mineral-insulated cable length	6 metres
Mineral insulated to flexible cable joint temperature	200°C
Flexible cable length	5 metres
Flexible cable temperature	200°C
Drift with temperature over operating range	> +/- 2% FS

Traditional tri-axial sensor configuration

Tri-axial capacitive sensors capable of surviving in high-temperature environments are classically complex assemblies of metal and ceramic components, Figure 9.5. Chivers (1989a), Chivers (1989b), Müller *et al.* (1997) and Gill *et al.* (1997) have utilised these sensors in turbine applications for blade tip-to-casing clearance measurement. This sensor will not operate with the authors' developed version of Grice *et al.*'s (1990) proximity electronics as the guard ring does not extend to the sensor tip. This typically introduces a 4 pF 'stray' linkage between electrode and outer screen, which is indistinguishable from the signal to the proximity electronics, and therefore takes the system out of its operating range, Table 9.2.

Stray capacitance is present in Chivers' (1989a) tri-axial designs as the guard does not extend to the sensor tip. A fully guarded sensor would typically have less than 0.1 pF stray capacitance, attributable to air linkage from electrode across the guard ring to earth. One could therefore utilise a fully guarded sensor with the authors developed from Grice *et al.*'s (1990) electronics. In so doing, they could use the same sensor to measure proximity to a solid target using their developed form of Grice *et al.*'s (1990) electronics, or to measure blade tip-to-casing clearance with Stringfellow *et al.*'s (1997) developed form of Chivers' (1989a) electronics.

New technology sensor

Sheard and Lawrence (1998) present the new technology (NT) sensor concept. The concept eliminates all ceramic components, Figure 9.5, maintaining electrical isolation by alumina coating the electrode and guard. The elimination of machined ceramic components enables guard extension to the sensor's tip, which is the key feature that effectively eliminates stray capacitance and makes the design suitable for use with both proximity and tip clearance electronics.

The electrode, guard and body comprise a set of inverted cones, which pre-load into one another. The use of inverted cones produces an intrinsically safe fully captive design. By pre-loading the cones into one another during sensor assembly, all components remain positively located at all times. This reduces susceptibility to high cycle fatigue. The employed design has the ability to withstand 500G acceleration loads at peak operating temperature.

It is unlikely that any tri-axial capacitive sensor will compete on cost with co-axial or multi-core capacitive sensors, which Monich and Bailleul (1993) and Bailleul and Albijat (1996) describe for use with Dooley's (1989a, b) or Foster's (1989) electronics. The primary consideration, however, must be a fully captured sensor design that will not fail mechanically.

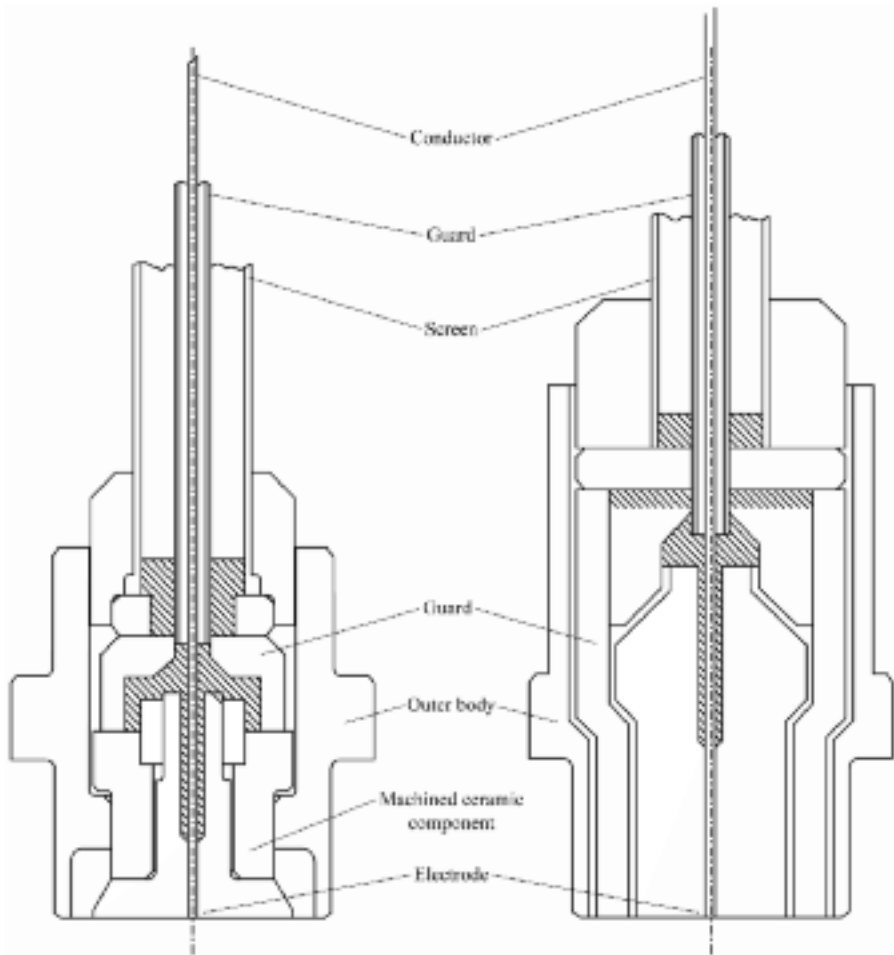


FIGURE 9.5. Traditional tri-axial capacitive sensor (left) originally developed by Chivers (1989a) and the new technology (NT) capacitive sensor (right) originally developed by Sheard and Lawrence (1998).

Sensor geometry

The objective of good sensor design is to give the maximum operating range for a given sensor diameter. A large guard ring improves sensor linearity by reducing stray capacitive linkage through the air from active electrode to sensor body. However, as the ratio between guard and active electrode diameter increases, the active electrode diameter must decrease if overall sensor diameter is to remain constant. As the active electrode diameter reduces, sensor range reduces. It is therefore apparent that there is an optimum ratio between guard and active electrode diameter that will maximise sensor range. The authors empirically assessed the trade-off between guard and active sensor diameter. They found that a ratio of 1.4 gave the greatest sensor range.

The authors performed a finite element analysis of the electrical field between sensor face and target for the optimised tip geometry. The predicted lines of constant voltage (Figure 9.6) across the sensor face indicated slight distortion of the field across the electrode-guard interface. Clearly, the guard is not perfect. However, the guard worked well enough to prevent distortion to the field in front of the electrode, therefore enabling maximum linkage between active sensor electrode and target.

Sensor range

The authors evaluated the new technology sensor range when attached to the developed proximity electronics, Figure 9.7. They achieved a range of approximately 75% overall sensor diameter. Grice *et al.*'s (1990) original sensors and proximity electronics typically have a guard to electrode diameter ratio of 2, which gives good linearity over a short range of approximately 50% overall sensor diameter, Figure 9.7. The new technology sensor and developed proximity electronics therefore increases overall sensor range by about 50% from 50% to 75% of overall sensor diameter.

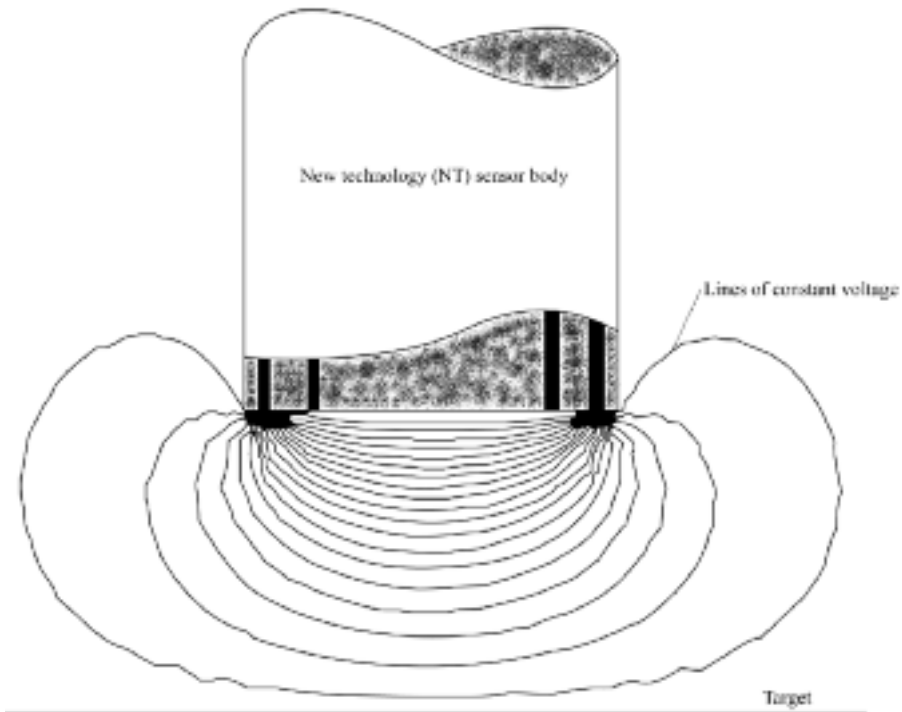


FIGURE 9.6. Finite element analysis of optimised new technology sensor tip. Predicted lines of constant voltage to target at one sensor diameter from the sensor tip.

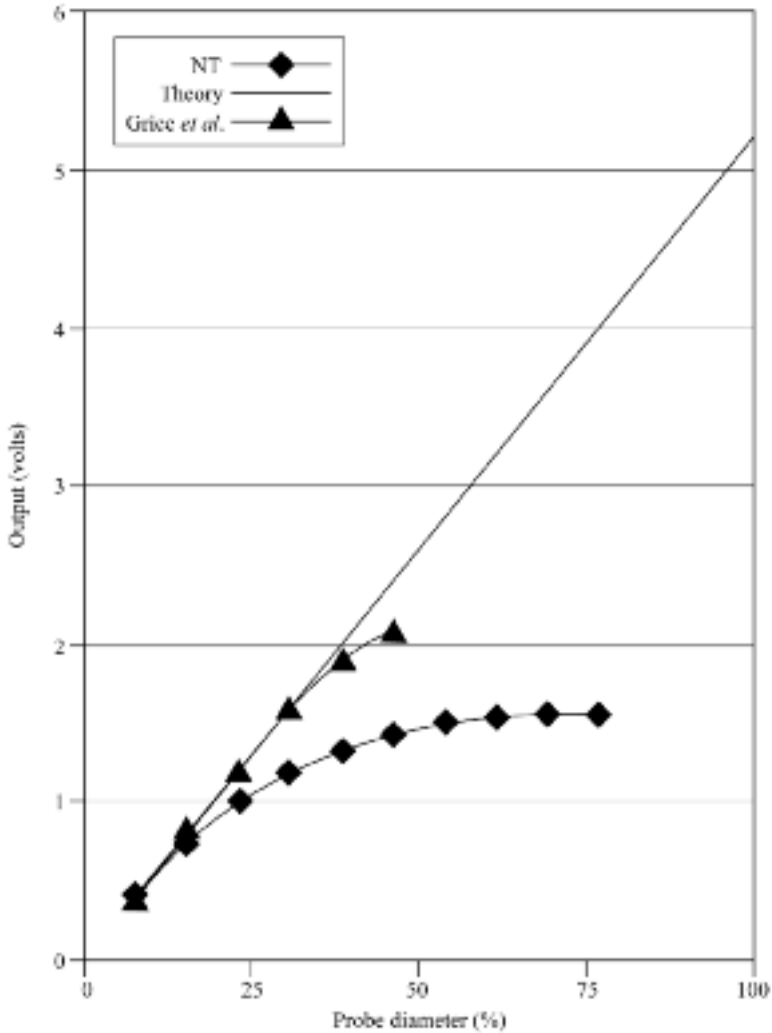


FIGURE 9.7. The new technology sensor range when coupled with authors' developed proximity electronics and the sensor range of Grice *et al.*'s (1990) original electronics and sensor design.

The authors also studied the performance of Stringfellow *et al.*'s (1997) blade tip-to-casing clearance electronics in combination with a new technology sensor. Range was 75% of overall sensor diameter, Figure 9.8. We can put the new technology sensor range into context via a comparison with the range of Stringfellow *et al.*'s (1997) blade tip-to-casing clearance electronics in combination with Chivers' (1989a) original sensors, Figure 9.8. It was this electronics and sensor technology combination that Gill *et al.* (1997) utilised and applied in a General Electric MS6001FA industrial gas turbine and compressor. Gill *et al.* (1997) conducted a planned over-speed trip, and concluded that immediately following the trip the

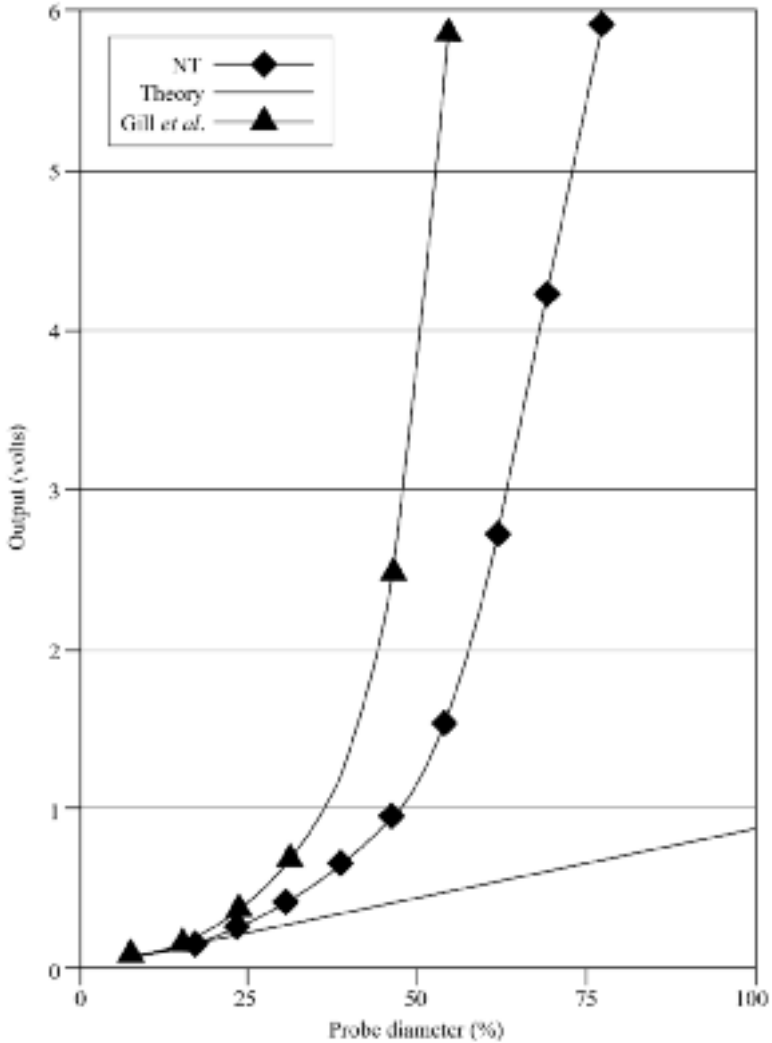


FIGURE 9.8. The new technology sensor range when coupled with tip clearance electronics of Stringfellow *et al.* (1997) and the sensor range achieved by Gill *et al.* (1997) when using tip clearance electronics of Stringfellow *et al.*'s (1997) and the original sensor design of Chivers (1989a).

sudden decrease in centrifugal load caused the blade tip-to-casing clearance to increase beyond the measurement system's range.

Müller *et al.* (1997) and Gill *et al.* (1997) each utilised Stringfellow *et al.*'s (1997) electronics in combination with Chivers' (1989a) original sensor design. Both Müller *et al.* (1997) and Gill *et al.* (1997) reported a sensor range that equated to approximately 40% of overall sensor diameter. Although insufficient in Gill *et al.*'s (1997) application, sensor range of 40% overall sensor diameter still represented an

improvement over Chivers' (1989a) original electronics in combination with Chivers' (1989a) original sensor design. The original electronics and probe combination were only able to achieve a sensor range of between 25% and 35% of overall sensor diameter.

The authors worked collaboratively with Gill *et al.* (1997), supplying new technology sensors for application in a General Electric MS9001EC industrial gas turbine. The improvement in range from 40% to 75% of overall sensor diameter enabled Gill *et al.* (1997) to successfully measure turbine blade tip-to-casing clearance during all phases of the gas turbine operating envelope. The recorded data remained necessarily confidential. However, Gill *et al.* (1997) were able to comment that the improvement in new technology sensor performance was a step towards the required capability for continuous, long-term blade tip-to-casing clearance monitoring in the harsh turbine environment.

CABLE DEVELOPMENT

A cable system links the sensor and capacitive displacement transducer amplifier, Figure 9.2. For high-temperature installations the only viable cable type is mineral-insulated (MI).

Mineral-insulated cable

Mineral-insulated cables are signal transmission cables which consist of an impervious sheath, an oxide insulator and a conductor. In the case of the tri-axial cable, the guard and second oxide layer separate the conductor from the outer sheath. The sheath material must suffer low oxidation at an elevated temperature, favouring stainless steel or Inconel® which are resistant to oxidation and maintain their structural integrity in high-temperature environments.

The insulator is a compressed metal oxide powder. The capacitive displacement transducer amplifier is insensitive to cable capacitance. Therefore, despite its high relative permittivity when compared to other materials, magnesium oxide (MgO or magnesia) is the preferred insulator.

MgO-filled cable

At the target cable operating temperature, 600°C (Table 9.3), the relative permittivity of magnesia changes by 7% from 6.3 to 6.7 (Table 9.4), which will result in a corresponding change in cable capacitance of 7%. For a typical cable configuration with approximately 2000 pF capacitance between conductor and guard and guard and sheath, a 100% change in cable capacitance affects system output by less than 2%. Consequently, the authors concluded that the performance of magnesia is adequate for the new technology sensor application.

SiO₂-filled cable

The principal advantage of silica (SiO₂) over magnesia is its low relative permittivity, Table 9.4. Below approximately 500°C the relative permittivity of silica is half that of magnesia, giving a cable of half the capacitance per metre. This enables cables of twice the length for the same overall capacitance as a magnesia-filled cable. Above 500°C the relative permittivity of silica increases rapidly (Table 9.4), therefore making silica-filled cable unsuitable for use. Silica is not the only low dielectric insulating material. However, it is the only readily available low-cost material.

Table 9.5 summarises the cable configuration which Stringfellow *et al.* (1997) present. The authors selected stainless steel for the centre wire and outer screen for strength at temperature. They chose nickel, a low electrical resistance metal, for the guard as low electrical resistance of the guard improves performance of both the author’s developed form of Grice *et al.*’s (1990) proximity measurement electronics and Stringfellow *et al.*’s (1997) clearance measurement electronics.

Table 9.4. *Relative permittivity of silica and magnesia.*

Temperature (°C)	Silica	Magnesia
20	3.0	6.3
100	3.0	6.3
200	3.0	6.4
250	3.1	6.4
300	3.1	6.4
350	3.1	6.5
400	3.2	6.5
450	3.5	6.5
500	3.9	6.5
550	4.7	6.6
600	6.2	6.7
650	11.9	6.9
700	21.0	7.3
750	26.7	7.8
800	29.2	8.6

Table 9.5. *Cable specification.*

Conductor material	Stainless steel
Guard material	Nickel
Outer screen material	Stainless steel
Insulating material	MgO or SiO ₂ , plus additives
Conductor to guard capacitance	130 pF/M (SiO ₂)
Guard to outer screen capacitance	130 pF/M (SiO ₂)
Guard resistance	0.2 ohms per metre
Overall cable diameter	3.00 mm

Flexible cable

The capacitive displacement transducer amplifier does not require the new technology sensor earth. For this reason one can use a co-axial poly-tetra-fluoro-ethylene (PTFE) cable to connect the guard and conductor to the new technology sensor, Figure 9.2. The tri-axial cable's outer screen performs the same function as the PTFE wrap around a co-axial cable, simply insulating the guard from earth.

SYSTEM PERFORMANCE

The following section summarises the new technology sensor's laboratory testing and presents the most significant data.

High-temperature sensor performance

As the cable and sensor are intimately connected, it is impossible to study sensor performance independent of the cable to which it is connected. To overcome this, the authors mounted probe components in a jig with no mineral-insulated cable attached to allow them to study the new technology sensor performance independently of the cable to which they would attach it in practical application.

The critical parameter at elevated temperature is isolation resistance between components. To ascertain change in isolation resistance with temperature of the jig-mounted components, the authors oven tested them. Results from the oven testing, Figure 9.9, were encouraging, with measured isolation matching theoretical resistivity for pure alumina well. With an isolation of 10 kOhms within the sensor, capacitive displacement transducer amplifier performance is unaffected. However, by 1 kOhm the system performance had collapsed. Oven tests indicated that at 1100°C parts maintained over 10 kOhms isolation, making them fit for purpose.

High-temperature cable performance

The authors studied cable samples to verify performance at temperature. The cable samples started to exhibit a thermoelectric effect above 700°C. The dissimilar metals which they used in the cable construction began to generate a voltage between screen and guard and guard and conductor, which was up to 50mV at 1100°C. This effect decoupled in the capacitive displacement transducer amplifier, and therefore did not affect system performance. However, it proved impossible to make an accurate measurement of isolation resistance above 700°C.

Below 700°C, change in isolation resistance with temperature was consistent with the theoretical resistivity for pure magnesia and silica. The authors predicted an isolation resistance of 10 kOhms at 800°C within silica-filled cable and 1200°C within magnesia-filled cable. This was consistent with the new technology sensor specification, Table 9.3.

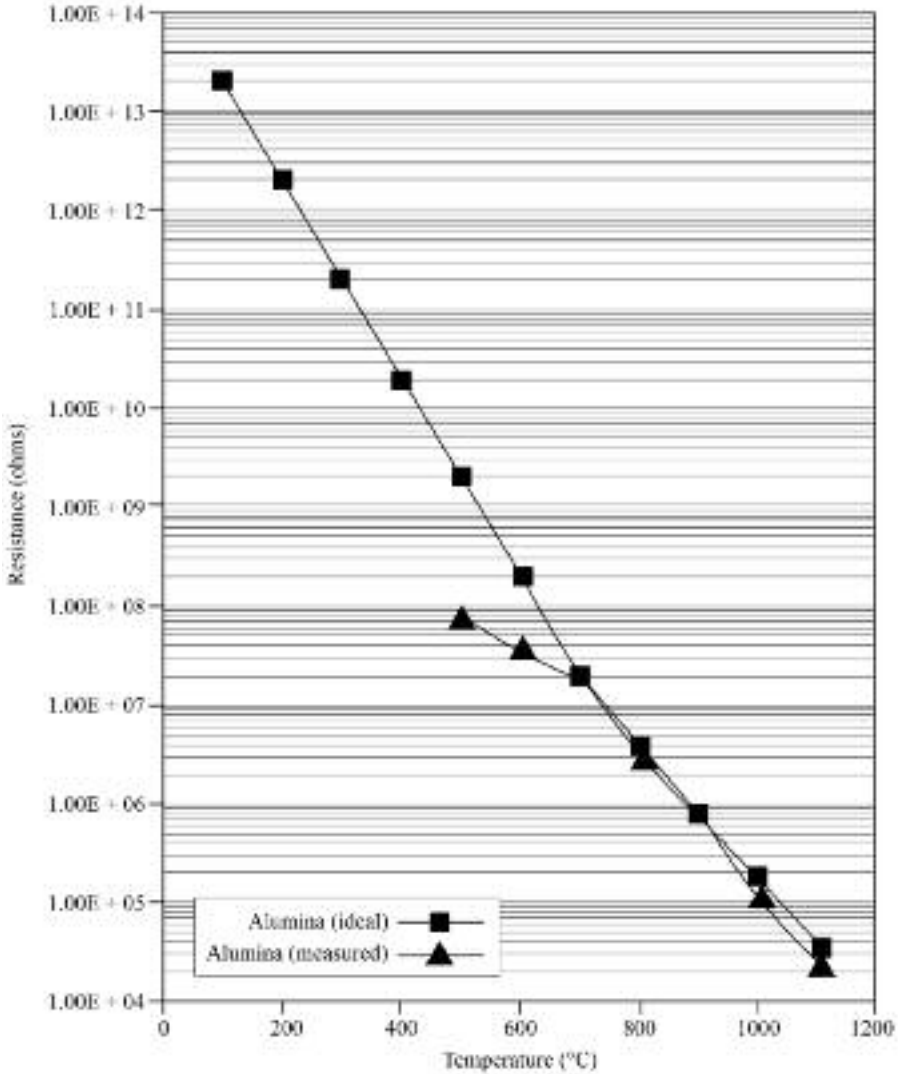


FIGURE 9.9. Measured and theoretical isolation resistance for alumina-coated sensor components.

Sensor and cable coupled performance

The authors decided to test the assumption that they could study sensor and cable performance separately. They attached a new technology sensor to a silica-filled cable and oven tested it. The isolation resistance with temperature was within the measurement uncertainty of a repeat cable-only trial. From this the authors concluded that there were no close-coupled interactions between sensor and cable, and that their study of probe and cable performance in isolation was valid.

Proximity measurement electronic system performance

The gas turbine-mounted capacitive displacement transducer amplifier operates by oscillating a voltage at 16 kHz on the guard, which induces an in-phase voltage on the centre wire. The authors noted that with a silica-filled cable, above 800°C the phase of the induced voltage on the centre wire shifted. By 950°C the return signal was flooded with quadrature and the system collapsed, Figure 9.10.

At a temperature of 800°C the silica's relative permittivity increased by an order of magnitude, Table 9.4. This increased cable capacitance by an order of magnitude. One may set up the capacitive displacement transducer amplifier to function with almost any required cable capacitance in practical applications. However, very large changes in cable capacitance do result in system collapse. The dramatic increase in silica's relative permittivity, therefore, was the primary cause of system collapse at 950°C.

To confirm that the sensor itself was not responsible for system collapse, the authors heated a sensor tip (attached to silica-filled cable) with a blow torch to approximately 1100°C. They checked system sensitivity, which remained stable to within 1%.

Measured system sensitivity with magnesia-filled cable remained virtually unchanged from ambient to 1100°C, Figure 9.10. The authors observed system output during the oven test. The phase of the induced voltage on the centre wire remained virtually unchanged, with no evidence of quadrature.

Clearance measurement electronic system performance

The authors considered the effect of guard resistance when using the new technology sensor with Stringfellow *et al.*'s (1997) clearance measurement system electronics. Conventional stainless steel cable with its inherent low conductivity can lead to measurement errors in Stringfellow *et al.*'s (1997) electronics. The guard resistance, when combined with guard to outer cable capacitance, develops a quadrature interference signal which can become significant.

The specific conditions needed for the quadrature to become significant occur at high cable temperature, when the cable guard to conductor resistance reduces, and leakage between the two becomes significant. The combined effect of guard resistance, guard to outer capacitance and guard to conductor leakage are responsible for the error in system output.

A second effect occurs with low isolation between cable guard and screen at high cable temperatures. As guard to screen leakage becomes significant, resistive leakage produces an interference signal that is 'in phase'. This error signal is indistinguishable from sensor to target signal capacitance.

The two effects described above become dominant with cable guard resistances above 10 ohms and isolation resistances below 10 kOhms. Cable guard resistances below 10 ohm and isolation resistances above 10 kOhms induce errors in system output of less than 1%, and therefore are negligible.

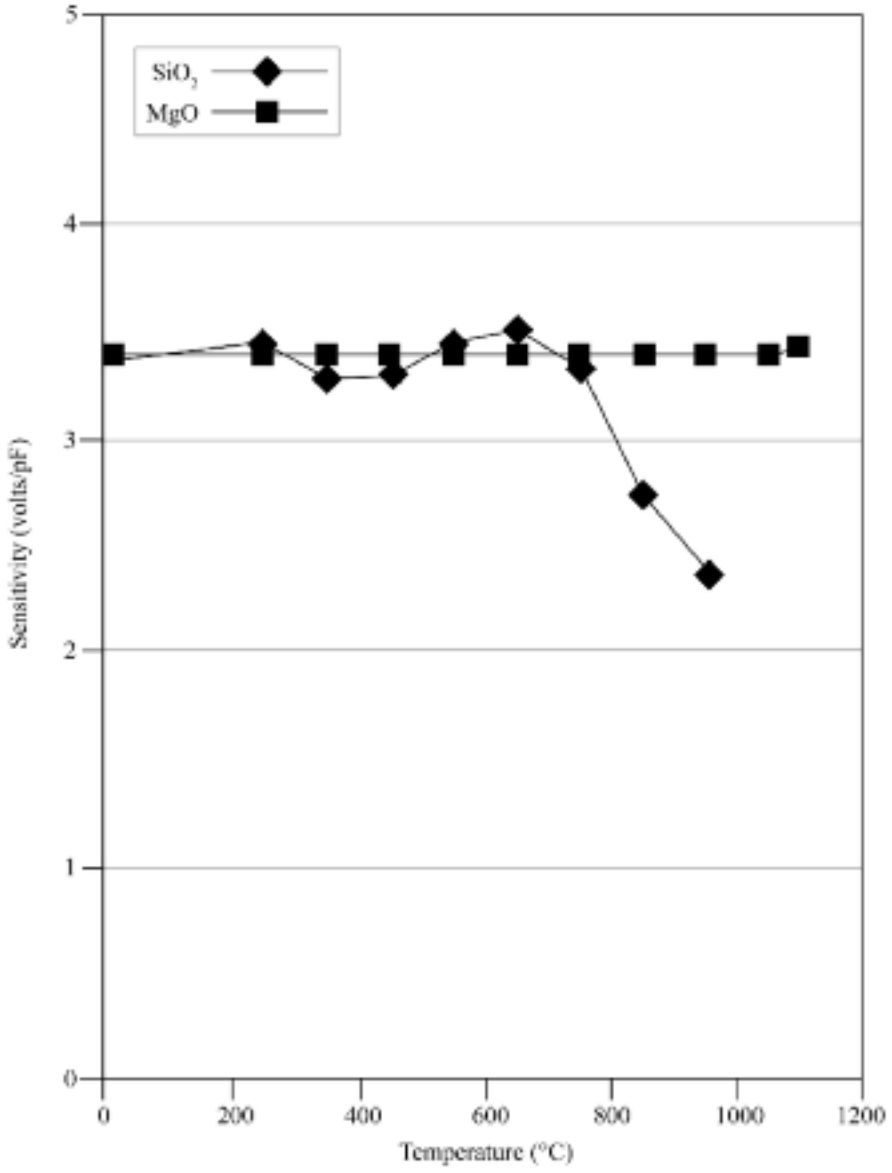


FIGURE 9.10. Proximity measured system sensitivity.

Stringfellow *et al.* (1997) considered the approach to minimising the two effects by using a tri-axial cable with low guard resistance, Table 9.5. In practical applications of the measurement system, the authors envisage that the provision of gas turbine-mounted electronics should facilitate the use of sensors with short enough mineral-insulated cable lengths to keep guard resistance close to 1 ohm. Flexible cables use a low-resistance copper guard, with a resistance per metre that is negligible.

CONCLUSIONS

The authors have developed a new proximity measurement system, with an extended operating temperature range making its installation in back-end compressor and turbine applications possible. They have also developed a novel electronic concept which enables tri-axial sensors to drive in a manner that is not susceptible to low-frequency changes in cable and sensor properties which changes in their operating temperature induce.

In addition, the authors characterised a novel sensor, which Sheard and Lawrence (1998) presented. The novel sensor eliminates ceramic components, thus avoiding thermal cycle fatigue due to mismatched component coefficients of expansion. The sensor has a fully captive design, and is therefore intrinsically safer than Chivers' (1989a) sensor design. The sensor range in practice was 50% greater than previous designs in both proximity and tip clearance applications.

The authors have produced tri-axial cables that successfully incorporate the requirement for low capacitance, low guard resistance and high working temperature, which Stringfellow *et al.* (1997) presented.

The new technology sensor can operate with either the authors' developed form of Grice *et al.*'s (1990) proximity electronics or Stringfellow *et al.*'s (1997) developed form of Chivers' (1989a) blade tip-to-casing clearance electronics. The new technology sensor is the first sensor concept that is suitable for routine uncooled turbine application at 1100°C.

REFERENCES

- Atkinson, W. (1994), 'Sensor Requirements'. *Proceedings of the 1st P&W International Clearance Sensor Workshop*.
- Bailleul, G.D. & Albijat, S. (1996), 'Review of Progress in the Development of Capacitive Sensors for Blade Tip Clearance Measurement'. *Proceedings of the American Society of Mechanical Engineers Turbo Asia Conference*. Jakarta, Indonesia, 5–7 November, Paper No. 96-TA-001.
- Barranger, J.P. & Ford, M.J. (1981), 'Laser Optical Blade Tip Clearance Measurement System'. *Transactions of the ASME, Journal of Engineering for Power*, vol. 103, pp. 457–60.
- Burr, R. (1994), 'Sensor Comparison'. *Proceedings of the 1st P&W International Clearance Sensor Workshop*.

- Chivers, J.W.H. (1989a), *A Technique for the Measurement of Blade Tip Clearance in a Gas Turbine*. PhD thesis, University of London.
- Chivers, J.W.H. (1989b), 'A Technique for the Measurement of Blade Tip Clearance in a Gas Turbine'. AIAA Paper No. 89-2916
- Dooley, K. (1989a), 'Capacitive Bridge-Type Probe for Measuring Blade Tip Clearance'. Patent No. US 4,818,948, 4 April.
- Dooley, K. (1989b), 'Capacitance to Voltage Conversion Bridge and a Capacitive Offset'. Patent No. US 4,795,965, 3 June.
- Foster, R.L. (1989), 'Linear Capacitive Reactance Sensors for Industrial Applications'. SAE Technical Paper No. 890974, doi:10.4271/890974.
- Gill, S.J., Ingallinera, M.D. & Sheard, A.G. (1997), 'Turbine Tip Clearance Measurement System Evaluation in an Industrial Gas Turbine'. *Proceedings of the 42nd American Society of Mechanical Engineers Gas Turbine and Aeroengine Congress*. Orlando, Florida, USA, 2–5 June, Paper No. 97-GT-466.
- Grice, N., Sherrington, L., Smith, E.H., O'Donnell, S.G. & Stringfellow, J.F. (1990), 'A Capacitance Based System for High Resolution Measurement of Lubricant Film Thickness'. *Proceedings of the Nordtrib '90, 4th Nordic Symposium on Tribology, Lubrication, Friction and Wear*. Hirtshals, Denmark, 10–13 June.
- Grzybowski, R., Foyt, G., Atkinson, W., Knoell, H. & Wenger, J. (1996), 'Microwave Blade Tip Clearance Measurement System'. *Proceedings of the 41st American Society of Mechanical Engineers Gas Turbine and Aeroengine Congress*. Birmingham, England, 10–13 June, Paper No. 96-GT-002.
- Hastings, M.M. & Jensen, H.B. (1996), 'A Novel Proximity Probe Unaffected by Shaft Electromagnetic Properties'. *Proceedings of the 41st American Society of Mechanical Engineers Gas Turbine and Aeroengine Congress*. Birmingham, England, 10–13 June, Paper No. 96-GT-004.
- Hughes, S.T. (1995), 'Sensors for Road Vehicles Based Upon Capacitance Variation'. *Proceedings of the Institution of Mechanical Engineerings Sensors - Autotech 95 Seminar 21*. Birmingham, England, 7–9 November, Paper No. C498/21/214.
- Monich, M. & Bailleul, G. (1993), 'New Digital Capacitive Measurement System for Blade Clearances'. *Proceedings of the 39th ISA International Instrumentation Symposium*. Albuquerque, New Mexico, USA, 2–6 May, pp. 419–30.
- Müller, D., Sheard, A.G., Mozumdar, S. & Johann, E. (1997), 'Capacitive Measurement of Compressor and Turbine Blade Tip-to-casing Running Clearance'. *Transactions of the American Society of Mechanical Engineers, Journal of Engineering for Gas Turbines & Power*, vol. 119, pp. 877–84.
- Sheard, A.G. & Lawrence, D.C. (1998), 'Gap Measurement Device'. Patent No. US 5,760,593, 2 June.
- Sheard, A.G. & Turner, S.R. (1992), 'An Electromechanical Measurement System for the Study of Blade Tip-to-casing Running Clearances'. *Proceedings of the 37th American Society of Mechanical Engineers Gas Turbine and Aeroengine Congress*. Cologne, Germany, 1–4 June, Paper No. 92-GT-50.
- Stringfellow, J.F., Wayman, L. & Knox, B. (1997), 'Capacitance Transducer Apparatus and Cables'. Patent No. WO 97/28418, 7 August.
- Sutcliffe, H. (1977), 'Principles of Eddy Current Distance Gauging'. *Transactions of the Institute of Electrical Engineers*, vol. 124, pp. 479–84.

Capacitance Transducer Apparatus and Cables

J.F. Stringfellow, L. Wayman and B. Knox

ABSTRACT

This Appendix is adapted from the patent ‘Capacitance transducer apparatus and cables’. The adaption aims to make the invention presented in the patent more accessible to the reader, without significantly altering the patent’s content.

A need to drive longer cable lengths between capacitive clearance measurement system electronics and sensor inspired the research resulting in the intellectual property that forms the basis of the patent. Historically, the tri-axial cable between electronics and sensor had been limited to 180 mm. The inventors of this patent extended the length to 10 metres when in combination with the sensor concept described in Appendix 2. Taken together, the electronics-cable-sensor combination facilitated practical embodiments of the capacitive clearance measurement system suitable for use in gas turbine development and production applications, as opposed to instrumentation research applications.

INTRODUCTION

The present invention relates to capacitance transducer apparatus, to cables and in particular, although not exclusively, to cables for use in transmitting signals to and from a frequency modulated driven guard capacitance detector. One can use frequency modulation driven guard capacitance transducers in the form of capacitance detectors which measure blade tip-to-casing clearance in gas turbines. Figure A1.1 shows an arrangement suitable for such an application.

The electronics in Figure A1.1 comprise an oscillator connected by a cable to a probe. The cable is tri-axial comprising an inner conductor, an outer protective layer and an intermediate layer between the outer layer and inner conductor. The inner

This chapter is a revised and extended version of Stringfellow, J.F., Wayman, L. and Knox, B. (1997), ‘Capacitance Transducer Apparatus and Cables’. Patent No. WO 97/28418, 7 August.

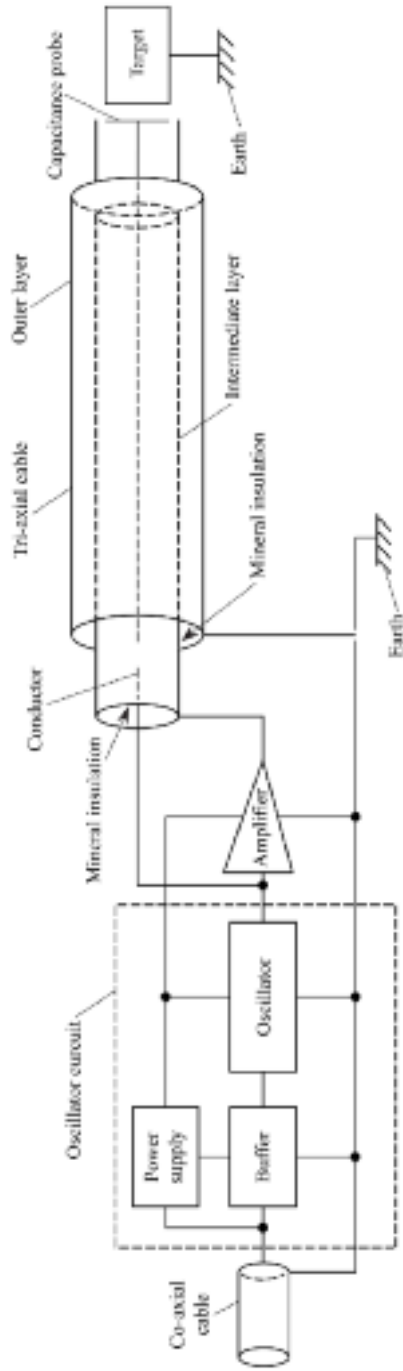


FIGURE A1.1. Schematic illustration of a prior art arrangement of a capacitive clearance measurement system oscillator circuit, tri-axial cable and probe arrangement.

conductor, intermediate layer and outer layer are all electrical conductors. The intermediate layer consists of a material that is different to that forming the outer layer and is of relatively high electrical conductivity. The resistance of the intermediate layer is preferably less than 1 ohm per metre, and ideally less than 0.1 ohm per metre, which one may achieve by forming the intermediate layer from a nickel-based material, and ideally from pure nickel. The reduction in the intermediate layer resistance can lead to the capacitive clearance measurement system's higher sensitivity by enabling a guard driver amplifier in the apparatus to drive the intermediate layer to the same instantaneous voltage as the inner conductor.

Figure A1.1 schematically depicts a target which could be a gas turbine blade and which is electrically connected to earth. Spaced from the target is a capacitance probe. In this configuration, the target acts as an earthed plate of a parallel plate capacitor and the probe as the other plate. A tri-axial cable electrically connects the probe to an oscillator circuit. The oscillator circuit comprises a power supply, a buffer and an oscillator. A unity gain amplifier electrically connects to a power supply and the oscillator output. The buffer, oscillator and unity gain amplifier each electrically connect to earth. A 50 ohm co-axial cable electrically connects to the power supply and buffer to connect the oscillator circuit to a detection circuit (not shown).

In the arrangement which engineers used until now, the tri-axial cable comprised a central stainless steel conductor, electrically connected to the oscillator's output. The tri-axial cable has a stainless steel outer layer which electrically connects to earth and a stainless steel intermediate layer which electrically connects to the amplifier's output. The outer layer acts as a screen against the high-frequency radiation that would otherwise occur. Between the conductor and intermediate layer and between the intermediate layer and outer layer is a mineral insulation material such as silica or aluminium oxide.

Manufacturers, until now, have used stainless steel for the intermediate and outer layers because it imparts the required strength, durability and heat resistance to the cable. In particular, in gas turbine environments, cables encounter high temperatures of approximately 1000°C; therefore, the cable's construction must be such that it will not degrade.

However, as gas turbine technology has advanced, the tri-axial cable length between the probe and oscillator circuit has had to increase. It is important for the oscillator circuit to be located away from the gas turbine's high-temperature body. As gas turbine size and complexity increases, so by necessity does the required cable length. The sensitivity of the frequency modulated driven guard blade tip-to-casing measuring devices using such cabling has decreased as the length of such cable has increased. The performance of existing embodiments of the capacitive clearance measurement device has become unsatisfactory as the cable length has approached about 3 metres.

The present invention's aim is to obviate or overcome disadvantages encountered in the prior art, whether referred to herein or otherwise. In accordance with the present invention's first aspect, the capacitance transducer apparatus comprises an oscillator connected by a cable to a capacitance, whose cable is tri-axial and comprises an inner conductor, an outer protective layer and an intermediate layer

between the outer layer and inner conductor. The inner conductor, intermediate layer and outer layer are all electrical conductors, in which the intermediate layer consists of a material that is different to that forming the outer layer and is of relatively high electrical conductivity.

In this specification, the inventors use the term 'tri-axial' in relation to a cable that has at least three layers. That is, a four-layer cable would still be tri-axial. Substantially reducing, as compared with the prior art, the intermediate layer's resistivity achieves increased sensitivity. Although engineers did not appreciate this before the present invention, it appears that the stainless steel intermediate layer's relatively high resistivity in the prior art has caused high impedance as a result of which the phase shift and amplitude are not maintained along the cable's length. Reducing the cable's total impedance (reactance) by increasing the intermediate layer's electrical conductivity enhances the apparatus' sensitivity considerably and makes accurate distance measurements possible using cable lengths of about 5 metres and more, typically up to about 10 metres (although this is not intended to be an upper limit for use of the present invention). Put another way, the guard driver amplifier needs to be able to drive the capacitance over the cable's full length, which it cannot do if the intermediate layer has a high resistivity.

Normally, the intermediate layer will consist of a different material from that in the outer layer and the central conductor, since one selects the materials employed for the different elements taking into account different properties which the elements require. The outer layer may comprise a drawn metallic material which is preferably capable of withstanding temperatures over about 1000°C, and which resists oxidation at such temperatures. The preferred material for the outer layer is stainless steel.

The intermediate layer will also need to withstand high temperatures, and will preferably have a melting point above 1200°C, but the intermediate layer must also exhibit a relatively low resistance rather than (as the outer layer is required to) oxidation resistance at elevated temperatures. Thus, the intermediate layer's conductivity is preferably substantially higher than that of stainless steel. Manufacturers may employ a nickel-based material for the intermediate layer because it can withstand the required temperatures for annealing the other stainless steel layers, whilst simultaneously exhibiting a sufficiently high conductivity. Preferably, the intermediate layer is a drawn metallic material.

Examples of nickel-based alloys that manufacturers may use for the intermediate layer include alloys of nickel with copper having between 25% and 75% nickel (all percentages given herein by weight) such as cupronickel (approximately 70% Cu and 30% Ni) and Monel (approximately 70% Ni and 30% Cu), and other alloys comprising nickel with chromium or cobalt, Ni Cr Fe Co alloys. Examples of such alloys include those sold under the trademarks Inconel and Incoloy (Incoloy 800 comprises 21% Ni, 0.1% C, 0.5% Cu and the remainder Fe). Alternatively, a manufacturer may employ pure nickel.

A manufacturer may also use non-nickel-based alloys; for example, one may form the intermediate layer from cobalt and cobalt-based alloys or carbon steel. Alternatively, a manufacturer may employ composite materials which have the necessary conductivity and high temperature performance. For example, an intermediate

layer of copper sheathed in stainless steel would have the appropriate conductivity by virtue of the copper and high-temperature strength by virtue of the stainless steel. Preferably, the intermediate layer's resistance is less than 1 ohm per metre and preferably less than 0.1 ohm per metre.

Preferably, the cable's resistance (that is to say, the end-to-end resistance) is less than 2 ohms, preferably less than 1 ohm and ideally less than 0.1 ohm. The central conductor, however, is preferably formed from a material that is relatively tough such as stainless steel. This is required in order to reduce or minimise the degree of powder damage to the central conductor as the cable draws down during manufacturing.

There is a mineral insulator between the inner conductor and intermediate layer and between the intermediate layer and outer layer. The mineral insulator preferably has a relatively low dielectric constant, preferably not more than five and ideally not more than four, in order to reduce the signal's attenuation which the cable transmits. Thus, the mineral insulator preferably is silica or aluminium oxide. However, depending on the cable's length, it is possible to employ higher dielectric constant insulants such as magnesium oxide.

TRI-AXIAL CABLE CONFIGURATION

The present invention provides a tri-axial cable suitable for use as part of a capacitance transducer apparatus, the cable comprising an inner conductor, an outer protective layer and an intermediate layer between the outer layer and central conductor. The intermediate layer consists of a different material from the outer layer and is of relatively high electrical conductivity. The tri-axial cable comprises a central stainless steel conductor, Figure A1.2, a stainless steel outer layer and a nickel intermediate layer. Between the central conductor and the intermediate layer and between the intermediate layer and outer layer is a mineral insulation material.

In its configuration and mode of operation the cable is similar to that in Figure A1.1. However, in the case of the cable according to the present invention, the nickel intermediate layer's substantially lower resistivity ensures maintenance of the phase shift and amplitude along the cable's whole length. This greatly improves the device's sensitivity as compared to that using a stainless steel intermediate layer as in the prior art. Performance over the full range of cable lengths up to 10 metres substantially improves and is significantly indistinguishable from performance at shorter lengths. Performance for all cable lengths should improve.

The tri-axial cable production described herein is within the capability of tri-axial cable manufacturers. By first drawing the central conductor in a known manner, a manufacturer can produce the tri-axial cable. The manufacturer draws and disposes the intermediate nickel layer and outer stainless steel layers concentrically about the central conductor and anneals the layers. The nickel layer is advantageous at this stage compared with, say, copper because it can withstand without significant degradation the required temperatures to anneal the stainless steel. The manufacturer fills the tri-axial cable with mineral insulants such as silica or aluminium oxide.

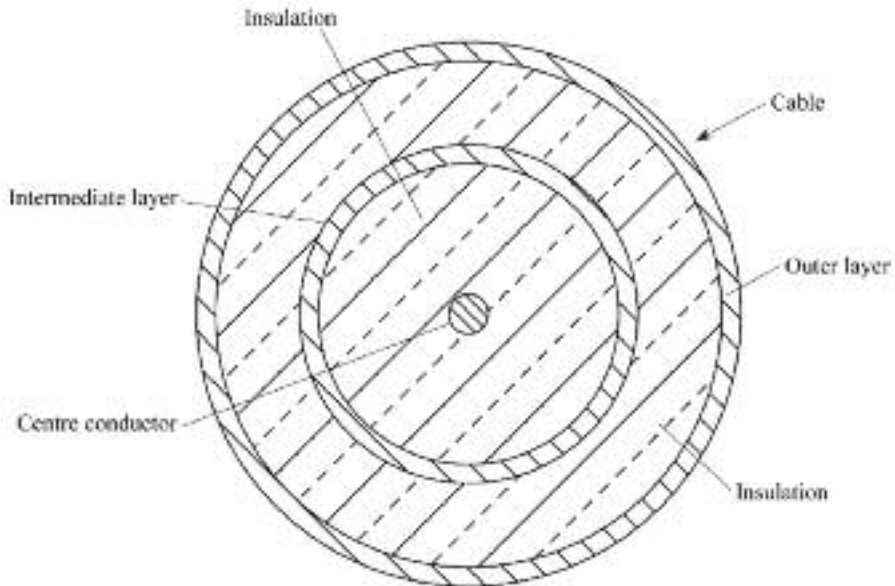


FIGURE A1.2. An enlarged cross-section through a tri-axial cable perpendicular to the longitudinal axis through a cable.

Whilst the inventors have described the cable in relation to its applicability and usefulness as part of a frequency modulated driven guard capacitive clearance measurement system, one can also use it advantageously as part of an amplitude modulation-based capacitance system.

CLAIMS

1. Capacitance transducer apparatus comprising a cable connecting an oscillator to a capacitance, in which the cable is tri-axial comprising an inner conductor, an outer protective layer and an intermediate layer between the outer layer and inner conductor, the inner conductor, intermediate layer and outer layer, all of which are electrical conductors, in which the intermediate layer consists of a material that is different to that forming the outer layer and is of relatively high electrical conductivity.
2. Apparatus as claimed in Claim 1, wherein the intermediate layer has a resistance less than 2 ohms per metre.
3. Apparatus as claimed in Claim 2, wherein the intermediate layer has a resistance less than 0.1 ohm per metre.
4. Apparatus as claimed in any one of Claims 1 to 3, wherein the cable has a resistance of less than 2 ohms.

5. Apparatus as claimed in Claim 4, wherein the cable has a resistance less than 0.5 ohm.
6. Apparatus as claimed in any one of Claims 1 to 5, wherein the intermediate layer comprises a nickel-based material.
7. Apparatus as claimed in Claim 6, wherein the intermediate layer comprises an alloy of nickel with copper, or with chromium or cobalt.
8. Apparatus as claimed in Claim 6, wherein the intermediate layer comprises pure nickel.
9. Apparatus as claimed in any one of Claims 1 to 5, wherein the intermediate layer comprises cobalt, a cobalt-based alloy, carbon steel, or a composite material.
10. Apparatus as claimed in any one of Claims 1 to 9, wherein the cable includes mineral insulation between the central conductor and intermediate layer and between the intermediate layer and the outer layer.
11. Apparatus as claimed in Claim 10, wherein the mineral insulation has a dielectric constant of not more than five.
12. Apparatus as claimed in Claim 10 or Claim 11, wherein the mineral insulation is silica or aluminium oxide.
13. Apparatus as claimed in anyone of Claims 1 to 12, which measures blade tip-to-casing clearance in a gas turbine.
14. A tri-axial cable suitable for use as part of a capacitance transducer apparatus, the cable comprising an inner conductor, an outer protective layer and an intermediate layer between the outer layer and central conductor, in which the intermediate layer consists of a different material from the outer layer and is of relatively high electrical conductivity.

Gap Measurement Device

A.G. Sheard and D.C. Lawrence

ABSTRACT

This Appendix is adapted from the patent 'Gap measurement device'. The adaption aims to make the invention presented in the patent more accessible to the reader, without significantly altering the patent's content.

A need to eliminate the capacitive link between a tri-axial cable's inner conductor and outer protective layer inspired the research resulting in the intellectual property that forms the basis of the patent. The inventors eliminated the capacitive link by extending a tri-axial cable's intermediate layer to the sensor's front face. It is the sensor's design with an intermediate guard extending to its front face that comprises the invention which this patent presents. In combination with the electronics and tri-axial cable described in the patent that forms the basis of Appendix 1, the electronics-cable-sensor combination facilitated practical embodiments of the capacitive clearance measurement system suitable for use in gas turbine development and production applications, as opposed to instrumentation research applications.

INTRODUCTION

The present invention relates to the measurement of gaps to discontinuous targets, especially to the blade tip-to-casing clearance measurement between gas turbine compressor and turbines blades, and the casings within which they run. The present invention also relates to the measurement of gaps to continuous targets, especially to clearance measurement between compressor and turbine discs and the static structural components within a gas turbine.

This chapter is a revised and extended version of Sheard, A.G. and Lawrence, D.C. (1998), 'Gap Measurement Device'. US Patent No. 5,760, 593, 2 June.

This invention provides a sensor for capacitively measuring the distance to an object. The sensor comprises an electrode that will couple capacitively with the object. A shield which is electronically isolated surrounds the electrode by means of an insulated layer. The intermediate layer is also electrically isolated from an outer protective layer by means of an insulation layer. One applies the insulation layer over at least part of the electrode, so that the insulation surrounds the electrode. Similarly, the shield is isolated from the outer protective layer by depositing a layer of insulation over at least part of the shield, so that the insulation surrounds the shield.

Background to the invention

In many fields and especially in the case of gas turbines, there is a need for a gap measurement sensor that is able to function at high temperatures, for example in the order of 1000°C or more, in order to improve gas turbine thermodynamic efficiency. Researchers are conducting studies to increase sensor working temperature to 1200°C or higher. In such environments it is not possible to employ sensors that rely on permanent magnetism of materials, and it is important to ensure that the use of all materials to manufacture the sensor can withstand the temperatures. For this reason, the inventors have proposed the use of capacitance sensors in turbine applications.

One use of such sensors in the case of turbines is to measure the clearance between the turbine blades' tips and the casing in which they run. It is highly desirable to minimise this clearance in order to maximise turbine efficiency. A gap of 1 mm would be typical of current turbines, although reducing this further is desirable. In order to achieve such small clearances, it is necessary to provide sensors that are located in the turbine casing and detect turbine blade presence as they pass the sensor. Such a sensor typically comprises four components. First, an electrode will couple capacitively with the turbine blade. Second, a shield is located between the electrode and the turbine casing. Third, a sensor body that surrounds the shield enables the sensor to fit precisely in the provided recess in the casing. Fourth, an insulator between both the electrode and shield and the shield and retainer electrically isolates the electrode and shield from the casing. The electrode connects to the tri-axial cable's centre conductor, and the shield to the cable's intermediate screen whilst the retainer or the housing connects to the cable's outer screen which removes the signals from the sensor. The signal from the electrode passes to the shield via a unity gain amplifier so that it screens the electrode signal from ground (the casing) by means of a buffered version of itself.

In the arrangement which manufacturers used until now the requirement for the sensor to operate at a temperature around 1000°C meant that the insulating elements within the sensor required manufacturing from machined ceramics. Furthermore, the insulating elements which are in the form of rings had as small a wall thickness as possible in order to maximise the electrode's size, which increased the sensor's sensitivity, but also increased the manufacturing difficulty. In addition, sensor assembly is a highly skilled operation which adds to the final product's cost.

Summary of the invention

According to the present invention, Figure A2.1, there is a device for capacitively measuring the distance to an object, which comprises an electrode that will couple capacitively with the object. A shield is located about the electrode and electrically isolates it from the electrode by means of insulation, and a layer of insulation that surrounds the shield, wherein deposition forms the insulation between the electrode and the shield and the insulation that surrounds the shield.

The device, according to the invention, has the advantage of a significantly reduced manufacturing cost due to the removal of two physical components (the ceramic insulating rings) that are difficult to machine, and their replacement by deposited layers which are simple and inexpensive to form. In addition, because of the insulation between the electrode and the shield, and the insulation surrounding the shield, it will be much thinner than the radial thickness of any preformed ceramic ring. The electrode's diameter can therefore significantly increase for any given sensor size, thereby increasing the sensor's sensitivity.

The sensor may, if desired, include a shield as a preformed part, in which case the insulation between the electrode and shield and the insulation between the shield and the casing may both deposit on the shield. Elimination of the machined ceramic components results in machining the sensor components solely from metal.

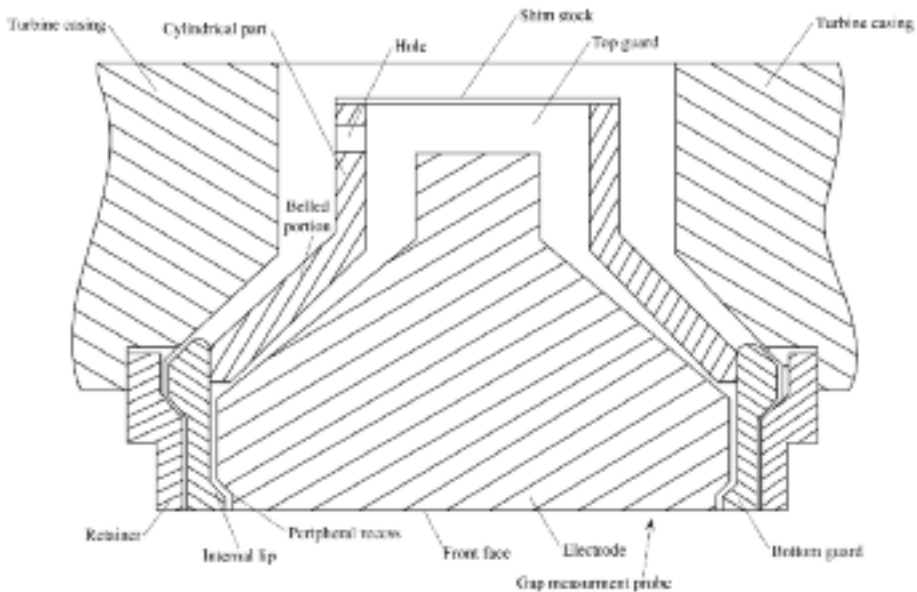


FIGURE A2.1. A section through a practical embodiment of the sensor's first form according to the invention.

Alternatively, the insulation between the electrode and the shield may deposit on the electrode instead of the shield. If desired, one may deposit the insulation between the shield and the housing on the shield. However one forms the shield, the preference is to enclose the electrode entirely with the exception of the electrode that will couple capacitively with the object. By enclosing the electrode completely, the sensor design eliminates capacitive coupling with any other elements such as a gas turbine casing. One may manufacture the sensor body as a separate part if desired. Alternatively, one may form the sensor body by depositing a metallic layer over an insulating layer which is already deposited on the shield. This sensor form has the advantage that it can form as a single, monolithic item, thereby not only removing the expensive machining operations for forming the ceramic insulation rings, but also removing the sensor's skilled assembly process.

An additional advantage of this sensor form is that it will not be the subject of differential thermal expansion of its component parts in operation. If one used a conventional sensor for turbine blade tip-to-casing clearance measurement, the metal and ceramic parts' differential thermal expansion could loosen them to some degree when the sensor heats to the normal operating temperature of about 1000°C. Also, the difference in pressure on either side of the turbine blades as they pass the sensor applies a vibrating force on the electrode at a frequency up to 6000 Hz. This causes the sensor electrode to apply a vibrating shearing force on the ceramic insulating rings. In some instances, for example with certain turbochargers, the vibrating force can have a frequency as high as 100 kHz. This shearing force could, after a prolonged operation time, cause damage to the ceramic rings which would lead to catastrophic system failure if the sensor became detached from the casing. In contrast, with the sensor according to the invention, the entire sensor can form substantially from the same material, thereby avoiding the problems of differential thermal expansion. Furthermore, removing the ceramic rings, which are relatively poor thermal conductors, can reduce temperature differences over the sensors' different regions.

Although for many purposes a solid metal body may form the electrode, this approach has the disadvantage that its operating temperature is limited to the metal's maximum operating temperature, for example around 1125°C in the case of steel. According to a preferred aspect of the invention, the electrode forms as a ceramic body and depositions form the shield, together with the layers of insulation between the electrode and the shield and between the shield and the housing. A layer of conductive material, for example metal, deposited on the ceramic can render the electrode conductive. Alternatively, the ceramic body could form as a conductive ceramic/metal composite. In this way, it is possible to form a sensor which contains no bulk metal parts, and so it can operate at significantly higher temperatures, for example up to 1200°C or higher. This method might make it possible to form a stoichiometric sensor for turbine use in which fuel burns a stoichiometric quantity of oxygen in order to maximise the gas turbine's thermodynamic efficiency.

Any method that will generate a layer that has the necessary adhesion and thermal stability to enable it to operate at the relevant temperature, for example 1500°C, may form the deposition layers. Deposition, for example, may form the layers in the condensed phase, for instance by sol-gel methods which involve the hydrolysis and

polycondensation of a metal alkoxide. These can include silicon tetraethoxide, titanium butoxide or aluminium butoxide which produce an inorganic oxide gel which a low-temperature heat treatment converts to an inorganic oxide glass. Alternatively, other deposition techniques may form the layers, for example, vacuum deposition methods such as plasma-assisted chemical vapour deposition, sputtering or, preferably, plasma deposition. All of these processes are well known and commercially employed for a number of purposes.

In the case of plasma deposition, the component spins in a vacuum whilst a ceramic or metal powder sprays through an arc or flame that flashes it into plasma. As the plasma hits the cold spinning part, it condenses, forming a layer of ceramic or metal. Each layer of insulation or metal may form as a single layer only, or if desired, may build up from a number of layers. One or more keying layers may provide improved adhesion between the top layer and the substrate. For example, a different vacuum deposition process or having a different stoichiometry from that of the top layer form the keying layer or layers so that the layers' properties are graded over the total thickness. The insulating layers that these methods deposit are generally metal or metalloid oxides and nitrides. These include aluminium oxides and nitrides, titanium, tantalum and silicon, or combined mixtures. Thus, the inventors also envisage the use of mixed metal oxides for the layers. However, the invention, at least in its broadest aspect, is not limited to any particular deposition technique.

Thus, another aspect of the invention provides a method of forming a device for capacitively measuring a turbine blade tip-to-casing clearance. This comprises forming an electrode that will couple capacitively with the turbine blade, depositing a layer of insulation over at least that part of the electrode that will be located in the casing, depositing a layer of metal over the insulation to form a shield, and depositing a second layer of insulation over the shield. One may employ this manufacturing method for forming any of the devices described above.

The layers may form to any thickness that is appropriate to the layer's function. For example, in the case of the shield and the electrode, a thickness from 0.01 to 1.00 μm , preferably from 0.10 to 0.20 μm , is appropriate in order to provide the necessary electrical conductivity, whilst for the layers of electrical insulation thicknesses from 0.20 to 0.50 μm are appropriate. However, according to a preferred aspect of the invention, the electrode part that faces the object (the 'front face'), especially where the sensor measures turbine blade tip-to-casing clearance, may form with a significantly greater thickness, for example, with a thickness greater than 0.5 mm, preferably in the range of 0.5 to 2 mm and especially from 0.75 to 1.5 mm. Such a layer can form so that the layer is softer than the material forming the turbine blade. The turbine blade must abrade it, thereby ensuring a very small and controllable gap between the blade and the electrode's front face.

Although one could manufacturer the sensor in its entirety before installation in the casing, it is possible to form the sensor without the electrode's front face, to install the sensor in the casing and only then to deposit the electrode's front face. One can then machine the electrode's front face to the required level leaving the sensor flush with the inside of the casing. During gas turbine operation, a blade tip could erode the casing liner and the sensor's front face, but still leave the sensor opera-

tional. This would result in the sensor giving an output of true blade tip-to-casing clearance after a rub as the sensor tip would still be flush with the casing inner diameter. In contrast, conventional sensors are not abradable, and are recessed in the casing. After the first rub, the distance from the sensor front face to the casing inner diameter changes and all clearance readings are incorrect from that point on.

Although described principally with reference to turbines (since the turbine within a gas turbine generally provides the most demanding environment), one can use the device according to the invention for gap measurement in general and can function at temperatures up to the limit of the materials from which it forms. One can employ it anywhere in a gas turbine, steam turbine or other turbomachinery, reciprocating engine or other equipment requiring measurement of gap size.

Detailed description of the invention

Referring to the accompanying drawings, Figure A2.1 shows the gap measurement sensor for determining the turbine blade tip's position (not shown) with respect to the turbine casing. The sensor comprises an electrode formed from steel having a front face that directs itself toward the turbine and across which the turbine blade tips pass as the turbine rotates. The electrode is located within a shield which comprises a bottom guard and a top guard, each of which is also machined from steel. The bottom guard has an internal lip that engages a peripheral recess in the electrode in order to ensure that the electrode cannot slide forward out of the bottom guard toward the turbine blades, and the top guard has a generally frusto-conical belled portion and cylindrical portion. The belled position is capable of engaging the electrode's rear shoulder to prevent the electrode sliding backwards into the gas turbine casing. A retainer which seats the bottom guard, top guard and electrode is located around the outside of the bottom guard within a recess in the gas turbine casing.

Plasma has deposited on the bottom guard with a 0.2 mm thick insulation layer formed from aluminium nitride. The deposited insulation layer covers the bottom guard's entire surface except for those parts which are in contact with the top guard. When assembled, the metal forming the top guard becomes electrically insulated from both the electrode and the turbine casing. The top guard is similarly coated, although it may entirely separate from both the electrode and the casing by means of an air gap. The electrode connects to the tri-axial cable's centre conductor (not shown) by conventional means, whilst the screen (which the top and bottom guards form) connects to the tri-axial cable's intermediate screen. A unity gain amplifier sets the screen voltage to that of the electrode, so that it will prevent any capacitive coupling between the electrode and the turbine casing which is at ground potential. The sensor forms in a simple and inexpensive manner, without the need to form any parts from ceramics by machining, and can withstand any temperature up to the steel parts' maximum working temperature.

In order to assemble the sensor, the top guard and the bottom guard slip over opposite ends of the electrode and butt together or otherwise engage so that they enclose the electrode in such a way that the internal lip firmly holds between the

bottom guard and the top guard's belled portion. Although there are clearances between the assembly's various parts, this is simply for the sake of clarity. It is best to weld the top guard and bottom guard and drill a hole through the top guard's cylindrical part, generally at the electrode's end to enable insertion of the tri-axial cable. Next, cut back the cable (not shown) and insert it through the hole and the cable's central wire, brazing it to the electrode's end face and brazing the intermediate screen to the top guard. Then, drop the sensor into the recess in the gas turbine casing and the retainer which is located around the electrode and top guard and welded to the casing. This prevents the sensor from sliding out of the casing recess toward the turbine blades. Then weld the tri-axial cable's outer screen to the gas turbine casing, and spot-weld a thin piece of shim stock over the top guard's end so that a shield surrounds the entire electrode which formed the top and bottom guards with the exception of the sensor front face. Then place a ceramic packing disc (not shown) over the end of the top guard's cylindrical portion and position a metal disc (not shown) over the packing disc to close the recess in the casing, and tack-weld it to the casing.

Figure A2.2 schematically shows a similar form of sensor to that in Figure A2.1, but in which the electrode has a first ceramic insulating layer over its entire surface (including the front face), followed by a 0.3 mm thick layer of platinum / iridium (excluding the front face) which forms the shield, and finally a further 0.2 mm thick layer of ceramic which insulates the shield from the turbine casing. The sensor corresponds to the electrode's assembly, bottom guard and top guard which Figure A2.1 shows. It can secure itself in the gas turbine casing's recess and operate exactly as the sensor which Figure A2.1 illustrates. The sensor has the advantage that the machining needs to form only one element, the electrode, thereby reducing manufacturing costs.

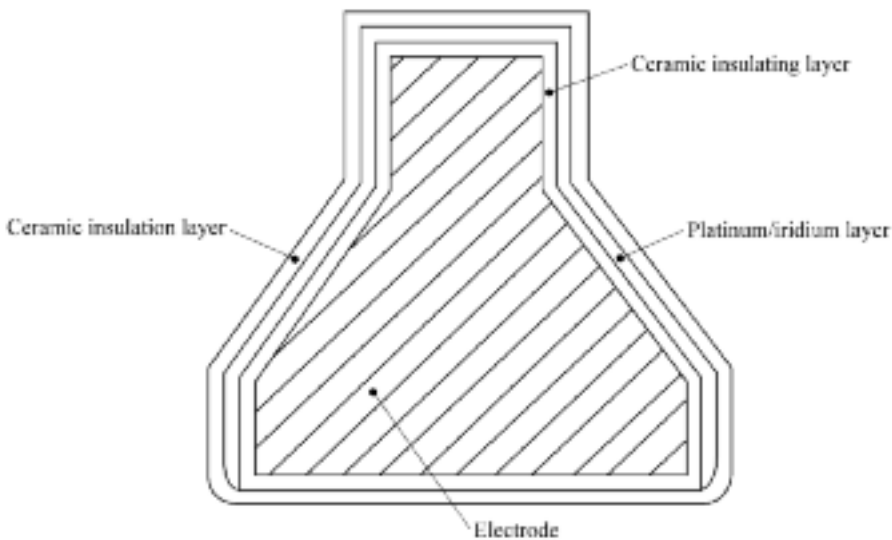


FIGURE A2.2. Schematic representation of the sensor's second form according to the invention.

Figure A2.3 shows a sensor modification (see Figure A2.2) in which a ceramic core forms an electrode body on which plasma deposition has deposited a platinum / iridium layer. The insulation layers and the shield form on the electrode as described above with reference to Figure A2.2. This sensor form has the advantage that it contains no metal parts. A ceramic component forms the only bulk part, and so it is possible for this sensor to withstand significantly higher temperatures, for example in excess of 1200°C without failing.

Figure A2.4 schematically shows a sensor improvement (see Figure A2.3) in which the electrode's front face forms as a relatively thick metal coating which has deposited in the form of a relatively low density, porous metal layer or a metal / ceramic composite. The layer forming the front face has about a 1 mm thickness and is relatively soft (compared with the ceramic or the turbine blade), so that, after installation, the turbine blades may abrade the electrode's front surface, thereby forming a small and controllable gap between the two.

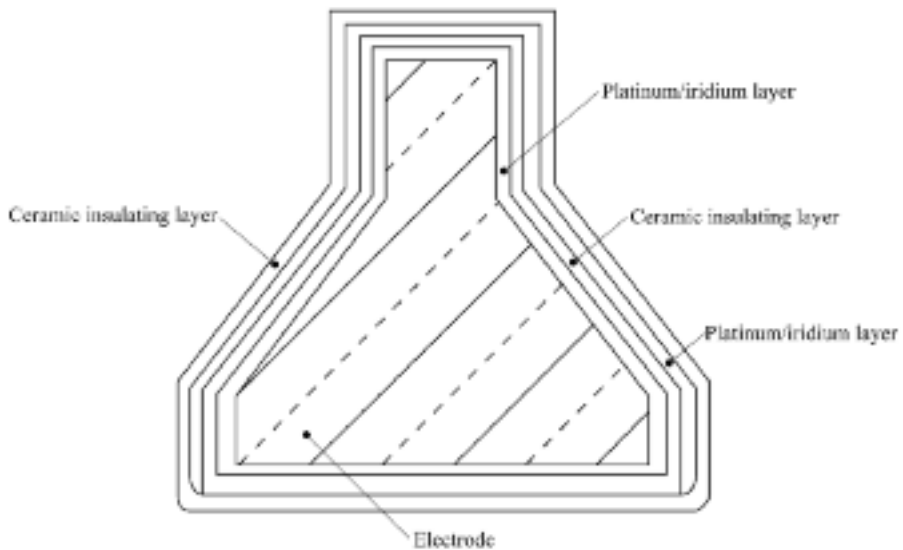


FIGURE A2.3. Schematic representation of the sensor's third form according to the invention.

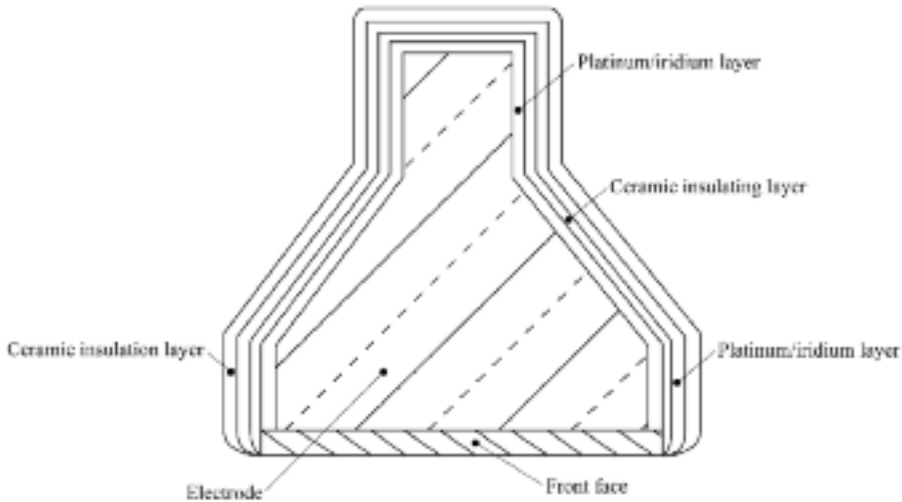


FIGURE A2.4. Schematic representation of the modified form of the sensor in Figure A2.3.

CLAIMS

1. A device for capacitively measuring the blade tip-to-casing clearance in the turbine of a gas turbine which comprises an electrode that will couple capacitively with the turbine blade. The device comprises the following: a part which faces the turbine blade, a deposited electrically conductive layer which faces the turbine blade, a shield that surrounds the electrode except in the electrically conductive layer, a deposited ceramic insulation coating between the electrode and shield such that the insulation electronically isolates the shield from the electrode, and a deposited ceramic insulation layer surrounds the shield.
2. A device, as claimed in Claim 1, which contains the shield as a preformed part, and the insulation between the electrode and the shield, and the insulation that surrounds the shield, have both been formed on the shield by deposition.
3. A device, as claimed in Claim 1, wherein the insulation located between the electrode and the shield has deposited on the electrode.
4. A device, as claimed in Claim 3, wherein the shield has formed on the insulation deposited on the electrode by deposition.

5. A device, as claimed in Claim 4, wherein the insulation that surrounds the shield has formed on the shield by deposition.
6. A device, as claimed in Claim 5, wherein the electrode forms as a solid metal body.
7. A device, as claimed in Claim 5, wherein the electrode comprises a solid ceramic body on which an electrically conductive layer has been deposited.
8. A device, as claimed in Claim 7, wherein the deposited electrically conductive layer on the electrode part that faces the turbine blades has a thickness of at least 0.5 mm.
9. A device, as claimed in Claim 8, wherein the deposited layer of insulation comprises a metal or metalloid oxide or nitride.
10. A device, as claimed in Claim 9, wherein one uses a vacuum deposition method to deposit any deposited layer.
11. A device, as claimed in Claim 10, wherein a chemical vapour deposition method, a sputtering method or a plasma deposition method has formed any deposited layer.
12. A device, as claimed in Claim 1, wherein that electrode's part which faces the turbine blades deposits an electrically conductive layer of a relatively low density, porous metal that is relatively soft so that the turbine blades can abrade the conductive layer, thereby forming a small and controllable gap.
13. A device, as claimed in Claim 12, wherein the deposited electrically conductive layer on the electrode part that faces the turbine blades is about 1 mm.
14. A device, as claimed in Claim 1, wherein the deposited electrically conductive layer on that electrode's part that faces the turbine blades is of a metal/ceramic composite that is relatively soft so that the turbine blades can abrade the conductive layer, thereby forming a small and controllable gap.
15. A device, as claimed in Claim 1, wherein the deposited electrically conductive layer on that electrode's part that faces the turbine blades is about 1 mm thick.

Capacitive Gap Measurement Device

A.G. Sheard

ABSTRACT

This Appendix is adapted from the patent ‘Capacitive gap measurement device’. The adaption aims to make the invention presented in the patent more accessible to the reader, without significantly altering the patent’s content.

A need to eliminate the mechanical joint between a tri-axial cable and sensor inspired the research resulting in the intellectual property that forms the basis of the patent. This mechanical joint has to survive in a hot and high-vibration environment, over a gas turbine’s compressor or turbine blades. The mechanical joint is a weak point in the capacitive clearance measurement system, and as a consequence of the harsh operating environment, prone to failure. The approach which this patent presents forms the basis of this Appendix and facilitates a practical embodiment of the tri-axial cable and sensor which form as a single component without a mechanical joint between the two. Although not required in research and development applications, elimination of the mechanical joint increases sensor life and makes it suitable for use in production gas turbine applications such as a closed loop clearance control system where the sensor must survive from one planned gas turbine maintenance outage to the next.

INTRODUCTION

In many fields, and especially during the development of gas turbines, there is a need for a gap measurement sensor that is able to function at high temperatures, for example in the order of 1000°C or more. A gas turbine can achieve improved thermodynamic efficiency with a higher turbine entry temperature. The inventor therefore conducted research to increase gap measurement sensor working temperature, for example to 1200°C or higher. In such high-temperature environments it is not

This chapter is a revised and extended version of Sheard, A.G. (2000), ‘Capacitive Gap Measurement Device’. Patent No. GB 2 325 305 B, 19 April.

possible to employ sensors that rely on the permanent magnetism of materials. It is important to ensure that all materials that one uses to produce the sensor can withstand the high temperatures involved. For this reason, the inventor proposed capacitance sensors for use in turbines.

One use of a high-temperature gap measurement device is in the turbines to measure the blade tip-to-casing clearance. It is highly desirable to minimise this clearance in order to maximise the turbine's efficiency. A 1mm gap is typical of current turbines, although it is desirable to reduce this further. In order to achieve such small clearances, it is necessary to provide sensors that are located in the casing within which the turbine blades rotate, with the sensor then detecting the presence of each blade as it passes the sensor. Such a sensor typically will comprise an electrode that will couple capacitively with the turbine blade, a shield that is located between the electrode and the turbine casing, a sensor body that surrounds the shield and enables the sensor to fit precisely in the recess in the casing, and insulation provided between the electrode and shield and also between the shield and retainer in order to electrically isolate the electrode and shield from the casing. The electrode connects to the tri-axial cable's centre conductor, and the shield to the cable's intermediate screen whilst the retainer or the housing connects to the cable's outer screen which removes the signals from the sensor from the turbine's vicinity. The signal from the electrode passes to the shield via a unity gain amplifier, screening the electrode signal from ground (the casing) by means of a buffered version of itself.

Such a sensor will function quite satisfactorily to enable maintenance of a blade tip-to-casing clearance at about 1 mm, but it is expensive to manufacture. The sensor should operate at an approximate temperature of 1000°C which means that the insulating elements require manufacturing from machined ceramics. Furthermore, the insulating elements, which are in the form of rings, will have as small a wall thickness as possible in order to maximise the electrode's size (which increases the sensor's sensitivity), thereby increasing the difficulty and cost of manufacturing. In addition, sensor assembly is a highly skilled operation which adds to the final product's cost.

According to the present invention, there is a method of forming a sensor for capacitively measuring the distance to an object together with a composite cable, which comprises the following four steps:

1. providing the interior of a metal tube with a longitudinally extending conductor and a mineral insulant (normally in the form of a compacted powder) so that the interior is substantially filled with the conductor and insulant;
2. locating the metal tube within the bore of a larger tube after the metal tube's exterior surface or the larger tube's interior surface has a deposited layer of insulating material;
3. drawing the assembly of tubes so formed through a reducing die with the exception of one end to form a smaller cable part diameter than the said one end, and;

4. providing an electrode at the assembly's said one end to form the sensor, which the electrode substantially extends over the entire surface of exposed mineral insulant and is in electrical contact with the conductor.

The method, according to the invention, has the advantage that it enables the manufacturing of a gap measurement sensor at a significantly reduced cost due to the removal of two physical components (the ceramic insulating rings) that are difficult to machine, and their replacement with mineral insulant and a deposited layer of insulation. The composite sensor and cable manufactured in accordance with the invention has the further advantage that the sensor's various component parts will suffer from differential thermal expansion in operation to a lesser extent than conventional sensors. If one were to use a conventional sensor for turbine blade tip-to-casing clearance measurement, differential thermal expansion of the metal and ceramic parts could cause them to loosen to some degree when heating the sensor to the normal operating temperature of about 1000°C. Also, the difference in pressure on either side of the turbine blades as they pass the sensor applies a vibrating force on the electrode at a frequency up to 6000 Hz, which causes the sensor electrode to apply a vibrating shearing force on the ceramic insulating rings. In some instances, for example with certain turbochargers, the vibrating force can have a frequency as high as 100 kHz. This shearing force could, after a prolonged operation time, cause damage to the ceramic rings which would lead to the system's catastrophic failure if the sensor became detached from the casing.

One may conduct the four steps in the manufacturing process in any appropriate order. For example, one may perform steps (step 1 and step 2) in either order: one may assemble the inner tube, conductor and mineral insulant, and then locate them in the metal tube, or alternatively, one may first coat either tubes' relevant surface with insulant, assemble the two tubes, and only then introduce the conductor and mineral insulant into the inner tube. It is possible to provide for either the metal tube's interior surface or the inner tube's exterior surface with the deposited layer of insulating material, although it is normally preferable, for ease of processing, for insulation to provide the inner tube's exterior surface.

It is possible for the initial, undrawn, assembly of tubes to have the appropriate diameter for the sensor, in which case the only drawing step(s) required are to reduce the diameter of that part of the assembly that will become the cable (step 3). However, in most cases, the process will require an initial drawing step in which the assembly of tubes' diameter substantially draws down to the sensor's intended final diameter. Such a method has the advantage that one may employ it to manufacture a range of different diameter sensors', the only difference is the size of the drawing die. In addition, one may use the initial drawing step for accurate sensor diameter dimensioning after one has assembled the various component parts of the assembly (the tubes, conductor and mineral insulant).

At some stage in the manufacturing process, it is preferable to seal the two tubes together at the end that forms the sensor, in order to prevent any escape of insulating material from between them. One may achieve this in a number of ways,

and at different steps in the process, but preferably a glass / ceramic sealing step performs this in which one chooses the material composition such that the material has a softening or melting point sufficiently high to withstand further processing or service conditions that one needs to complete the manufacturing of the composite structure and to which one will subject the sensor in service.

A suitable material for such a seal is glass powder, or pre-form of the necessary dimensions, having a melting point at least 100°C above the sensors' maximum operating temperature intended application. In addition, the material is advantageously impervious to and unreactive with moisture and should have sufficient adhesion to the composite structure's components (tubes in particular) to withstand the dynamic (vibration and shear) forces associated with manufacturing. Producing a thin oxide layer on the tubes using a controlled oxidation treatment may improve adhesion/sealing. It is preferable to perform the sealing step after drawing down the assembly of tubes, but before electrode application.

Normally, there is a recess in the mineral insulant's exposed surface after the drawing step (and sealing step, if any) and a layer of ceramic material deposits on the assembly's end. The ceramic material isolates the tube's interior which forms the guard from the electrode. After the layer of ceramic has been deposited, one cleans the exposed end of the conductor and fills the recess with metal to form the electrode. One may form the electrode as a separate component that inserts into the recess, or may deposit it.

The layer that deposition forms (the layer of insulating material between the tubes) and any other layer that deposition forms, may form by any method that will generate a layer that has the necessary adhesion and thermal stability to enable it to operate at the relevant temperature, for example, at 1000°C, 1200°C or 1500°C. Deposition may form the layers, in principle, in the condensed phase, for instance, by sol-gel methods or other deposition techniques. This can be vacuum deposition methods such as plasma-assisted chemical vapour deposition, by sputtering or, preferably, by plasma deposition, all of which processes are well known and commercially employed for a number of purposes. In the case of plasma deposition, the component spins in a vacuum whilst one sprays a ceramic or metal powder through an arc or flame that flashes it into a plasma. As the plasma hits the cold spinning part, it condenses, forming a layer of ceramic or metal.

Each layer of insulation or metal may form as a single layer only, or if desired may build up from a number of layers. For example, one or more keying layers may improve the adhesion between the top layer and the substrate, the keying layer(s) forming, for example, by a different vacuum deposition process or having a different composition or stoichiometry from that of the top layer so that the layers' properties are graded over the total thickness. The insulating layers, which these methods deposit, are generally oxides and metal or metalloid nitrates. For example, they can be oxides and aluminium, titanium, tantalum and silicon nitrates, or mixtures thereof with themselves or with other oxides or nitrides. Thus, the inventor envisages use of mixed metal oxides for the layers. Note, however, that the invention, at least in its broadest aspect, is not limited to any particular deposition technique.

The layers may form to any thickness that is appropriate to the layer's function. For example, in the case of the electrode, a thickness from 0.01 to 1.00 μm , preferably from 0.10 to 0.20 μm will be appropriate in order to provide the necessary electrical conductivity, whilst for the electrical insulation layer, thicknesses from 0.20 to 0.50 μm will be appropriate. However, according to a preferred aspect of the invention, the electrode may form with a significantly greater thickness, for example, with a thickness greater than 0.5 mm, preferably in the range from 0.5 to 2 mm, and especially from 0.75 to 1.5mm. This is especially useful where one intends to use the sensor to measure turbine blade tip-to-casing clearance. Such a layer can form so that the layer is softer than the material forming the turbine blade, and the turbine blade can abrade it, thereby ensuring a very small and controllable gap between the blade and the electrode's front face.

Although a manufacturer could produce the sensor in its entirety before installation in the casing, it is possible to form the sensor without the electrode's front face, to install the sensor in the casing and only then to deposit the electrode's front face. One can then machine the electrode's front face back to the required level, leaving the sensor flush with the casing. During gas turbine operation a blade tip could erode the casing liner and the sensor's front face, but still leave the sensor operational. This would result in the sensor giving an output of true tip clearance after a rub as the sensor tip would still be flush with the casing inner diameter. In contrast, conventional sensors are not abradable, and are recessed in the casing. After the first rub, the distance from the sensor front face to the casing inner diameter changes and all clearance readings are incorrect from that point on.

According to another aspect, the present invention provides a device for capacitively measuring the distance to an object comprising an assembly having a sensor and a cable formed integrally with the sensor. The assembly includes a tri-axial cable with a solid central conductor, a shield that surrounds the conductor and is insulated by means of a mineral insulant. An outer metal tube surrounds the shield and is insulated by means of a solid insulating material. The tri-axial cable has a generally constant diameter, but an increased diameter at one end part which forms the sensor. It also has an electrode that extends over the sensor's electrode which electrically connects to the central conductor and is electrically isolated from the shield and from the outer metal tube.

Although described principally with reference to turbines (since such applications generally provide the most demanding environment), one can use the sensor formed according to the invention for gap measurement in general and it can function at temperatures up to the limit of the materials from which it forms. One can employ it anywhere in a gas turbine, steam turbine or other turbomachinery, reciprocating engine or other equipment requiring measurement of gap size.

The following narrative will now describe one sensor form according to the present invention by way of example with reference to Figure A3.1, a schematic section through the composite sensor and tri-axial cable. A composite sensor and cable for capacitively measuring a clearance to a turbine blade comprises a sensor and a tri-axial cable part formed integrally therewith. The sensor and cable part each comprise

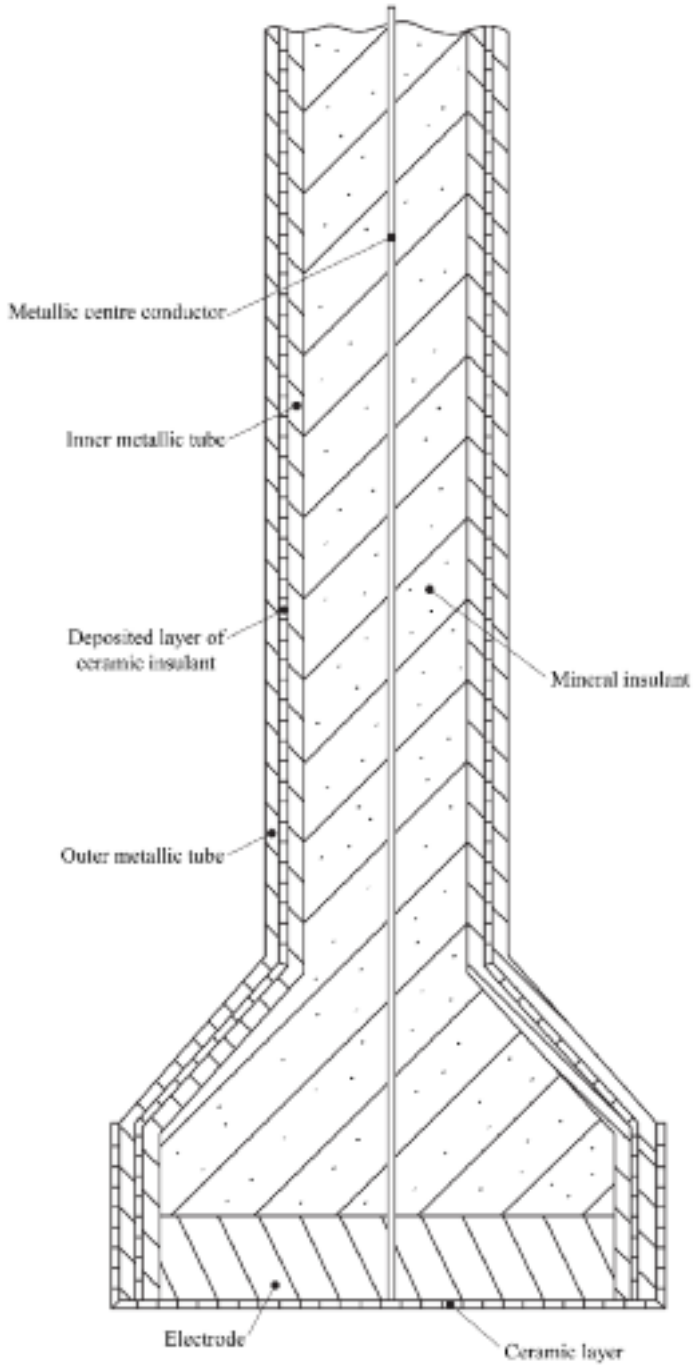


FIGURE A3.1. Schematic section through the composite sensor and tri-axial cable.

a central conductor that is located centrally along the length of an inner tubular part that forms a screen and which is located within an outer tubular part that forms a guard. One fills the interior of the inner tubular part that is not occupied by the conductor with a mineral insulant, for example magnesium oxide or silica. The guard is located in a recess in the turbine's housing, and a deposited layer of ceramic insulant electrically insulates it from the screen. There is a recess in the mineral insulant's end surface in which an electrode connected to the central conductor is located. A thin layer of ceramic covers the assembly's end forming the sensor.

One forms the composite assembly by first forming a pre-form comprising a hollow stainless steel tube of outer diameter of about 8 mm which contains a central nickel or stainless steel conductor rod and mineral insulant by methods that are conventional for forming mineral-insulated cable. The pre-form will have a length in the range of 1 to 10 metres depending on the turbine's dimensions and geometry which the assembly intends to fill. One then deposits a ceramic insulating layer about 0.1 mm in thickness on the hollow tube's outer surface by means of a flame-spraying method, and then slides the tube into a tube whose internal diameter is such as to enable the coated tube to fit snugly.

The assembly passes through one or more die drawing steps until the tube's outer diameter corresponds to the sensor's intended final diameter (other than any changes that the sensor's coating will cause), for example about 6 mm. The assembly is then subjected to a further drawing step in which the assembly's part that constitutes the cable (the assembly's entirety with the exception of one end which will form the sensor) draws down further to a diameter of about 3 mm.

After drawing the assembly to the required size, fused glass or silica seal the ends of the tubes in order to seal the insulating layer between the tubes. A recess then forms in the sensor's end by removing all the mineral insulant to a depth of about 0.5 mm. One then flame sprays a thin layer of ceramic over the recessed end in order to coat the tube's exposed internal surface. One then cleans the central conductor's exposed end by forming the recess in the mineral insulant to remove the flame-sprayed ceramic. One also flame sprays an electrode to form a 0.5 mm thick metal (usually nickel) layer into the recess. Finally, one flame sprays the sensor's entire end and side face with ceramic in order to protect the underlying metalwork.

CLAIMS

1. A method of forming a sensor for capacitively measuring the distance to an object together with a composite cable, which comprises four steps:
 - (1) providing the metal tube's interior with a longitudinally extending conductor and a mineral insulant so that the interior is substantially filled with the conductor and insulant;
 - (2) locating the metal tube within a larger tube's bore after the larger tube's interior surface's or smaller tubes exterior surface receives a deposited layer of insulating material;

- (3) drawing the so-formed tube assembly through a reducing die with the exception of one end to form a smaller diameter cable part than the said one end;
- (4) providing an electrode at the assembly's said end to form the sensor, which the electrode substantially extends over the entire exposed mineral-insulant surface and is in electrical contact with the conductor.
2. A method, as claimed in Claim 1, wherein the metal tube's exterior surface has the insulating material applied in step 2.
3. A method, as claimed in Claim 1 or Claim 2, which includes an initial drawing step in which the assembly of tubes' diameter substantially draws down to the sensor's intended final diameter.
4. A method, as claimed in any one of Claims 1 to 3, wherein the inner tube is located within the outer tube before the conductor and the mineral insulant are located in the inner tube.
5. A method, as claimed in any one of Claims 1 to 4, wherein a vacuum deposition method provides the electrode.
6. A method, as claimed in any one of Claims 1 to 5, wherein a recess is formed in the exposed mineral insulant at the assembly's said one end in order to accommodate the electrode.
7. A method, as claimed in Claim 6, which includes depositing a layer of insulating material on the assembly's said one end after formation of the recess in the mineral insulant in order to isolate the electrode from the inner tube.
8. A device for capacitively measuring the distance to an object comprising an assembly having a sensor and a cable formed integrally. The assembly includes a tri-axial cable with a solid central conductor, a shield that surrounds the conductor and is insulated by means of a mineral insulant. There is an outer metal tube that surrounds the shield and is insulated by means of a solid insulating material. The tri-axial cable has a generally constant diameter, but an increased diameter at one end, part of which forms the sensor. It has an electrode that extends over the sensor's electrode which electrically connects to the central conductor and electrically isolates itself from the shield and from the outer metal tube.

Bibliography

Page numbers in italics refer to figures or tables

- Amsbury, C.R. & Chivers, J.W.H. (1978), 'System for the Measurement of Rotor Tip Clearance and Displacement in a Gas Turbine'. *AGARD Conference Proceedings, Seal Technology in Gas Turbine Engines*, vol. 234, 2, 30, 31
- Atkinson, W. (1994), 'Sensor Requirements'. *Proceedings of the 1st P&W International Clearance Sensor Workshop*, 218
- Bailleul, G.D. & Albijat, S. (1996), 'Review of Progress in the Development of Capacitive Sensors for Blade Tip Clearance Measurement'. *Proceedings of the American Society of Mechanical Engineers Turbo Asia Conference*. Jakarta, Indonesia, 5–7 November, Paper No. 96-TA-001, 219
- Baker, L.C., Grady, G.E. & Mauch, H.R. (1978), 'Turbine Tip Clearance Measurement'. US-ARTL-TR-78-4, 56
- Barranger, J. (1978), 'An In-Place Recalibration Technique to Extend the Temperature Capability of Capacitance-Sensing Rotor Blade Tip Clearance Measuring Systems'. *Society of Automotive Engineers Aerospace Meeting*. San Diego, USA, Paper No. 781003, 31, 56, 57, 82
- Barranger, J.P. & Ford, M.J. (1981), 'Laser Optical Blade Tip Clearance Measurement System'. *Transactions of the ASME, Journal of Engineering for Power*, vol. 103, pp. 457–60, 28, 56, 117, 212
- Belsterling, C.A. (1970), 'Sensing with Air'. *25th ISA Conference*. Philadelphia, USA, 30
- Bindon, J.P. (1986), 'Visualization of Axial Turbine Tip Clearance Flow Using a Linear Cascade'. Cambridge University Engineering Department Report CUED/a-Turbo/TR 122, 190
- Brandt, D.E. & Wesorick, R.R. (1994), 'GE Gas Turbine Design Philosophy'. *GER3434D, 38th GE Turbine State-of-the-Art Technology Seminar*, 194
- Burr, R. (1994), 'Sensor Comparison'. *Proceedings of the 1st P&W International Clearance Sensor Workshop*, 191, 212, 212
- Calvert, W.J., Ginder, R.B., McKenzie, I.R.I. & Way, D.J. (1989), 'Performance of a Highly-Loaded HP Compressor'. *Proceedings of the 34th American Society of Mechanical Engineers Gas Turbine and Aeroengine Congress*. Toronto, Canada, 5–8 June, Paper No. 89-GT-24, 62, 149
- Chivers, J.W.H. (1989), 'A Technique for the Measurement of Blade Tip Clearance in a Gas Turbine'. AIAA Paper No. 89-2916, 4, 25, 54, 56, 58, 66, 117, 140, 179, 183, 219
- Chivers, J.W.H. (1989), *A Technique for the Measurement of Blade Tip Clearance in a Gas Turbine*. PhD thesis, University of London, 1, 2–3, 4, 31, 41, 53–4, 57–8, 60–1, 82, 83–4, 89, 162, 163, 164, 165, 169, 173, 191, 219, 222, 223, 224, 64, 169, 213, 220, 223
- Davidson, D.P., DeRose, R.D. & Wennerstrom, A.J. (1983), 'The Measurement of Turbomachinery Stator to Drum Running Clearances'. *Proceedings of the 28th American Society of Mechanical Engineers Gas Turbine and Aeroengine Congress*. Phoenix, USA, 27–31 March, Paper No. 83-GT-204, 2, 4, 9, 15, 20, 22, 23, 30, 82, 113, 116, 117, 120, 139–40, 151, 153, 159, 10, 16, 17, 18, 116, 152, 155

- Denton, J.D. (1993), 'Loss Mechanisms in Turbomachines'. *Transactions of the ASME, Journal of Turbomachinery*, vol. 115, pp. 621–56, 189
- Denton, J.D. & Cumpsty, N.A. (1987), 'Loss Mechanisms in Turbomachinery'. *Proceedings of the IMechE International Turbomachinery Conference*. Robinson College, Cambridge, UK, 1–3 September, Paper No. C260/87, 190
- Denton, J.D. & Johnson, C.G. (1976), 'An Experimental Study of the Tip Leakage Flow around Shrouded Turbine Blades'. CEGB Report RIM1N848, 190
- Dooley, K. (1989a), 'Capacitive Bridge-Type Probe for Measuring Blade Tip Clearance'. Patent No. US 4,818,948, 4 April, 219
- Dooley, K. (1989b), 'Capacitance to Voltage Conversion Bridge and a Capacitive Offset'. Patent No. US 4,795,965, 3 June, 219
- Dring, R.P. & Joslyn, H.D. (1981), 'Measurement of Turbine Rotor Blade Flows'. *Transactions of the ASME, Journal of Engineering and Power*, vol. 103, pp. 400–5, 190
- Drinkuth, W., Alwang, W.G. & House, R. (1974), 'Laser Proximity Probes for the Measurement of Turbine Blade Tip Running Clearances'. *Proceedings of the ISA Aerospace Instrumentation Symposium*. Paper No. 74228, pp. 133–40, 28, 56, 104
- Ford, M.J. (1980), 'Clearance Measurement System'. Report NASA CR 159402, 28, 56
- Foster, R.L. (1989), 'Linear Capacitive Reactance Sensors for Industrial Applications'. *SAE 40th Annual Earthmoving Industry Conference*. Peoria, Illinois, USA, Paper No. 890974, 191, 219
- Freeman, C. (1985), 'Effect of Tip Clearance Flow on Compressor Stability and Engine Performance'. *Von Karman Institute for Fluid Dynamics Lecture Series 1985–05, Tip Clearance Effects in Axial Turbomachines*, 26
- Gill, S.J., Ingallinera, M.D. & Sheard, A.G. (1997), 'Turbine Tip-Clearance Measurement System Evaluation in an Industrial Gas Turbine'. *Proceedings of the 42nd American Society of Mechanical Engineers Gas Turbine and Aeroengine Congress*. Orlando, Florida, USA, 2–5 June, Paper No. 97-GT-466, 54, 219, 222–3, 223, 224
- Ginder, R.B. (1991), 'Design and Performance of Advanced Blading for a High Speed HP Compressor'. *Proceedings of the 36th American Society of Mechanical Engineers Gas Turbine and Aeroengine Congress*. Orlando, Florida, USA, 3–6 June, Paper No. 91-GT-374, 62
- Ginder, R.B., Britton, A.J., Calvert, W.J., McKenzie, I.R.I. & Rarker, J.M. (1991), 'Design of Advanced Blading for a High Speed HP Compressor Using an S1-S2 Flow Calculation System'. *Proceedings of the IMechE Conference on Turbomachinery*, Paper No. 423/007, 62
- Grice, N., Sherrington, L., Smith, E.H., O'Donnell, S.G. & Stringfellow, J.F. (1990), 'A Capacitance Based System for High Resolution Measurement of Lubricant Film Thickness'. *Proceedings of the Nordtrib '90, 4th Nordic Symposium on Tribology, Lubrication, Friction and Wear*. Hirtshals, Denmark, 10–13 June, 212, 213, 215, 219, 221, 222
- Grzybowski, R., Foyt, G., Atkinson, W., Knoell, H. & Wenger, J. (1996), 'Microwave Blade Tip Clearance Measurement System'. *Proceedings of the 41st American Society of Mechanical Engineers Gas Turbine and Aeroengine Congress*. Birmingham, England, 10–13 June, Paper No. 96-GT-002, 212

- Haffner, K., Kempe, A., Rösgen, T. & Schlamp, S. (2008), 'Method and an Apparatus for Determining the Clearance Between a Turbine Casing and the Tip of a Moving Turbine Blade'. US Patent No. 7,400,418, 15 July, 75
- Hall, L.C. & Jones, B.E. (1976), 'An Investigation into the Use of a Cone-jet Sensor for Clearance and Eccentricity Measurement in Turbo Machinery'. *Proceedings of the Institution of Mechanical Engineers 1847–1982*, vol. 190, pp. 23–30, 30
- Hardy, H.D. (1972), 'Use of Laser-powered Optical Proximity Probe in Advanced Turbofan Engine Development'. *Symposium on Airbreathing Propulsion, Progress in Astronautics and Aeronautics*, vol. 34, 28
- Hastings, M.M. & Jensen, H.B. (1996), 'A Novel Proximity Probe Unaffected by Shaft Electromagnetic Properties'. *Proceedings of the 41st American Society of Mechanical Engineers Gas Turbine and Aeroengine Congress*. Birmingham, England, 10–13 June, Paper No. 96-GT-004, 211–12
- Hughes, S.T. (1995), 'Sensors for Road Vehicles Based Upon Capacitance Variation'. *Proceedings of the Institution of Mechanical Engineerings Sensors - Autotech 95 Seminar 21*. Birmingham, England, 7–9 November, Paper No. C498/21/214, 191, 212
- Kappler, G., Moore, R. & Hourmouziadis, J. (1992), 'Hochleistung-Turbo-Fan-Triebwerke ein Familienkonzept'. DGLR Paper No. 92-03-043, 162
- Kaye, G.W.C. & Laby, T.H. (1956), *Tables of Physical and Chemical Constants*. Longman's Green & Co., London, 32
- Kempe, A., Schlamp, S., Rösgen, T. & Haffner, K. (2003), 'Low-coherence Interferometric Tip-clearance Probe'. *Optics Letters*, vol. 28, pp. 1323–5, 75–7
- Kempe, A., Schlamp, S., Rösgen, T. & Haffner, K. (2006), 'Spatial and Temporal High-Resolution Optical Tip-Clearance Probe for Harsh Environments'. *Proceedings of the 13th International Symposium on Applications of Laser Techniques to Fluid Mechanics*. Lisbon, Portugal, 26–29 June, 75, 77
- Killeen, B., Sheard, A.G. & Westerman, G.C. (1991), 'Blade-by-blade Tip-Clearance Measurement in Aero and Industrial Turbomachinery'. *Proceedings of the 37th ISA International Instrumentation Symposium*. San Diego, California, USA, 5–9 May, pp. 429–47, 4, 58–60, 78, 85, 162
- Knoell, H., Schedl, K. & Kappler, G. (1981), 'Two Advanced Measuring Techniques for the Determination of Rotor Tip Clearance During Transient Operation'. *Fifth International Symposium on Airbreathing Engines*. Bangalore, India, 30, 31, 56–7
- Lawson, C.P. (2003), *Capacitance Tip Timing Techniques in Gas Turbines*. PhD thesis, Cranfield University, 77
- Lawson, C.P. & Ivey, P.C. (2005), 'Tubomachinery Blade Vibration Amplitude Measurement Through Tip Timing With Capacitance Tip Clearance Probes'. *Sensors and Actuators A: Physical*, vol. 118, pp. 14–24, 77
- Monich, M. & Bailleul, G. (1993), 'New Digital Capacitive Measurement System for Blade Clearances'. *Proceedings of the 39th ISA International Instrumentation Symposium*. Albuquerque, New Mexico, USA, 2–6 May, pp. 419–30, 219
- Morrison, R. (1991), 'Grounding and Shielding in Instrumentation'. *Proceedings of the 37th ISA International Symposium of Measurement Techniques*, pp. 989–96, 86

- Müller, D., Sheard, A.G., Mozumdar, S. & Johann, E. (1997), 'Capacitive Measurement of Compressor and Turbine Blade Tip-to-casing Running Clearance'. *Transactions of the ASME, Journal of Engineering for Gas Turbines & Power*, vol. 119, pp. 877–84, 54, 77, 190, 192, 196, 199–200, 212, 215, 219, 223, 55
- Parish, C.J. (1990), 'Fast Response Tip Clearance Measurement in Axial Flow Compressors — Techniques and Results'. *Proceedings of the IMechE Part G: Journal of Aerospace Engineering*, vol. 204, pp. 51–6, 4
- Pavey, P.G. (1993), Private communication with Mr. P.G. Pavey, Rolls-Royce plc, Engineering Manager Measurement and Test, 140, 192
- Poppel, G.L. (1979), *Analysis and Preliminary Design of an Optical Digital Tip Clearance Sensor for Propulsion Control*. Report NASA-CR-159434, 31–2
- Ramachandran, J. & Conway, M.C. (1996), 'MS6001FA – An Advanced Technology 70-MW Class 50/60Hz Gas Turbine'. *39th GE Turbine State-of-the-Art Technology Seminar*, GER-3765B, 54, 194, 207
- Rubinshtein, Ya.M. & Trubilov, M.A. (1958), 'A Steamjet Method for Measuring Clearance in Steam Turbines'. *Teploenergetika*, vol. 5, pp. 68–74, 30
- Sheard, A.G. (1989), *Aerodynamic and Mechanical Performance of a High Pressure Turbine Stage in a Transient Wind Tunnel*. DPhil thesis, University of Oxford, <http://ora.ouls.ox.ac.uk/objects/uuid:73ecb15e-efde-474d-ae30-3f8f7e1d6f4e>, 54
- Sheard, A.G. (2011), 'Blade-by-blade Tip-Clearance Measurement'. *International Journal of Rotating Machinery*, vol. 2011, Article ID 516128, pp. 1–13, 82–3, 89–90, 91, 104, 117
- Sheard, A.G. (2000), 'Capacitive Gap Measurement Device'. Patent No. GB 2 325 305 B, 19 April, 162
- Sheard, A.G. (1993), 'A System for Measuring Blade and Stator Radius During Compressor Build and Overhaul'. *Proceedings of the 9th International Turbomachinery Maintenance Congress*. Amsterdam, Netherlands, 18–22 October, pp. 1–12, 56
- Sheard, A.G. & Killeen, B. (1995), 'A Blade-by-blade Tip-Clearance Measurement System for Gas Turbine Applications'. *Transactions of the ASME, Journal of Engineering for Gas Turbines & Power*, vol. 117, pp. 326–31, 75, 186, 76
- Sheard, A.G. & Killeen, B. (1993), 'Hybrid System for High-Temperature Tip-Clearance Measurement'. *Proceedings of the 39th ISA International Instrumentation Symposium*. Albuquerque, New Mexico, USA, 2–6 May, pp. 379–94, 75, 140, 144, 148, 153, 190, 76
- Sheard, A.G. & Lawrence, D.C. (1998), 'Gap Measurement Device'. US Patent No. 5,760,593, 2 June, 54, 77, 162, 183, 192, 197, 199, 207, 213, 219, 213, 220
- Sheard, A.G. & Turner, S.R. (1992), 'An Electromechanical Measurement System for the Study of Blade Tip-to-Casing Running Clearances'. *Proceedings of the 37th American Society of Mechanical Engineers Gas Turbine and Aeroengine Congress*. Cologne, Germany, 1–4 June, Paper No. 92-GT-50, 1, 54, 63, 75, 82, 89, 113, 139–40, 162, 173, 175, 176, 191, 194, 212, 55, 177
- Sheard, A.G., Killeen, B. & Palmer, A. (1993), 'A Miniature Traverse Actuator for Mapping the Flow Field between Gas Turbine Blade Rows'. *Proceedings of the IMechE: Machine Actuators & Controls Seminar*. London, UK, 31 March, pp. 1–11, 62, 86, 140, 151

- Sheard, A.G., O'Donnell, S.G. & Stringfellow, J.F. (1999), 'High Temperature Proximity Measurement in Aero and Industrial Turbomachinery'. *Transactions of the ASME, Journal of Engineering for Gas Turbines & Power*, vol. 121, pp. 167–73, 58, 162, 173, 183, 192, 194, 197, 199, 207
- Sheard, A.G., Westerman, G.C. & Killeen, B. (1992), 'An On-Line Calibration Technique for Improved Blade-by-blade Tip-Clearance Measurement'. *Proceedings of the 38th ISA International Instrumentation Symposium*. Las Vegas, Nevada, USA, 26–30 April, pp. 32–51, 75, 117, 120–1, 124, 134, 140, 144, 149, 119
- Sheard, A.G., Westerman, G.C., Killeen, B. & Fitzpatrick, M. (1994), 'A High-Speed Capacitance-Based System for Gauging Turbomachinery Blading Radius During the Tip-Grind Process'. *Transactions of the ASME, Journal of Engineering for Gas Turbines & Power*, vol. 116, pp. 243–9, 56, 86, 153
- Stringfellow, J.F., Wayman, L. & Knox, B. (1997), 'Capacitance Transducer Apparatus and Cables'. Patent No. WO 97/28418, 7 August, 54, 58, 77, 162, 164, 165, 191, 219, 222–3, 225, 228, 230, 55, 223
- Sutcliffe, H. (1977), 'Principles of Eddy Current Distance Gauging'. *Transactions of the Institute of Electrical Engineers*, vol. 124, pp. 479–84, 211
- Valentini, E., Lacitignola, P. & Casini, M. (1988), 'Progress on Measurement Techniques for Industrial Gas Turbine Technology'. *Proceedings of the 33rd American Society of Mechanical Engineers Gas Turbine and Aeroengine Congress*. Amsterdam, Netherlands, 6–9 June, Paper No. 88-GT-113, 5
- White, S.D. (1977), 'Turbine Tip Clearance Measurement'. USARTL-TR-77-47, 28, 56
- Winfield, D.P. (1991), Private communication with Mr D.P. Winfield, Rolls-Royce plc, Product Engineering Manager Repair and Overhaul ATO, 134, 135

Author index

Page numbers in italics refer to figures or tables

- Albijat, S., 219
Alwang, W.G., 28, 56, 104
Amsbury, C.R., 2, 30, 31
Atkinson, W., 212, 218
- Bailleul, G.D., 219
Baker, L.C., 56
Barranger, J.P., 28, 31, 56, 57, 82, 117, 212
Belsterling, C.A., 30
Bindon, J.P., 190
Brandt, D.E., 194
Britton, A.J., 62
Burr, R., 191, 212, 212
- Calvert, W.J., 62, 149
Casini, M., 5
Chivers, J.W.H., 1, 2–3, 4, 25, 30, 31, 41, 53–4, 56, 57–8, 60–1, 66, 82, 83–4, 89, 117, 140, 162, 163, 164, 165, 169, 173, 179, 183, 191, 219, 222–3, 224, 64, 169, 213, 220, 223
Conway, M.C., 54, 194, 207
Cumpsty, N.A., 190
- Davidson, D.P., 2, 4, 9, 15, 20, 22, 23, 30, 82, 113, 116, 117, 120, 139–40, 151, 153, 159, 10, 16, 17, 18, 116, 152, 155
Denton, J.D., 189, 190
DeRose, R.D., 2, 4, 9, 15, 20, 22, 23, 30, 82, 113, 116, 117, 120, 139–40, 151, 153, 159, 10, 16, 17, 18, 116, 152, 155
Dooley, K., 219
Dring, R.P., 190
Drinkuth, W., 28, 56, 104
- Fitzpatrick, M., 56, 86, 153
Ford, M.J., 28, 56, 117, 212
Foster, R.L., 191, 219
Foyt, G., 212
Freeman, C., 26
- Gill, S.J., 54, 219, 222–3, 224
Ginder, R.B., 62, 149
Grady, G.E., 56
Grice, N., 212, 213, 215, 219, 221, 222
Grzybowski, R., 212
- Haffner, K., 75–7
Hall, L.C., 30
Hardy, H.D., 28
Hastings, M.M., 211–12
Hourmouziadis, J., 162
House, R., 28, 56, 104
Hughes, S.T., 75, 140, 144, 148, 153, 190, 191, 212, 76
- Ingallinera, M.D., 54, 219, 222–3, 224
Ivey, P.C., 77
- Jensen, H.B., 211–12
Johann, E., 54, 77, 190, 192, 196, 199–200, 212, 215, 219, 223, 55
Johnson, C.G., 190
Jones, B.E., 30
Joslyn, H.D., 190
- Kappler, G., 3, 30, 56–7, 162
Kaye, G.W.C., 32
Kempe, A., 75–7
Killeen, B., 4, 56, 58–60, 62, 75, 78, 85, 86, 117, 120–1, 124, 134, 140, 144, 148, 149, 151, 153, 162, 186, 190, 76, 119
Knoell, H., 30, 31, 56–7, 212
Knox, B., 54, 58, 77, 162, 164, 165, 191, 219, 222–3, 225, 228, 230, 55, 223
- Labey, T.H., 32
Lacitignola, P., 5
Lawrence, D.C., 54, 77, 162, 183, 192, 197, 199, 207, 213, 219, 213, 220
Lawson, C.P., 77
- Mauch, H.R., 56
McKenzie, I.R.I., 62, 149
Monich, M., 219
Moore, R., 162
Morrison, R., 86
Mozumdar, S., 54, 77, 190, 192, 196, 199–200, 212, 215, 219, 223, 55
Müller, D., 54, 77, 190, 192, 196, 199–200, 212, 215, 219, 223, 55

- O'Donnell, S.G., 58, 162, 173, 183, 192, 194, 197, 199, 207, 212, 213, 215, 219, 221, 222
- Palmer, A., 62, 86, 140, 151
- Parish, C.J., 4
- Parker, J.M., 62
- Pavey, P.G., 140, 192
- Poppel, G.I., 31–2
- Ramachandran, J., 54, 194, 207
- Rösgen, T., 75–7
- Rubenshtein Ya M., 30
- Schedl, K., 30, 31, 56–7
- Schlamp, S., 75–7
- Sheard, A G, 1, 4, 54, 56, 58–60, 62, 63, 75, 77, 78, 82–3, 85, 86, 89–90, 91, 104, 113, 117, 120–1, 124, 134, 139–40, 144, 148, 149, 151, 153, 162, 173, 175, 176, 183, 186, 190, 191, 192, 194, 196, 197, 199–200, 207, 212, 213, 215, 219, 222–3, 224, 55, 76, 119, 177, 213, 220
- Sherrington, L., 212, 213, 215, 219, 221, 222
- Smith, E.H., 212, 213, 215, 219, 221, 222
- Stringfellow, J., 54, 58, 77, 162, 164, 165, 173, 183, 191, 192, 194, 197, 199, 207, 210, 212, 213, 215, 219, 221, 223, 225, 55, 222, 223
- Sutcliffe, H., 211
- Trubilov, M.A., 30
- Turner, S.R., 1, 54, 63, 75, 82, 89, 113, 139–40, 162, 173, 175, 176, 191, 194, 212, 55, 177
- Valentni, E., 5
- Way, D.J., 62, 149
- Wayman, L., 54, 58, 77, 162, 164, 165, 191, 219, 221, 223, 225, 228, 230, 55, 222, 223
- Wenger, J., 212
- Wennerstrom, A.J., 2, 4, 9, 15, 20, 22, 23, 30, 82, 113, 116, 117, 120, 139–40, 151, 153, 159, 10, 16, 17, 18, 116, 152, 155
- Wesorick, R.R., 194
- Westerman, G.C., 4, 56, 58–60, 75, 78, 85, 86, 117, 120–1, 124, 134, 140, 144, 149, 153, 162, 119
- White, S.D., 28, 56
- Winfield, D.P., 134, 135

Subject index

Page numbers in italics refer to figures or tables

- Alstom GT26, 75, 77
axial thermal movement, 75
- blade-by-blade tip clearance measurement,
53–78 *see also* gas turbine blade-by-
blade tip clearance measurement; gas
turbine blade tip clearance measurement;
on-line calibration for blade-by-blade tip
clearance measurement
- accuracy 66
Alstom GT26 75, 77
average clearance, 53
axial thermal movement, 75
blade analyser unit, 58–9
BR700 development gas turbine, 54–6
C147 compressor at DRA Pystock, 75, 76
calibration of system, 67–8, 69–71
without datuming, 72
Chivers' capacitive system, 53–6
commissioning spinning rig and blade
analyser, 64–7
complete measurement system, 60
conclusions, 77–8
error in measurement, 67, 70, 74
establishing accuracy, 64–7
experimental programme, 64–75
facility requirements, 60–1
blade offset from longest blade, 62
capacitance probe and touch wire mounting,
63
spinning rig, 61, 63–4
flame noise, 75
FM capacitance probe:
ground station, 57
Hartley oscillator, 58
principle of operation, 57–8
root mean square voltmeter, 57
triaxial cable, 57
unity gain amplifier, 58
further developments, 75–7
hybrid probe, 76
limitations of various measurement systems,
75–7
mark space ratio, 60
blade tip-to-casing running clearance *see* com-
pressor and turbine blade tip-to-casing
running clearance
- BMW Rolls-Royce joint venture, 54–5, 56–7
BR700 development gas turbine, 54–6
- calibration uncertainty, 172, 173
Chivers' capacitive system, 53–6
Cold Flow Rig (UCF6), 16
aerodynamic probes, 15
with first generation measurement system, 17
and mini measurement systems, 18
gas angles and Mach numbers, 15
gas-to-wall temperature ratios, 15
pressure ratio and non-dimensional speed,
15
probe tip region, 21
Reynolds numbers, 15
total temperature and pressure conditions,
15
compressor and turbine blade tip-to-casing run-
ning clearance, 161–88 *see also* electro-
mechanical measurement of
tip-to-casing running clearance, 1–23
blade passing and staircase signal, 166
cable, 174
calibration:
curve, 171
procedure, 169–71
uncertainty, 172, 173
casing replica, 170
calibration and system uncertainty, 169–73
comparison between gas turbine and cold build
clearances, 179
compressor tip-rub data, 180
conclusions, 186–8
data from electromechanical system, 177
data logging, 174–5
demodulator, 165–7
phase locked loop, 165
voltage-controlled oscillator, 165
deviation from mean clearance, 184
dynamic data analysis, 186
dynamic output of opposed capacitance
probes, 187
gas turbine cranks, 178
ground station, 174–5
high-pressure turbine measurement in cold sta-
bilisation test, 185
individual blade clearance data, 182

- installation and operation uncertainty, 172, 173
- lineariser, 167
- mean compressor blade clearance data, 181
- measurement on development gas turbines, 176
- measurement system performance and specification, 168–9
- amplification factor, 168
- capacitive clearance system specification, 168
- signal-to-noise ratio, 168
- staircase module, 168
- system resolution, 167
- voltage controlled oscillator, 168
- module description, 163–7
- operating experience, 175–86
- oscillator and guard amplifier, 165
- oscillator, 174
- performance curve, 179–83
- probe, 173–4
 - cable assembly, 164
 - durability and long-term uncertainty, 183–6
 - positions around compressor, 178
- running in procedure, 178–9
- schematic block diagram, 163
- speed module, 167
- system:
 - concept, 162–9
 - evaluation on a core gas turbine, 176
 - installation, 173–5
 - uncertainty and analysis, 172, 173
- turbine measurement, 183
- C147 compressor:
 - with blade-by-blade measurement system, 152
 - design parameters, 151
 - at DRA Pystock, 75, 76
 - and fittings, 152
 - stage 5 clearance, 155
- Coulombe-Probe, 31
- CTR1, 21
- electromechanical actuator:
 - electronics module, 7, 9
 - micro version, 9, 10
 - mini version, 8, 10
 - mounting tower, 7
 - overall size, 7
 - probe electrode, 7
 - probe-actuator assembly, 7
 - stepper motor drive assembly, 7
- electromechanical measurement of tip-to-casing
 - running clearance, 1–23 *see also* compressor and turbine blade tip-to-casing running clearance
 - calibration of electromechanical actuator, 13–14, 15
- carbon brush fitting, 3
- Cold Flow Rig (UCF6), 16
 - aerodynamic probes, 15
 - with first generation and mini measurement systems, 18
 - with first generation measurement system, 17
 - gas angles and Mach numbers, 15
 - gas-to-wall temperature ratios, 15
 - pressure ratio and non-dimensional speed, 15
 - probe tip region, 21
 - Reynolds numbers, 15
 - total temperature and pressure conditions, 15
- compressor test rig, 19, 20
- CTR1: probe tip region, 21
 - direct current capacitive principle, 4
 - electromechanical principle, 4
- external gearbox, 3
 - first generation electromechanical system, 2, 15–16
 - Amsbury and Chivers, 1978, 2
 - full scale spool test, 22
 - FM capacitive measurement principle, 4
 - full scale spool (FSS):
 - installation design for mini system, 21
 - installation geometry, 20
 - liner segments, 20
 - with mini measurement system, 22
 - probe loading, 20–2
 - test, 20–2
- high-pressure compressor, 2
- high-pressure turbine, 2
- laboratory tests, 13–15
- measurement specification:
 - accuracy, 27
 - air cooling passages, 27
 - blade-to-space ratio, 27
 - casing lining, 26
 - component efficiency, 27
 - dynamic response, 27
 - environment, 27
 - range, 26
- microwave principle, 4
- optical principle, 4
- probe cartridge:
 - datum face, 7
 - electrical discharge, 7
 - float, 7
 - outer datum, 7
 - removal from mini system actuator, 10
 - stepper motor, 7
- second generation electromechanical system:
 - actuator, 7–10

- actuator's rack-mounted electronic controller, 5
 - Cold Flow Rig (UCF6), 15–18
 - commissioning, 13–22
 - cooling requirements, 11
 - electronic controller, 11, 12–13
 - four stage commissioning, 2
 - insulated electrode, 5
 - internal datum, 5
 - low-energy electrical discharge, 5
 - mechanical design, 1–2
 - mini electromechanical actuator, 4
 - performance review, 2
 - probe cartridge design, 5–6, 7
 - probe-actuator assembly design, 15
 - probe's mechanical design and operation, 5
 - schematic layout, 3
 - system concept, 5–13
 - system specification, 9
 - test conclusions, 23
 - test vehicle conditions, 15
 - self-calibrating system, 3
 - spark-discharge technique, 2
 - spring-loaded probe, 3
 - stepper motor driven probe, 2
 - thermal effects, 2
 - thermal errors, 3
 - users, 4
- Fenlow probe, 2, 28, 82
 - flame noise, 75
 - FM capacitance probe, 83–4
 - demodulator unit, 83
 - ground station, 57
 - Hartley oscillator, 58
 - principle of operation, 57–8, 83–4
 - root mean square voltmeter, 57
 - triaxial cable, 57
 - unity gain amplifier, 58
 - FM capacitive clearance measurement system, 35
 - FM oscillator 33–35
 - with active guarded electrode, 25
 - first generation electromechanical system, 2, 15–16 *see also* second generation, electromechanical system
 - Amsbury and Chivers, 1978, 2
 - on Cold Flow Rig 17, 18
 - full scale spool test, 22
 - full scale spool (FSS)
 - installation design for mini system, 21
 - installation geometry, 20
 - liner segments, 20
 - with mini measurement system, 22
 - probe loading, 20–2
 - test, 20–2
 - gas turbine blade-by-blade tip clearance measurement, 139–59 *see also* blade-by-blade tip clearance measurement; gas turbine blade tip clearance measurement; on-line calibration for blade-by-blade tip clearance measurement
 - actuator 148
 - and probe, 147
 - blade tip-to-casing vs blade number data, 157
 - C147 compressor:
 - with blade-by-blade measurement system, 152
 - and fittings, 152
 - stage 5 clearance, 155
 - clearance measured over longest blade, 141
 - clearance vs blade data set after subtracting mean clearance, 158
 - commissioning, 151–8
 - conclusions, 159
 - cooling requirements, 148
 - distance from system datum to C147, 154
 - electromechanical actuator, 144–8
 - electronic controller, 149
 - PC software, 149
 - probe, 144, 145, 148
 - and actuator, 147
 - schematic view of installation, 144
 - probe tip with electrode, 146
 - specification, 146
 - system concept, 140–9
 - test facility, 149–51
 - C147 design parameters, 151
 - interrelationship between ground station, actuator and host computer, 150
 - test vehicle conditions, 151
 - turbine exit gas angle, 142
 - typical capacitance probe output voltage, 156
 - gas turbine blade-tip clearance measurement, 25–50 *see also* blade-by-blade tip clearance measurement; gas turbine blade-by-blade tip clearance measurement; on-line calibration for blade-by-blade tip clearance measurement
 - blade-tip-to-casing data comparison, 42–3
 - capacitance sensor, 36
 - capacitive measurement technique, 32–3
 - casings' thermal growth, 26
 - and combustion gas composition, 34
 - complex impedance, 31
 - compressor bearings, 3
 - compressor evaluation, 39–45
 - clearance measurements during flight, 44
 - discussion of results, 42–5
 - prototype, 40
 - test programme, 41

- cone-jet sensors, 30–1
- Coulombe-Probe, 31
- direct current capacitance probe, 31
- electromechanical-based, 30
- environmental conditions, 33
- in a flight environment, 25
- fluidic-based displacement, 30
- FM capacitive clearance measurement system, 35
- FM oscillator with active guarded electrode, 25
- guard amplifier:
 - calibration factors, 38–9
 - design criteria, 37–9
 - helium-neon laser principle, 28
 - laser optical clearance system, 27–8, 29
 - laser proximity probe, 27–8, 29
 - laser triangulation, 27–8, 29
 - measuring probe sensor, 35–7
 - mechanical actuators, 30
 - optical triangulation, 27–8, 29
 - optical-based technique (Poppel), 31–2
 - oscillator, 37
 - pneumatic back-pressure sensors, 30
 - prototype capacitance probe, 46
 - rotor thermal growth, 26
 - specific fuel consumption, 26
 - specification, 26–32
 - standing capacitance, 31
 - surge line, 26
 - survey of previous work, 27–32
 - system design for gas turbine measurement system, 33–7
 - FM oscillator, 33–5
 - measuring probe modulator, 37
 - technique evaluation and selection, 32–3
 - tip-to-casing clearance data, 48–9
 - turbine evaluation, 45–8
 - capacitance probe calibration rig, 47
 - discussion of results, 48
 - dry cranks, 47
 - flight cycles, 47
 - square cycles, 47
 - on the test bed, 47–8
 - turbine liner, 46
 - and variation of relative permittivity of air, 34
 - vidicon tube, 28
 - working line, 26
- GE MS6001FA turbine capacitance probe, 193
 - cross section, 195
 - installation, 194
 - stage 1 turbine blade tip geometry, 197
- Hartley oscillator, 58
- helium-neon laser principle, 28
- high-speed system for gauging radius during tip grind, 111–38
 - commissioning high-speed gauging system: CNC lathe and fittings, 121
 - dial gauge, 121
 - offset of JT8 stage 11 compressor, 122
 - phase I, 120–30
 - phase II, 131–7
 - pin-fixed blade root fixing, 131
 - radius of JT8 stage 7 compressor blades, 132
 - radius of JT8 stage 11 compressor blades, 123
 - after 0.05mm cut, 125
 - after 0.10mm cut, 126
 - after 0.15mm cut, 127
 - after 0.20mm cut, 128
 - after 0.25mm cut, 129
 - after deburring, 136
 - after final 0.25mm cut, 133
 - after following Winfield's recommendation, 135
 - repeatability test, 130
 - conclusions, 137
 - layout of measurement head, 119
 - measurement head, 119
 - radius over every blade, 116–18
 - blading of typical compressor drum, 117
 - capacitance-based measurement system, 119–20
 - schematic view of blade disc assembly, 118
 - radius to the longest blade, 113–16
 - measurement system actuator and probe cartridge, 115
 - measurement system probe and actuator, 114
 - measurement technique selection, 113–15
 - operating procedure, 115–16
 - system commissioning, 120–37
 - tip-grind machine with electromechanical measurement system, 116
 - V2500, 112
- high-temperature proximity measurement in turbomachinery:
 - cable performance, 226
 - cable specification, 225
 - capacitive displacement transducer, schematic of, 216
 - clearance measurement electronic system performance, 228–30
 - clearance sensor comparison, 212
 - component parts and cable configuration, 214
 - conclusions, 230

- drive electronic specification, 218
- eddy current sensor, 211
- finite element analysis of optimised new technology sensor tip, 221
- flexible cable, 226
- gas turbine-mounted CDT amplifier, 215
- measured and theoretical isolation resistance, 227
- MgO-filled cable, 224
- mineral insulated cable, 224
- new technology sensor with proximity electronics, 222
- principle of operation, 213–17
- proximity measured system sensitivity, 229
- proximity measurement electronic system performance, 228
- rare earth magnets, 211
- relative permittivity of silica and magnesia, 225
- schematic of proximity measurement system, 217
- sensors, 213–15
 - comparison with older technologies, 223
 - development, 218–24
 - geometry, 220–1
 - new technologies, 219–20, 223
 - comparison with older technologies, 223
 - performance, 226
 - proximity, 215
 - range, 220–4
 - specification, 218
 - traditional with new technology, 213, 220
 - traditional tri-axial configuration, 219
- signal conditioning, 215–17
- sensor and cable coupled performance, 227
- SiO₂-filled cable, 225
- system performance, 226–30
- hybrid probe, 76

- industrial gas turbine tip clearance measurement evaluation, 189–209
 - average clearance at location 7, 206
 - blade passing outputs from Systems 1 and 2, 204
 - calibration curves for average from Systems 1, 2 and 3, 198
 - calibration, initial evaluation and uncertainty analysis, 196–201
 - capacitive measurement, 191
 - configuration of system components, 202
 - eddy current principle, 191
 - electromechanical principle 191
 - error analysis, 199–201
 - evaluation systems, 191
 - calibration, 197–8
 - prior experience, 192
 - fluidic principle, 191
 - future applications/potential improvements, 208
 - GE MS6001FA turbine capacitance probe, 193
 - cross section, 195
 - installation, 194
 - stage 1 turbine blade tip geometry, 197
 - geometric system uncertainty, 199
 - histogram of measured blade fence thickness *versus* nominal blade fence thickness, 200
 - installed performance, 201–3
 - isometric view of tip clearance probes, 196
 - measuring and diagnostics of probes and electronics, 207–8
 - microwave principle, 191
 - operating experience, 201–8
 - optical principle, 191
 - plot of clearance and speed *versus* time for Systems 1 and 2, 205
 - schematic of the 16 evaluation probes, 195
 - system concept, 191–3
 - calibration of 1, 2 and 3, 196–7
 - requirements, 192–3,
 - target geometry, 194–6
 - temperature dependency limitations, 199
 - test conclusions, 209
 - test results, 203–7
 - turbine evaluation, 193–5
 - typical equivalent thermal mass to flanges at horizontal joint, 207
 - vendor provided generic system requirements and specifications, 192
- laser triangulation, 27–8, 29

- measurement systems *see also* first generation electromechanical system; second generation electromechanical system,
 - establishing accuracy of, 64–7
 - limitations of various, 75–7
- microwave principle, 4, 191

- on-line calibration for blade-by-blade tip clearance measurement, 81–108 *see also* blade-by-blade tip clearance measurement; gas turbine blade-by-blade tip clearance measurement; gas turbine blade tip clearance measurement,
 - blade analyser unit, 85, 86

- peak detect and reset circuit, 86
- capacitance probe calibration, 92–9, 96
- data sets from actuator positions, 93
- error in system output, 100
- longest blade of each data set, 95
- refinement, 99–101
- system output against clearance, 98
- capacitance probes' limitations, 81–3
- clearance measurement, 101–8
 - blade tip thickness, 104
 - deviation of system output from refined calibration, 103
 - error in measure clearance, 106
 - over each blade, 105
 - over each blade around compressor disc, 107
 - system output against corrected clearance, 102
- conclusions, 108
- demodulator unit:
 - phase comparator, 83
 - pulse train, 83
 - voltage-controlled oscillator, 83
- experimental programme, 91–2
 - cycle scrapped components, 91
- FM capacitance probe, 83–4
 - demodulator unit, 83
 - principle of operation, 83–4
- ground station, 83, 89–90
- integrated capacitance probe and calibration systems:
 - ground station, 83
 - measurement head, 83
- measurement head, 86–7, 88, 89
 - actuator carriage, 86
 - encoder, 87
 - integrated probe, 88
 - stepper motor, 87
 - traverse actuator, 86, 89
 - yaw module, 86
- optical clearance measurement systems, 75
- pulse train, 58
- spark-discharge technique, 82
- spinning rig, 61
 - capacitance probe and touch wire mounting, 63
 - for Chivers' system, 64
 - differences from gas turbine test, 67
 - geometry, 62
 - traverse actuator, 64
 - system output against known clearance, 65, 69
 - for each blade, 73
 - with tri-axial frequency modulated probe, 82–3
 - optical principle, 4, 191
 - optical triangulation, 27–8, 29
 - optical-based technique (Poppel), 31–2
- Reynolds numbers, 15
- second generation electromechanical system *see also* first generation electromechanical system
 - actuator, 7–10
 - actuator's rack-mounted electronic controller, 5
 - Cold Flow Rig (UCF6), 15–18
 - commissioning, 13–22
 - cooling requirements, 11
 - electronic controller, 11, 12–13
 - four stage commissioning, 2
 - insulated electrode, 5
 - internal datum, 5
 - low-energy electrical discharge, 5
 - mechanical design, 1–2
 - mini electromechanical actuator, 4
 - performance review, 2
 - probe cartridge design, 5–6, 7
 - probe-actuator assembly design, 15
 - probe's mechanical design and operation, 5
 - schematic layout, 3
 - system concept, 5–13
 - system specification, 9
 - test conclusions, 23
 - test vehicle conditions, 15
- spinning rig, 61, 63
 - capacitance probe and touch wire mounting, 63
 - commissioning, 64–7
 - for Chivers' system, 64
 - differences from gas turbine test, 67
 - geometry, 62
 - traverse actuator, 64
- stepper motor, 2, 7, 87
- tip-to-casing running clearance *see* compressor and turbine blade tip-to-casing running clearance; electromechanical measurement of tip-to-casing running, clearance
- UCF6 *see* Cold Flow Rig (UCF6)